UNIVERSITAT POLITÈCNICA
DE CATALUNYA
BARCELONATECH

PhD Thesis

Energy storage systems integration into PV power plants

Hector Beltran San Segundo

Barcelona, October 2011

Energy Storage Systems Integration into PV Power Plants

Hector Beltran San Segundo

Supervisors: Dr. Pedro Rodríguez Cortés & Dr. Enrique Belenguer Balaguer

Dissertation submitted to the PhD Doctorate Office of
the Universitat Politècnica de Catalunya in partial
fulfillment of the requirements for the degree of
Doctor of Philosophy by the

UNIVERSITAT POLITÈCNICA DE CATALUNYA

**Electrical Engineering Department
Research Center on
Renewable Electrical Energy Systems**

OCTOBER 2011

seer
Sistemes Elèctrics
d'Energia Renovable

UNIVERSITAT POLITÈCNICA
DE CATALUNYA
UPC BARCELONATECH

Energy storage systems integration into PV power plants

ACTA DE QUALIFICACIÓ DE LA TESI DOCTORAL

Reunit el tribunal integrat pels sota signants per jutjar la tesi doctoral:

Títol de la tesi: Energy storage systems integration into PV power plants

Autor de la tesi: Hector Beltran i San Segundo

Acorda atorgar la qualificació de:

☐ No apte

☐ Aprovat

☐ Notable

☐ Excel·lent

☐ Excel·lent Cum Laude

Barcelona,…… de…..................…………….. de 2011

El President   El Secretari   El vocal

…………………….   …………………….   …………………….
(nom i cognoms)   (nom i cognoms)   (nom i cognoms)

A la Carol …

Quan surts per fer el viatge cap a Ítaca,
has de pregar que el camí sigui llarg,
ple d'aventures, ple de coneixences.

Has de pregar que el camí sigui llarg,
que siguin moltes les matinades
que entraràs en un port
que els teus ulls ignoraven,
i vagis a ciutats
per aprendre dels que saben.

Tingues sempre al cor la idea d'Ítaca.
Has d'arribar-hi, és el teu destí,
però no forcis gens la travessia.
És preferible que duri molts anys,
que siguis vell quan fondegis l'illa,
ric de tot el que hauràs guanyat
fent el camí, sense esperar
que et doni més riqueses.

Ítaca t'ha donat el bell viatge,
sense ella no hauries sortit.
I si la trobes pobra, no és que Ítaca
t'hagi enganyat. Savi, com bé t'has fet,
sabràs el que volen dir les Ítaques.

Més lluny, heu d'anar més lluny
dels arbres caiguts que ara us empresonen,
i quan els haureu guanyat
tingueu ben present no aturar-vos.
Més lluny, sempre aneu més lluny,
més lluny de l'avui que ara us encadena.
I quan sereu deslliurats
torneu a començar els nous passos.
Més lluny, sempre molt més lluny,
més lluny del demà que ara s'acosta.
I quan creieu que arribeu,
sapigueu trobar noves sendes.
Més lluny, sempre molt més lluny,
més lluny del demà que ara ja s'acosta
i, quan sereu deslliurats,
tingueu ben present no aturar-vos.

Bon viatge per als guerrers
que al seu poble són fidels,
afavoreixi el Déu dels vents
el velam del seu vaixell,
i malgrat llur vell combat
tinguin plaer dels cossos més amants.
Omplin xarxes de volguts estels
plens de ventures, plens de coneixences.

C om diu el poema de Kavafis, musicat per Llach, el procés per completar aquesta tesi ha sigut sense cap mena de dubte "un camí llarg, ple d'aventures i ple de coneixences". Si els meus peus van xafar terra d'Ítaca per primer cop el dia que vaig complir els 31, avui crec que puc dir que he arribat per segon cop a l'illa. No ha sigut un camí senzill, ningú no va dir que ho seria, de fet, per aconseguir-ho ha calgut treballar molt i superats innumerables i enormes obstacles. Queda clar que, com deia Edison: el ingeni o l'èxit té un ú per cent d'inspiració i un noranta nou per cent de transpiració, és a dir, suar. I és que una de les coses que més clares m'han quedat al llarg d'aquests anys és que fer una tesi doctoral és un camí personal... que ningú farà per tu. Però també, que és un camí que no es fa sol. De fet, dur a terme aquesta tesi doctoral no hagués estat possible sense l'ajuda tant professional com personal i emocional d'un conjunt de persones i institucions a les que m'agradaria citar i reconèixer en aquest punt.

En primer lloc, m'agradaria iniciar els agraïments pels meus dos codirectors: el Dr. Pedro Rodríguez de la Universitat Politècnica de Catalunya i el Dr. Enrique Belenguer de la Universitat Jaume I de Castelló. Quique i Pedro o Pedro i Quique, vosaltres sous els principals responsables tant de l'inici d'aquest viatge com del fet que haja arribat a bon port. Gracies Quique, moltes gracies per haver-me mostrat un camí a la vida allà per l'any 2003 i haver-me ajudat a remar al llarg de tots i

cadascun d'aquests anys. Gracies Pedro, moltes gracies a tu també per haver-me permès formar part del teu grup de recerca, lloc on he pogut desenvolupar i completar aquesta tesi. Gracies per ajudar-me a retrobar el camí oferint-me tota mena d'informació, ajuda i recursos. Si Quique ha estat les veles, tu has estat el vent.

En segon lloc, vull donar les gracies a tots aquells que d'una manera o altra, en major o menor mesura, heu ajudat a donar forma i contingut a aquest document. Entre vosaltres, m'agradaria destacar: a Nico, per la teua inestimable ajuda en aquells durs inicis en que va caler tractar tantes dades; a Barthe, per les teues interessantíssimes pinzellades sobre venda d'electricitat; a Nacho Peña, per tindre sempre un moment per tirar un cable i resoldre eixe dubte; a Emilio, perquè la teua inestimable ajuda final m'ha permès donar-li cos a aquest treball, sense tu, aquesta tesi no seria ni la meitat del que és; a Néstor, per ser l'inseparable company de fatigues a qui no cal explicar res d'aquest procés, veritat que m'entens, Nestor?; a Fran, pels teus sempre savis consells tant sobre word... com sobre tantes altres coses; a Leo i a Lola, pels vostres ànims, pel vostre entusiasme i per llegir eixes pàgines amb el que tant m'heu aportat; a Guti, pels seu "Jazz" que, havent arribat en un moment molt important per a mi, tanta companyia em van fer i m'han fet en les hores d'escriptura d'aquest document.

En tercer lloc, voldria agrair a nivell d'institucions a l'Institut de Tecnologia de l'Energia d'Aalborg, i a la seua gent, per obrir-me les portes d'un lloc tan distingit (mange tak). Igualment, agrair als membres d'Ikerlan a Arrasate l'haver-me permès estar uns dies amb ells, dedicar-me tants recursos i temps i, sobretot, fer-me sentir un més entre vosaltres (Eskerrik asko). Fer record també de l'Institut de Tecnologia Elèctrica de València, on tot açò va començar, i on vaig passar dos meravellosos anys. Igualment, a la Fundació Balaguer-Gonel Hermanos de Castelló pel seu suport. Finalment, donar les gracies a la gent que forma el grup SEER a Terrassa, perquè vosaltres em vau ensenyar com es treballa per fer una tesi.

Per altra banda, aprofite per agrair a tots aquells amics que us heu anat interessant per l'evolució d'aquest treball a pesar de saber que durant molt de temps ha sigut tema tabú (recordeu la paraula prohibida). Destacats sou els qui viviu o vivíeu a Barcelona, qui m'heu anat acollint a les vostres cases en diverses vegades. Especialment, Dani, per haver-me cedit la teua habitació durant prop de tres mesos. Vull agrair també d'entre els amics aquells que vau fer l'esforç de vindre a donar-me

suport a Dinamarca, gracies Manu, i molt remarcablement l'amic Christian qui va repetir visita per tal d'ajudar-me en el retorn. Quina quilometrada, eh Chris?

Vull agrair especialment aquesta tesi a la meua família. A l'amor i suport incondicional d'uns pares que sempre m'han estimat i han confiat en mi, i que són els primers responsables d'haver arribat fins a ací. Aquesta tesi també és fruit del vostre esforç, de l'educació i exemple que m'heu donat, i de com em vau inculcar des de ben menut la cultura de l'esforç. Gracies als dos per rebre'm sempre amb un somriure. Igualment al meu germà, amb la seua ajuda personal i ben emotiva en tants moments complicats. Gracies per la revisió del text, nene. I per últim, com no, a la meua "abuelita" i al meu iaio (que en pau descanse i a qui sempre tinc present com exemple) així com a altres familiars propers. GRACIES a tots amb majúscules.

I finalment, moltíssimes gràcies a tu, Carol. Pels teus ànims. Per la teua paciència i comprensió. Per estar ahí sempre que t'he necessitat. I en definitiva per ser com eres. Però també, gracies a la vida, per haver-me donat aquesta segona oportunitat. Una segona oportunitat que m'ha dut fins a ací i que em permetrà emprendre de nou i amb tu, la meua companya de viatge, almenys una vegada més, el viatge a Ítaca.

Castelló, Setembre de 2011

"*Don't give up!!! That which does not kill us makes us stronger.*" – Friedrich Nietzsche

"*Don't be fearful! Fear is the path to the dark side. Fear leads to anger. Anger leads to hate. Hate leads to suffering.*" – Master Yoda, Star Wars

ABSTRACT

The boom experienced by renewable sources in recent years has changed their consideration as a marginal component of the electrical system mix into a major player with an important role in the demand coverage in many countries. Regarding the PV technology, its weight within the electrical systems in countries such as Germany, Spain and Japan suggests that integration problems may arise if the current installation trends are maintained. Most of these problems are connected to one of its main handicaps: its stochasticity and its high level of intermittency, both characteristics clearly dependent on weather.

This work is dedicated to the analysis of one of the best solutions to achieve a higher penetration rate of the photovoltaic technology in the grid which is, according to the literature, the introduction of an energy storage system in parallel with photovoltaic plants. The ultimate objective in the study reported in this Thesis dissertation is to provide PV power plants with the ability to generate solar energy in a controlled and, if possible, constant way so that these could access both the day and intraday electricity markets.

The analysis of the storage system characteristics , focusing the interest on the amount of energy and power that this system would require when operating the photovoltaic plant in accordance with a specific energy management strategy while avoiding saturations, requires a good knowledge of solar resource. At present, there has not been any major and exhaustive

campaign to measure the radiation with sampling periods below 15 minutes. Therefore, the solar resource can only be estimated by using statistically-based data and weighted averages. These data come from sources in the space (satellite images) and from meteorological stations in the Earth's surface. This work uses information extracted from one of the most commonly accepted solar radiation databases, the PVGIS database developed by the European Union. Moreover, real data measured in a particular place in the south of the Iberian Peninsula, where the analysis of the energy storage requirements has been centered, are also used. Both data sets have been cross validated in order to verify their credibility and agreement degree.

On the other hand, there are multiple energy storage technologies that can be currently identified as potential candidates to be included in photovoltaic power plants to integrate future hybrid plants with controlled production. A review of these technologies, along with a description of their main features highlighting their strengths and limitations, is included in this Thesis work. Using the comparison as a method, which has been performed considering various factors associated to the storage technology itself (geographical dependence, state of development, energy and power rated levels achieved by each technology) but also taking into account the operation conditions at which the storage will be subject in a photovoltaic power plant, one technology is highlighted as the candidate to be used in this application.

Finally, this Thesis proposes various energy management strategies to control power production in photovoltaic power plants integrating an energy storage system. Some of these strategies are directed to incorporate the plant to the electricity market while others simply pretend to reduce the variability of the production. For each of them, an estimate of the energy storage system required energy capacity has been obtained. These estimates allow having a rough approximation of the energy requirements, as well as an estimate of the additional cost, that this solution would imply. Among the various energy management configurations proposed, some of them provide results technically feasible on the one hand and, on the other hand, also interesting outcomes from an economic point of view, as the regulatory framework governing the electricity markets becomes gradually adapted to the new and evolving reality of the electric power system.

Resum

El gran boom experimentat per les energies renovables al llarg dels darrers anys ha suposat que aquestes deixen de ser considerades com un element marginal del sistema elèctric per passar a tindre un rol fonamental en la cobertura de la demanda de molts països. Pel que fa a la tecnologia fotovoltaica, el seu pes en sistemes elèctrics com és el cas d'Alemanya, Espanya o Japó fa pensar en els possibles problemes d'integració que es poden plantejar de seguir amb aquesta tendència causats per un dels seus principals handicaps: la seua elevada estocasticitat i el seu nivell d'intermitència, dependents ambdós en tot moment de les condicions meteorològiques.

El present treball està dedicat a l'anàlisi de les característiques de la que ja queda destacada en la bibliografia com una de les solucions òptimes per tal d'aconseguir una major índex de penetració de la tecnologia fotovoltaica en la xarxa elèctrica: la introducció de sistemes d'emmagatzematge d'energia en paral·lel amb les plantes fotovoltaiques. La finalitat última en l'estudi realitzat en aquest treball es atorgar a les plantes fotovoltaiques la capacitat de generar la seua energia de forma controlada i, de ser possible, constant per tal de poder accedir als mercats d'energia elèctrica tant diaris com intradiaris.

Per tal d'analitzar les característiques del sistema d'emmagatzematge òptim, centrant l'anàlisi en la quantitat d'energia i de potència que aquest sistema requeriria per tal de fer funcionar la planta fotovoltaica d'acord amb una estratègia de control de potència

determinada i evitant en la mesura d'allò possible saturacions del sistema d'emmagatzematge que suposarien perdudes del control de la planta, resulta fonamental un bon coneixement del recurs solar. A dia d'avui, no s'han realitzat grans campanyes de mesura de la radiació amb freqüències de mostreig inferiors als 15 minuts enlloc, pel que el recurs solar sols pot ser estimat utilitzant dades ponderades i mitjanes estadístiques. Aquestes provenen tant de fonts a l'espai (imatges de satèl·lit) com d'estacions meteorològiques a la superfície terrestre. En aquest treball s'utilitza informació extreta d'una de les bases de dades de radiació solar més acceptades comunament, la PVGIS de la Unió Europea, així com dades reals mesurades en un lloc concret del sud de la península Ibèrica on s'ha centrat l'estudi. Ambdós grups de dades han estat creuats per tal de verificar la seua versemblança i validesa.

Per altra banda, són múltiples els sistemes d'emmagatzematge d'energia que poden ser identificats en l'actualitat i que podrien ser candidats a ser integrats en les futures plantes fotovoltaiques de producció controlada. Aquest treball realitza una revisió d'aquestes tecnologies, descrivint les seues principals característiques i ressaltant els punts forts així com les limitacions de cadascuna d'elles. De la comparació entre els distints sistemes, tenint en compte diversos factors propis (dependència geogràfica, estat de desenvolupament tecnològic, nivells de potència i energia assolits per la tecnologia) així com de funcionament a les plantes fotovoltaiques, surt una tecnologia com a candidata a ser utilitzada.

Finalment, aquest treball proposa diverses estratègies de control de la producció d'energia per a plantes fotovoltaiques amb emmagatzematge d'energia. Algunes més orientades a fer funcionar la planta de cara al mercat i altres simplement buscant reduir la variabilitat de la producció. Per a cadascuna d'elles, s'ha realitzat una estimació de la capacitat energètica necessària del sistema d'emmagatzematge. Açò permet tindre una idea ben aproximada dels requeriments energètics d'aquestes solucions així com una estimació del cost suplementari que representa la seua inclusió en les plantes fotovoltaiques. De entre les diverses solucions, alguna d'elles dóna resultats tant viable a nivell tècnic, com interessant des d'un punt de vista econòmic, sempre i quan el marc regulador del mercat elèctric fora progressivament adaptat a la nova i canviant realitat del sistema.

CONTENTS

Energy is the cornerstone for the economic, political and social development of societies and civilizations. Controlling the energy resources has historically meant to have advantage over the others. This trend has been further accentuated during the second half of the twentieth century with the enormous industrialization development and the massive use of coal and oil in the developed countries. As a consequence to the high levels of pollution derived from the use of these fossil fuels, society has started to internalize a certain climate change concern. Moreover, there is also, maybe not on the society but in high political circles, an emerging concern about the threat over the economies and the further development of these countries represented by the high energy dependence on fossil fuels, which are mainly produced by politically unstable countries. Both concerns, environmental and politico-economical, have encouraged policy makers and researchers to seek for alternative sources of energy.

A direct consequence of this new energy policy scenario in the period 1995-2010 is the rapid development experienced worldwide by distributed generation technologies, highlighting those based on renewable energy sources such as wind and solar. According to the International Energy Agency (IEA), this huge development has achieved more than 198 GWe and 40 GWe, respectively, over that period; all together represents an average annual growth above 20 % for each of these technologies. These evolutions contrast with the growth estimated for conventional generators well below the 3 % during the same period. Since the introduction of renewable sources has not been homogeneous around the world, a massive

installation can be identified in different countries such as Germany, Denmark, Spain, Japan and the USA. Therefore, a high percentage of the production mix is already covered by renewables during certain periods of time in these countries. This phenomenon can pose serious problems in the coming future for the grid stability if this evolution is maintained. Problems derived essentially from the intermittent and stochastic power production nature associated to these technologies. Therefore, for a further integration into the grid, renewable sources, and especially the PV technology, will have to evolve from its currently stochastic weather dependent power production into a more constant and predictable controlled production. Such a production will be better managed to balance the electric power system and will make possible to trade it in electricity markets as it is done with the rest of conventional power generators production.

This Thesis work addresses several key aspects on the design and control of future PV power plants which, supported by energy storage systems (ESS), will present these production characteristics. In this sense, the solar resource is described and analyzed; the different energy storage (ES) technologies are updated and reviewed; also, different energy management strategies (EMS) for the PV plant with storage are defined, simulated and tested; and finally the energy storage requirements to allow the PV plant accomplishing the different operation modes are analyzed and defined. The results and conclusions from this work can be profited by PV power plant developers to get a rough estimation of the control possibilities to facilitate a further integration of PV plants with storage into the grid on the one hand, but also of the energy capacity requirements demanded by the storage to perform in such a way.

Motivation

As can be deduced from this brief introduction which establishes the framework and the topic of this Thesis, the main motivation that has driven to its development is the Author's concern about the global warming, the climate change and its blind trust in the renewable energies importance for a future sustainable development of the planet.

Nonetheless, not only these are the initial motivations to undertake the Thesis on this domain, but also a clear interest for the PV and the energy storage technologies themselves as well as their continuous evolution, which represents for the Author a real challenge and a very exciting world that deserves being investigated.

In this sense, for the correct understanding of the PV power plants production profile, which highly defines the amount of storage that has to be integrated in order to be able to control the plant production, not only it is important to know about the PV technology itself but also about the nature of the solar resource, which will ultimately be the responsible for the PV production variability. This encourages the Author to investigate on the solar resource characteristics and on those databases which could provide information on the irradiation availability and on the PV potential worldwide.

Similarly, many different ES technologies are nowadays being developed or already commercialized around the world. And many of them have already been considered for applications at consumer or grid levels, or even with some renewable technologies. However, not a clear ES solution has been proposed yet in the literature to be integrated into PV power plants. This situation prompts the Author to update and review these technologies, to get a global panorama of the state of the art, and to try to define the best energy storage alternative according to the operating conditions that it should face when connected to a PV power plant and to the storage technology characteristics.

It is essential for the viability of these PV power plants to integrate energy storage systems, not only to combine components but also to implement optimal EMS which allow generating the maximum profit from this hybrid technology. The definition of new EMS to control these power plants implies to think on the type of production which is desired to achieve. This concerns the goal of this production or, in other words, how the new controlled production will be beneficial not only for the electric power system but also for the economic viability of the hybrid power plant. This motivates the study and analysis of the Spanish electricity market in such a way that the proposed EMS can take advantage of the market structure and of the current regulatory frame in order to optimize the incomes.

Finally, the difficulty to precisely forecast the real PV production, so dependent on current weather conditions, that is going to be experienced at a certain location at any given moment, motivates the Author to perform the analysis of the PV+ES operation and the ESS energy capacity requirements evaluation on an annual timeframe basis. This will allow obtaining results which are somehow independent of the daily, or even seasonal, weather variations. The idea of the Author would be to provide some energy storage sizing estimations or reference values, as generalized as possible, which could be used in the coming future by PV plant developers or professionals of the PV industry for their PV+ES power plant projects.

Goals

According to the motivation, the main objective of this Thesis is to propose a solution for the further integration of PV power plants into the EPS; a solution based on the introduction into these intermittent power plants of an ESS with which an advanced control of plant power production can be achieved. This advanced control capability allows approaching the performance of these stochastic renewable energy sources to that of the conventional dispatchable power plants. In order to achieve this goal, a series of partial objectives have been defined and are enumerated in the following:

- To analyze the EPS evolving structure and to proceed with an overview of the current RES state of development and their future trends, focused on the PV technology.

- To identify future problems derived from the massive integration of renewables into the EPS and to analyze possible solutions.

- To analyze the possible applications or functionalities for the grid, the demand side or the renewables integration associated to the ESS.

- To study the solar resource characteristics and its availability, as well as to review those solar data sources which can be consulted in order to obtain information on the PV potential for any location.

- To compare the different solar databases and to determine which is the most interesting from the point of view of the solar data required in this work.

- To contrast the standard PV production curves obtained for a determined location from the solar radiation data bases with real PV production data registered in that location throughout one year.

- To review the different ES technologies in order to determine which would be the most suitable ESS to be integrated within PV power plants.

- To review the configuration and the control strategies implemented in already existing hybrid plants which combine PV with other renewables and storage.

- To propose some new EMS which allow converting the instantaneous weather-dependent PV production into a more regular and predictable power production. It would be desirable that some of these EMS were defined so as to provide the PV power plant with capability to trade their energy production in the electric pool.

- To model and simulate a PV power plant with ES so as to check the performance of the system under the different EMS.

- To analyze the ESS power and energy capacity ratings which are needed to operate the PV plant with storage according to each of the proposed EMS.

- To define what would be, both technically and economically, the most viable energy management strategy which could be implemented into PV plants with storage in such a way that these could participate and trade in the electricity markets. This would be the strategy which allows this participation while requiring the smallest ESS.

Summary

This Thesis dissertation is structured in such a way that it successively introduces the work carried out while approaching the results obtained in the search of the goals. In this sense, the document is divided into six chapters which can be summarized as follows.

Chapter I introduces the current EPS and generation mix structure (with the high level of penetration of the DGs, many of them presenting the big handicap of producing power intermittently). This is analyzed together with the future RES installation trends, especially for the case of the PV technology. In the same way, an overview of the problems associated to these renewable technologies installation tendencies is presented in this chapter. Finally, the introduction of ESS is contemplated as possible solution to the integration problems and the multiple functionalities and applications which can be obtained when these are introduced are also analyzed.

Chapter II is devoted to the review of the solar resource characteristics, the current solar radiation modeling techniques and the solar resource data information sources. After that, the PVGIS database is chosen as the optimal to provide PV production models for the analysis. Finally, a detailed analysis of the solar radiation resource in the south of Spain, comparing real irradiation data with theoretical models extracted from the PVGIS database is performed. This analysis confirms the validity of the real data used for the further analysis.

Chapter III presents an updated and complete compilation of the current state of the art of the multiple types of ES technologies that can be found nowadays around the world and that could be applied for renewable energies applications. Their historical evolution, their current state of development, their strengths and weaknesses, the estimated costs and the existing installations are enumerated among other specific characteristics for each of the

technologies. To conclude the chapter, a comparison of the different ES technologies and a selection of the optimal technology to be used within PV power plants is discussed according to different factors.

Chapter IV discusses about some possible EMS which are proposed to be implemented in PV power plants with ES. Each of the strategies pursues a different goal in terms of improved operability of the PV plant. For doing so, a power plant model which combines PV panels with an ESS is first introduced. Then, the two main EMS which are proposed to be used in order to control such a plant are described. Thereafter, some complementary control options, which can be optionally overlapped to any of the two main EMS, are also described. Finally, some simulation results, derived from the application of these EMS to the PV power plant with ES, are set out. The simulation results presented in this chapter are exclusively focused on the PV production cumulative probability distribution reorganization and on the PV production frequency spectrum modification that can be achieved when introducing an ESS into a PV power plant.

Chapter V is devoted to the presentation of the PV+ES system annual performance and the ESS sizing results for that period. In this sense, ES capacity requirements are established, in an annual basis, in order to achieve a proper PV+ES power plant performance when operating under the various EMS introduced in the previous chapter. To do that, the Matlab programs which have been developed and used to perform the annual analyses are first introduced. Thereafter, the corresponding sizing analyses are described for each of the EMS possible configurations. Note the different improved-operation goals of each of the EMS configurations and the optional introduction of a series of complementary energy adjustment controls (which do highly modify the operation of the plant). As a result to these two observations, very different ES sizing requirements are obtained in the different analysis. This will pave the way to the economic viability of some control strategies, closing the door to the others. Apart from the various sizing analysis carried out, some experimental results are also obtained in a laboratory test bench which implements a package of ultracapacitors as energy storage technology. A Lithium Ion battery ageing analysis is also presented in this chapter. To finish the chapter, some conclusions based on a comparison of the results obtained for the different sizing analysis are introduced.

Finally, Chapter VI contains the main conclusions obtained presenting the most relevant contributions. Thus, future research lines that arise from this Thesis work are proposed.

CHAPTER
1

Introduction

The classical electric power system structure has been characterized worldwide by the centralized power generation philosophy, a way of operating a power system in which almost all the electrical energy is generated by, or almost all capacity lies in, large central power plants, normally based on fossil fuels, nuclear and hydraulic power.

Despite the global financial crisis which has been hitting the worldwide economies since 2007, the energy consumption around the world did only experience a certain reduction over the year 2009 recovering again in 2010 an overall increase of 5.4 %, even higher than the average of the last 10 years [1]. Therefore, more and more power needs to be increasingly generated every year. However, the increase in the cost of the fossil fuels due to a higher demand of these energy primary resources in developing countries and a certain political instability periodically present in the exporting countries, combined with an increasing concern about the global warming and the climate change (which was made clear with the major ratification of the Kyoto protocol) has boosted the development of new power technologies, notably based on renewable energy sources but also on nuclear power (technology which has been also experiencing a renaissance till the recent accident in Fukushima Daiichi, Japan). The development of these alternative sources of energy helps reducing, or limiting, the CO_2 emissions as well as achieving a certain energetic independence from the countries producing fossil fuels; goals highly intended by politicians in most of the developed countries.

As a consequence to the evolution of the worldwide energy production panorama, most of the electric power systems (EPS) around the world are also experiencing changes in their organization and structure. This reorganization is being forced by the increasing introduction of renewable resources and combined heat and power units producing small-medium scale amounts of electric power in many different places around the geography (where the natural resources or the use of the energy can be better profited).

Therefore, these EPS do not consist anymore of a few centralized generators (big power plants) injecting power into the grids at certain established locations. On the contrary, the new philosophy of EPS consists on a large amount of distributed generators (DGs), with power levels well below that of the conventional ones (capacity levels usually accepted vary between 0.1 and 50 MW), which inject their power into the grid as well as transport level as at the distribution level [2, 3].

A demonstration scheme of the distributed generation philosophy can be appreciated in Figure 1.1. It can be clearly appreciated in this example how different generation technologies are integrated, being some of them directly connected to local networks and consumers, and how the whole system is well interconnected.

Distributed generation involves a large number of different generation technologies. These range from small turbines with a steam organic Rankine cycles to gas turbines or micro turbines, through diesel or gas-fuelled reciprocating engines, Stirling engines, fuel cells (at high or low temperature), photovoltaic (PV) systems, wind turbines or even small hydro turbines. Note that although many DG technologies use fossil fuels, most of them can also be run using renewables such as biofuels.

However, not all these technologies present the same state of development and are unequally introduced around the world. In fact, some of them are still emerging and have high investment costs, e.g. fuel cells, while others are already widely deployed. So much so that wind power plants, for example, cannot be considered anymore as marginal power sources in the electricity domain neither included as a distributed generator, given the capacity power that these have achieved. It is important to highlight in this sense the case of different countries where the share of their electricity demand covered in 2010 with wind power was very significant. These are: Denmark with a 22 %, Portugal with a 21 %, Spain with a 15.4 %, and Ireland with a 10.1% [1].

Figure 1.1 Scheme of DGs in the electrical network. Source: Electric Power Research Institute.

In order to get an updated overview of the frame where this Thesis is placed, this chapter presents in the following a short description of the current panorama for the different renewable energy sources, with especial attention to the photovoltaic technology. The problems associated to their increasing degree of penetration are stated along the chapter. Then, the Spanish EPS and its associated electricity market are described. These are introduced in order to discuss the current regulatory framework in the country where the Thesis work study is focused, and how a further integration of renewables could be achieved. Finally, the possible applications or functionalities that can be provided by or achieved thanks to the energy storage systems (ESS), as a possible solution for the renewable integration problems, are enumerated and described.

1.1. Renewable energy sources panorama.

Conversely to conventional energy sources, renewable energy sources (RES) can be defined as those providing energy which comes from inexhaustible natural resources such as the sunlight, the wind, the rain, the tides and the geothermal heat; that is, energy sources which are replaced rapidly by natural processes. It has already been stated that RES are not anymore a minor agent in the energy consumption domain in different countries. Those highlighting are: Germany which met 11 % of its total final energy consumption with

renewables, the USA whose RES accounted for about the 10.9 % of the domestic primary energy production, or China where an estimated 29 GW of grid-connected renewable capacity was added in 2009 [1]. This importance can be extrapolated to the worldwide level as can be appreciated in Figure 1.2.

This figure stands out that during the year 2009 the global final energy consumption share around the planet contained a 16 % which was provided by the different RES technologies. This percentage stands for: 10 % coming from traditional biomass (used primarily for cooking and heating in rural areas of developing countries), and 3.4 % from hydropower (growing modestly but from a historical large base). New renewables (small hydro, modern biomass, wind, solar, geothermal, and biofuels) accounted for another 2.8 % but these are growing very rapidly in developed as well as in some developing countries.
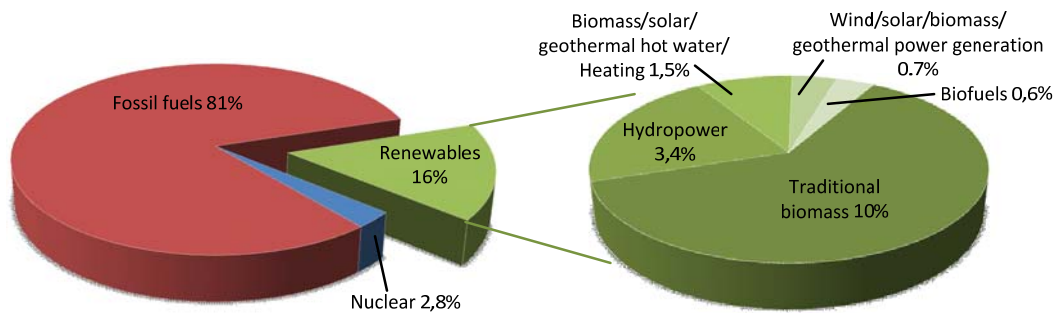
Figure 1.2 Global final energy consumption share as of 2009. Source: [1]**.**

Apart from the actual share in the energy consumption, it is important to highlight the evolution of these technologies in the recent years, with many of them presenting growth rates annually-averaged well above the 15% during the period 2005 - 2010. But not only that, it stands out that some technologies, as it is the case for the PV power, have achieved evolutions over that period as high as 50 % from one year to the following in their installed capacity [1]. This can be observed in Figure 1.3 in which the annual evolution from 2009 to 2010 together with the average evolution in the period 2005-2010 is represented for eight different RES technologies. Just behind the solar PV technology, biodiesel, solar thermal and wind power has to be noted with sustained growths over 20 %. It stands out however the different evolutions these are following. While the wind power has been increasing at a constant rate, the growth rate for solar thermal has experienced a great boom in 2010 and, on the other hand, the growth rate for biofuels have progressively declined in the recent years due to different factors till the 7 % registered for the biodiesel last year and with the only

exception of the ethanol which was up again in 2010 to recover a 17 %. Finally, the three last technologies (hydropower, biomass power and heat, and geothermal power and heat) are growing at rates of 3 – 9 % per year, more similar with the global growth rates for fossil fuel based technologies (normally being registered in the range 1 – 4 %).
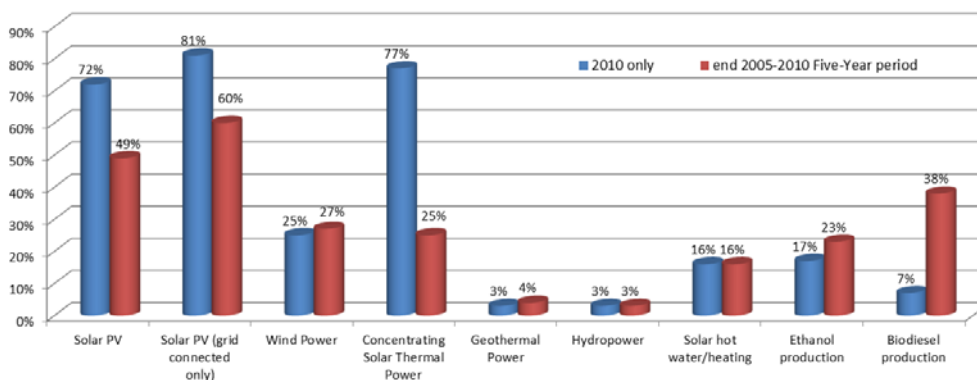
Figure 1.3 Average annual growth rates for RES capacity and biofuels production. Source: [1]**.**

However, it must be stated that of course this growth is not homogeneous around the globe and the different regions present different degrees of penetration of renewables. Apart from the USA, China and Germany, the European Union (EU) as a whole must be highlighted in this sense for the ambitious deployment plans approved in the last five years. Despite the important difficulties to get agreements on any matter which arise at the EU level, given its enormous structure with 27 members and different policies and national interests, a unified approach towards RES was agreed at a European Council meeting which took place in Brussels on March 2007. From then on, the Council endorsed a binding target of a 20 % share of RES in the overall EU energy consumption by 2020 (what constitutes a 37 % of Europe's electricity production from RES), and a 10 % binding minimum target to be achieved by all Member States for the share of biofuels in overall EU transport petrol and diesel consumption [4]. This target was supported on the corresponding regulatory framework defined by the Directive 2009/28/EC on the promotion of the use of energy from renewable sources and amending and subsequently repealing Directives 2001/77/EC and 2003/30/EC [5].

The individual targets established in the Annex I of the Directive 2009/28/EC for the different Member States are represented in Figure 1.4. These are defined as an overall percentage for the share of energy from RES in the gross final consumption for each of the states, establishing also the partial evolutions these should follow along the plan period.
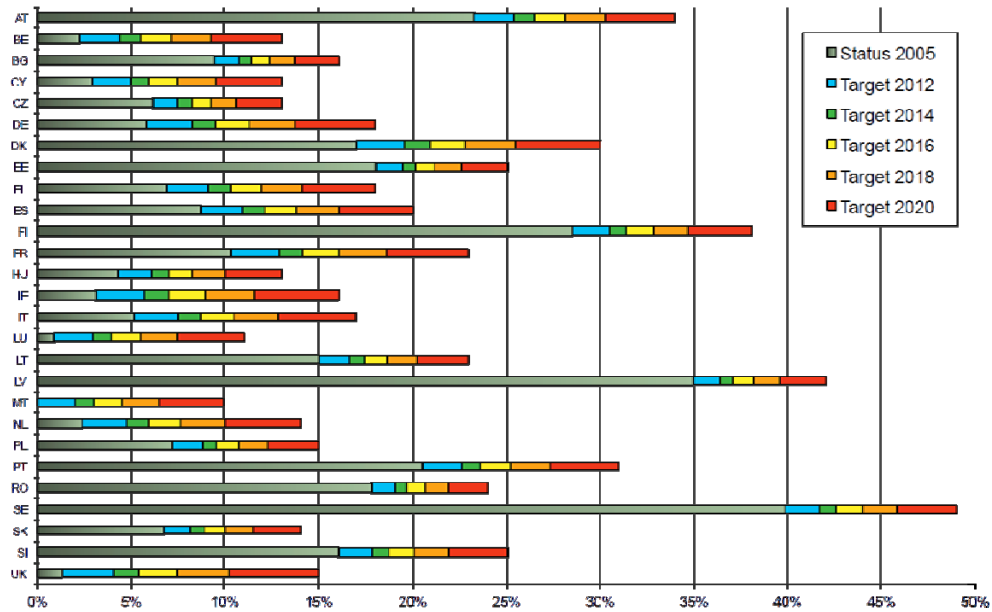
Figure 1.4 Trajectory to reach the share of renewables in the EU in 2020. Source: [4]**.**

It can be observed in the figure how, although the Council made an effort to unify the EU energy policy, the initial situation and the final target vary to a great extent from some Member States to the others. In fact, apart from establishing the final targets and the trajectory, the Directive allows each state to decide on what kind of technologies to utilize in order to reach its targets and what kind of national regulations or energy policies to fix.

The targets represented in Figure 1.4 also stand out that this Directive is much more ambitious than the previous Directives, already cited, as well as the EU White and Green Papers on "Energy for the Future: Renewable Sources of Energy" and "Towards a European Strategy for the Security of Energy Supply", respectively, approved in 1997 and 2000. Note that previous legislation had been passed to meet the CO_2-reductions compromise acquired by the EU in the Kyoto Protocol but also to lower the European dependence on energy imports. The new extended targets can be understood by the fact that the renewables industry response to the goals established in those documents (12 % of the total and 21 % of electric energy in the European Union by 2010) was so good that the initial targets have been not only accomplished but even overwhelmed in some of the technologies (a 3 GW was established for PV while 29 GW were already installed in 2010).

Therefore, RES as a source of primary energy, or its share in the final energy consumed, presents a promising future supported on favorable energy policies around the world.

When focusing on the share of RES in the electricity generation mix, the situation can be also defined as increasingly positive. As for the year 2010, renewables already represented around the 19 % of the electricity production, with 16 % of the global electricity coming from hydroelectricity and 3 % from the rest of recently incoming RES. This share can be observed in Figure 1.5. Note that renewables provided even more electricity than the nuclear power plants last year.
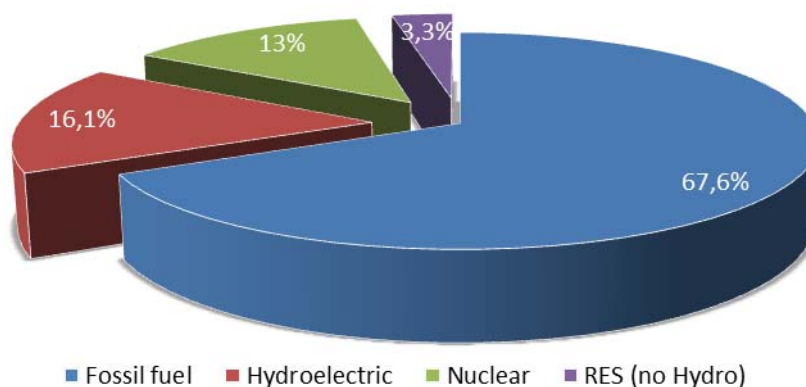
Figure 1.5 Global electricity production mix in 2010. Source: [1]**.**

The positive evolution is validated by the fact that RES technologies accounted for approximately half of the estimated 194 GW of new electric capacity added globally during 2010 (an increment of almost 8 % from 2009), bringing the cumulative capacity of RES generating power to 1320 GW [1]. This installed capacity represents about a quarter of the total global power generating capacity which was estimated of around 4950 GW at the final of the year 2010. However, this renewable capacity did only supply around the 19.5 % as has been shown in Figure 1.5.

If hydroelectric power is left apart, given that it is quite a traditional technology, the evolution presents an even higher rate with an increment of 25 % in the installed capacity in 2010 with regard to that of 2009 (312 GW against 250 GW). In this sense, two technologies can be highlighted: the wind power which increased its global capacity in 2010 by 39 GW, and the PV power which did the same by almost 17 GW. The latter will be examined in depth in the following section.

As described for the case of the RES evolution in the final energy consumption, their application for electricity production is not homogeneous around the world. Different countries lead the list on renewable although the ranking varies depending on the optional introduction of the hydroelectric power within the renewable mix. Therefore, countries such as China, the USA, Brazil, Canada, India Germany or Spain stand out [1]. When analyzing each of them separately, interesting figures are obtained:

- China is already the world leader in the installation of RES with an estimated addition of 29 GW of grid-connected renewable capacity in 2010, mainly wind turbines and solar thermal systems. This increase brought the cumulative installed capacity to 263 GW, which accounts for about 26% of China's total installed electric capacity [1].

- USA achieved an 11.6 % of existing electric capacity from RES in 2010 thanks to an estimated 25% of electric capacity additions during that year. This represents being the third country in annual additions just behind China and Germany. However, RES provided just over 10.3% of total domestic electricity [1].

- India introduced around 2.7 GW of new grid-connected RES power capacity during the year 2010, mainly from wind but also from biomass, small hydropower, and solar capacity. This capacity addition brought the cumulative power to a total of nearly 19 GW by January 2011. However, most of the electricity coverage from RES still comes from large hydropower plants which generated about one-quarter of India's electricity in 2010, with other renewables accounting for just over 4% of the generation [1].

- Canada and Brazil generate around 61 % and 80 % of their electricity with hydropower (an accumulated of 75.6 GW and 80.7 GW in 2010, respectively), what situates them in the third and fourth position in the ranking of countries with more RES capacity installed including hydro. Apart from that, Canada is not among the top five countries for any other technology. Conversely, Brazil can be highlighted in the ethanol and the biodiesel production as the second in the ranking after the USA and Germany, respectively. Moreover, Brazil is nowadays the second larger power producer from biomass also after the USA, what represents an installed capacity which reached the 7.8 GW by the end of 2010.

- European Union presented an estimated increase for RES in 2010 of approximately 41% with regard to 2009, what represents incrementing the capacity in 22.6 GW (note that only PV technology accounted for around 13.2 GW). The RES share in the total

electricity production around the EU was nearly 20% in 2009 what approaches the 2010 target established in 2005. Note that 42 % of this production was not hydroelectric. And among the EU 27 Member States, of course, Germany must be highlighted. This country achieved in 2010 a RES power production level which covered 16.8 % of its electricity consumption, despite a 4.3% increase in the Germany electricity demand that year. Among the renewable technologies which provided this energy, wind power was the most important, accounting for nearly 36% of RES generation, followed by biomass, hydropower and PV [1].

Finally, special attention is paid to the case of Spain for the interest of this Thesis work. In Spain, the introduction of renewables started thanks to the Law 54/1997 for the Electricity Sector [6], which established the liberalization of the electricity in Spain and set a 2010 target to reach 12 % of the primary energy consumption from RES. This objective was established according to the proposed recommendation in the "White Paper on Renewable Energies" published by the EU, which expressed a general interest in this type of energy. The Spanish law provided for that purpose the preparation of a plan for the promotion of the RES, which was approved in December 1999 [7]. It was called "Plan de Fomento de las Energías Renovables" and it analyzed the situation and the potential of the RES and established specific targets for different technologies.

As in many European countries, the early years of the decade were hard for the effective deployment of renewables and only wind power seemed to be doing its way. Therefore, the Spanish government decided to reinforce the regulatory framework and clearly bid for a RES energy policy passing a new plan for RES in 2005. The so-called "Plan Nacional de Energías Renovables" or PER [8] was defined as a roadmap for RES for the period 2005 - 2010. This new plan kept the target of 12% from RES in the primary energy consumption by 2010 and added two new targets for that year: 5.83% of biofuels in petrol and diesel consumption for transport, and a minimum contribution of RES to gross electricity consumption of 29.4 %. Moreover, the PER was supported by a series of Royal Decrees which established very generous feed-in tariffs. This fact fostered the final breakthrough of the renewables in Spain and most of the targets set by the PER were achieved by the end of the application period.

In summary, out of the 99 GW of installed power capacity in Spain at the end of 2010, RES accounted for 44.9 GW. These are mainly represented by wind power (20.1 GW), hydroelectric power (17.6 GW) and PV power (3.8 GW). Given that the hydropower did not register any new addition in 2010, these installed power capacity values represent an

increment of around the 15 %, in average for the rest of renewable technologies, with regard to 2009. The share for each generating technology in the Spanish electricity production mix can be observed in percentage in Figure 1.6.
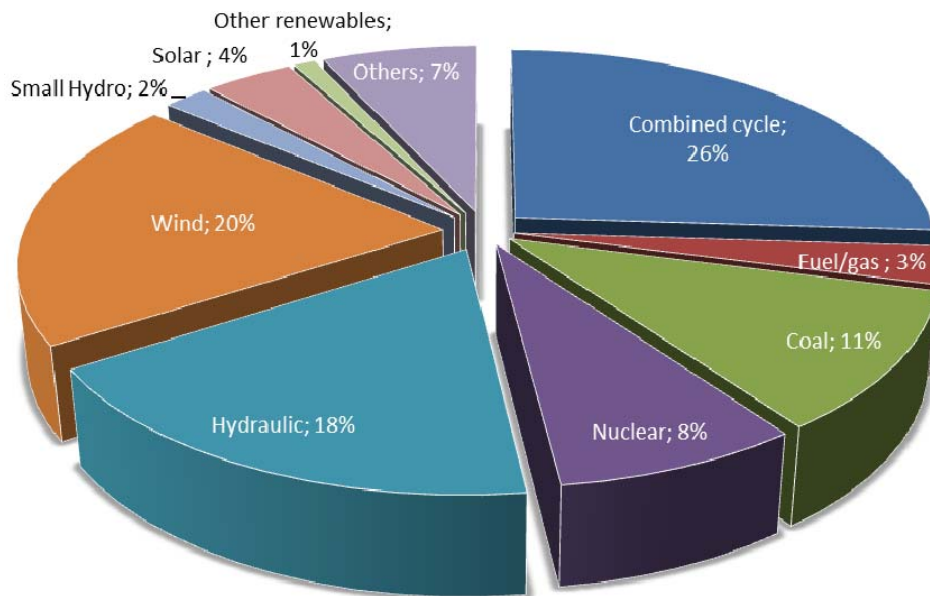
Figure 1.6 Spanish electricity capacity mix (installed power). Source: [9]**.**

However, although representing a 45 % of the installed capacity in 2010, these RES only provided 13.2 % of the final energy production and generated 32.3 % of electricity, up from 9.3 % and 26 %, respectively, in 2009 [9]. The percentages of electricity consumption can be observed in detail in Figure 1.7. Therefore, some targets of the plan have been even overcome, as it is the case for the gross electricity consumption from RES.

From this point on, the new European scenario is established by the already cited Directive 2009/28/EC [5] on the promotion of the use of energy from renewable sources for the coming years. This Directive encourages and forces the Member States to set the national energy policies which allow achieving its targets. In Spain, this Directive has been already transposed and it is reflected on the recently approved (2010) "Plan de Acción Nacional de Energías Renovables" or PLANER [10], and in the currently under development "Ley de Eficiencia Energética y Energías Renovables". These are proposed for the period 2011-2020 and, together with the "Ley de Economía Sostenible" [11] passed this year, constitute the three fundamental pillars on which the promising future of the sector rests.
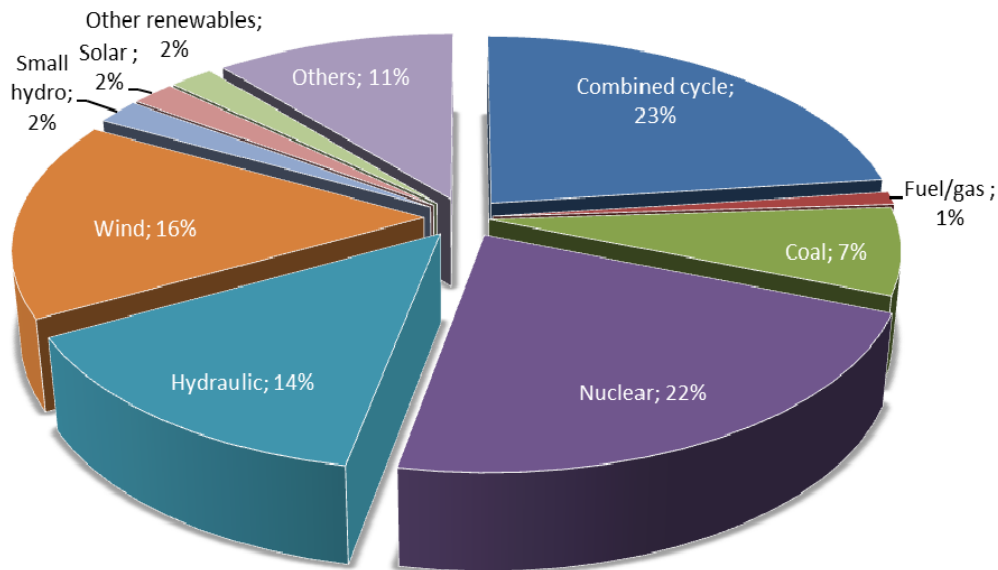
Figure 1.7 Spanish gross electricity consumption share (electric energy). Source: [9]**.**

Therefore, according with the present state of evolution of RES and its coming installation trends, everything indicates that their degree of penetration is going to increase progressively. This poses some technical issues over the future operation of the grids and the structure of the electricity markets, which have been already expressed by experts in reports as the Communication to the European Parliament and the Council entitled "Renewable Energy: Progressing towards the 2020 target" published on the 31st January 2011 [12]. This document states the progress of the Member States towards achieving the renewable electricity targets established by the Directive 2001/77/EC. But also, the communication further pointed out the following interesting affirmation: "Based on Member States' plans, renewable energy should constitute 37% of Europe's electricity mix by 2020. … The Energy 2020 Strategy highlighted how the rise of electricity produced from renewable sources also has implications for the electricity market as a whole. Multiple, flexible, smaller scale distributed forms of electricity generation need different grid and market design rules compared to traditional large, centralized power sources" [12]. Thus, this EU report is prompting the states to assign priority to RES electricity production by increasing the investment on these technologies but also to start studying what market rules should be modified and what infrastructures should be integrated in the grid so as to make RES integration easier and possible.

1.2. Photovoltaic power technology panorama.

As far as photovoltaic technology is concerned, the evolution during the last 10 years has been amazingly extraordinary. As already introduced, the average increase registered from 2005 is around the 50 % annually, with an aggregated annual average of more than 20 % since 2002. This can be appreciated in Figure 1.8 which shows the annual evolution in detail representing for each of the years those countries which mainly participated in the PV growth. This tendency has been confirmed, or even reinforced despite the financial crisis during the last year 2010, as can be appreciated in Figure 1.8 but also in Figure 1.3. This year 2010, a global PV capacity was installed in such a quantity that the PV market more than doubled its figures of 2009. In this sense, an estimated 17 GW of capacity was added worldwide (compared with some 7.3 GW in 2009), bringing the global total to about 40 GW which represents a total amount more than seven times the capacity in place five years before [13].
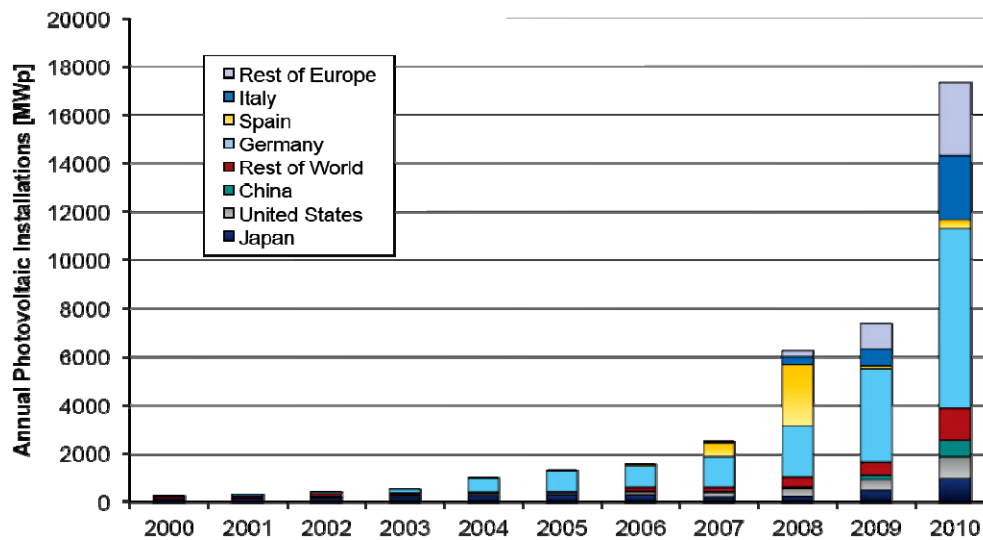
Figure 1.8 Annual evolution of the PV installed capacity. Source: [13]**.**

With these figures, photovoltaic power plants should not be considered anymore a marginal renewable power source to be installed exclusively as a local solution to feed isolated consumers or integrate low voltage networks as another low power DG. So much so that the current trends are focused on large utility-scale PV plants with power capacities over 200 kW [14]. In all, the number of systems with these characteristics exceeded 5000 in 2010, an increase of 1800 with regard to 2009, with nine of the world's 15 largest PV plants

completed that year [15]. These large scale facilities comprehended around 9.7 GW of capacity by the end of 2010, an increase of more than 3 GW during the year and accounted for almost 25% of the overall global PV capacity.

As of November 2010, the largest PV power plant in the world is the Finsterwalde Solar Park, located in Germany, with a total capacity of 80.7 MW. But, not only this installation is over the 50 MW nowadays, others which can be also highlighted are: the Sarnia PV Power Plant in Canada with 80 MW, the Olmedilla PV Park in Spain with 60 MW, the Strasskirchen and the Lieberose Photovoltaic Parks both in Germany with 54 MW and 53 MW respectively, or the Puertollano PV Park also in Spain with 50 MW. Moreover, the boom does not finish there and new projects are arising with proposals of hundreds of MWs. Note the Topaz Solar Farm, proposing to install 550 MW of solar photovoltaic in the northwest of California Valley (USA) at a cost of over $1000 millions, or the High Plains Ranch II installation, proposed by Sun Power with 250 MW of solar photovoltaic to be built on the Carrizo Plain, also in the northwest of the California Valley (USA).

This demonstrates the increasing interest on the photovoltaic technology which, once it is consolidated as a mature technology, is demonstrating to be economically and technically viable for large scale installations, what is fostering its future enormous deployment supported by favorable policies according to [4, 14]. The planned future developments in two important regions such as the European Union and China can be appreciated in Figure 1.9. In fact, these two regions have to be highlighted because, on the one hand, the EU dominated the global PV market, accounting for the 80 % of the PV installed capacity worldwide in 2010 while, on the other hand, although China did not install more than 0.6 GW last year (accumulating a total rounding 1 GW) this country is the world production leader by far and its PV installing plans are not negligible at all. It is important to note that for the case of the European Union, 2010 was the year when there was for the first time a higher increase in the PV capacity installed than in that of the wind capacity (around 13.2 GW against 9.5 GW) [1].

When analyzing the countries, one after another, situation for photovoltaics differ substantially among them. This is due to different energy policies and public support programs for RES and especially for photovoltaics, as well as the varying grades of liberalization of domestic electricity markets. The distribution by countries of the global accumulated PV capacity, as for the end of the year 2010, can be observed in Figure 1.10.
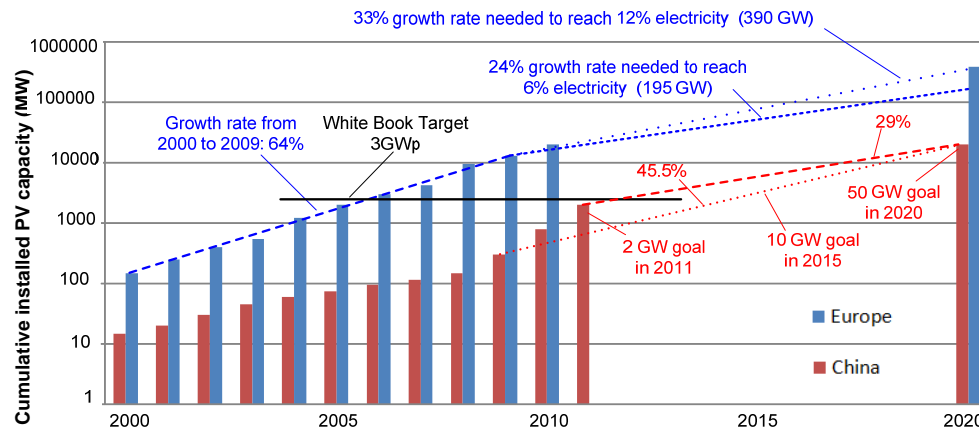
Figure 1.9 Cumulative installed photovoltaic capacities in the EU and Chine, estimates for 2010 and target for 2020. Source: [4]**.**

The first one to be highlighted is the worldwide leader on the PV domain: Germany. It installed by itself 7.4 GW, more PV capacity in 2010 than the entire world did the previous year. In this way, Germany culminated the year with an overall PV capacity of 17.3 GW, which provided 2.75 TWh of electricity during the first quarter of 2011 [16].

In a second place, it stands out Italy with 2.3 GW of new PV capacity added to the grid in 2010, bringing the total to nearly 3.5 GW and an even stronger impulse in 2011 which, according to official sources, elevated the connected to the grid in June to 5.8 GW [13].

In the third place, the Czech Republic profited of a high feed in tariffs policy to experience the second strongest year after the momentum registered in 2009. An overall of 1.5 GW were installed to accumulate around 2 GW which represent accomplishing the government prevision for 2020 according to the National Renewable Action Plan in only two years. It must be noted that this country accounted no PV capacity as far as in 2008 [13].

Apart from these three major actors in the European panorama, others can be cited including France, which added 0.7 GW in 2010 to achieve 1.05 GW in all, Belgium with 0.4 GW achieving 0.79 GW, and Greece which in spite of its economic problems installed almost 0.2 GW bringing its total capacity to about 205 MW, but which is not expected to evolve largely in the coming future due to restrictive changes in the regulations. The United Kingdom introduced in 2009 interesting feed-in tariffs for some months also which fostered the installation of around 55 MW (to a cumulative 85 MW) but these were reduced again in March 2011, what enables a new stagnation to be imagined.
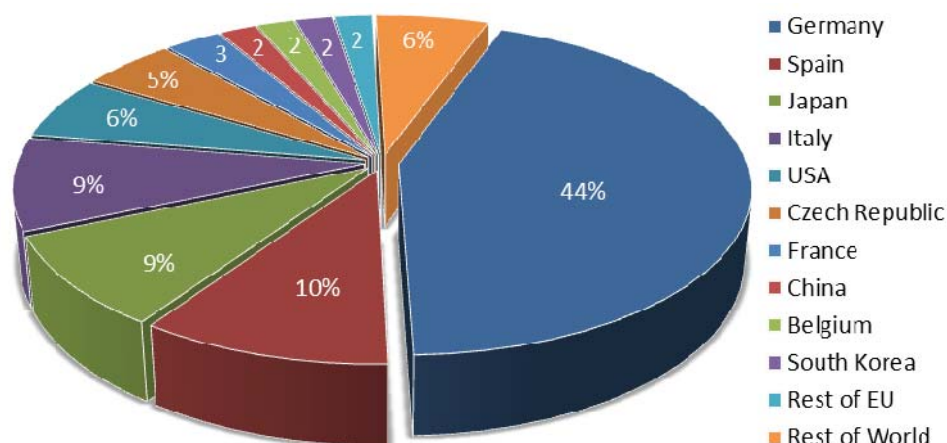
Figure 1.10 PV capacity worldwide installed till 2010 (Distribution by countries). Source: [1]**.**

Out of Europe, only North America and Asia have experienced a significant PV deployment. Regarding North America, the USA stands out in the first place. A PV capacity of close to 900 MW was installed across the United States of America in 2010, with the State of California taking the lead, to reach a cumulative PV capacity of 2.5 GW. Moreover, spectacular plans to install another 16.6 GW before 2014 are confirmed. With regard to the Canadian situation, the new feed-in tariffs approved in Ontario in 2009 promoted the installation of MW new PV systems in 2010, more than tripling its cumulative installed PV capacity to about 420 MW.

On the other hand, the Asia region, including some countries from the Pacific, is experiencing a very quick and large development of PV system installations. Countries such as Japan, China, India, South Korea and Australia show a very positive upward trend which has been clearly fostered by their governments' commitment.

The largest PV market in Asia has traditionally been Japan with 2.6 GW of installed capacity till the year 2009 which evolved to 3.6 in 2010 (a 1 GW increment). Moreover, after the nuclear accident in Fukushima the current government seems to be concerned on the need to push renewables up to the 20 % of the whole countries' production by 2020, including an ambitious plan for PV installations in the residential sector [13].

After Japan, China can be identified as the second market in Asia but everything suggests that it will be the first one in brief. The Chinese PV market grew around 600 MW in 2010, completing a cumulative installed capacity of about 1 GW. However, this only represents a 5 to 7 % of the total Chinese PV production. Therefore, they have the capability to easily

increase their PV production park with more than enough local resources and this situation is likely to change given that the National Energy Administration has recently doubled its capacity target to 10 GW in 2015 and further up to 50 GW in 2020, as it has already been stated in Figure 1.9.

In a third place, South Korea keeps being important in the PV market and installed 180 MW during 2010 which brought the cumulative capacity to a total of 705 MW. However, this is an amount similar to that of the previous year what suggests something is not going as expected. In fact, changes in regulation have slowed the evolution of PV installation in Korea and the signs are that the tendency is going to keep the same in 2011.

On the other hand, India has to be highlighted for showing the opposite trend. Although official estimates for PV systems installed in 2010 are only between 50 to 100 MW (being most of them off-grid installations) a new plan called "The Indian National Solar Mission" was launched at the beginning of 2010 to make India a global leader in solar energy and which envisages installing a solar generation capacity of 20 GW, focusing on the grid-connected market, by 2020. This plan is going to offer the first results in 2011 with 1 GW expected for 2013.

And finally, Australia is the new big incomer in the PV market. The pacific country experienced a 383 MW increase to achieve a cumulative capacity of 571 MW [17]. This boom in the PV integration in Australia has been supported, as for the rest of the countries, on a decided political concern about the development of renewables which is going to be kept, and even reinforced, in Australia in the coming years.

Apart from these countries, some interesting initiatives for the PV development and installation are being taken in other countries such as Thailand, Malaysia, Indonesia, Bangladesh, The Philippines and Vietnam. However, as for the case of India but with lower perspectives or ambitions, the midterm plans which are being settled to push forward renewable energies and the corresponding changes in regulations in these countries are too recent to already show important results. In this sense, none of these countries present yet a total capacity installed above 100 MW but this is to come for sure throughout 2011.

It is important to highlight at this point, and before concluding this section, the case of Spain. This is an especially important country for this Thesis work since all the study and the analysis performed is focused on a Spanish southern location.

The Spanish PV market has followed quite a peculiar development during the last 5 years mainly due to changes in the Spanish energy policy. The evolution of the Spanish PV market with both the annually installed PV capacity and the accumulated value can be observed in Figure 1.11.
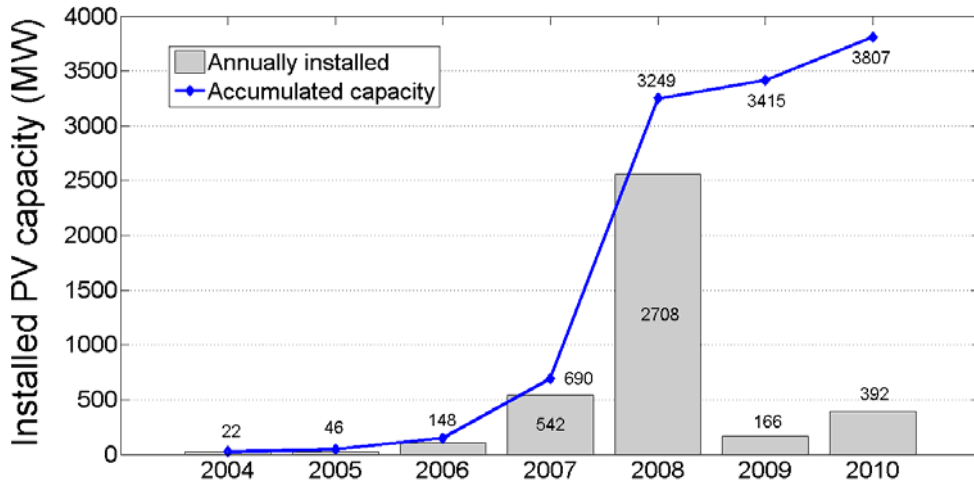
Figure 1.11 Evolution of the Spanish PV market. Source: MICyT.

In spite of the enormous solar resources existing in such a sunny country as it is Spain, it took some time to the PV industry to ingrain in Spain and it was not until August 2005 when, thanks to the already cited "Plan de Energías Renovables" (PER) approved by the Spanish Government, it started to experience a drastic market expansion. Among the targets defined in the plan, the PV technology was confirmed with a 500 MW objective already defined in the previous plans. However, the main reason for the expansion of the PV industry during the period 2006-2008 was that the new renewables plan was supported on generous feed-in tariffs, set one year before by the Real Decreto 436/2004 (Royal Decree dated 12 March 2004 [18]). These feed-in tariffs were so favorable that boosted the development of the PV market in that period in a drastic way (the PV capacity was brought from 22 MW to 690 MW in only two years). Then, since initial objectives of the plan were quickly approached (and even exceeded), the government approved a new Royal Decree in 2007 (the RD 661/2007, dated 25 May 2007 [19]) which established an increased PV capacity goal of only 1.2 GW. As a consequence of the already consolidated PV industry in Spain and its installation capacity at that moment on the one hand, and of the limited goal on the other hand, a race among industrials was triggered on to get permits to enter this quota and install multi-megawatt ground-mounted PV power plants which profited the favorable feed-in tariff. This

huge and quick development represented exceeding the quota limit in only one year, with an addition of 2.7 GW installed in 2008 to achieve a total cumulative PV capacity of 3.4 GW [20]. That year, Spain was the biggest PV market worldwide, as can be observed in Figure 1.8. This fact led to a new revision of the PV legislation in 2008. Thus, a new Royal Decree (the RD 1758/2008, dated 26 September 2008) was passed and it considerably reduced feed-in tariffs for new PV installations, limiting at the same time the annual PV capacity quota to a 500 MW amount. Moreover, out of this amount, two-thirds were assigned to rooftop mounted installations and could not be assigned to ground-mounted large scale systems. This new regulatory situation resulted in a PV installed capacity of about 150 MW in 2009. And in 2010, around 400 MW of new PV power plants were installed and the total PV capacity achieved in this way the 3.8 GW, what represents that Spain keeps being the second biggest market regarding the total cumulative installed PV capacity [14]. This second consecutive year with an activity well below the 2008 peak was mainly experienced as a consequence of the quota limit but also due to the uncertainties associated with the continuously changing regulatory framework. In fact, during the year 2010, the Spanish Government passed two new Royal Decrees (RD 1565/2010, dated 19 November 2010 and RD-Law 14/2010, dated 23 December 2010) which modified the policy on renewables once again in such a way that the new framework basically allows only the development of the roof-top PV market. On the one hand, the first of these RDs established limits on the validity of the feed-in tariffs to 28 years while, on the other hand, the RD-Law reduced the tariffs, mainly for ground-mounted installations, by 10% and 30% until 2014 [13]. This reduction is done in this case using the mechanism of introducing a limit on the number of hours for which the producer will receive the full tariff each year till 2014. From that year onwards, this limit will be set according to the geographical location of the PV power plant [14].

Then, according to this new regulatory framework, current tariffs for new projects are:

- 0.289 €/kWh for building-integrated & roof-top installations under 20 kWp.
- 0.204 €/kWh for building-integrated & roof-top installations from 20 kWp to 2 MW.
- 0.135 €/kWh for ground-mounted installations of up to 10 MW.

Moreover, since these regulations are retroactive all the capacity installed in previous years is involved, what has led the Spanish Solar Industry Association (ASIF) [20] to announce taking legal actions against them. As can be understood, the future remains unclear for Spain under a regulatory framework as the currently defined by these RDs.

To conclude with this section, it is to be highlighted that the vast majority of the installed PV capacity today is grid-connected, with the off-grid sector accounting for a declining share with each passing year (6% of the demand in 2008, 5% in 2009 and around the 3% in 2010) [21]. Therefore, if the present installation trends and the plans of expansion for the PV technology in different countries are confirmed and consolidated, the PV power is going to be a key agent in the electric power systems in many of these countries in the near future. Therefore, electricity markets and the regulations driving the technical connection of renewables will have to be probably adapted in order to cope with all this incoming power while making the operation of the system viable. This is the reason why, the Spanish EPS and its associated electricity markets, as target electric system and electricity market for the analysis performed in this Thesis work, are reviewed in the following section.

1.3. Spanish electric power system & the associated electricity market.

Electric power systems and electricity markets present very different characteristics around the world. Their configuration and structure strongly depends on the generation mix that these contained and in the number of different agents participating in the market. As far as this Thesis work is concerned, only the Spanish electric power system and its associated electricity market are of interest. Therefore, a short description of these two structures is presented in the following.

1.3.1. Spanish electric power system.

After the approval of the Law 54/1997 for the Electricity Sector [6], which established the liberalization of the sector, the power production in Spain is an activity that any company can undertake in order to participate in the competitive electricity market. In this sense, any new power generator entering the system is classified within some of the two following groups: those which form the so-called Ordinary Regime and those forming the so-called Special Regime. These groups are defined as and include the following technologies:

- Ordinary Regime: It is simply defined as the electricity generated by all those facilities which are not classified within the Special Regime. These include conventional technologies such as coal, fuel oil, natural gas, combined cycle and nuclear [9].

- Special Regime: It is defined as the group of electrical energy producers which falls under a unique economic regime established by the Royal Decree RD 661/2007 [19],

consisting of facilities with installed power not exceeding 50 MW and whose production is originated according to any of the four groups or categories identified in that Royal Decree [9]. These are:

o Group a) for cogeneration (CHP) or other forms of electricity generation associated with non-electrical activities (profiting residual energies), always involving an a high energy-efficiency.

o Group b), is the largest one and contains different types of generators that use renewable non-consumable energies such as mini-hydro, wind, solar PV, biomass, geothermal, biogas or any type of biofuel as a primary energy source…

o Group c) for plants which use non-renewable or agricultural waste, livestock, urban and service sector waste as primary energy sources, with energy recovery entailing a high energy yield and not included in category b). Their installed power lower is limited to 25 MW.

o Group d) for treatment and waste reduction.

The economic regime settled by the RD 661/2007 allows these facilities selling their production at a supported sales price which consists of either assigning a fix price per unit of energy produced (different for each technology) or offering a premium which is added to the market price for facilities that choose negotiating their production in the spot markets. The selected option normally depends on the dispatchability of the plant. If the power production can be anticipated and dispatched, the power plant operator will usually access electricity markets because higher revenues can be achieved with the market price plus the premium. On the contrary, the supported fix price option will be the solution for intermittent power plants whose production cannot be assured in advance and is much affected by external factors such meteorological conditions.

Although the Spanish electricity generation mix and final consumption share were already introduced in Figure 1.6 and Figure 1.7 respectively, more precise figures for each of them are presented in Table 1.1. Moreover, capacity and production figures are categorized for each technology according to the just introduced production groups, what allows getting a precise idea of the current importance of both groups in the Spanish electric power system. The annual increment from 2009 to 2010, registered for each of the technologies can be also observed. This information can be consulted every year in the power system annual report published by the Spanish system operator [9].

	Installed capacity		Generated energy	
	MW	% 10/09	GWh	% 10/09
Hydraulic	17561	0,0	38653	62
Nuclear	7777	0,8	61990	17,5
Coal	11380	0,2	22097	-34,7
Fuel/gas	2860	-4,9	1825	-12,4
Combined cycle	25235	9,4	64604	-17,5
Total ordinary regime	**64813**	**3,4**	**189169**	**-0,9**
Hydraulic	1991	0,5	6811	24,4
Eolic	20057	5,8	43355	15,9
PV solar	3458	13,3	6027	2,2
Thermoelectric solar power	682	141,6	692	569,5
Other renewables	1050	5,1	4981	6,2
Non renewables	6992	6,2	29036	8,4
Total special regime	**34230**	**7,4**	**90903**	**13,1**
Total	99043	4,7	273399	3,5

Table 1.1 Spain electricity production at the end of 2010. Distribution by technologies.

To conclude this section, it must be pointed out that all these different power generation systems, together with the transport network and part of the distribution network (both used to make the energy demanded by the users arrive from the places where the generators produced it), are managed in Spain by the Spanish system operator (Red Eléctrica de España, REE). This company, which is partially public, not only manages the electric energy transport but also owns much of the high voltage transport grid. Once the configuration of the electric power system has been introduced, its associated market can be described.

1.3.2. Spanish electricity market.

Conversely to the electric power system with its technical issues, the electricity market in Spain is operated by the company "Operador del Mercado Eléctrico" (OMEL) which is being transformed now into a new company called "Operador del Mercado Ibérico de la Electricidad" (OMIE) which includes the management of the Spanish and the Portuguese electricity markets, the recently integrated Iberian market.

a) Organization of the electricity market.

Following the liberalization of the electricity sector started with the already cited Law 54/1997, the Spanish peninsular system has developed a competitive power production market similar to that of other countries. It is structured in different markets which can be

appreciated in Figure 1.12. Some of them are managed by OMEL: the daily or dayahead market and the six intraday markets. Some others regarding technical operating issues are managed by REE: the operational restrictions market, the ancillary services market and the balancing markets. Finally, the spot markets which anticipate future production and where supply contracts are negotiated (forward markets) are managed by other companies and utilities such as Endesa, Comisión Nacional de la Energía (CNE) or The Iberian Energy Derivatives Exchange (OMIP).
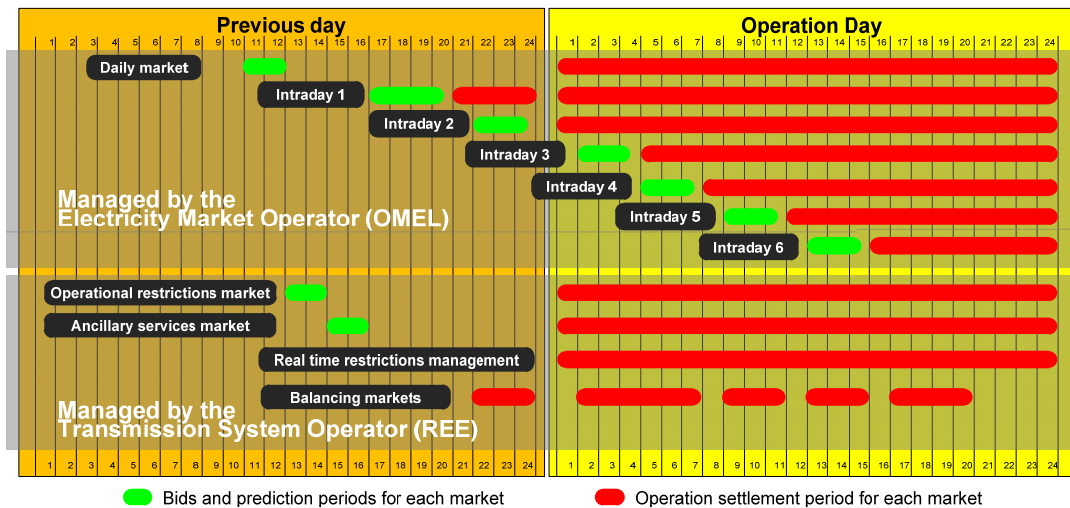
Figure 1.12 Iberian Electricity Market (MIBEL) temporal sequence. Source: [22]**.**

Among the different markets, the daily market is the most important one since it is there where the power transactions for the coming day take place. This power exchange, also known as pool market, conducts auctions for generators seeking to sell energy to serve consumers which offer energy purchase bids. The power exchange process is organized by matching the bids for sale and purchase starting from the cheapest offer until demand is matched in each programming period (for each hour). This process determines the market clearing prices or marginal price (price at which the purchase and sell offers do cross each other), and those generator units which have bid below the clearing price are scheduled for generation (known as 'merit order' or power commitment). The matching process and the final result offered by OMEL can be appreciated in Figure 1.13.
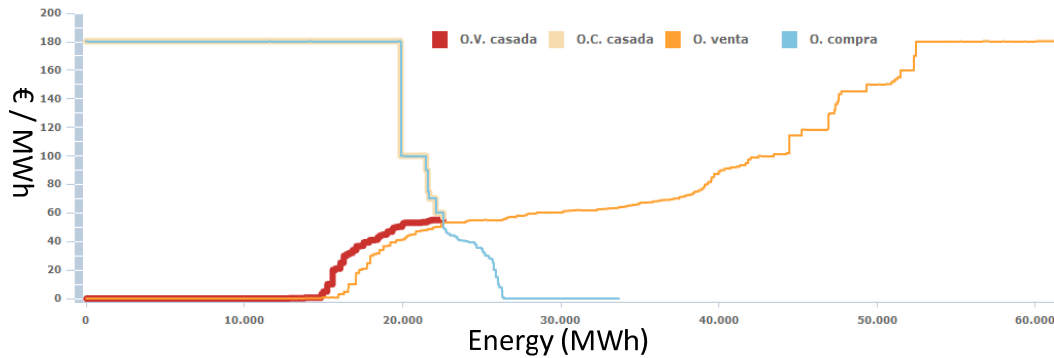
Figure 1.13 Process of matching the bids for sale and purchase of electricity. Source: OMEL.

The resulting production program is only a first adjustment between the supply and the demand but performed one day in advance. To cope with possible deviations in the daily schedule coming from the generation (generator unexpected unavailability) or from the demand side (consumption prediction error), six intraday market sessions are organized. The timing for these markets can be also observed in Figure 1.12. During their corresponding bid and prediction period, new energy offers for sale and purchase can be accepted to adapt the operation to any new situations which may arise [23]. Note that this structure existing in Spain based on six intraday markets is unique and most of the countries present a continuous electricity market with real time recalculations and balance operations. Moreover, it must be pointed out that recent news indicate that the OMEL has proposed to the Spanish Ministry of Industry a restructuration of the system which would involve the following main changes:

- The existence of eight intraday markets (one every three hours), instead of six.

- The reduction of the time gap between the final of the negotiation (bids and prediction) period and the beginning of the operation settlement period (OSP) from the current 2:15h to 1:10h for each of the eight intraday markets.

Apart from the organized markets, producers and consumers also have the possibility to conclude individual bilateral contracts, although these are not the majority in Spain as they are in other countries such as Germany. The resulting daily market schedule together with the bilateral agreements allows setting the so-called operation daily program (PDBF), which defines hourly the energy sales and acquisitions.

It must be pointed out that the ultimate function of the EPS is to supply electric energy, obtained from power generators, to the customers via the transmission and distribution

(T&D) system. To ensure this goal compliance and support the delivery of electricity from seller to purchaser with the security, reliability and certain quality requirements of the power supply, the system operator provides a series of system adjustment services which enable to change the production schedule in the short time [22]. These services can be multiple and depend on the EPS operator and the regulatory framework for each country. As an example, the following Table 1.2 presents a list of adjustment services and their common definitions according to the Federal Energy Regulatory Commission (USA).

1. System Control	Scheduling generation and transactions ahead of time, and controlling some generation in real time to maintain generation/load balance.
2. Reactive Supply & Voltage Control	The generation or absorption of reactive power from generators to maintain transmission system voltages within required ranges.
3. Regulation	Minute-by-minute generation/load balance within a control area to meet EPS standards.
4. Spinning Reserve	Generation capacity that is on-line but unloaded and that can respond within 10 minutes to compensate for generation or transmission outages. "Frequency-responsive" spinning reserve responds within 10 seconds to maintain system frequency.
5. Supplemental Reserve	Generation capacity that may be off-line or curtailable load that can respond within 10 minutes to compensate for generation or transmission outages.
6. Energy Imbalance	Correcting for mismatches between actual and scheduled transactions on an hourly basis.
7. Load Following	Use of online generation equipment to track the intra- and inter-hour changes in customer loads
8. Backup Supply	Generation available within an hour, for backing up reserves or for commercial transactions.
9. Real Power Loss Replacement	Generation that compensates for losses in the T&D system.
10. Dynamic Scheduling	Real-time control to electronically transfer either a generator's output or a customer's load from one control area to another.
11. Black Start	Ability of a power source to go from a shutdown condition to an operating condition, energizing part of a grid, without outside assistance after a blackout occurs.
12. Network Stability	Real-time response to system

Table 1.2 List of ancillary services in the USA and their common definitions.

For the case of Spain, the system adjustment services are, according to the Spanish Royal Decree RD 1454/2005 [24], grouped in three main categories: the real time restrictions management, the deviations management in the balancing markets and the ancillary services.

I. The <u>restrictions management</u> must be supported by all the generators taking part in the market according to that defined in the system operator operational procedure P.O. 3.2. It consists of different resolution processes distinguished according to their time horizon:

    o   technical constraints that may arise in the PDBF.

    o   technical constraints that may arise in the updated programs resulting from the different intraday markets.

    o   technical constraints that may arise during real time operation.

    After incorporating the required modifications, to solve the PDBF technical constraints, the daily provisional viable production program (PDVP) is obtained.

II. The <u>ancillary services</u> correspond in the Spanish electricity market to the operations performed in order to cooperate with the frequency and voltage regulation of the grid. The spinning reserve is divided in two categories: fast response and conventional.

    o   Fast response spinning reserve: the power capacity must be kept in a state of 'hot standby' so it can respond to network abnormalities in seconds. Power generators included in this group contribute to the EPS *primary reserve*. Thus, these are power sources kept online and synchronized to the grid that can increase their output immediately responding to a major generator or transmission outage and can reach full output within 10 minutes). This service is usually defined by the system operator regulations in each country. In Spain, it is defined by the REE operating procedure P.O. 7.1 [25].

    o   Conventional spinning reserve: the power capacity requires a slower response time of approximately 5 - 15 minutes. Power generators included in this group contribute to the EPS *secondary and tertiary reserves*. The secondary reserve is the same as the primary but does not need to respond immediately; therefore units can be offline but still must be capable of reaching full output within the required 10 minutes. The tertiary reserve is the same as secondary, but with a 30-minute response time, and it is used to restore primary and secondary reserves to pre-contingency status. These services are defined in Spain by the system operator operating procedures 7.2 [26] and 7.3 [27], respectively.

Ancillary services are completed in Spain with the grid voltage control, regulated by the P.O. 7.4 [28] and the black start capability, which will be regulated in brief by the P.O. 7.5 (still under development).

III. The <u>deviations management</u> in the balancing markets is a process indispensable to ensure the balance between production and demand in between intraday markets while guaranteeing the availability of the regulatory reserves at any moment.

Finally, regarding the costs incorporated by the system adjustment services, these are calculated according to the operational procedure P.O.14.4 which sets the procedure to determine the payment obligations or collection rights. In addition, this operational procedure indicates how to calculate the measured deviations (difference between the energy measured at the power plant bars and that scheduled in the market) and which also generate both collection rights and payment obligations [23]. Figure 1.14 compiles the contribution to the electricity final average price in 2010 of the different processes.

Precio (€/MWh)	E	F	M	A	M	J	J	A	S	O	N	D	Total
Mercado diario	32,14	29,66	21,08	28,88	38,05	40,96	43,56	43,85	47,52	43,71	42,75	48,37	38,37
Restric. técnicas PBF	3,12	2,46	3,95	1,95	1,49	1,19	2,33	2,62	1,89	2,17	2,32	1,81	2,30
Mercado intradiario	-0,03	-0,02	-0,02	0,00	-0,01	-0,01	-0,01	-0,01	-0,03	-0,07	-0,03	-0,04	-0,02
Banda de regulación	1,03	0,98	0,99	0,47	0,54	0,43	0,34	0,42	0,51	0,84	0,82	0,93	0,70
Restric. técnicas T. Real	0,36	0,21	0,40	0,18	0,18	0,09	0,22	0,16	0,24	0,51	0,28	0,28	0,26
Desvíos	0,68	0,37	0,45	0,60	0,42	0,65	0,23	0,29	0,61	0,86	0,83	0,83	0,57
Excedente desvíos	0,32	0,25	0,13	-0,24	-0,15	-0,24	-0,09	-0,08	-0,17	-0,20	-0,04	-0,16	-0,05
Pagos por capacidad	4,11	4,14	3,44	3,23	1,98	2,88	3,62	1,33	2,15	1,95	2,92	3,92	3,00

Figure 1.14 Electricity final average price components in 2010. Source: [9]**.**

Therefore, this is the electricity market structure in which RES must be fitted. Different solutions can be adopted as it is explained in the following.

b) Renewables within the electricity market.

The treatment received by renewables within electricity markets around the world is very diverse. Spain has traditionally presented the scheme commonly called of "feed-in tariffs", the same set in countries like Germany and Denmark. As previously described, this is based on supporting a sales price for electricity coming from renewables or, as it is called in the Spanish regulations, any producer included within the Special Regime. The support to this sales price consists of either assigning a fix price per unit of energy produced (different for each technology) or offering a premium which is added to the market price for facilities that pretend to trade their production in the spot markets. Low power technologies usually choose to ascribe the production fix price system. Conversely, some technologies such as wind

power or medium size CHP participate in the spot market, profiting the premium which complements the market clearing or marginal price.

This scheme has drawn successful scenarios for the renewable energy deployment in those countries where it has been implemented. This feed-in tariffs and premiums system is justified by the strategic and environmental benefits of renewable energy and aim to ensure a reasonable return on investment while learning curves and economies of scale are putting the different technologies in top condition to fight, side by side, with conventional sources.

The feed-in tariffs' system for Special Regime generators (with its already cited different subgroups) was firstly organized by the already cited RD 436/2004, which was substituted later on by the also cited RD 661/2007. However, new regulations have modified the premium levels established by the RD 661/2007 for certain technologies, as it is the case already described in Section 0 for PV. Therefore, the energy policy towards this technology has not been certainly stable, what introduces doubts on investors and has influenced on its evolution deceleration.

For the economic viability of the proposal defined in this Thesis work, that of integrating ESS into PV power plants to achieve a controlled and constant production, the PV regulatory framework should be corrected again. If PV production can be guaranteed to be constant with a high liability, these power plants could also participate in the electricity markets. Thus, these could profit the variations in the hourly price of the electricity to achieve an economic income optimization. Moreover, due to production forecasting problems, PV power will very probably require to attend all the intraday markets. In this sense, the proposal from OMEL to introduce two new intraday markets and reduce the time gap between programming and operation periods would facilitate the market participation for these extremely stochastic power plants. An option which would help reducing PV deviations from its power commitments and, hence, reducing the economic penalties.

Finally, it seems essential that the income obtained by PV power plants with ES in the spot market would have to be also complemented by a premium, offered to PV installations as the one the regulatory frame already fixes for wind power or CHPs. A thorough discussion must be started in this regard. If a higher integration of this technology is desired, PV systems will compulsory have to improve their production predictability to avoid high system unbalances. In this sense, if PV plants can grant a constant hourly production thanks to the ESS integration, these can be considered as almost dispatchable power plants which

participate in the market in a similar way to that of conventional generators. This would solve the integration problem and the PV technology could assume an important share of the production. Therefore, a proper energy policy which set increased premiums for controllable PV production, making it economically viable, should be established.

1.4. Contribution of energy storage to the integration: applications of energy storage systems.

ES technologies development and implementation stands out as one of the most promising solutions to help solving the issue related to the capacity of the EPS to integrate a higher degree of penetration of RES in general and PV systems in particular. As it has already been anticipated along this chapter, the introduction of a certain amount of ES into PV power plants would make possible to control the PV production. Thus, PV power plants would not be any more a problem for the EPS from the energy balancing point of view. The increment in the power plant cost due to the ESS integration should be compensated by a new regulatory framework more beneficial for this kind of power plants. An increase in the economic compensations could be justified by many reasons: energetic independence of the country, improved share of renewables with the corresponding environmental benefits, a higher controllability of the system thanks to the presence of storage, etc…

Different ES technologies can be found worldwide nowadays with varying degrees of development, energy and power ratings and special characteristics. These are presented in detail along the Chapter III introducing some examples of installations for each technology.

As a function of the ES technology features, there are many different applications or functionalities which can be identified for them. Some of these, compiled from different publications, are enumerated in Table 1.3 where these are gradually classified as a function of the time these require the ESS to provide energy for accomplishing the desired service.

However, among the extensive list of possible specific functionalities for which ESS can be used, some are highlighted by most of the authors [29-32] and can be classified into three main groups [33, 34]: grid system applications, customer/end-use applications and renewables applications. These three groups, which are explained in detail below, cluster the possible ESS applications depending on their possible beneficiary.

Storage Capacity	Energy Storage Features
Transient (microseconds)	Voltage sags compensation Ride through capability during disturbances (backup systems) Regenerate electrical motors Improve harmonic distortion and power quality
Very short term (cycles of the grid frequency)	Cover load during startup and synchronization of backup generators Compensate transient response of renewable-based electronic converters Increase system reliability during fault management Keep computer and telecommunication systems alive for safe electronic data backup
Short term (minutes)	Cover load during short-term load peaks Smooth renewable energy deficits for online capture of wind or solar power Decrease needs of startup backup generator Improve maintenance needs of fossil fuel-based generators Allow ride-through of critical medical, safety, and financial procedures
Medium term (a few hours)	Store renewable energy surplus to be used at a later time Compensate for load-leveling policies Allow stored energy to be negotiated on net-metering basis Integrate surplus energy with thermal systems
Long term (several hours to a couple of days)	Store renewable energy for compensation of weather-based changes Provide reduction in fuel consumption and decrease waste of renewable energy Possible elimination of fossil fuel-based generator backup Require civil constructions for hydro and air systems Produce hydrogen from renewable sources
Planning (weeks to months)	Concern large power storage systems, such as pumped hydro and compressed air systems Use of fossil fuel storage to offset economic fluctuations Store hydrogen from biomass or renewable-based systems

Table 1.3   Possible uses and applications for ES systems.

1.4.1. Grid level applications.

The first group establishes what applications or functionalities can be found for ESS at the grid level. Most of them are well known and have been considered for long [35], although factors such as the ES technologies state of development or their corresponding costs have limited their introduction for practical large scale applications [30, 31, 36].

a) Energy arbitrage

Energy arbitrage involves the purchase of inexpensive electricity available during periods of low electricity demand (cheap energy), to charge the ESS, so that the low priced energy can be used or sold at a later time when the price for electricity is high earning in this way an economical profit. This activity can also be used to influence in the demand side, by using higher peak prices to induce a reduction in peak demand through demand charges, real-time pricing, or other market measures.

As an example, the Irish and Australian electricity markets which trade on spot market organized in 30 minutes trading periods, assigning a unique cost for the unit of electricity

generated (€/MWh) in that period [37-39]. This price can vary significantly over a 24-hour period due to the relative change in electricity demand. It is stated in [40] that the average electricity price on the Irish electricity market in 2009 at 18:30h was approximately 300% the average electricity price at 04:00h. Similar figures can be found in the Spanish electricity markets, operated by OMEL (Operador del Mercado Eléctrico) who recently reported that the difference between maximum and the minimum electricity prices was over 30 €/MWh in the 56.7% of the days during the last 12 months period under analysis (May'10-April'11) [41]. These variations respond to the big differences in demand that can be appreciated in the Spanish daily aggregated load curve, represented with the orange line in Figure 1.15, together with the price variation in the Iberian electricity market along one winter day. These data can be obtained from the Iberian market operator, "Operador del Mercado Eléctrico" (OMEL). Thus, the range for potential economic benefits with this application seems important.
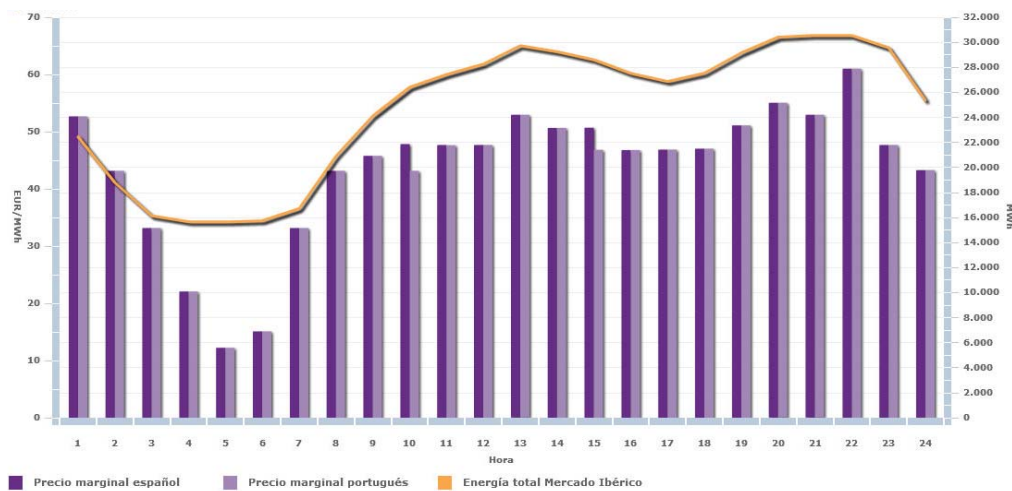
Figure 1.15 Load demand and electricity prices evolution along one day in the Iberian market.

b) Distribution networks support

ESS may be used to improve distribution networks performance by compensating for electrical anomalies or disturbances and stabilizing the system after a fault occurs on the network. This can be achieved by absorbing or delivering power (active or reactive) when needed to keep generators connected and turning at the same speed. The different unexpected faults induce anomalies such as voltage sags, voltage and frequency irregularities, phase shifts and presence of sub-synchronous resonances that can be corrected by the ESS.

Consequently, fast response and high power ratings are essential for this application. The result is a more stable system with improved performance (throughput).

Table 1.4 establishes different ways in which ESS can provide such a network support.

Transmission Stability Damping	Increase load carrying capacity by improving dynamic stability.
Sub-Synchronous Resonance Damping	Increase line capacity by allowing higher levels of series compensation by providing active and/or reactive power modulation at sub-synchronous resonance modal frequencies.
Voltage Control and Stability	1. Transient Voltage Dip Improvement Increase load carrying capacity by reducing the voltage dip which follows a system disturbance. 2. Dynamic Voltage Stability Improve transfer capability by improving voltage stability.
Under-frequency Load Shedding Reduction	Reduce load shedding needed to manage under-frequency conditions which occur during large system disturbances.

Table 1.4 Various types of transmission and distribution support. Extracted from [33]

c) Load Management

Apart from helping to stabilize the distribution system, ESS can cooperate to reduce the distribution network capacity requirements by managing the load and thus avoiding distribution congestions during peak hours.

Typically, the distribution network is built to handle the maximum load required at any moment and hence they are most of the time only loaded in part. However, since load demand is growing faster than the distribution networks installed capacity is usually enlarged, congestion occurs more and more frequently, mainly during peak demand hours.

ESS can avoid this overcharge phenomenon by the "Load Leveling" and "Peak Shaving" mechanisms, Figure 1.16. These involve storing low-priced off-peak electric energy and then discharging it during the peak demand hours. In this way, the load on the distribution network can be reduced. Both actions, load leveling and peak shaving are similar. These only differ on the degree of energy shifted and, hence, on the ESS energy capacity they require. Thus, ESS can provide, by means of these two load management mechanism, another service to the grid known as distribution network "Congestion Relief", which is somehow complementary with the energy arbitrage application.
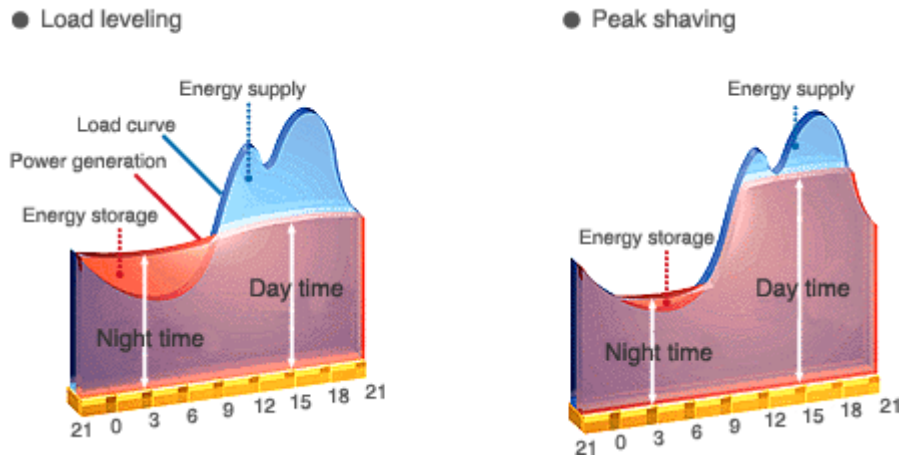
Figure 1.16 Load leveling and peak shaving energy management mechanisms.

Source: NGK Insulators Ltd. web site.

In the same way, if the distribution network capacity is not exceeded thanks to the introduction of ESS and the load managing functionalities, upgrades can be avoided or deferred. These upgrades are usually separated by decades and must be built when necessary to accommodate likely load and generating expansions. Consequently, ESS could be used instead of upgrading the distribution network till the moment when it becomes economical to do so; that is, it allows delaying utility investments in distribution systems by using relatively small amounts of optimally located ESS. Therefore, apart from favoring a further use of the utility assets and helping reduce the investment financial risk, the ESS introduction would be much more economical than the large capital investments always associated to the development of new distribution network infrastructures. Note for example that the costs to build and upgrade distribution network infrastructures in areas with high intermittent RES potential is estimated between $200 and $1000 per kW [31, 42-44]. On the other hand, the value of deferring distribution network would have an estimated benefit of approximately $500 per kW, and could be as high as $1200 per kW if the energy can be transported to shave peak loads at different locations [31, 34]. This extended service, included within load leveling application advantages, is also known as distribution network "Upgrade Deferral".

A similar mechanism also included within load management is the "Load Following". It consists on the ESS acting as a sink when demand falls below production levels and acting as a source when demand is above production levels. Therefore, the storage can be used to maintain ancillary services and reserve on the electricity grid.

ESS for load management usually require power ratings ranging from the kW scale to several hundreds of megawatts along with a storage capacity of 1 to 3 hours and fast response times [45]. New technologies, which are not restricted by geographic limitations, have already been proposed as suitable for large scale load leveling [46, 47].

d) Central Generation Capacity Optimization

This functionality is extremely related to the previous one. Thanks to load managing actions, ES could be used to defer and/or to reduce the need to negotiate new generation capacity in the wholesale electricity marketplace under certain circumstances of the EPS operation. Instead of adding inefficient and expensive centralized power plants normally "on the margin" which would be connected to the EPS exclusively, when the system risks a blackout, ESS could be used. In this sense, the peaking capacity costs would be somewhat reduced. This application would require the system operators to grant access to the electric system's "wires" (transmission and distribution power lines) to distributed ES suppliers.

1.4.2. Customer / End-use applications.

Apart from functionalities and applications for improving the grid operation and functioning, a second group clusters all those ESS applications which could help energy customers to improve their power supply, both technically and economically. Depending on the author, these applications can get different names.

a) Demand Side Management (DSM)

DSM involves actions that encourage end-users to modify their level and pattern of energy usage to reduce both energy consumption (during peak hours) and peak power demands (at any moment) reducing their overall costs for electricity. These actions are very similar to the load management grid applications, although these are exclusively focused on energy customers. Somehow, this DSM application is also similar to arbitrage though electricity prices are here based on the customer's tariff whereas the price for electricity in grid level energy arbitrage at any given time is that prevailing in the wholesale market. An example of DSM application using batteries in parallel with a PV power plant can be found in [48].

In general, the two possible DSM actions regarding customer habits are: to try to distribute the energy consumption regularly on the one hand and to avoid big differences in

the power demand along the time to optimize network utilization on the other hand, Figure 1.17. These actions are supported by the following mechanisms:

- The Time-of-Use Energy Cost Management – It involves the end-user to charge the ESS during off-peak time periods when the electricity price is low, to then discharge it during times when on-peak energy prices apply. The energy bill is in this way reduced for the installation.

- The Power Demand Charges Management – This second mechanism for grid customers involves using the ESS in order to reduce the overall costs for electric service by reducing its on-peak power needs; i.e. avoiding extra demand charges associated with a given kW of peak load. Thus, customers must avoid using power during peak demand periods, which are the times when demand charges apply, or exceeding certain power demand limits (according to the contract established with the energy provider). It is normally set up that, if large loads exceed the power limit for just one 15 minute period along the month, a peak demand charges is applied for the whole month bill. Then, the stored energy can be used to supply some loads during those periods when demand charges apply or to avoid exceeding that certain power demand limit which would increment the overall cost.

Typically, although depending on provisions of the applicable tariff, ESS should operate for five to six hours in this application.

Currently, many countries are promoting the use of DSM as a tool for facilitating the integration of RES, using similar principals with ESS and providing certain specific tariffs [49]. Therefore, as smart networks become more advanced, it must be pointed out that DSM, either with or instead of ES, could become a realistic alternative [50].

As can be easily deduced and although each circumstance is different, the use of ESS for DSM is compatible with some other end-use functionalities such as the energy arbitrage or, even, ancillary services which could provide benefits to customers if they were allowed to participate in the wholesale energy marketplace as small energy producers. In fact, DSM can facilitate a reduction in the amount of ES capacity required in other grid applications to improve the EPS.
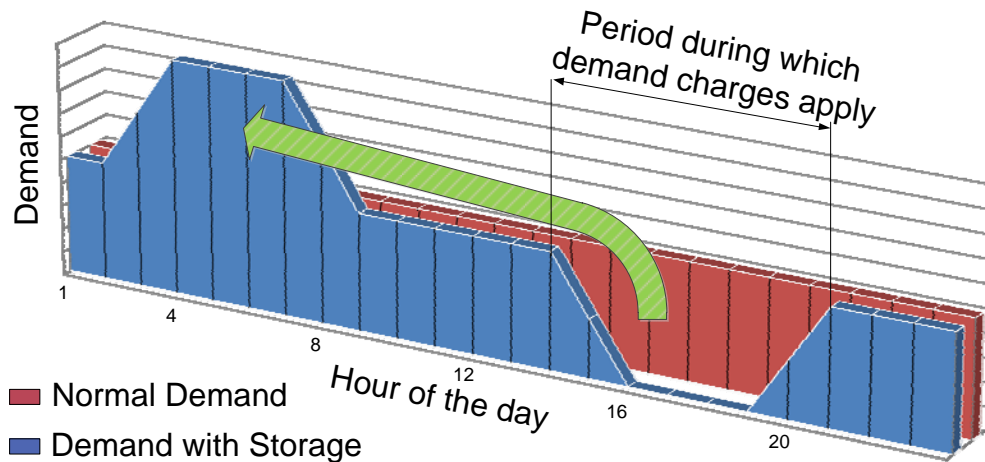
Figure 1.17 On-peak Demand-Charge Reduction using Energy Storage.

b) Electric service reliability (back up)

The electric service reliability application entails use of the ESS to provide highly reliable electric service; that is, using the ESS as an uninterruptable power supply (UPS), except for the fact that the units must have longer ES capacities (energy back up systems). In the event of a complete power outage lasting more than a few seconds the ESS will provide enough energy so as to guarantee one of the three following actions:

- ride through outages of extended duration (ride through capability) maintaining generation units connected to the grid during the system disturbance

- proceed with a complete and orderly shutdown of the loads.

- transfer to on-site alternative generation resources.

Depending on the option selected by the end-use customer, the energy capacity requirements of the ESS will vary. If an orderly shutdown is the objective, then discharge duration may be an hour or more. If the goal is to transfer supply to another generation device, a few minutes of discharge duration is needed. In any case, ES units used for this application must yield power with sufficient quality and reliability.

c) Power conditioning and supply continuity

This functionality involves the use of ESS to protect downstream loads against short duration events taking place in the grid which can affect the continuity and condition of the power delivered to the load. Some manifestations of these phenomena include:

- variations in voltage profile (e.g. short-term spikes or dips, longer-term surges or sags, short blackouts, flicker).

- variations in the frequency at which power is delivered.

- low power factor (voltage and current excessively out of phase with each other).

- interruptions in service, of any duration, from a fraction of a second to minutes.

Traditionally, UPS units have been used for this type of applications, used on sensitive processing equipment and thus with required capacities usually under 10 MW. Furthermore, the discharge duration time required for any power and supply quality application ranges from a few seconds to about one minute. Thus, development of short-term and fast response times ESS could help to provide end-users immunity against these phenomena, even substituting UPS units and offering local voltage and frequency control or support, or ride-through capability.

1.4.3. Applications associated to RES.

These are a series of arising applications associated to ESS which involve granting some extended functionalities to RES thanks to the combined installation of both technologies. In fact, contrary to the situation for grid applications which have not pushed ES technologies development for many years, the ESS application to cooperate with renewables operation is a very promising market which is expected to experience a great development in the coming years, hand in hand with the RES expansion. In fact, this has been, together with the new future transport applications associated to the electric vehicle, the two main factors for the great research effort being performed on some among the different ES technologies reviewed in Chapter III during the last years [30, 31].

a) Ancillary services provided by renewables with ES

The first application which deserves to be highlighted is that, thanks to the introduction of different ES technologies within intermittent RES, these will be able to cooperate with the grid operation by providing some ancillary services and maybe being even used as baseload power plants in the coming future.

Classical power generators have traditionally provided these services and system operators have not forced new DG suppliers and RES to offer them till recently, allowing these power generators to focus on selling as much energy as possible. However, with the

continuous increase in the penetration of RES, the need for these ancillary services is growing and operators have already started to ask large scale RES power plants (wind farms) to cooperate with some of these services. It is well known nowadays that ESS can help renewables to provide some of these ancillary services [29, 35], pointing out that ESS implemented must be reliable and capable to provide a rapid start-up and a good ramping behavior [33].

Thus, electricity markets must evolve and system operators should create competitive scenarios modifying grid codes and market regulations to push RES with ES to cooperate in the power system operation. In fact some of the ES technologies have already started to provide this kind of services, with others planning to compete in this field in the near future thanks to their great responsiveness. It is the case for Compressed Air or Pumped-hydro ES facilities which are capable to come to full power within 10 minutes or even less, whereas natural gas turbines can require 25 minutes and combined cycles 45 minutes in some cases. Other smaller ES units could also offer services at a local level, providing voltage control and energy balancing. Therefore, not only conventional generators and large scale traditional ESS will be able to provide ancillary services, but also low and medium scale intermittent power plants with ES could participate on each of them in the following way:

I. <u>Frequency control as spinning reserve:</u> most of the ES technologies are connected to the grid by means of power converters, which can facilitate the participation in the grid frequency control of RES power plants with ES. These can act as spinning reserve units by exchanging the accumulated energy with the grid when needed [51, 52]. This is an application which has been a renewables' aspiration for more than 30 years [53], although it has not been possible to the moment without the ES technologies support.

Application of ESS in this domain includes transient grid-frequency stability support. To contribute to the frequency stabilization during short transients, a functionality called grid angular stability (GAS) in [29, 54], low or medium capacity ESS are needed because the GAS operation consists of injection and absorption of active power during short periods of time, 1–2 s. This application contributes, for example, to the frequency stability of isolated utilities based on diesel generators [52, 55]. In the same way, low and medium capacity ESS would be needed by RES to participate in the frequency primary control, or frequency stability, operating as fast response spinning reserve or emulating the inertia of the synchronous generators in conventional power plants. This could be achieved, for example in Spain, with an ES consisting on power capacity levels of only 1.5 % of the

RES power plant rated power and energy capacities large enough so as to provide this amount of power for up to 15 min (values currently established for conventional generators within the Spanish operating procedures according with the relative weight of the Spanish electric system within the UCTE - Union for the Coordination of the Transmission of Electricity in Europe [56]). As an alternative solution, the frequency primary control or the inertia emulation could also be provided by RES by forcing their power converters to operate below their optimal power production point, presenting in this way the possibility to increase "instantaneously" their production in case of need. The problem with this operation mode is that it penalizes the energy production of the RES [57]. Finally, a third option for this application could be to also allow the RES to overcharge for a period of time with this 1,5 % rated extra power, although this strategy risks the equipment lifespan. As for the rest of generators, the frequency control or support offered by the RES would be regulated by the corresponding legislations, such as the Spanish operational procedure P.O. 7.1, P.O. 7.2 and P.O. 7.3. These regulations should probably be adapted to include the participation of RES in the corresponding service. Applications in this field with different ES technologies have already been published [52, 55, 58].

II.   Voltage Control: the ESS introduction makes it possible for intermittent RES power plants to further support the local voltage control in distribution lines [59]. Not only the reactive power management, usually controlled with the power converter, would be available to support voltage but also an energy reserve (accumulated within the ESS) would be available to allow an economically efficient active power control (retailing and storing) so as to keep the voltage within ranges at any time. Thus, this service would involve a trade-off between the amounts of active and reactive energy produced and that exchanged between the generators, the ESS and the grid [29, 59]. Operation of the RES providing this service would be regulated by the corresponding legislations, such as the Spanish operational procedure P.O. 7.4, or equivalent ones including the participation of RES. Some examples of this application can be already cited [51, 60-63].

III. Black Start Capability: it is the ability to energize part of a grid without outside assistance after a blackout occurs. This has traditionally been one of the limitations for RES which could be now achieved thanks to the introduction of ESS and the accumulated energy this units could offer in order to start-up a grid partial operation [64].

Finally, it is to point out that the different ancillary services which could be offered by these RES integrating a variety of ESS should be regulated in the different National Grid Operation Codes, adapting current operation procedures. Apart from the technical conditions of operation, new regulations should reflect clearly their financial and economical frame, being this as generous as possible so as to encourage participation. Thus, the electricity market, its competitors and the associated industry could plan their investments and calculate their return time being based on the existing feed-in tariffs and the free market operations.

b) ESS as providers of quality in the supply from renewables

Feeding intermittent power into the EPS can certainly affect its supply quality [59, 65]. The impact depends primarily on the degree to which the intermittent RES contribute to the instantaneous load but can pose serious problems to the stability. Phenomena such as clouds or objects passing over the array of panels produce power spikes on PV power plants production, and wind turbines produce intermittently as a function of the wind speed and its gusts, apart from the power oscillations and flicker produced as the blade sweeps over the tower. All of them may reduce system stability and transmission capability mainly in weak or isolated grids [66, 67] where quality power requirements are quite strict, contrary to larger power system where more flexibility is accepted. For large power systems, supply quality issues arising from RES fluctuations need to be addressed when voltage variations go beyond the 10 % of the rated value during more than 5% of the time, or if a voltage dip with a value below 15 % of the rated voltage occurs [68]. In addition, wind turbines, especially inductive machines, tend to absorb reactive power from the system and produce a low power factor. If wind turbines absorb too much reactive power, the system can become unstable [69]. Furthermore, as already indicated most of the ESS are connected to the grid by means of power converters, notably for solar photovoltaic and wind power plants. These converters introduce several undesired harmonics that can have a negative impact on electronic equipment [70] and can cause unexpected tripping due to protections operation.

Therefore, all these problems can be reduced by installing some kind of ES device connected to the point of common coupling (PCC) of the RES power plant. The ESS can act as an UPS unit, as an active filter or as any electronic device needed to compensate the most important problems introduced by the RES power plant at that PCC. In this way, it would isolate the RES from the grid, and fluctuations produced by the RES would have no effect on the EPS, and vice versa. Some examples of applications in this domain can be already found in the literature, such as [71] where the supply quality and the stability of a wind farm is

improved using a STATCOM which is supported with a hybrid battery. Another cases presented as grid voltage stability in [54] involves immunity against degraded voltage by providing additional reactive power and some active power for durations of up to 2s.

ES technologies that deal with the mentioned supply quality related issues require low energy capacities although high power ratings, high capacity to survive cycling and fast response rates [72]. The ES capacity required is even lower for ride-through capability applications, where the electric load or RES generator must stay connected during an EPS disturbance at the PCC, given that part of the energy can be obtained from the grid during a certain undervoltage period [72].

This supply quality improvement capability assigned to ESS when implemented together with intermittent DG is strongly associated to the way the hybrid power plant can dispatch its energy. And this is defined by the energy management strategy implemented. There are several strategies depending on the goal. These are presented in the next section.

c) Renewables Energy Management

Several energy management strategies can be implemented on RES integrating an ESS. With the increasing introduction and penetration of intermittent RES, the EPS control in the dynamic balance between generation and load [73] is more and more difficult to be achieved due to the additional variability and unpredictability of the power generation mix. In this sense, if properly placed, ESS can not only help providing ancillary services or improving quality service to the grid but also these can help mitigating many of the issues caused by intermittent production of RES. Some examples of applications in this regard can be already cited [66, 74-78]. Considering the increasing amount of energy capacity that the different energy management strategies would require to operate adequately, they can be identified, ordered and shortly described as presented below:

I. Production leveling, smoothening and regulation: although it is not currently a grid connection requirement for RES, a general reduction in the short term fluctuations (or a minimum stabilization on their intermittent generated power) seems desirable or even essential and can be required in the near future by the system operators to guarantee a stable and balanced functioning of the EPS. This reduction can be obtained by running the ESS as a kind of low-pass filter, i.e. reducing the variability of the production referred to an average value. This strategy, called smoothening or production leveling, uses the following criterion for the stabilization: the diminution in the difference between the

maximum and the minimum values of the generated power with regard to a moving average power value calculated within a certain time window. The flattening degree of the inputted renewable energy obtained with this strategy will depend on the ESS power and energy capacities. Note that this strategy is not considered to be excessively energy demanding since its operating time horizon would stretch from seconds up to one hour. A similar strategy can be highlighted here, it is named "regulation" and is used in some publications due to its equivalence with the corresponding adjustment service [31, 69, 79]. Regulation focuses on the minute-by-minute customers load variations and, normally by means of an Automatic Generation Control scheme, compares it to the forecasted value in order to tell one or more generating units if these need to lightly modify their power output in response to short load variations for keeping the system balanced [80]. Thus, it slightly differs from the smoothening strategies which, instead of focusing on the customers load variations, focuses on the RES production variations and compares it with the forecasted production to decide the power reference. However, energy requirements for both strategies are quite the same. Examples implementing these strategies have already been developed [81, 82]. Some of them claim that the required ES capacity for such application is 20% of the RES output capacity, calculated for a wind farm [74], and others even assure that they can provide with that capacity a 90% smooth output [83]. Similar values are stated out by [79], with a combination of good ramp rates, i.e., 10–20 MW/s for wind farms, and a power capacity with the ability to provide rated power for at least one hour. The operability improvement obtained by a generic PV power plant with ES when implementing these short-term horizon energy management strategies is analyzed in Chapter IV and Chapter V of the present PhD Thesis dissertation.

II.   <u>Renewables Availability & Predictability Improvement</u>: the expected massive introduction of intermittent RESs into the EPS, and specially the PV technology for the interest of this Thesis work, may force these technologies to evolve from their current intermittent and stochastic production into not only a smoothed power production source but even into a more deterministic system whose production could be completely controlled (dispatchable). The goal of this strategy is to be able to forecast the amount of power the intermittent RES will be capable to inject into the EPS in the coming hours with a certain degree of confidence. This strategy could be called something like short term Unit Commitment. Thus, thanks to the ESS introduction, RES power plants not only could reduce the intermittency (smoothening) but also could assure a constant percentage of its nominal power for a given time under proper weather conditions, or even under

adverse conditions with an increased availability. That means that the RES plant operator would be able to offer, according with the weather forecast and with the power plant characteristics, a forecasted amount of power to be delivered to the EPS at a given time, and during a certain period, with a high degree of confidence. In some countries, as it is the case for Spain, it is an EPS requirement to deliver a production forecast to participate in the market. The difference between forecasted and real time production results in financial consequences. Therefore, utilization of ESS for this functionality could represent a direct benefit for RES as far as there will be significant penalties for those which deviate from their scheduled power production due to inaccurate generation forecasts. Examples can be already found in this sense, the Bonneville Power Administration used to charge $100 / MWh for deviation from scheduled power delivery [69]. The time horizon for this strategy would range from 30 minutes to 24 hours [79]. Therefore, it can be classified as a medium-term energy management strategy. This is the main ESS applications considered and studied in this Thesis work. Its energy and power requirements have been analyzed when implemented in a PV power plant operating under different control configurations.

III. Renewables Production Shifting, Peak Shaving and Load Following: this third energy management strategy represents shifting the RES production to peak demand periods and not when the renewable resource (wind or sun) is available. In other words, one can say that with this functionality the RES production and its power delivery are decoupled by using the ESS energy capacity in order to optimize the economic income of the plant [53]. Variations in the demand in Spain along the day can be appreciated in the Spanish daily aggregated load curve, Figure 1.18. A curve which is provided every day by the system operator, REE. In that figure, the aggregated power generated along the day by the Spanish wind farms can be observed on the green curve on the top right, together with its percentage of share in the overall production. One can conclude that the wind production is stochastic and does not track the Spanish load curve. Thus, as for the case of the grid application, the peak shaving functionality associated to renewables with ES would consist in using that off-peak renewable power, instead of storing electric energy from the EPS, to charge the ES device and subsequently allowing it to discharge during peak demand periods of the system [84]. This functionality can favor customers and RES facility owners with higher economical incomes (energy arbitrage) on one hand and utilities or energy providers with benefits by avoiding connection of non-renewable central generation inefficient facilities on the other hand. Therefore, not only does this

enable the ES unit to maximize its profits, but it can also reduce the cost of operating the system. As for the case of the "regulation" strategy (classified within the short term group) another strategy could be defined here derived from the ancillary services, the "load following". It consists on using the online generation equipment to track the intra- and inter-hour changes in customer loads [85]. This could be implemented too in RES units with ES to help coping with the customer load curve [79]. All these mid-term strategies would typically imply a contract and/or power purchase agreement.
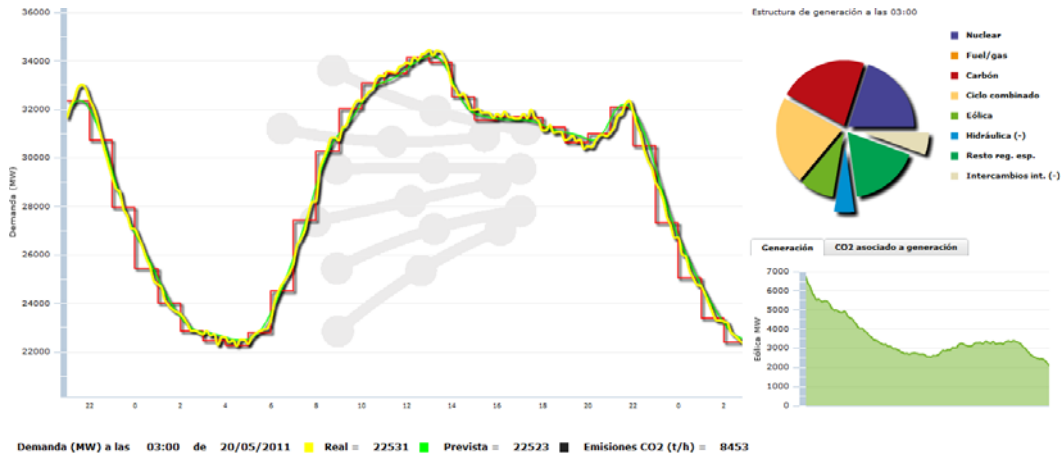

Figure 1.18 Typical daily demand curve in the Spanish electric system. Source: [49]**.**

IV.   Long-term Load Leveling, Unit Commitment and Seasonal Storage: when incorporating large amounts of ES, long-term load leveling and other applications as long term unit commitment or seasonal storage could be obtained. Unit commitment, which involves finding the least-cost dispatch of available generation resources to meet the forecasted electrical load, presents a general horizon of one day to one week, with time increments rounding one hour [69] but depending on the country. On the other hand, seasonal storage, which is designed to retain energy for long periods, comprehends monthly energy balances [86]. Such an amount of energy capacity and the corresponding time horizons could even mean the use of RES power plants with ES as baseload power plants or to even enable an increase in the predictability for technologies such as PV to nearly 100% for large periods of time. Regarding unit commitment applications, these would be beneficial in a deregulated EPS where electricity price variations could justified the joint dispatch of RES and ESS [87-90]. Thus, the added value in the combined operation of a wind farm with ESS is considered to be approximately $62,500/year for energy arbitrage with uncertainty in wind production [31]. Another study centered in a large wind farm

fixes a payback time of the installation in 7 years [78]. Regarding seasonal storage, it would require so much ES that its cost might not justify the benefits due to the reduction that would be experienced in the marginal returns. In other words, after a certain amount of installed capacity, ESS used for multiple purposes might lose the incremental benefit of one of its purposes. These strategies would also imply a contract and/or power purchase agreement and due to their energy capacity requirements these are probably beyond the PV power plants scope and clearly not to be considered in this Thesis work.

Some extra functionalities or applications can be enumerated for the RES energy management; although these can be integrated within the first strategy since are somehow concrete applications of the smoothening functionality. These are:

- *dP/dt limitations*: a limit on the RES output power steepness can be fixed. This is a service that limits the rate of change in the produced power which allows a better integration of high fluctuating RES into the EPS [81].

- *Soft stop*: ESS allow RES to present this functionality which provides them with the capability to ramp down the power plant more slowly than the primary energy resources (wind or solar irradiation) get extinguished, giving other energy sources time to start up.

Therefore, it seems clear that the ESS requirements and its potential benefits will be different as a function of the energy management strategy to implement. While high cyclability and fast response rates are needed for short-term applications, at the opposite end for the case of seasonal storage, large energy capacity and low self-discharge are necessary together with power density and cycle efficiency which are moderately important. Access time and ramp rates bear little significance for seasonal storage.

In any case, to be a viable and interesting option for intermittent RES applications, any ESS should be scalable and modular, to accommodate for various size requirements (from a few kW for rooftop solar power to multiple MW for wind farms). Furthermore, any ESS should also require low maintenance and have a long lifespans to decrease costs associated with replacements, maintenance and operations.

Finally, note that many of the different ES applications introduced are compatible with each other and, although each case is unique, if the RES power plant with ES is used for one certain medium-long term application it will probably have energy capacity enough so as to provide other benefits such as: 1) revenues from or avoided cost for on-peak energy, 2)

avoid/deferred need to build new transport and distribution facilities, 3) avoid transmission access or congestion charges, 4) transmission support, and 5) ancillary services.

A good dimensioning of the system and a good analysis of the marginal returns when providing each of the different functionalities must be analyzed to determine the economic viability of future installations. A future scenario which is not far away since, as it has been cited along this section, new guidelines have already been passed in some national grid codes to regulate the parallel operation of intermittent RES with the medium voltage grid asking them to start providing some kind of stability support to the network operation [91, 92].

1.4.4. Applications comparison.

To summarize all the information presented along this section, a comparison of the different applications enumerated in the preceding paragraphs can be established. For so doing, Figure 1.19 is introduced. It contains the different ESS potential applications represented as a function of the amount of time and rated power these would require to the ESS. This figure has been elaborated by compiling different comparisons already performed in the literature [30, 31, 93].
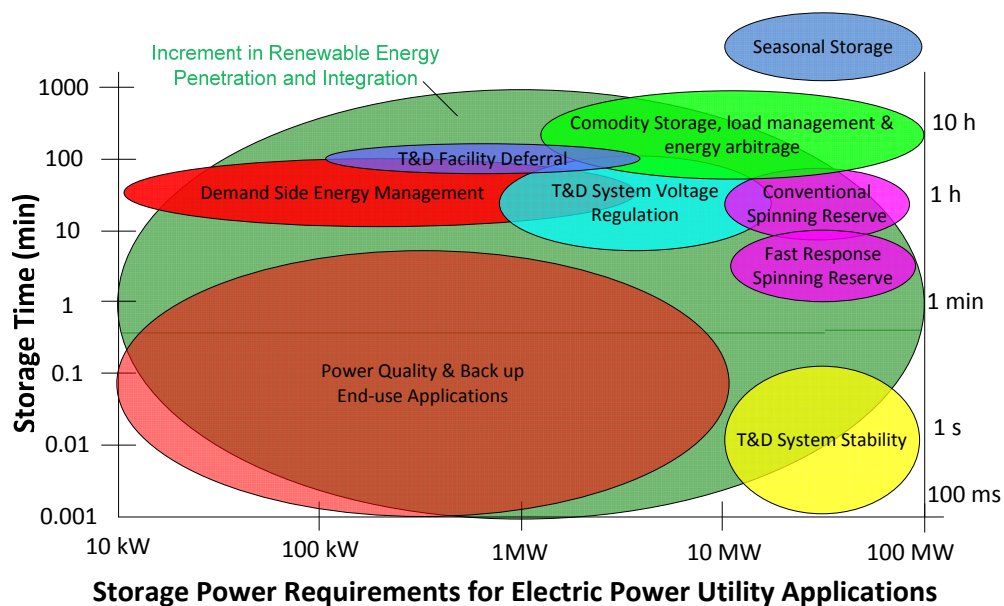

Figure 1.19 Storage time vs. storage power requirements for ESS applications.

Thus, it is clear that very different ranges of power and energy are required for the different applications. Therefore, it can be concluded for each of the different applications

there will be an ES technologies which will be the one fitting the best. This analysis is performed after the ES technologies analysis in Chapter III.

1.5. References

[1] Ren 21 Steering Comittee, "Renewables 2011 global status report," REN21 Secretariat, Paris, 2011.

[2] T. Ackermann, G. Andersson and L. Soder, "Distributed generation: a definition," *Electr. Power Syst. Res.,* vol. 57, pp. 195-204, 4/20, 2001.

[3] K. Alanne and A. Saari, "Distributed energy generation and sustainable development," *Renewable and Sustainable Energy Reviews,* vol. 10, pp. 539-558, 12, 2006.

[4] A. Jaeger-Waldau, "PV status report 2010," JRC Scientific and Technical Reports (EUR collection), Italy, Tech. Rep. JRC59708, 2010.

[5] The European Parliament and the Council of the European Union, "Directive 2009/28/EC on the promotion of the use of energy from renewable sources " 2009.

[6] Gobierno de España, "Ley 54/1997, del Sector Eléctrico," 28 de noviembre de 1997, 1997.

[7] Gobierno de España - Ministerio de Industria y Energía, "Plan de Fomento de las Energías Renovables en España," 1999.

[8] Gobierno de España - Ministerio de Industria, Turismo y Comercio, "Plan de Energías Renovables en España 2005-2010," 2005.

[9] Red Eléctrica de España (REE). Informe del sistema eléctrico español. Madrid (Spain). 2010.

[10] Gobierno de España - Ministerio de Industria, Turismo y Comercio, "Plan de Acción Nacional de Energías Renovables 2010-2020," 2010.

[11] Gobierno de España, "Ley 2/2011, de Economía Sostenible," 4 de marzo 2011, 2011.

[12] The European Comission. Communication to the european parliament and the council - renewable energy: Progressing towards the 2020 target. 2011.

[13] A. Jaeger-Waldau, "PV status report 2011," JRC Scientific and Technical Reports (EUR collection), Italy, Tech. Rep. EUR 24807 EN - 2011, 2011.

[14] European Photovoltaic Industry Association. Global market outlook for photovoltaic until 2015. EPIA Publications. Belgium. 2011 [Online]. Available: http://www.epia.org/publications/ photovoltaic-publications-global-market-outlook/global-market-outlook-for-photovoltaics-until-2015.html.

[15] PV resources. [Online]. *2011(Accessed: June 10, 2011),* Available: http://www.pvresources.com/.

[16] Anonymous Germany hits new solar power record in Q1 2011. *Newsletter, EnergyMarketPrice. Com .*

[17] International Energy Agency. Photovoltaic power systems programme - national reports. [Online]. *(Accessed: June 18, 2011),* 2010. Available: http://www.iea-pvps.org/index.php?id=93.

[18] Gobierno de España - Ministerio de Industria, Turismo y Comercio, "Real Decreto 436/2004, por el que se establece la metodología para la actualización y sistematización del régimen jurídico y económico de la actividad de producción de energía eléctrica en régimen especial," 12 de Marzo, 2004.

[19] Gobierno de España - Ministerio de Industria, Turismo y Comercio, "Real Decreto 661/2007, por el que se regula la actividad de producción de energía eléctrica en régimen especial." 25 de Mayo, 2007.

[20] ASIF. Asociación de la industria fotovoltaica en españa. [Online]. *(Accessed: August 10, 2011),* 2011. Available: http://asif.org/.

[21] P. Mints. Solar PV market analysis: Unstable boom times continue for PV market. *Renewable Energy World International Magazine (July-August),* 2010.

[22] A. Carbajo Josa, "Los mercados eléctricos y los servicios de ajuste del sistema," *Economía Industrial,* pp. 55-62, 2007.

[23] N. Aparicio, "Nuevas estrategias para la contribución de los parques eólicos al control de frecuencia de los sistemas eléctricos," 2011.

[24] Gobierno de España - Ministerio de Industria, Turismo y Comercio, "Real Decreto 1454/2005, por el que se modifican determinadas disposiciones relativas al sector eléctrico." 2 de diciembre, 2005.

[25] Red Electrica de España (REE), "Servicio complementario de regulación primaria," vol. PO 7.1, 1998.

[26] Red Eléctrica de España (REE), "Regulación secundaria," vol. PO 7.2, 2009.

[27] Red Eléctrica de España (REE), "Regulación terciaria," vol. PO 7.3, 2009.

[28] Red Eléctrica de España (REE), "Servicio complementario de control de tensión de la red de transporte," vol. PO 7.4, 2000.

[29] A. Mohd, E. Ortjohann, A. Schmelter, N. Hamsic and D. Morton, "Challenges in integrating distributed energy storage systems into future smart grid," in *Industrial Electronics, ISIE. IEEE International Symposium on,* 2008, pp. 1627-1632.

[30] S. Vazquez, S. M. Lukic, E. Galvan, L. G. Franquelo and J. M. Carrasco, "Energy Storage Systems for Transport and Grid Applications," *IEEE Transactions on Industrial Electronics,* vol. 57, pp. 3881-3895, 2010.

[31] M. Beaudin, H. Zareipour, A. Schellenberglabe and W. Rosehart, "Energy storage for mitigating the variability of renewable electricity sources: An updated review," *Energy for Sustainable Development,* 2010.

[32] H. Ibrahim, A. Ilinca and J. Perron, "Energy storage systems—Characteristics and comparisons," *Renewable and Sustainable Energy Reviews,* vol. 12, pp. 1221-1250, 6, 2008.

[33] J. M. Eyer, J. J. Iannucci and G. P. Corey, "Energy storage benefits and market analysis handbook," Sandia National Laboratories, Tech. Rep. SAND2004-6177, 2004.

[34] J. Sayer, "Guide to estimating benefits and market potential for electricity storage in new york," Distributed Utility Associates, New York, 2007.

[35] P. F. Ribeiro, B. K. Johnson, M. L. Crow, A. Arsoy and Y. Liu, "Energy storage systems for advanced power applications," *Proc IEEE,* vol. 89, pp. 1744-1756, 2001.

[36] A. Joseph and M. Shahidehpour, "Battery storage systems in electric power systems," in *Power Engineering Society General Meeting. IEEE,* 2006, pp. 8.

[37] A. Gonzalez, B. Gallachóir, E. McKeogh and K. Lynch, "Study of electricity storage technologies and their potential to address wind energy intermittency in ireland," University of Limerick, Ireland, 2004.

[38] I. MacGill, "Electricity market design for facilitating the integration of wind energy: Experience and prospects with the Australian National Electricity Market," *Energy Policy,* vol. 38, pp. 3180-3191, 2010.

[39] S. R. Thorncraft and H. R. Outhred, "Experience with market-based ancillary services in the australian national electricity market," in *Power Engineering Society General Meeting. IEEE,* 2007, pp. 1-9.

[40] D. Connolly, H. Lund, B. V. Mathiesen and M. Leahy, "Modelling the existing Irish energy-system to identify future energy costs and the maximum wind penetration feasible," *Energy,* vol. 35, pp. 2164-2173, 2010.

[41] OMEL, "Evolución del mercado de energía eléctrica," Operador del Mercado Eléctrico, Madrid (Spain), Tech. Rep. April, 2011.

[42] A. Mills, R. Wiser and K. Porter, "The cost of transmission for wind energy: A review of transmission planning studies," Citeseer, Tech. Rep. LBNL-1471E, 2009.

[43] P. Denholm and R. Sioshansi, "The value of compressed air energy storage with wind in transmission-constrained electric power systems," *Energy Policy,* vol. 37, pp. 3149-3158, 2009.

[44] R. Sioshansi and P. Denholm, "The Value of Concentrating Solar Power and Thermal Energy Storage," *Sustainable Energy, IEEE Transactions on,* vol. 1, pp. 173-183, 2010.

[45] D. Connolly, "A review of energy storage technologies," 2009.

[46] B. P. Roberts, "Sodium-sulfur (NaS) batteries for utility energy storage applications," in *Power and Energy Society General Meeting - Conversion and Delivery of Electrical Energy in the 21st Century, 2008 IEEE,* 2008, pp. 1-2.

[47] D. K. Nichols and S. Eckroad, "Utility-scale application of sodium sulfur battery," in *Proceedings of the IEEE International Stationary Battery Conference (Battcon'03),* pp. 1–9.

[48] Y. Hida, Y. Ito, R. Yokoyama and K. Iba, "A study of optimal capacity of PV and battery energy storage system distributed in demand side," in *Universities Power Engineering Conference (UPEC), 2010 45th International,* 2010, pp. 1-5.

[49] Red Eléctrica de España (REE), "Proyecto INDEL. atlas de la demanda eléctrica española," 1998.

[50] R. E. Brown, "Impact of smart grid on distribution system design," in *Power and Energy Society General Meeting - Conversion and Delivery of Electrical Energy in the 21st Century, 2008 IEEE,* 2008, pp. 1-4.

[51] S. W. Mohod and M. V. Aware, "Energy storage to stabilize the weak wind generating grid," in *Power System Technology and IEEE Power India Conference, POWERCON. Joint International Conference on,* 2008, pp. 1-5.

[52] P. Mercier, R. Cherkaoui and A. Oudalov, "Optimizing a Battery Energy Storage System for Frequency Control Application in an Isolated Power System," *Power Systems, IEEE Transactions on,* vol. 24, pp. 1469-1477, Aug. 2009.

[53] S. T. Lee and Z. A. Yamayee, "Load-Following and Spinning-Reserve Penalties for Intermittent Generation," *Power Apparatus and Systems, IEEE Transactions on,* vol. PAS-100, pp. 1203-1211, 1981.

[54] S. Eckroad and I. Gyuk, *Handbook of Energy Storage for Transmission & Distribution Applications.* EPRI-Department of Energy, 2003.

[55] F. Schorr and N. Brochard, "Advances in energy-efficient, power quality and energy storage, and implications for utility grid frequency stabilization," in *Telecommunications Energy Conference, 2007. INTELEC 2007. 29th International,* 2007, pp. 604-608.

[56] European Network of Transmission System Operators for Electricity (ENTSOE), "UCTE - Union for the Coordination of the Transmission of Electricity," vol. 2011, .

[57] G. Costales Ortiz, A. Lara Cruz, J. M. Carrasco Solís, E. Galvan Diez and L. Garcia Franquelo, "System for conditioning and generating/storing power in electrical distribution networks in order to improve the dynamic stability and frequency control thereof," WO Patent WO/2003/023,933, 2003.

[58] Lin Cui, Dahu Li, Jinyu Wen, Zhenhua Jiang and Shijie Cheng, "Application of superconducting magnetic energy storage unit to damp power system low frequency oscillations," in *Electric Utility Deregulation and Restructuring and Power Technologies, 2008. DRPT 2008. Third International Conference on,* 2008, pp. 2251-2257.

[59] R. Hara, H. Kita, T. Tanabe, H. Sugihara, A. Kuwayama and S. Miwa, "Testing the technologies," *Power and Energy Magazine, IEEE,* vol. 7, pp. 77-85, 2009.

[60] J. Shi, Y. J. Tang, L. Ren, J. D. Li and S. J. Chen, "Application of SMES in wind farm to improve voltage stability," *Physica C: Superconductivity,* vol. 468, pp. 2100-2103, 2008.

[61] N. R. Ullah, T. Thiringer and D. Karlsson, "Voltage and Transient Stability Support by Wind Farms Complying With the E.ON Netz Grid Code," *Power Systems, IEEE Transactions on,* vol. 22, pp. 1647-1656, Nov. 2007.

[62] Z. Jun-xing and W. Tong-xun, "A novel dynamic voltage restorer with flywheel energy storage system," *Journal of Mechanical & Electrical Engineering,* vol. 2, 2010.

[63] L. Ji-ru, Y. Zhong-dong and Y. Quan-qing, "Research on Superconducting Magnetic Energy Storage Based on Dynamic Voltage Restorer," *High Voltage Engineering,* vol. 3, 2008.

[64] K. C. Divya and J. Østergaard, "Battery energy storage technology for power systems--An overview," *Electr. Power Syst. Res.,* vol. 79, pp. 511-520, 2009.

[65] L. Caihao and D. U. Xianzhong, "Distributed generation and its impact on power system," *Automation of Electric Power Systems,* vol. 12, pp. 53-56, 2001.

[66] I. Ngamroo, A. N. Cuk Supriyadi, S. Dechanupaprittha and Y. Mitani, "Power oscillation suppression by robust SMES in power system with large wind power penetration," *Physica C: Superconductivity,* vol. 469, pp. 44-51, 1/1, 2009.

[67] D. Weisser and R. S. Garcia, "Instantaneous wind energy penetration in isolated electricity grids: concepts and review," *Renewable Energy,* vol. 30, pp. 1299-1308, 7, 2005.

[68] J. O. G. Tande, "Grid integration of wind farms," *Wind Energy,* vol. 6, pp. 281-295, 2003.

[69] P. S. Georgilakis, "Technical challenges associated with the integration of wind power into power systems," *Renewable and Sustainable Energy Reviews,* vol. 12, pp. 852-863, 4, 2008.

[70] J. H. R. Enslin, "Interconnection of distributed power to the distribution network," in *Power Systems, IEEE PES. Conference and Exposition,* 2004, pp. 726-731.

[71] A. Arulampalam, M. Barnes, N. Jenkins and J. B. Ekanayake, "Power quality and stability improvement of a wind farm using STATCOM supported with hybrid battery energy storage," *IEE Proceedings - Generation, Transmission and Distribution,* vol. 153, pp. 701-710, 2006.

[72] C. Abbey and G. Joos, "Supercapacitor Energy Storage for Wind Energy Applications," *IEEE Transactions on Industry Applications,* vol. 43, pp. 769-776, 2007.

[73] T. E. Lipman, R. Ramos and D. M. Kammen, "An assessment of battery and hydrogen energy storage systems integrated with wind energy resources in california," California Energy Commission, California, Tech. Rep. CEC-500-2005-136, 2005.

[74] Y. Iijima, Y. Sakanaka, N. Kawakami, M. Fukuhara, K. Ogawa, M. Bando and T. Matsuda, "Development and field experiences of NAS battery inverter for power stabilization of a 51 MW wind farm," in *Power Electronics Conference, IPEC, International,* 2010, pp. 1837-1841.

[75] T. Kinjo, T. Senjyu, N. Urasaki and H. Fujita, "Terminal-voltage and output-power regulation of wind-turbine generator by series and parallel compensation using SMES," in *Generation, Transmission and Distribution, IEE Proceedings-,* 2006, pp. 276-282.

[76] A. Nourai and D. Kearns, "Batteries Included," *Power and Energy Magazine, IEEE,* vol. 8, pp. 49-54, 2010.

[77] K. Mattern, A. Ellis, S. E. Williams, C. Edwards, A. Nourai and D. Porter, "Application of inverter-based systems for peak shaving and reactive power management," in *Transmission and Distribution Conference and Exposition, 2008. T&D. IEEE/PES,* 2008, pp. 1-4.

[78] S. Faias, P. Santos, F. Matos, J. Sousa and R. Castro, "Evaluation of energy storage devices for renewable energies integration: Application to a portuguese wind farm," in *Electricity Market, 2008. EEM 2008. 5th International Conference on European,* 2008, pp. 1-7.

[79] E. Hirst and B. Kirby, "Separating and measuring the regulation and load-following ancillary services," *Utilities Policy,* vol. 8, pp. 75-81, 6, 1999.

[80] N. J. Schenk, H. C. Moll, J. Potting and R. M. J. Benders, "Wind energy, electricity, and hydrogen in the Netherlands," *Energy,* vol. 32, pp. 1960-1971, 2007.

[81] N. Kakimoto, H. Satoh, S. Takayama and K. Nakamura, "Ramp-Rate Control of Photovoltaic Generator With Electric Double-Layer Capacitor," *Energy Conversion, IEEE Transactions on,* vol. 24, pp. 465-473, 2009.

[82] D. S. Callaway, "Tapping the energy storage potential in electric loads to deliver load following and regulation, with application to wind energy," *Energy Conversion and Management,* vol. 50, pp. 1389-1400, 5, 2009.

[83] I. Fuel Cell Energy, "Stationary fuel cell power systems with direct FuelCell technology - tackle growing distributed baseload power challenge," 2004.

[84] B. H. Chowdhury, "Central-station photovoltaic plant with energy storage for utility peak load leveling," in *Energy Conversion Engineering Conference, 1989. IECEC-89., Proceedings of the 24th Intersociety,* 1989, pp. 731-736 vol.2.

[85] Y. Hida, R. Yokoyama, K. Iba and K. Tanaka, "Practical load following operation of NaS battery," in *8th WSEAS International Conference on POWER SYSTEMS,* Cantabria, Spain, 2008, .

[86] T. Schmidt, D. Mangold and H. Müller-Steinhagen, "Central solar heating plants with seasonal storage in Germany," *Solar Energy,* vol. 76, pp. 165-174, 3, 2004.

[87] Ruey-Hsun Liang and Jian-Hao Liao, "A Fuzzy-Optimization Approach for Generation Scheduling With Wind and Solar Energy Systems," *Power Systems, IEEE Transactions on,* vol. 22, pp. 1665-1674, 2007.

[88] E. D. Castronuovo and J. A. P. Lopes, "On the optimization of the daily operation of a wind-hydro power plant," *IEEE Transactions on Power Systems,* vol. 19, pp. 1599-1606, 2004.

[89] D. J. Swider, "Compressed Air Energy Storage in an Electricity System With Significant Wind Power Generation," *IEEE Transactions on Energy Conversion,* vol. 22, pp. 95-102, 2007.

[90] J. L. Angarita, J. Usaola and J. Martínez-Crespo, "Combined hydro-wind generation bids in a pool-based electricity market," *Electr. Power Syst. Res.,* vol. 79, pp. 1038-1046, 7, 2009.

[91] Red Eléctrica de España (REE), "Technical requirements for wind power and photovoltaic installations and any generating facilities whose technology daes not consist on a synchronous generator directly connected to the grid," vol. PO 12.2 Outline, 2008.

[92] W. Bartels and R. Hüttner, "Erzeugungsanlagen am mittelspannungsnetz," in *Schutz- Und Leittechnik 2008 - 3. ETG-/BDEW-Tutorial,* Fulda, 2008, .

[93] Electricity Storage Association. [Online]. 2010). Available: http://electricitystorage.org.

The solar resource

O utside the Earth's atmosphere, the solar radiation intensity hitting our planet presents a constant value equal to 1366.1 W/m^2. This value is known as the "solar constant" [1], which includes all the frequency spectra of solar radiation and not just the visible light. A surface exposed to the Sun rays should only receive this value in case of being placed normal to the direction of the radiation. Any deviation from this direction leads to a reduction of the incident radiation. Thus, the solar constant radiation intensity corresponds to the maximum possible value of radiation which would occur at the Earth's surface if it were unhindered by the atmosphere and the horizon. Unfortunately, or luckily, the atmosphere is there and the solar radiation on the Earth's surface is not constant or homogeneous, presenting always lower values. Furthermore, solar radiation hits the planet with different inclinations, depending on the latitude and the different relative positions that the Earth adopts with regard to the Sun along the day and the year, Figure 2.1, according with the multiple Earth movements (changes in the orbit, in its tilt and wobble movements). Either way, it is important to be able to understand the physics, the nature and the distribution of the solar radiation and the daylight, particularly to determine the amount of energy intercepted by the Earth's surface (solar potential) at any locations. Note that solar radiation and daylight are essential to life since it affects the Earth's weather processes determining the natural environment. In addition, its presence at the Earth's surface is necessary for the provision of food for mankind since daylight is a need for the production of

all our agricultural products and sustains the food chain through the process of photosynthesis. That is why, the Sun and its emitted radiation variations have been studied for centuries. Note that the first record of sunspots dates to around 800 BC in China and the oldest surviving drawing of a sunspot dates to 1128 CE. However, the scientific understanding of the climatological phenomena and a statistical study of radiation is comparatively new [2]. In fact, it was not till the beginning of the twentieth century that some initial research, concerned with the relationship between irradiation and the sunshine duration, was carried out by Ander Ångström [3-5]. In this sense, comprehensive statistical observations and measurements have been only performed along the last 50 years. Thus, first serious studies on solar radiation where not published until the 1960s decade [6, 7], a time when there were only three stations in north-west Europe with irradiation records exceeding a 25 year period [8]. Similarly, daylight was not recorded on a continuous basis at that time and, for example, up to 1970 only seven sites across the UK measured horizontal illuminance. Since then, research in this field has come a long way.
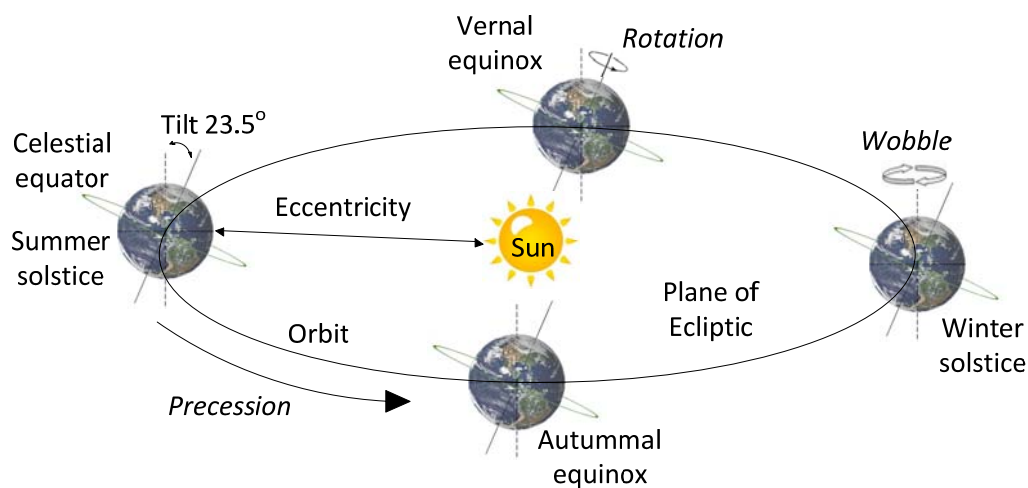

Figure 2.1 Relative position of the Earth versus the Sun. Source: Purdue University.

These lines of research have been favored by new economic interests. In fact, not only for life and natural processes it is important to understand solar radiation, for some time now the solar resource availability is also a key parameter for the solar energy industry which requires more and more detailed information on the solar characteristics and potential in order to both optimize new solar based technologies and select optimal places where new solar power facilities have to be installed, respectively. The solar industry is evolving so much and so quickly that have produced lately surprising news such as that recently

published in the Science Magazine [9] which affirms that, after comparing natural photosynthesis with present technologies for photovoltaic-driven electrolysis of water to produce hydrogen, the latter is the most efficient process when measured on an annual basis. Therefore, given that the work presented in this thesis is based on the solar radiation evolution along one year and its comparison with the statistically-averaged radiation values in order to model an energy storage system's ratings and characteristics, being a work profitable by this solar industry, an overview and the corresponding analysis on the solar radiation resource characteristics, models and sources of information has been considered convenient. These are the contents presented in this chapter but, prior to deepen into that overview and its analysis, some definitions should be pointed out here. Different terms are frequently used along the solar radiation related literature which are sometimes confusing and that the author considers should be clarified. Solar radiation (measured in W/m^2) and luminance (candela/m^2 (cd/m^2)) refer to the energy emanating from the Sun, being the latter only that energy contained within the visible part of the solar radiation spectrum (0.39 - 0.78 µm). Instead, irradiance (W/m^2) and illuminance (lm/m^2) refer to the instantaneous energy incident on a surface. Finally, the term irradiation (Wh/m^2 or J/m^2) and illumination (lumen-hour $(lmh)/m^2$) refer to the cumulative energy incident on a surface along a given period of time.

2.1. The solar resource analysis and modeling.

Solar irradiance data provide information, as already introduced, on how much of the Sun's energy strikes a surface at a location on the Earth during a particular period of time. Unlike wind resource, which varies in a stochastic way with a statistical distribution of the wind speed close to that of a Weibull distribution [10-13], the solar resource cannot be so clearly assimilated to any statistical distribution. Nevertheless, as previously indicated, the irradiance level knowledge is needed for effective research into solar energy applications and economic viability of new PV installations.

2.1.1. Solar radiation components.

The global solar radiation incident on any type of inclination surface consists of three different components: direct, diffuse and reflected components. These can be described as:

- Direct: usually known also as beam or direct normal irradiance, it is the solar radiation experienced at a given location on Earth by any surface perpendicular to the

Sun's rays. It is equal to the solar constant minus the atmospheric losses due to absorption and scattering. These losses depend on the time of day (length of light's path through the atmosphere depending on the solar elevation angle), the cloud cover, the moisture content, and others such as aerosols, ozone, mixed gases…

- Diffuse: is the solar irradiance which is scattered or reflected by atmospheric components in the sky, reaching measurement surfaces with multiple angles.

- Reflected component: it is mainly exclusively considered for inclined surfaces since it is basically a ground reflected component, hence very influenced by the albedo parameter. Albedo is synonym for reflectance and denotes the reflection coefficient of the Earth surface in the visible range of the solar spectrum. Thus, this component may be quite important in northern European latitudes where Sun elevation is low for a large part of the year, a phenomenon which is further increased by the permanent presence of a highly-reflecting snow cover, with an elevated albedo value, as can be appreciated in Table 2.1 , together with some other typical values.

Type of surface, soil or vegetation	Albedo Value (%)
Black earth, dry	14
Black earth, moist	8
Grey earth, dry	25-30
Grey earth, moist	10-12
Ploughed field, moist	14
White sand	34-40
River sand	43
Light clay earth	30-31
Fresh snow cover	75-95
Old snow cover	40-70
Rock	12-15
Densely built-up areas	15-25
High dense grass	18-20
Sea ice	36-50
Water surface, sea	3-10
Lawn: high Sun, clear sky	23
Lawn: high Sun, partly cloudy	23
Lawn: low Sun, clear sky	25
Lawn: overcast day	23
Dead leaves	30
Grass	24
Wheat	26
Tomato	23
Pasture	25
Heather	14
Bracken	24
Deciduous woodland	18
Coniferous woodland	16

Table 2.1 Typical Albedo values for different types of surfaces. Source: [2]

Therefore, taking into account these three components, the global irradiance on a plane tilted α degrees from the horizontal, Figure 2.2, can be evaluated from the well-known equation:

$$I_\alpha = I_n \cos\beta + I_d R_d + \gamma I R_{gr} \qquad (2.1)$$

being I_n the direct normal irradiance, β the angle of incidence of the Sun rays on the tilted plane, I_d the diffuse horizontal irradiance, R_d the diffuse transposition factor, γ the foreground's albedo, I the global horizontal irradiance, and R_{gr} the ground reflection transposition factor. Furthermore, the different irradiance components are interrelated by the following equation:

$$I = I_n \cos\phi + I_d \qquad (2.2)$$

being ϕ the instantaneous Sun's zenith angle.

Regarding the rest of the components in (2.1), while the calculation of the tilted direct component is purely a geometric matter when its value on the horizontal plane is known and, in this manner calculated straightforward ($I_n \cos\beta$), the computation of the diffuse component on a surface of a given orientation and tilt is not so simple. The evaluation of the ground-reflected diffuse irradiance is dependent on the R_{gr} factor. It is to note that generally the ground reflection process is considered ideally isotropic, hence R_{gr} can be simplified into:

$$R_{gr} = (1 - \cos\alpha)/2 \qquad (2.3)$$

In addition, the foreground albedo (γ) can be experimentally measured on-site or modeled [14], although using approximated values of γ, as those in Table 2.1, together with the isotropic approximation for R_{gr}, do introduce some uncertainties in the irradiance estimation.

Finally, R_d is usually the most difficult component to determine. If the diffuse irradiance is considered to be ideally constant over the whole sky hemisphere, R_d would be obtained straight from another simple isotropic approximation:

$$R_d = (1 + \cos\alpha)/2 \qquad (2.4)$$

But, reality shows that depending on the orientation of the surface under consideration the radiation that it receives will differ. A plane of tilt α facing the Sun receives more diffuse

radiation than a plane with the same tilt in the opposite direction. Hence, various anisotropic diffuse models have been proposed to estimate this anisotropy and calculate a refined value of R_d [2, 14-16]. Most of them will be shortly explained along this section.
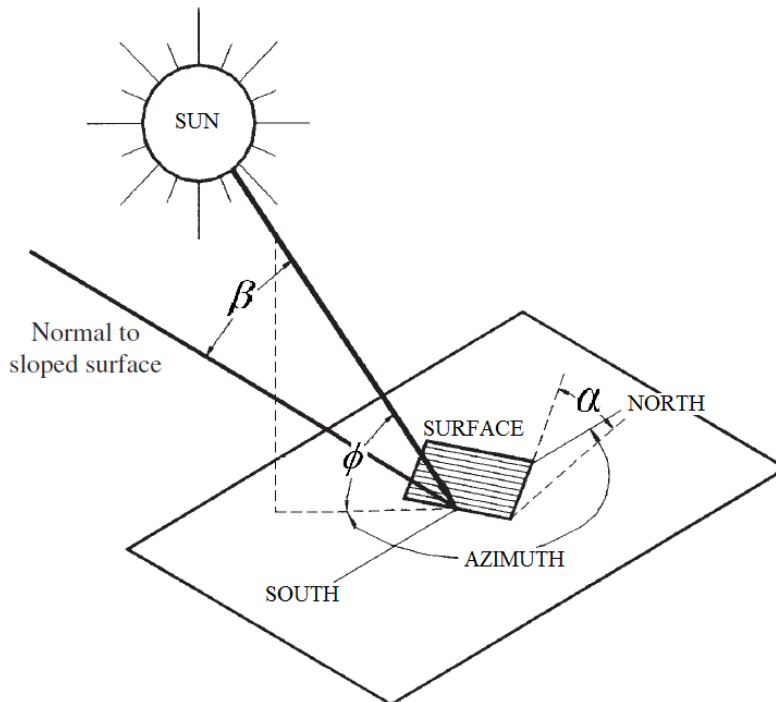

Figure 2.2 Solar geometry of a sloped surface. Source: [2]**.**

The expression in (2.1) can only be used in the case that the three different irradiances (I, I_n and I_d) are known, or when two of them are known and the third one can be estimated by using (2.2). If only one of them is available, the other two must be estimated.

Due to the cost and difficulty on measuring the different irradiance components, the three of them are not normally available [17-19], and even less for tilted surfaces. Usually, meteorological stations do register the global irradiation on a horizontal surface recorded on a day-integrated basis. Not so usually, some stations incorporate further measurements such as the diffuse irradiation, recorded also on a day-integrated basis, or even both diffuse and global horizontal irradiation but preciously recorded on a detailed hourly-integrated basis. Finally, some rare cases of stations do record irradiation values on different orientations and tilted surfaces as well as the normal direct irradiance by means of a pyrheliometer [2]. Therefore, because of the usual lack of measured data, mathematical models need to be

developed to generate, normally from the global irradiance data, the corresponding expected components at a certain location and over any possible tilted plane. The normal procedure for the determination of these radiation components can be observed in Figure 2.3. It presents various steps of calculation, using various mathematical models and approximations at every step, what induces a reduction in the final accuracy. When statistical data on daily sunshine hours or monthly-averaged daily horizontal global radiation are not available, other calculation strategies have been developed in order to achieve similar results. Figure 2.4 represents the different steps which can be followed in order to determine the hourly radiation received on a sloped surface when only atmospheric parameters such as sunshine, temperature, humidity or atmospheric pressure are available. As for the case of the calculation procedure in Figure 2.3, accuracy of the estimation is reduced with every step. Normally, the accuracy of the intermediate and final estimations is considered to be higher with the increasing number of known input parameters for the models.
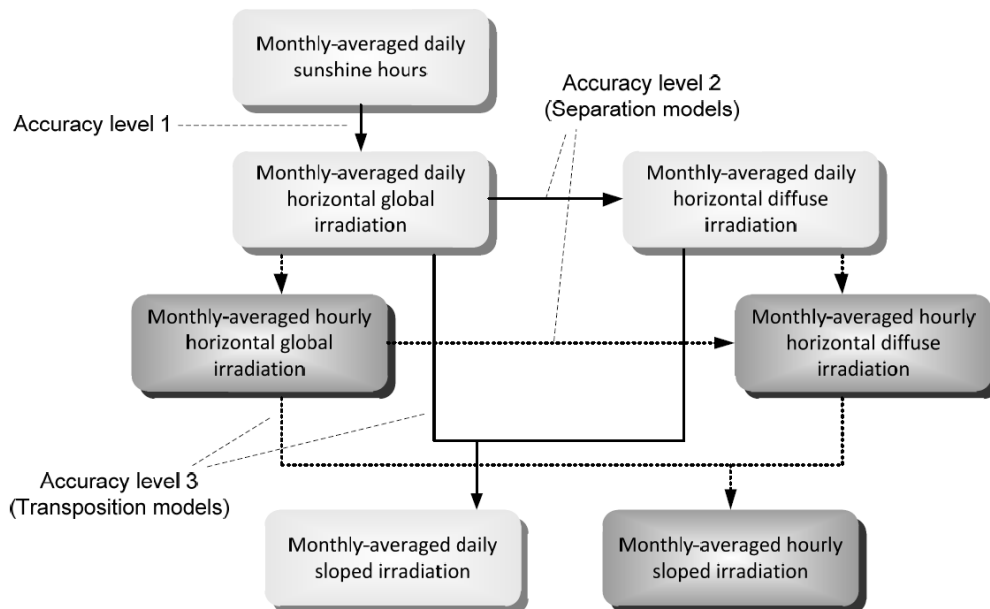
**Figure 2.3 Flow diagram for the monthly-averaged daily and hourly sloped irradiation calculus.
Source:** [2]**.**

The coming section aims to present a slight review of the different mathematical models proposed with computational purposes for the successive calculation steps introduced in Figure 2.3 and Figure 2.4 which allow estimating the various radiation components on horizontal and tilted surfaces.

2.1.2. Solar radiation modeling.

It has already been referred that the frequency at which solar radiation data are required depends on the application. Although monthly-averaged daily irradiation has traditionally been the basic temporized radiation parameter and various models were developed to analyze its components, it is now possible with the advent of cheap and powerful desk-top computers to perform energy-system simulations using hourly or sub-hourly data. Such simulations, however, require reliable estimates of irradiation on tilted or slope surfaces, values which may be computed from the corresponding horizontal global and diffuse energy data. However, long-term hourly data for these latter two quantities are rarely available too. Therefore, methods are required for estimations to be carried out from long-term records of daily irradiation, Figure 2.3, or other meteorological parameters, Figure 2.4. Therefore, models which enable computation of hourly or instantaneous irradiance data are found also, leading with this increased sampling frequency to a more accurate modeling of solar energy processes.

In all, the multiple mathematical models related with solar radiation can be classified into two main groups: separation and transposition models or methods. These groups are described and some of the main methods for each of them presented in the following.

a) Separation models

These models have been developed in order to separate the direct and diffuse components of the radiation when only the global horizontal irradiation is initially known. Some of them deal with the estimation of hourly diffuse irradiation from monthly-averaged daily irradiation and meteorological records (Liu-Jordan, meteorological radiation model…) while others determine the hourly diffuse irradiation on a horizontal surface in a more precise way from the records of hourly global irradiation (Orgill-Holland, Erbs, Reindl, Maxwell…) In all, a great number of studies and proposals have been introduced in the literature being most of them only local adaptions of general models. Therefore, among the different proposals, the following can be highlighted and are shortly introduced:

- Liu and Jordan regression method [20]: this approach is based on computing monthly-average values of daily diffuse irradiation from long-term averages of hourly diffuse irradiation, once the ratio of hourly to daily diffuse irradiation is known. The method presents a theoretical model for this ratio which shows good agreement with measured data for North America, as confirmed by some studies. Some latter

proposals suggested the possibility of refinement of the model by incorporating the dependence of the transmission coefficient (τ_D) on the clearness index (K_t), and including the angle of incidence in the relationship. Anyway, Liu–Jordan model may only be used to obtain hourly irradiation data from long-term records of monthly-averaged daily values. Therefore, some other models were needed for locations with absence of measured irradiation data.

- The meteorological radiation model (MRM) [21]: proposed by Muneer in 1998, it estimates the horizontal direct and diffuse components from just ground-based meteorological data such as air and wet-bulb temperatures, atmospheric pressure and sunshine duration. Such data is readily available worldwide, making MRM method an extremely useful tool. This model estimates the direct transmission through the terrestrial atmosphere based on its attenuation due to mixed gases (such as oxygen, nitrogen and carbon dioxide), water vapor, ozone and aerosols. Moreover, the model can estimate the horizontal solar components (diffuse, direct and global irradiance) on an hourly, monthly-averaged hourly, daily or monthly-averaged daily basis. It is not the only historic approach used within meteorological radiation models domain, but it is the most complete and its functioning structure is perfectly represented by the scheme depicted in Figure 2.4.

- Orgill-Hollands model [22]: this univariate model, using global irradiance as the only independent value and presented in 1977, was based on the analysis of hourly diffuse radiation on a horizontal surface registered along four years in Toronto (Canada). It mainly presents an equation to determine the hourly ratio of diffuse-to-total radiation received in a horizontal surface, being one of the first attempts of finding a regression model correlatating the hourly values of diffuse ratio I_D/I_G and the hourly clearness index (K_t).

- Erbs separation method [23]: the model by Erbs, introduced in 1982, is also univariate. The work followed the procedure of Orgill and Hollands to develop a regression model although Erbs used 65 months hourly pyrheliometer and pyranometer data for four USA locations. The model establishes in this way also a relationship between the hourly diffuse fraction and the hourly clearness index (K_t). This relationship was verified with a set of three years of data from Highett (Australia) and agreement was within a few percent. However, its regression equation was considered to be location dependent, what was ratified later by [24].
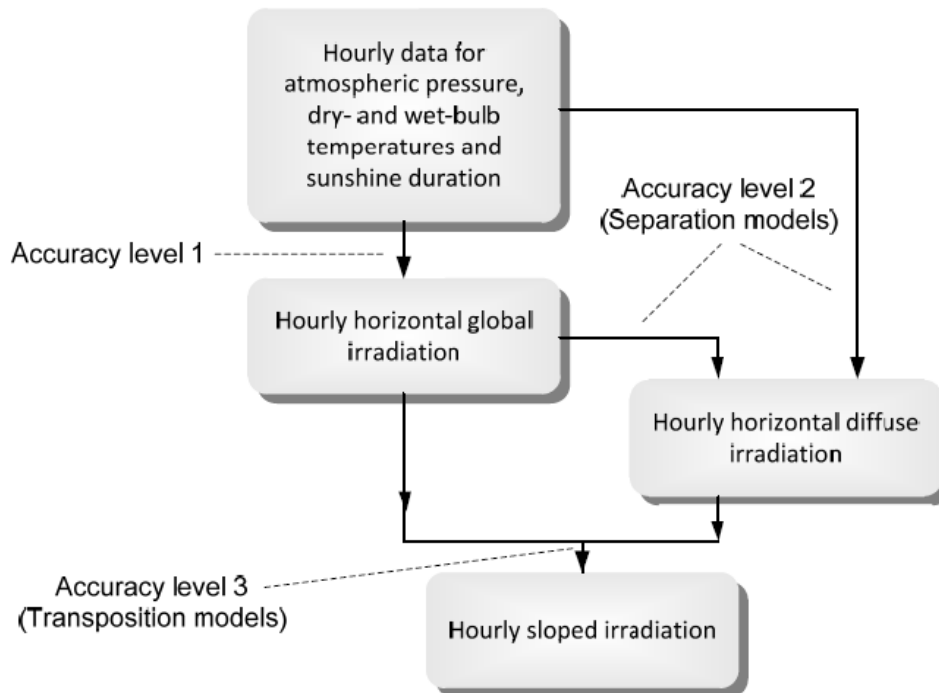
Figure 2.4 Flow diagram for the hourly sloped irradiation calculus from measured meteorological parameters. Source: [2]**.**

- Bugler model [25]: an alternative approach to obtain the diffuse component from measured hourly global irradiation on a horizontal surface was presented in 1977 by Bugler. The diffuse component is calculated using three different relationships; the appropriate equation is selected according to the value of the ratio of measured hourly global irradiation to hourly global irradiation computed for clear sky conditions. The method has been checked using measured hourly values in Melbourne over a five year period of irradiation on both a horizontal surface and a plane inclined at 38° to the horizontal facing north. The differences between the computed hourly values and the measured hourly values were found to be approximately normally distributed around zero with a standard deviation of 0.16 MJ/m^2. Bugler claims that its regression equations is independent of the location although its performance has been found to be inferior to that of Orgill and Hollands, as reported also in [24]. In fact, Bugler's procedure requires monthly data of precipitable water vapor and dust content, a clear disadvantage over the simpler approach of Orgill and Hollands.

- Maxwell model [26]: since different research studies showed limitations in the use of a univariate regression functions which do not adequately characterize the relationship between the diffuse or the direct fraction and the clearness index (K_t), Maxwell proposed in 1987 a bivariate model which separates the direct radiation and the diffuse radiation using a suite of functions of global irradiance and the Sun's zenith angle. This model is based on data obtained from 14 sites in Europe and the US. An improved version of this model was presented in [27], where the proposal was to split the Maxwell regression into two regressions, the first one correlating direct irradiation and clearness index when $K_t < 0.5$, and the second for the remainder range of the K_t where the diffuse ratio – clearness index regression was suggested to be kept.

- Reindl model [16]: among the various versions of the Reindl model, the most detailed approach is a also a multivariate regression. The direct/diffuse fraction is made dependent in this model not only on the clearness index but also on the Sun's zenith angle, the dry-bulb temperature and the relative humidity. Therefore, this model is, in essence, similar to the MRM model. Hourly data from five European and North American locations were used to develop this model.

Comparisons of the different models performance can be found in [24, 28], but although [24] distinguishes Orgill-Hollands' approach as being the best, not a clear optimal model is found in [28], what can be appreciated on the results presented in Table 2.2 (N = total number of measurements).

Component	Global		Diffuse		Direct	
Model	MBE (%)	RMSE (%)	MBE (%)	RMSE (%)	MBE (%)	RMSE (%)
All-sky, N = 116,927 Reference (W/m2)	543.5		173.8		598.2	
Meas. Global + Orgill	-0.4	4.5	-8.2	46.9	2.1	14.9
Meas. Global + Erbs	-0.4	4.5	-10.6	47.4	2.8	15.1
Meas. Global + Maxwell	-0.4	4.5	-24.6	48.2	6.7	14.9
Meas. Global + Reindl	-0.4	4.5	1.1	46.6	-0.6	14.2
Clear sky, N = 58,871 Reference (W/m2)	620.5		90.7		855.1	
Meas. Global + Orgill	-0.9	4.7	39.6	55.4	-4.9	7.1
Meas. Global + Erbs	-0.9	4.7	32.3	49.5	-4.1	6.7
Meas. Global + Maxwell	-0.9	4.7	-8.6	39.6	0.2	5.2
Meas. Global + Reindl	-0.9	4.7	57.8	82.7	-6.8	9.1

Table 2.2 Results for horizontal irradiance estimation performed by different mathematical models. Source: [28]**.**

Note the statistical parameters which have been considered to proceed with the comparison of the different mathematical models accuracy: the standard deviation (SD), the mean bias error (MBE), and the root mean square error (RMSE). These parameters have been used not only in this table but in all those represented in this section.

Apart from these separation models presented above, some other mathematical models stand out which can be classified as separation models since they are used to derive the different irradiation components from satellite images. These are:

- Ineichen or Perez model [29, 30]: this model was developed in 2002 to define a modified air mass independent Linke turbidity coefficient parameterization. It uses hourly radiance images from geostationary weather satellites, daily snow cover data, and monthly averages of atmospheric water vapor, trace gases, and the amount of aerosols in the atmosphere to calculate the hourly total insolation (Sun and sky) falling on a horizontal surface. Linke turbidity, atmospheric water vapor, trace gases, and aerosols are derived from a variety of sources.

- ESRA model [31, 32]: this separation model was developed in the frame of the European Solar Radiation Atlas (ESRA) and used in Heliosat-2 (2002). It is based on previous high accuracy analysis of the integral Rayleigh optical thickness which provided improved Linke turbidity assessments [33]. The input parameter for this model is the Linke turbidity coefficient, measured under air mass 2 conditions (equal to a zenith angle of 60 degrees).

- SOLIS model [34]: it was developed as a new spectral clear sky transmittance model in the frame of the European project Heliosat-3 (2005). The model is based on the radiation transfer model (RTM) calculations and on a modified Lambert-Beer function; it offers the possibility to obtain a good match between fitted and calculated values using only two zenith angle RTM calculations. The irradiance components are obtained by integration over the solar spectrum. For this model, the input parameters are the ozone content, the water vapor content in (measured in kg/m^2 and representing the precipitable water content of the atmosphere for one square meter) and the aerosol optical depth (AOD) at 550 nm.

- Bird-Hulstrom model [35, 36]: this is a simple model for calculating clear-sky direct and diffuse spectral irradiance on horizontal but also on tilted surfaces. It is based on previous simple algorithms and on comparisons with rigorous RTM calculations and

limited outdoor measurements which allowed the authors to developed a transmittance expression for the different attenuation processes in the atmosphere (Rayleigh scattering; aerosol scattering and absorption; water vapor absorption; and ozone and uniformly mixed gas absorption). The model needs mainly three input parameters: the water vapor column, the broadband AOD (calculated from the spectral attenuation at two wavelengths commonly used by meteorological networks: 380 and 500 nm), and the ozone column. But other input parameters are also included: the solar zenith angle, the collector tilt angle, the atmospheric turbidity, surface pressure, and the ground albedo.

- Molineaux model [37]: this model is based on the equivalence between the atmospheric AOD weighted over the whole solar spectrum and the monochromatic AOD at a certain wavelength. This key wavelength is ~0.7 μm, which is only slightly influenced by air mass and aerosol content. On the basis of this result, the model proposes simple relations to predict monochromatic AOD from pyrheliometric data and vice versa. The global irradiance component cannot be evaluated with this model. The input parameters are: the water vapor column in [cm] and the broadband AOD (or AOD at 700 nm).

- CPCR2 model [38]: a two band radiation (UV/Visible band (0.29–0.7 μm) and infra-red band (0.7–2.7 μm)) modeling technique is developed for clear sky conditions. For each band, the transmittance function of each extinction layer (ozone, water vapor, mixed gases, molecules and aerosols) is parameterized. Therefore, the direct and diffuse radiation components are obtained as functions of these layer transmittances. The photosynthetically active radiation (0.4–0.7 μm) and illuminance (0.39–0.76 μm) components can be easily derived from the UV/Visible band irradiances. The aerosol input to the model is the Angström size coefficient α (1.3 was used in the two bands) and the Angström turbidity coefficient β, which are related to the aerosol optical depth by the Angström relation.

- REST2 model [39]: this is a high-performance model to predict cloudless-sky broadband irradiance, illuminance and photosynthetically active radiation from atmospheric data. Its derivation uses the same two-band scheme as in the previous CPCR2 model, but with numerous improvements. Great attention is devoted to precisely account for the effect of aerosols, in particular. As for CPCR2, the main input parameters to the model are the water vapour content of the atmosphere.

- Kasten model [40]: The basis of this model is to calculate the irradiances by taking into account the atmospheric absorption and diffusion at two different altitude levels: 2500 m and 8000 m. The input to the model is the Linke turbidity also at air mass 2 conditions.

All stations	Normal direct average: 909 W/m²			Horizontal direct average: 497 W/m²			Horizontal global average: 547 W/m²			Horizontal diffuse average: 51 W/m²		
Model	Bias	RMSE	SD	Bias	RMSE	SD	Bias	RMSE	SD	Bias	RMSE	SD
Ineichen	-16	30	35	-10	19	16	-1	25	20	-10	26	19
ESRA	5	27	29	4	15	14	22	33	21	17	30	19
SOLIS	2	29	29	-1	14	14	10	27	21	11	25	18
Bird	8	29	33	4	18	16	17	33	21	13	26	18
Molineaux	1	27	28	0	14	13	-	-	-	-	-	-
CPCR2	-14	28	33	-9	18	15	12	28	21	21	30	18
REST2	-25	27	37	-12	18	14	2	24	20	14	26	18
Kasten	6	34	38	8	20	17	14	32	24	6	36	32

Table 2.3 Results for the three radiation components calculated with eight different separation models on 16 data banks (based on the clearest input conditions). Source: [41]**.**

A comparison for these eight clear sky solar irradiance separation models from satellite images has also been evaluated and can be consulted in [41]. A set of 16 independent data banks covering 20 years/stations, altitudes from sea level to 1600 m and a large range of different climates has been taking for analysis in that work. The results of the study, evaluated on very clear condition measurements, are within 4% in term of standard deviation as can be observed in Table 2.3. Therefore, it can be concluded that the accuracy of the input parameters such as the turbidity is crucial in the validity of the obtained radiation components, and that the choice of a specific separation model is secondary. In this sense, the model selection criteria should be based upon either implementation simplicity, input parameter availability (Linke turbidity or aerosol optical depth) or the capacity of the model to produce spectral radiation.

b) *Transposition models*

Once models for separating incident horizontal diffuse and global irradiation have been introduced, the next step is to obtain the incident slope direct and diffuse energy. This estimation is performed by means of different transposition models compiled in the literature.

For the case of a tilted surface, the direct component can be mathematically calculated as it was already presented after equation (2.1), using the expression $I_n \cos \beta$. On the contrary, it stands out that the diffuse irradiance consists now of sky-diffuse and ground-reflected components. Since the latter highly depends on the type of soil (or surface) where the

measurement is performed, it is very difficult to model, being usually treated in a statistical way and using typically established parameters, Table 2.1. So, most models focus on the diffuse component over slope surfaces determination.

Among the different proposed transposition methods, the following can be highlighted according to their historical development [2]:

- Isotropic model: it is the simplest of all slope irradiance models, and being classified within the first generation models group, it assumes an isotropic sky. Therefore, equation (2.4) can be applied to determine the diffuse irradiation. However, it has already been demonstrated that this radiation component is not isotropic in nature [42] and that, on the contrary, it is a function of the solar altitude and azimuth.

- Circumsolar model: this model is also classified within the first generation group although it was published in 1983. It assumes that the sky-diffuse radiation, together with the direct radiation, emanate from the direction of the solar disc [43]. It can only be adopted under exceptionally clear-sky conditions although even under those circumstances cannot be considered a serious contender.

- Threlkeld's model: this is the first of the second generation group of models. This group which includes Threlkeld's, Temps-Coulson, Klucher's, Hay's, Skartveit-Olseth and Reindl's models, introduces a differentiation between the radiance distribution of clear and overcast skies offering some accuracy improvement with regard to the first generation group. However, these models do not separate their generic development from the isotropic case and as such normally revert to the latter under overcast conditions. Focusing on the Threlkeld's model [44], presented in 1962, it was derived only from clear-sky radiation data, measured exclusively on vertical planes. Even like that, a numerical fit to Threlkeld's data was some time later adopted by the American Society of Heating, Refrigerating and Air-Conditioning Engineers (ASHRAE), which generalized the model by simply specifying the isotropic formula for all tilts different from vertical [45]. This composite ASHRAE model is important in practice since it is used routinely by building engineers for solar heat gain and cooling load calculations.

- Temps-Coulson model: contrary to the previous one, this model which was introduced for the first time in 1977 [46] suggests another anisotropic modification to

the clear-sky diffuse radiance model trying to solve deficiencies of the isotropic model near the horizons and in the circumsolar region of the sky.

- Klucher's model: this model, published in 1979 [47], represents a progress of the previous one by extending the anisotropy from clear to all sky conditions, correcting in this way overestimation under overcast conditions.

- Hay's model: the same year 1979, Hay presented its model [48] which assumes diffuse radiation incident on a surface to be composed of circumsolar and uniform background sky-diffuse components. Both are weighted in the model.

- Skartveit-Olseth model: this is a model presented in 1986 which focuses on high latitude locations and, therefore, presents an equation adapted to them [49].

- Reindl's model: this model was presented in 1990 and it is a combination of the Hay and Klucher's models. It simply proposes a new equation, based on those models, for the calculation of the diffuse irradiance [16].

- Moon-Spencer model: this is the first one of the third generation group of models. This group, which includes Gueymard's, Perez's and Muneer's models, treats the sky diffuse component as completely anisotropic, decomposing non-overcast irradiance as the sum of different components. For the case of the Moon-Spencer model, it was presented in 1942 [50] and pretended to demonstrate a relationship between the luminance of a patch of an overcast sky and its zenith angle. Although not really representing a model for the diffuse radiation on slope surfaces, this work was used as a base in the three third generation models explained later on.

- Steven-Unsworth model: this model was also used as reference or support for the three coming third generation models. The work was presented in 1980 [51] and found some discrepancies with the previous models, justifications could be found for those variations though. Furthermore, this model already divided the predicted irradiation on an inclined surface into the circumsolar and the background components, establishing an equation which determines them, and hence the global irradiation, only as a function of the inclination of the surface and of the radiance distribution index (parameter called "*b*" which the authors report in their work only for overcast and clear sky conditions, what represents a problem for other sky conditions in this model).

- Gueymard's model: presented in 1987 [14], the main assumption used in it to point out that the radiance of a partly cloudy sky may be considered as a weighted sum of radiances of a clear and an overcast sky. Thereupon, based on Steven-Unsworth's work, Gueymard introduces the concept of the weighted normalized radiances.

- Perez model: contrary to the previous, and to all the rest of models which only consider two components, this model, introduced in 1990 [15], is based on a three-component treatment of the sky-diffuse irradiance. These three components are modified by parameters such as the circumsolar or the horizon brightness coefficients or by terms accounting for the respective angles of incidence of circumsolar radiation on the tilted or horizontal surfaces. Values for these parameters were tabulated simplifying the calculation of the model.

- Muneer's model: finally, the last of the third generation models' is the Muneer's model. It was presented progressively in 1987, 1990 and 1995[52, 53] being adapted to studies on different locations. The novelty of this method is that it treats the shaded and the sunlit surfaces separately. Furthermore, it distinguishes between overcast and non-overcast conditions of the sunlit surface. Moreover, the value of the radiance distribution index is here used too, and its value is proposed to be obtained by finding a linear curve fit between vertical surface irradiance and horizontal diffuse irradiance.

To summarize, a similar comparison to that presented for the separation methods can be found in [28]. On this reference, ten different transposition methods (accounting most of those introduced here) are compared under different quality conditions of the input data provided to them (real measurements or estimations obtained from four different separation methods). The main conclusion extracted from the comparison is that the estimation accuracy of the different transposition methods is quite similar, as can be appreciated in Table 2.4, with the exemption of the models using isotropic approximations (isotropic and ASHRAE) which underestimate systematically the radiation. In this sense, for the rest of models, a good estimation of the solar radiation components on a tilted plane is also concluded to be much more influenced by the quality of the input data introduced to the transposition model than by the type of model itself. Therefore, the major part of the uncertainty in the predicted tilted irradiance at a sunny site is generally caused by the direct/diffuse separation obtained by empirical models whenever these components are not measured locally.

The same statistical parameters have been considered again in Table 2.4 to proceed with the comparison. Results are obtained in this case for three different surfaces: a fix surface south oriented and tilted 40º, a fix surface south oriented and tilted 90º (vertical) and a surface tracking the Sun. These are in percentage referring to the mean plane-of-array irradiance Is for each plane. Top pane: results for real-sky conditions; bottom pane: results for clear-sky conditions only.

Plane	40ºS		90ºS		Tracking	
Real-sky, N = 116,927	MBE (%)	RMSE (%)	MBE (%)	RMSE (%)	MBE (%)	RMSE (%)
Mean I_S (W/m²)	643.2		432.3		835.9	
Isotropic	-5.1	7.8	-5.8	11.6	-8.1	9.6
ÁSHRAE	-5.1	7.8	6.5	13.4	-8.1	9.6
Temps	1.3	6.0	4.8	11.3	-4.5	6.6
Klucher	-1.4	4.6	0.3	8.5	-6.0	7.5
Hay	-2.1	5.5	-2.7	8.2	-1.9	6.1
Skartveit	-2.4	5.7	-4.3	9.3	-2.2	6.4
Reindl	-1.8	5.3	-0.4	7.7	-1.5	5.9
Gueymard	-0.8	4.3	5.2	10.6	-0.9	4.2
Perez	-2.7	6.7	-4.7	12.0	-2.3	5.8
Muneer	-0.4	5.2	2.5	9.4	-5.4	7.0
Clear-sky, N = 58,871						
Mean I_S (W/m²)	763.0		523.5		1019.6	
Isotropic	-3.6	4.9	-4.9	8.1	-5.5	6.2
ÁSHRAE	-3.6	4.9	0.1	4.5	-5.5	6.2
Temps	-0.9	2.7	-0.3	5.0	-4.0	4.7
Klucher	-1.0	2.8	-0.5	5.1	-4.1	4.8
Hay	-1.0	3.2	-2.2	5.2	-0.3	2.7
Skartveit	-1.0	3.2	-2.2	5.2	-0.3	2.7
Reindl	-0.9	3.1	-1.2	4.7	-0.1	2.7
Gueymard	-1.1	2.7	-0.2	3.8	-1.2	2.1
Perez	-0.7	2.6	-0.4	3.9	-1.0	2.1
Muneer	0.4	2.8	2.0	5.1	-3.3	4.0

Table 2.4 Performance of ten transposition models when using optimal input data (direct + diffuse) and a whole 12-month dataset basis. Source: [28]**.**

As for the case of the separation models, more detailed information can be found in the cited literature but an accurate analysis for each of them is beyond the scope of this thesis.

2.1.3. Summary.

Therefore, it can be concluded from this section that many empirical functions have been proposed aiming to model the solar irradiance values at any location. In summary, one could start a quick review with the regression type model based on sunshine duration which was first investigated in [6] and applied later to different locations [54-57]. And from there on, different regression models incorporating trigonometric functions which were proposed by

[18, 58] as well as others incorporating multiple meteorological variables [52]. Nevertheless, it must be noted that linear regression models generally present considerable limitations when used in nonlinear systems. Thereupon, irradiance data have also been modeled using harmonic analysis methods due to its time dependent characteristics [59-61]. Furthermore, some statistical techniques have also been proposed, which model the irradiance with different resulting distributions. In this sense, while a Weibull distribution is identified in [62], other authors concluded that solar irradiance is better fitted by a Beta distribution [63] or even a Bimodal distribution [64, 65]. Resulting variations depend, among other factors, on the sampling time of the input irradiance signal and the location where the irradiance is studied [19, 65-67], which is a key parameter. Finally, to end with this final review, artificial intelligence, and more precisely, neural networks have been equally used as an advanced technique to forecast local irradiance [68, 69]. Good results have been reported for Arabia Saudi and Egypt by [70] and [71], respectively.

However, since models are locally adapted and depend on different assumptions and approximations, none of them can assure an exact instantaneous irradiance prediction in a generic location at any time. Only approximated estimations representing statistically-averaged values can be forecasted. As a matter of fact, these forecasted values largely vary as a function of the instantaneous atmospheric phenomena (clouds) which take place on many orders of magnitude, regarding both space and time. The scales of these phenomena range from local clouds on length scales of hundreds of meters and timescales of seconds to seasonal variations on global geographic scales. Therefore, constant instantaneous variations with regards to the standard solar radiation estimation are going to be faced at any location.

Even like that, a general estimation of the available solar resource in one determined location has to be considered prior to the investment when analyzing the economic and financial viability of a new installation. This is a main factor to be studied by investors. Thus the liability and precision of that estimation turns to be a key point for the solar PV industry.

An important number of solar resource data information sources can be identified. Most of them are introduced in the following section.

2.2. Solar resource data information sources.

As previously introduced, the solar resource information needs really differ depending on individuals interested on it. On one hand, solar industry manufacturers or regulators defining policies on the electric solar generation sector do generally have enough information with

solar radiation monthly-averaged values or solar radiation probability statistics to define the financial viability of new PV projects and conceive optimal support programs. On the other hand, solar power plant developers need detailed time series of direct normal irradiance derived from high resolution, high accuracy data sources to estimate their production and optimize the power plant operation. Equally, map-based time series of global irradiance are needed to predict and analyze possible electric grid power flows in regions with large penetration of renewable, notably PV plants. Thus, real-time data flow is required for large-scale PV systems operation and monitoring and for the forecasting of solar electricity generation to optimize supply/demand patterns in the electricity grid.

A good number of databases can be consulted nowadays for accessing solar radiation and associated climatic data. Some of them integrate geographic information systems (GIS) which allow for spatial analysis taking into account temperatures, elevations of the terrain, shadows… All of them present modeled global irradiance data approximations obtained from two main sources: in situ (ground) and satellite observations. Thus, from the measured data, models capable of exploiting geostationary satellite (Meteosat, GOES, MSAT, etc.) images on the one side [29] (most of the separation methods presented in the previous section), and models or methodologies for the calculation of the solar radiation from surface meteorological observations [72] on the other side have been widely developed. There is an inherent difference between the two types of databases and the methods how their data are processed. Advantages and disadvantages can be found on any of them.

On one hand, databases interpolated from ground observations (e.g. Meteonorm, ESRA, and PVGIS Europe) are sensitive to the quality of measured data and to the density of measuring stations. Furthermore, they typically represent only statistical values. So, their accuracy is not homogeneous and, due to the accumulation of estimation and interpolation errors can be certainly low for some locations placed far away from any substation.

On the other hand, the satellite-derived databases are affected by higher uncertainty in the cloud cover assessment when the ground is covered by snow and ice, near the coast or for low Sun angles. Thus, satellite-derived maps are more sensitive to errors in high mountains and high latitudes, due to low observation angles and complex interactions with terrain. However, they are closer to the real time and site specific values [73] since they present spatially continuous (grid) data with consistent accuracy, measured by the satellites at frequent and regular time sampling. Spatial resolution of satellite derived products is in a wide range of 1 to 300 km. The relative accuracy of the estimations, measured by the RMS,

is approximately about 20 to 25% for hourly values, and 15 to 20% for daily values, and less than 15% for monthly averages (with some seasonal variation). So, unlike interpolated maps from ground stations, where the accuracy depends on their spatial distribution, the accuracy of satellite assessments is spatially more stable and practically without bias. In this sense, it can be concluded that the meteorological geostationary satellites have a high potential in the field of solar irradiance derivation and, although affected by some factors, when compared to ground measurements interpolation they present a greater spatial and temporal coverage [41].

2.2.1. Satellite data derived databases.

Geostationary weather satellites have been distinguished as an important source for developing solar radiation databases at global and regional scales. Some databases which base their results on images obtained from satellites can be highlighted. These database use different mathematical models, some already introduced in this chapter, which have been developed to calculate high resolution and quality solar radiation databases from the corresponding satellite images. Note that some of these models are being refined lately in order to improve more and more the calculation capacity as well as to increase the spatial and temporal accuracy of the radiation components.

Therefore, the following databases derived from satellite images can be highlighted.

a) Helioclim [74]

These databases are an on-going effort of the Ecole des Mines de Paris/Armines, Center for Energy and Processes (France). Helioclim-1 provides information on solar radiation using Meteosat prime satellite images, at reduced resolution with a grid cell of about 30 km × 30 km at the equator. The database consists of daily global irradiation for a period 1985-2005, covering Europe, Africa, southwest Asia and part of the South America. The higher resolution database HelioClim-2 contains time-series of hourly irradiance calculated from Meteosat-8 satellite since February 2004. These databases run since 1985. They can be accessed through the SoDa service.

b) Solar Energy Mining (SOLEMI) [75]

SOLEMI is a service set up by the Deutsches Zentrum für Luft- und Raumfahrt (DLR, German Aerospace Agency) which provides high-quality irradiance data mainly based on Meteosat satellites with a nominal spatial resolution of 2.5 km and half-hourly temporal resolution. Solar radiation maps, high frequency time series and direct normal irradiance are

available under request for almost half of the Earth's surface. Together with related GIS services (STEPS), these data are used mainly in preparatory stages of renewable energy projects.

c) SATEL-LIGHT [76]

The European Database of Daylight and Solar Radiation (Satel-light) was funded by the European Union (Directorate General XII) from 1996 to 1998. It provides data for Western and Central Europe of statistical type: monthly averages, frequency distributions of half hourly values. The data can be also consulted for free in the form of active maps or in the form of a report for the chosen site. They represent a period of 1996-2000 and were derived from Meteosat images (solar radiation, and daylight) and ground measurements (temperatures). Registration is compulsory.

d) NASA Surface Meteorology and Solar Energy (SSE) [77]

The NASA's Surface Meteorology and Solar Energy (SSE) data set was developed by the project Prediction of Worldwide Energy Resource (POWER). The data set is freely available and it contains over 200 satellite-derived meteorology and solar energy parameters. It represents monthly averaged from 22 years of data (1983-2005) interpolated to $1° \times 1°$ grid regions (grid size of about 111 km at the equator) covering the entire globe. It provides data tables for a particular location, color plots on both global and regional scales. Finally, it contains average daily global solar radiation data for 1195 ground sites from the 30 years period (1964 - 1993), extracted from World Radiation Data Centre (WRDC) data set. The data are considered accurate for preliminary feasibility studies of renewable energy projects and their purpose is to fill gaps where ground measurements are missing. It is used as data provider for two free of charge software design tools:

- HOMER: The Hybrid Optimization Model for Electric Renewables (HOMER) which is used for designing standalone electric power systems that employ some combination of wind turbines, photovoltaic panels, or diesel generators to produce electricity.

- RETScreen[®]: the RETScreen[®] International Clean Energy Project Analysis Software is a decision support tool which can be used worldwide to evaluate the energy production and savings, costs, emission reductions, financial viability and risk for various types of Renewable-energy and Energy-efficient Technologies (RETs).

e) *ECMWF Archive* [78]

This climatic data archive is the resulting product of data assimilation and numerical weather modeling from both ground measurements and satellite images. The data assimilation concerns different reanalysis projects performed by the European Centre for Medium - Range Weather Forecasts (ECMWF). Three of these reanalysis can be highlighted: the ERA-15 reanalysis (comprehending years from 1979 to 1993), the ERA-40 reanalysis (years from 1957 to 2002) and the ERA-Interim reanalysis (1989 to 2011). Reanalysis datasets are created by assimilating ("inputting") climate observations using the same climate model throughout the entire reanalysis period in order to reduce the effects of modeling changes on climate statistics. This effort involves recovery, quality control and assimilation of data from all available observations.

Thus, the data provided in this archive are commercially available at the resolution of $2.5° \times 2.5°$ or even higher through the extended web services, and they are useful for validating long-term model simulations, for helping develop a seasonal forecasting capability and for establishing the climate of EPS (Ensemble Prediction System) forecasts needed for construction of forecaster-aids such as the Extreme Forecast Index.

f) *ESRL Archive* [79]

This archive, updated and maintained by the Earth System Research Laboratory (ESRL) from the National Oceanic & Atmospheric Administration (NOAA, U.S. Department of Commerce) comprehends also different reanalysis datasets. In this case, the three highlighted reanalysis are: the National Centre for Environmental Prediction (NCEP) / National Centre for Atmospheric Research (NCAR) NCEP/NCAR reanalysis I (comprehending form 1948 to the present), the NCEP/DOE (Department of Energy) reanalysis II (1979-2010) and the 20th Century Reanalysis (V2) (1871-2008).

The global archive presents a grid resolution of 210 km (at the equator) and it is available without restrictions. It contains also flux parameters, including global downward shortwave radiation. Daily values are accessible also through SoDa portal, presented below in this chapter.

Further information on climatological reanalysis databases can be found in the web page: http://reanalyses.org/.

2.2.2. Ground measurements derived databases.

As previously introduced, a second important source of information for developing solar radiation databases are ground measurements registered at ground meteorological stations. These stations are worldwide located with randomly distribution what generates accuracy problems in the solar radiation estimation for certain regions. Furthermore, the measurement of daily global horizontal radiation is more common in most of the stations than the measurement of both global and diffuse values. In addition, rarely any of them measures radiation on inclined surfaces. Finally, few stations measure radiation values on an hourly basis rather than in a day-integrated basis. To overcome these handicaps, other measured parameters such as sunshine duration or cloud cover are used together with empirical solar radiation estimation models, as those presented before along this chapter, are used. Beside those models estimating diffuse radiation values as well as radiation on inclined surfaces, interpolation techniques are implemented in this ground measurements based databases in order to get spatially continuous solar data information connecting the different sites (substations). So, quite a lot of estimations and approximations (together with the pyranometer accuracy) are performed, which impacts the overall accuracy of the database, dropping for certain regions, especially those placed far away from any substation.

Some of the main databases derived from ground measurements are the following.

a) National Meteorological Agencies

The different national weather services have registered climatic data in their ground meteorological stations for more than 50 years. Measurements made by these meteorological departments in most countries are in a manner such that the different climatic and geographical regions are covered. Some meteorological agencies which can be outlined are:

- The Japanese Meteorological Agency [80]: http://www.jma.go.jp/jma/indexe.html

- The Spanish Agency [81]: http://www.aemet.es/es/portada

Several institutions collect data from national files and archive them into global databases, as it is the case for the World Meteorological Organization (WMO) [82] which, supported by the UNESCO, compiled a CD-Rom with monthly and annual averages of measured parameters worldwide for the period 1961 to 1990. This organization also provides links and access to the National Meteorological Services and promotes projects which have resulted in different international databases.

b) *Global Energy Balance Archive (GEBA)* [83]

The GEBA is a database developed under one of the project fostered by the WMO. It was launched in 1988 and is maintained by the ETH Zurich. This database holds about 250000 records of monthly mean energy fluxes measured at more than 2000 stations worldwide, Figure 2.5. It incorporates various energy balance components, with a total of 19 different variables. These include, for example, global radiation, short- and long-wave radiation and turbulent heat fluxes. The database is regularly updated, with great importance being attached to a series of quality control procedures.
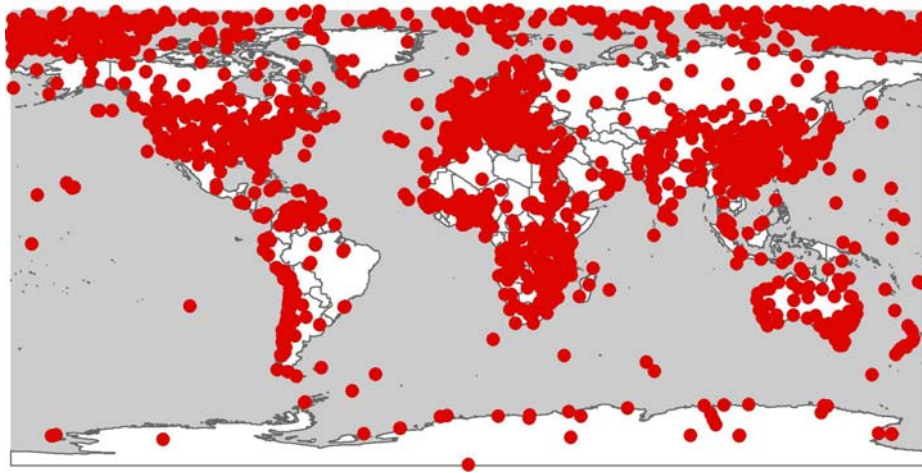
Figure 2.5 Location of ground substations used by the GEBA database. Source: GEBA Website.

g) *Baseline Surface Radiation Network (BSRN)* [84]

This is another project sponsored by the WMO to support climate research. It aimed at detecting long-term variations in irradiances at the Earth's surface, which are believed to play an important role in climate change. Measurements of irradiances are at 1Hz, and the 1-min statistics (mean, standard deviation, and extreme values) with quality flags stored at a centralized data archive at the World Radiation Monitoring Center (WRMC) in Zurich, Switzerland. The data are quality controlled both at any of the 39 stations and at the WRMC. The original 1-min irradiance statistics are stored at the WRMC for 10 years, while hourly mean values are transferred to the World Radiation Data Center in St. Petersburg, Russia. The BSRN covers the Earth's surface from 80 degrees N to 90 degrees S. The BSRN radiation measurements are used to validate the radiation schemes in climate models and to calibrate satellite algorithms.

h) World Radiation Data Center (WRDC) [85]

Headquartered in St Petersburg, Russia, it is one of the World Data Centers associated to the WMO. It counts with its own archive which contains data from about 1200 stations. The measurements are unevenly distributed in time and space. Mainly global horizontal irradiation and sunshine duration can be mainly retrieved (hourly, daily and monthly values), being diffuse irradiation also available for some stations.

i) International Daylight Measurement Program (IDMP)[86]

This program was set up in 1991 by the Commission Internationale de l'Eclairage (International Lighting Commission) based in Vienna, Austria. It operates a network with 48 stations, specialized in high frequency and high quality daylight and solar radiation measurements, and 15 stations measuring the distribution of light over the sky vault. This program seems quite stuck since no updates have been done for a long time. Furthermore, the accessibility to the data from each station depends on the policy of the particular institution involved.

2.2.3. Advanced databases.

There are information systems which cannot only be considered as a simple online database to be consulted for determined location's solar radiation information. These systems present advanced functionalities such as interactive maps, dedicated software packages and support services which provide the customer with extended information and tools so as to exploit the basic solar radiation data and achieve an improved assessment for solar energy projects. The most important ones are briefly presented here.

a) European Solar Radiation Atlas (ESRA) [87]

Made on behalf of the European Commission within the JOULE II Program, it comprehends, as its name suggests, a solar radiation atlas for Europe up to the Ural Mountains and including neighboring Mediterranean territories. In fact, it can be considered a comprehensive publication documenting the state of the art in solar energy and applications in Europe at the end of 1990s. It was developed from the best available measured solar data during the period 1981-1990, complemented with other climatic or meteorological data, producing digital maps for the European continent. Satellite-derived maps helped in improving accuracy in the spatial interpolation. The radiation data can be obtained either in

the form of those maps (average values over ten-years for each month), or in the form of long-term time series for several tens of selected measuring stations.

b) Photovoltaic Geographical Information System (PVGIS) [88]

The PVGIS is an online tool for geographical assessment of the solar resource and the performance of the PV technology developed by the Joint Research Centre of the European Commission. It offers map-based information of solar radiation based on statistics, modulated by temperature and other climatic parameters for two different regions: the European subcontinent computed from ground measurements obtained during the period 1981-1990 (1 km x 1 km grid resolution), and the Mediterranean Basin, Africa and South-West Asia developed by processing and spatial enhancing of the HelioClim-1 satellite database, register during the period 1985-2004 (with a 2 km x 2 km grid resolution). This information system will be explained in detail in the following section.

c) Meteonorm [89]

Meteonorm is a comprehensive meteorological reference database. It provides access to meteorological data (solar radiation, temperature, humidity, wind speed, precipitation), estimated by interpolation, for solar applications, solar systems design and a wide range of other applications for any location in the world. It contains a database of ground station measurements collected from various sources such as the Swiss Meteorological Institute, the GEBA or the WMO, etc. The main period of the measurements was between 1961 and 1990. Very high resolution direct and global radiation maps (0.1-1 km) are provided, with cheaper prices for lower resolution ones (30 km).

d) Solar GIS [90]

SolarGIS is a web based system that includes high-resolution climate databases, maps and software for solar energy applications. It mainly features four map-based applications: iMaps (interactive maps), climData (access to solar radiation and air temperature data), pvPlanner (high-performance PV simulator with extensive reporting capabilities) and PVSpot (provides estimated electricity production of any defined PV system for certain period of time (e.g. a day, a week, a month, a year or a user specified period of time) according to the SolarGIS data with a 15-min time step. The solar radiation database is derived from Meteosat satellites data and atmospheric parameters using in-house computing infrastructure and high performance algorithms. Data are available from January 1994 or

January 1999 (depending on the region) up to present with a 3 km x 3 km grid. Any of the products require registration.

e) *National Renewable Energy Lab (NREL)* [91]

The NREL provides on its webpage and for the USA solar radiation data and derived products such as overview static maps, or even dynamic maps created by the NREL Geographic Information System team, as well as a range of publications, algorithms, and source codes. The maps include monthly-averaged and annually-average daily production estimations for two technologies such as photovoltaic (PV) or concentrating solar power (CSP). And these averages are also calculated in two different grids, or over surface cells of 0.1 degrees in both latitude and longitude (about 10 km in size), or on grid cells of approximately 40 km by 40 km in size. Note that NREL provides too a solar calculator named PVWATTS which can be used for performance estimates of grid-connected PV systems.

Solar maps provide monthly-averaged daily total solar resource information on grid cells. The insolation values represent the resource available for a flat plate collector, such as a photovoltaic panel, south-oriented at an angle from horizontal (tilt angle) equal to the latitude of the collector location. This is a typical practice for PV system installation, although other orientations are also used.

f) *SoDa – Solar Data Radiation* [92]

The Solar Radiation database (SoDa) was developed by the Centre Energétique et Procédés (CEP) from the School of Engineers Mines Paris-Tech and ARMINES. It offers a one-stop access to a large set of information relating to solar radiation and its use. This service itself is not a database but an innovative application, made of an Intelligent System (SoDa IS), which builds links to other databases from around the world. When request for some information, the SoDa service cooperates with other web servers to elaborate the appropriate answer using the data and software maintained on remote sites. For example, values of Linke turbidity factor which are provided by the HelioClim-1 can be accessed through the SoDa Web service (the database of the Linke turbidity factor is available for the whole world). Other sites integrated in SoDa by means of standard protocols are: Meteotest, ESRA, Satel-light, NCEP/NCAR, etc. Finally, it is important to point out that it offers two different sections with available information: one with free data and another one only available after registration.

g) *Solar and Wind Energy Resource Assessment (SWERA)* [93]

Developed by the United Nations Environment Program (UNEP), the SWERA project provides solar products with information on the solar resource at a specific location in developing countries that is available for use by solar technologies. These products include maps and data of available solar resource, as well as documentation on the methodology employed to generate these solar resource estimates. The data products and resource maps are derived from models, satellite images and global weather observations and do not contain site-specific measurement information.

2.2.4. Comparison.

With the goal of summarizing this section, the following Table 2.5 and Table 2.6, extracted from [94], are represented. A comparison of the technical parameters and the methods used in the calculation of primary and derived parameters, for each of the six most important international solar radiation databases, are presented respectively on them.

Database & availability	Data inputs	Period	Time resolution	Spatial resolution (study region)	RMSE/MBE (%)
PVGIS Europe *(internet)*	566 meteorological stations	1981-1990	Monthly averages	1 km x 1 km + on-fly disaggregated by 100m DEM	4.7/-0.5
Meteonorm 6.1 *(CDROM and internet)*	Meteo stations + satellite data	1981-2000	Monthly averages	Interpol. (on-fly)+ Satellite; disaggregated by 100 m DEM	6.2/0
ESRA *(CDROM)*	566 meteorologic stations + SRB satellite data	1981-1990	Monthly averages	5 arc-minute x 5 arc-minute	~7.5/-
Satel-Light *(internet)*	Meteosat 5, 6, 7	1996-2000	30-minute	4.6 - 6.2 km x 6.1 - 14.2 km	21.0/-0.6
HelioClim-2 *(internet)*	Meteosat 8 and 9 (MSG)	2004 - 2007	15-min	3.1 - 4.2 km x 4.1 - 9.6 km	25.3/2.2
NASA SSE 6 *(internet)*	GEWEX/SRB 3 + ISCCP satel. clouds + NCAR reanalysis	1983-2005	3-hourly	1 arc-degree x 1 arc-degree	8.7/0.3

Table 2.5 Technical parameters of the main solar radiation databases. Source: [94]

Where, as for the case of Table 2.2 and Table 2.4, RMSE is the Root Mean Square Error (comparable only for data with same time resolutions) and MBE is the Mean Bias Error of the database, referred to yearly averages.

Finally note that, besides databases and web pages offering more or less treated radiation data, there several software packages on the market, aimed for sizing, simulation, monitoring, and economic assessment of PV systems. Apart from the already cited HOMER

and RETScreen international software, there are other different commercial packages and many of them include or provide an access to meteorological and/or PV components databases. Some of them can be highlighted: PV F-Chart, PV DesignPro, PVSYST, TRNSYS, PV*SOL, INSEL, etc.

Database/ system	Global horizontal radiation	Diffuse fraction	Inclined surface (diffuse model)	Simulation of time series	Derived parameters*
PVGIS Europe	3D spline Interpol. of ground data + model r.sun: Suri & Hofierka 2004	Measured at 63 stations, the rest estim. by Czeplak 1996	Muneer 1990	Simulation of daily profile from monthly averages by Suri & Hofierka 2004	G, D, terrain shadowing (beam only)
Meteonorm ver. 6.1	3D inverse distance interpol. by Zelenka et al 1992 and Wald & Lefevre 2001; Heliosat 1 for sat. data	Perez et al. 1991	Perez et al. 1987	Synthetic time series from monthly averages by Aguiar et al 1988, and Aguiar & Collares-Pereira 1992	G, D, B, terrain shadowing (beam and diffuse)
ESRA	Interpol. of ground data by co-krigging: Beyer et al. 1997	Measured at 63 stations, the rest estimated by Czeplak 1996	Muneer 1990	Simulation of daily average profile by Collares-Pereira & Rabl 1979, and Liu & Jordan 1960	G, D,B, clearness, zones
Satel-Light	Heliosat 1 (Dumortier diffuse clear sky model)	Skartveit et al. 1998	Skartveit & Olseth 1986	Real 30-minute data	G, B, D, illuminances, ext. statistics
HelioClim ver. 2	Heliosat-2 (Rigollier et al. 2004)	N/A	N/A	Real 15-minute data	G
NASA SSE rel. 6	Satellite model by Pinker & Laszlo 1992	Erbs et al. 1982	Retscreen method by Duffie & Beckman 1991	Simulation of daily average profile by Collares-Pereira & Rabl 1979, and Liu & Jordan 1960	G, B, D, extended number of parameters & statistics

Table 2.6 Methods used in calculation of primary and derived parameters. Source: [94]

2.3. The Photovoltaic Geographic Information System (PVGIS).

The Photovoltaic Geographic Information System (PVGIS) [88] is not only a solar radiation database but a whole web-based knowledge distribution system that provides climate data and tools needed for the performance assessment of photovoltaic (PV) technology in Europe. Fostered by the European Commission Joint Research Centre (JRC), it comprehends geodatabases and simulation models interlinked with a user friendly web interface, Figure 2.6, thus providing easy-to-use access [73].
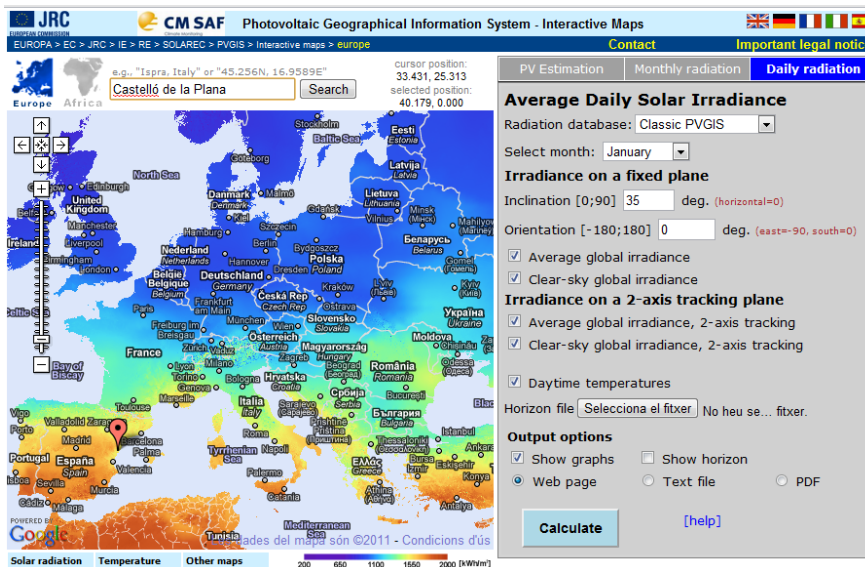
Figure 2.6 PVGIS web user interface. Source: [88]**.**

The PVGIS database was developed combining the solar radiation model r.sun [95], whose algorithms are based on equations published in the European Solar Radiation Atlas (ESRA) [74], with spatial interpolations. The radiation model is integrated into the GIS software GRASS [96, 97], estimating values for direct, diffuse and reflected components of the global irradiance/irradiation for horizontal or inclined surfaces under both clear and real-sky conditions for any location around Europe or Africa. Thus, PVGIS provides the calculated clear and real sky irradiance daily profiles which can be experienced in any location during a whole standard year, monthly averaged, as a function of the cloud cover.

Note that clear sky values represent those that would be measured in a place when no clouds were present, ideal conditions, while real sky values represent the average irradiance that would be measured along the whole month taking into account the number of clear and cloudy days statistically registered in that month.

Therefore, the database consists of maps representing monthly averages and one annual average of daily sums of global irradiation for horizontal surfaces, as well as those inclined at angles of 15, 25, and 40 degrees. Besides these data, raster maps of clear-sky irradiation, the Linke turbidity and the ratio diffuse to global radiation are computed in the database (although not all of them are calculated but integrated into the database from real measurements). As previously introduced, it stands out that PVGIS is a database which uses

solar radiation ground measurements collected at 566 ground meteorological stations over the period the period 1981 to 1990 (although it is now being updated with satellite images also).

2.3.1. PVGIS database inputs and outputs.

The different parameters introduced in the solar radiation model are:

- The clear-sky coefficients. These are used to convert the direct and diffuse irradiance values, calculated by the model for clear-sky conditions, to the real-sky values. These coefficients are derived from the monthly average ratios of diffuse to global irradiation measurements, which were registered in the same 566 meteorological stations. These were collected and harmonized within the ESRA project [74] together with the daily global irradiation on a horizontal surface and the clear-sky index, which characterizes the cloudiness of the sky. It should be noted here that the diffuse irradiation measurements are available only for 63 stations, for the other 503 locations the diffuse component has only been statistically estimated from global irradiation [73].

- The Linke atmospheric turbidity which represents the average optical state of the cloudless atmosphere for each month. Data which are extracted from [98], available also at the SoDa service [92], and adapted to the spatial resolution of the solar model.

- A digital elevation model (DEM) derived from SRTM-2 and SRTM-30 data [99]. Thus the PVGIS database accounts for shadows produced by local terrain features, calculated from the DEM.

- The ground albedo. This is assumed to have a constant value of 0.2, according with values represented in Table 2.1. Nevertheless, the model allows to use spatially distributed values for each grid point (if available) to improve the estimates.

From these input data and, by means of the solar radiation model and some implemented programs which use a unified grid of points for the different data layers with a spatial resolution of 1km by 1km, the following steps were processed in the database:

- Computation the clear-sky global irradiation on horizontal surfaces.

- Calculation and spatial interpolation of the clear-sky index and computation of the raster map of global irradiation for real-sky conditions on horizontal surfaces.

- Computation of the diffuse and direct components of the overcast global irradiation and the raster maps of global irradiations on inclined surfaces.

Hence, various products that are related to solar generation can be extracted from this web-based database. These are:

- The global irradiation for horizontal and inclined surfaces at any location.

- The monthly average clear and real-sky daily profiles of irradiances (taking into account possible shadows introduced by the terrain).

- The average direct, diffuse and reflected components of the global radiation every month at any location.

- The yearly-averaged electricity generation from fixed and tracking PV systems.

- The optimum inclination (optimized slope) and orientation (optimized azimuth) of fixed PV modules to annual maximize energy yields.

- The expected electricity output of a PV power plant as function of the PV technology, the temperature, the PV plant rated power and the estimated losses of the PV plant.

The different solar results or products can be downloaded for further processing. One point to keep in mind, especially for those results comprehending daily local irradiation or temperature profiles, is that the data provided by the PVGIS database are referred to the true solar time, i.e. the maximum irradiation value is always at noon.

An example of the results provided by PVGIS can be observed in Figure 2.7, where the time shown in the table of Figure 2.7 corresponds to the solar time. To find the GMT equivalent time, 0.40 hours have to be added. The different columns correspond to:

- G: Global irradiance on a fixed plane (W/m^2)

- G_d: Diffuse irradiance on a fixed plane (W/m^2)

- G_c: Global clear-sky irradiance on a fixed plane (W/m^2)

- A: Global irradiance on 2-axis tracking plane (W/m^2)

- A_d: Diffuse irradiance on 2-axis tracking plane (W/m^2)

- A_c: Global clear-sky irradiance on 2-axis tracking plane (W/m^2)

- T_d: Average daytime temperature profile (°C)

89

Time	G	G_d	G_c	A	A_d	A_c	T_d
07:07	0	0	0	0	0	0	7.1
07:22	17	17	10	8	7	5	7.2
07:37	101	38	129	262	62	382	7.4
07:52	159	59	206	379	107	541	7.6
08:07	221	81	291	458	124	657	7.8
08:22	273	92	365	515	132	742	8.1
08:37	323	103	437	560	139	809	8.3
08:52	370	113	505	597	144	863	8.6
09:07	414	121	569	627	149	906	9.0
09:22	456	128	630	652	153	941	9.3
09:37	494	135	687	672	156	971	9.6
09:52	529	140	739	689	158	995	10.0
10:07	561	145	787	703	160	1020	10.3
10:22	589	149	830	715	161	1030	10.7
10:37	614	152	868	724	163	1050	11.0
10:52	636	155	901	732	163	1060	11.4
11:07	654	157	928	738	164	1060	11.7
11:22	668	159	950	743	164	1070	12.1
11:37	679	160	967	746	165	1080	12.4
11:52	687	161	978	748	165	1080	12.8
12:07	690	162	984	749	165	1080	13.1
12:22	690	162	984	749	165	1080	13.4
12:37	687	161	978	748	165	1080	13.7
12:52	679	160	967	746	165	1080	14.0
13:07	668	159	950	743	164	1070	14.2
13:22	654	157	928	738	164	1060	14.5
13:37	636	155	901	732	163	1060	14.7
13:52	614	152	868	724	163	1050	14.8
14:07	589	149	830	715	161	1030	15.0
14:22	561	145	787	703	160	1020	15.1
14:37	529	140	739	689	158	995	15.2
14:52	494	135	687	672	156	971	15.2
15:07	456	128	630	652	153	941	15.2
15:22	414	121	569	627	149	906	15.2
15:37	370	113	505	597	144	863	15.1
15:52	323	103	437	560	139	809	15.0
16:07	273	92	365	515	132	742	14.8
16:22	221	81	291	458	124	657	14.6
16:37	159	59	206	379	107	541	14.3
16:52	28	28	16	14	12	8	13.9
17:07	17	17	10	8	7	5	13.5
17:22	0	0	0	0	0	0	13.1
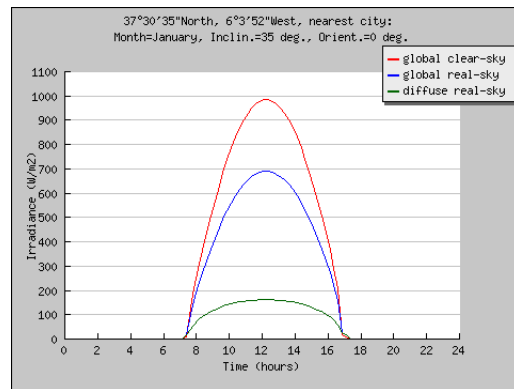
Fix PV installation
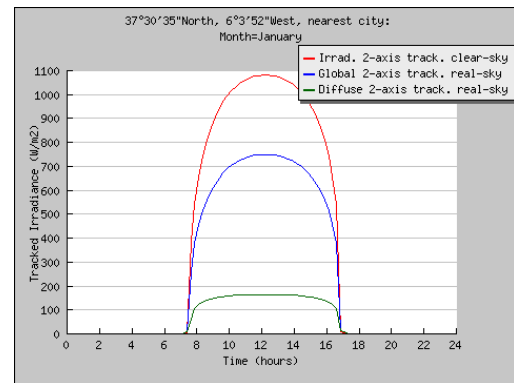
Two axis tracking PV installation
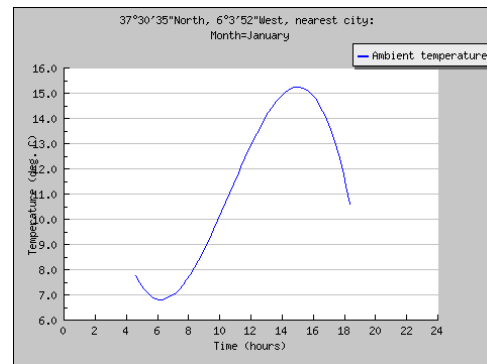
Temperature

Figure 2.7 Results from PVGIS for the city of Sevilla (Spain) in January. Inclination of plane: 35deg. Orientation (azimuth) of plane: 0 deg. Source: [88]**.**

2.3.2. Accuracy of the PVGIS database

The accuracy of this model providing the irradiation information for any location in Europe was evaluated taking as reference for the comparison those locations where real meteorological data measurements were originally available [88, 100, 101]

First, the interpolation deviation of the clear-sky coefficients was analyzed for each site. Comparing the yearly averages of the daily sum of global horizontal irradiation, for the stations with complete data (539 of them), the Mean Bias Error (MBE) was accounted as 8.9 $Wh/m^2/day$ (0.3%) and the Root Mean Square Error (RMSE) is 118 $Wh/m^2/day$ (3.7%). The monthly RMSE when comparing to the original data varies every month within an interval of 68 to 209Wh/m^2. In relative terms, it is within the interval of 3.2% to 7.8%, being the RMSE peak values during winter months, Figure 2.8. The deviation of PVGIS estimates of yearly sum of global horizontal radiation from the original observations stays within the range of 5% for 92% of the stations. In 12 locations (2.2% of all stations), the model outputs depart from the original values by more than 8%.
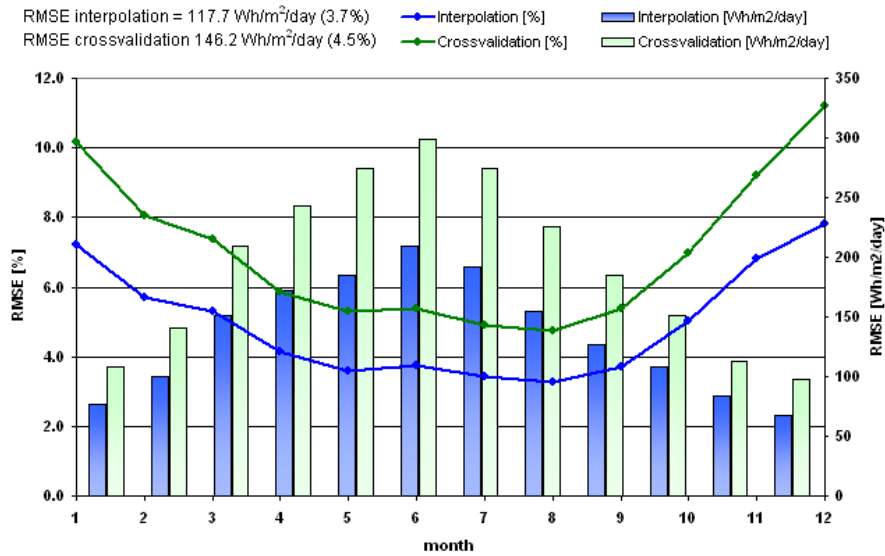
Figure 2.8 Root Mean Square Error calculated for the PVGIS. Source: [88]**.**

The comparison of the ESRA interpolation approach, Figure 2.9, shows that although the overall accuracy is practically the same (the yearly average of the RSME for ESRA is 113Wh/m^2, i.e. 3.5%), the PVGIS modeled values can be appreciated to be slightly better during the period from October to April and poorer during summer months.

Secondly, it is important to know not only the accuracy at the locations for which the original values were known, but also it is so to determine what uncertainty can be expected for any selected point outside these locations. Hence, a cross-validation was applied in order to estimate the predictive accuracy of the "r.sun" modeling approach in between different meteorological stations. Thus, the cross-validation error, which can be appreciated also in Figure 2.8, shows the maximum possible error that might occur at a given point if it was not taken into consideration in the interpolation. The average yearly MBE for the corss-validation is smaller, around $1.1Wh/m^2$ (0.03%) but the range of monthly averages of MBE is higher, from -2.5 Wh/m^2 in January to $4.4Wh/m^2$ in August. Furthermore, the RMSE is higher, and the yearly average is $143Wh/m^2$ (4.5%). It ranges from the lowest value in December, $97Wh/m^2$ (4.7%), to the highest in June, $299Wh/m^2$ (11.2%).
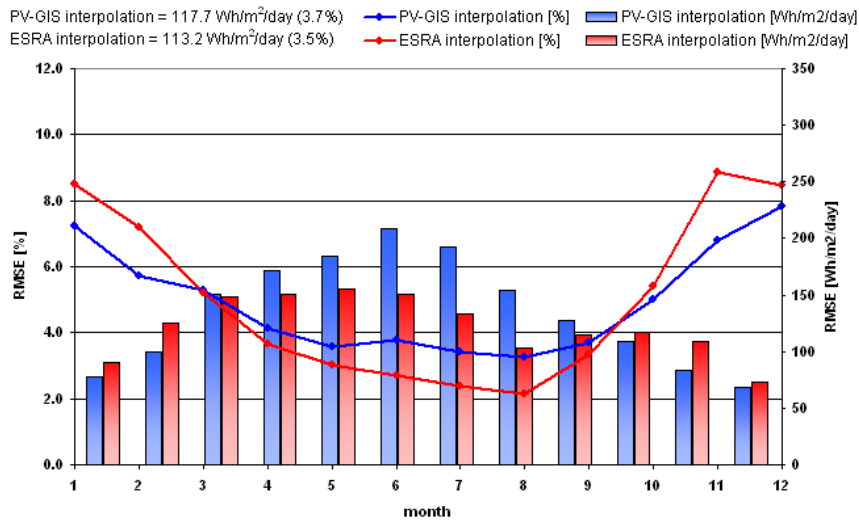
Figure 2.9 Root Mean Square Error. PVGIS vs. ESRA. Source: [88]

However, the overall cross-validation indicators do not provide an insight to the geographic distribution of the cross-validation errors—the estimate of yearly global horizontal irradiation for 90% of the station locations falls within the 7.2% of error margin, and in 19 locations (3.5% of all stations) the uncertainty is higher than 10%. However, with increasing distance between stations (37% of stations have the nearest neighbor at distance of 100 km or more), the information value of this indicator fades away.

Finally, it can be highlighted that for improving the database accuracy, some modifications have been proposed and are already under way along two parallel main lines for the PVGIS system [100]:

- Implementing a new solar resource database that is derived from a 20-years series of Meteosat satellite images. This will provide higher regional accuracy and better statistics solving the problem of low density and heterogeneous distribution of ground stations.

- Incorporation of technological and socio-economic parameters to the database that will enable analyses of economic, technological and environmental aspects, such as cost of PV energy generation, energy payback time, and avoidance of CO_2 emissions.

2.3.3. Solar resource results obtained with PVGIS.

With the different outputs provided by the PVGIS database, multiple studies to analyze the solar resource availability at different locations have been performed [102-105]. It stands out the one based on PVGIS solar radiation maps, as that in Figure 2.10, performed by Marcel Šúri in [100]. The global solar resource around Europe is identified on it.

Thus, according to [100], when analyzing the photovoltaic potential around Europe as a function of the solar resource availability, five climatic regions can be clearly identified.

- The highest potential region for solar electricity generation comprehends the southern countries mainly along the Mediterranean region (Malta, Cyprus, most parts of Spain, Italy and Croatia, Southern France and Corsica, Greece and Southern Turkey) and including Portugal. A typical annual electricity generation for a PV power plant ranges from 1100 to 1330 kWh per installed kWp mounted horizontally along this region.

- The second most favorable climatic region comprehends the Northern parts of Spain and Italy, and countries such as Croatia, Macedonia, and those around the Black Sea (Romania, Bulgaria and Turkey). The solar resource for them is in the range of 1000 to 1100 kWh/kWp in the horizontal plane per year.
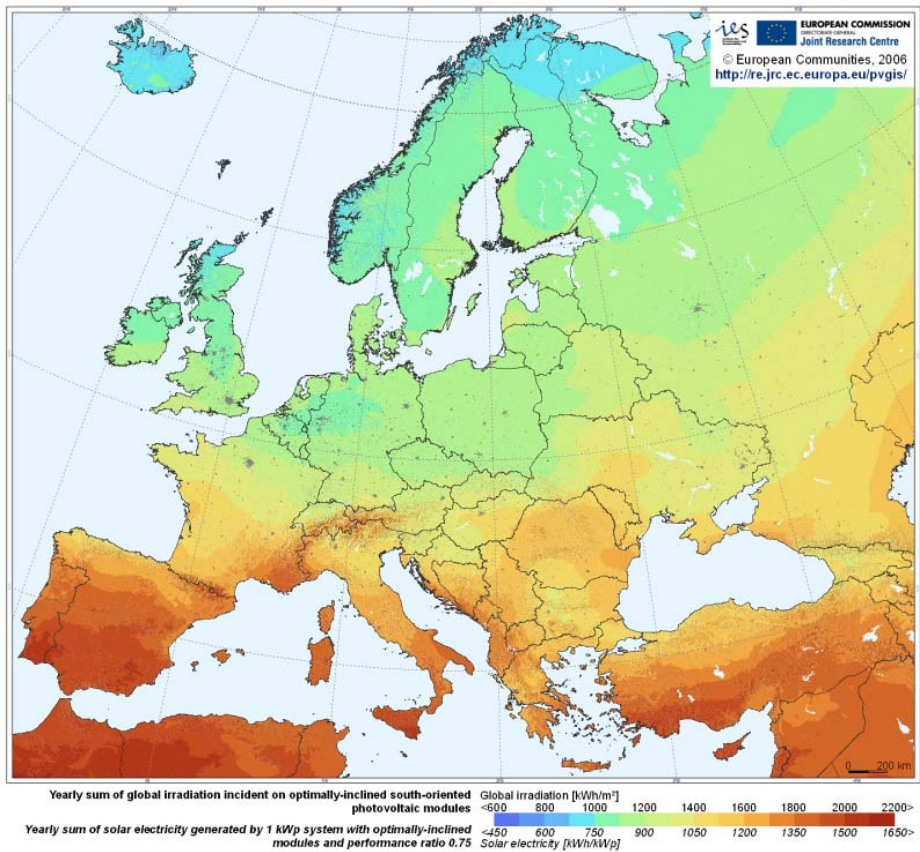
Figure 2.10 Photovoltaic Solar Electricity Potential in European Countries. Source: [88]**.**

- The third region which still presents acceptable conditions embraces France (except its North) and most of the countries in Central Europe (Hungary, Slovenia, Austria, Slovakia and Southern Germany). Their continental climate provides them with sunny summers with an annual overall generation in the range of 800 to 1000 kWh/kWp.

- Then, a group of regions where the solar resource is reduced to the interval from 700 to 800 kWh/kWp can be identified. These regions include the Northwest of Europe (encompassing Southern Ireland, England, Wales, North of France, Germany, Benelux, and Denmark), the Northern part of Central Europe (Poland, and most parts of the Czech Republic) and the Baltic States (Estonia, Latvia and Lithuania) including also South Sweden and Finland.

- Finally, the poorest regions in the European Union for PV power plants installations are Scotland and the North of Sweden and Finland, where yearly generation falls below 700 kWh per installed kWp.

These regions can be appreciated in Figure 2.10 and Figure 2.11. In the latter, the regional differences of solar electricity generation, calculated in [100] for a 1 kWp system, being the modules mounted at the optimum angle and compared to the country's average, can be appreciated.

So, a great potential for PV power plants development is identified within vast regions, mainly in the south of Spain and Turkey, which could be, and will probably be, profited to install large PV power plants which will help achieving the 2020 PV targets (indicated by the European Union and presented previously in the thesis).
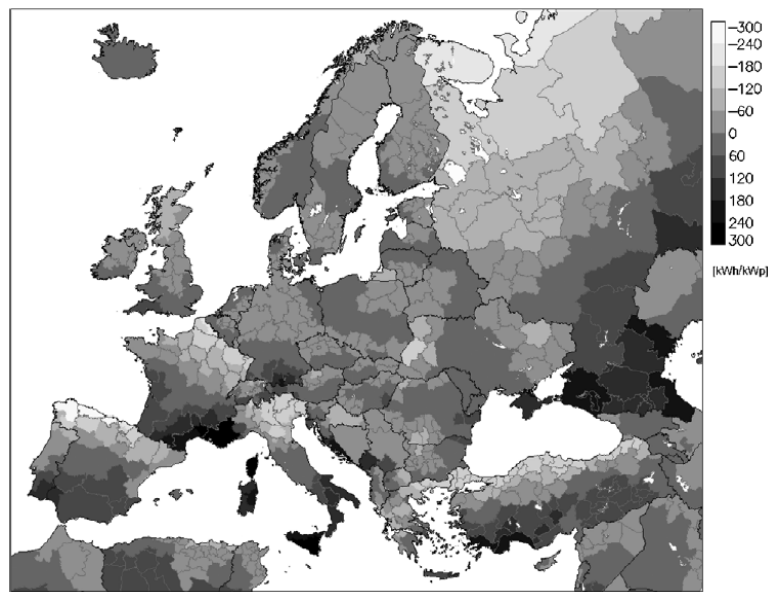
Figure 2.11 Regional differences of solar electricity generation from 1kWp systems. Source: [100]**.**

2.3.4. Study case applying PVGIS.

The research and analysis performed in this thesis is focused on one specific location in the south of Spain which is considered, according to the climatic European divisions already presented, one of the highest potential regions for PV installations. The ideal or theoretical radiation data and the real solar radiation data which have been employed in the analyses performed in this thesis for that location are here described and evaluated.

a) *Ideal irradiation values data sets*

The standard and expected monthly-averaged daily irradiance profiles were extracted from the PVGIS database. These two sets of 12-curves, provided by PVGIS, present values every 15 minutes. So, they need to be interpolated to adapt to the real measurements sampling time. The two sets correspond to the already introduced real and clear sky profiles datasets, obtained in this case for an optimal tilted plane (around 34° in the south of Spain), and they can be observed in Figure 2.12. The first 12-months dataset, the clear sky conditions solar radiation represented on the left hand side in Figure 2.12, is useful to determine the maximum expectable PV production while the second 12-months dataset, the real sky conditions solar radiation represented on the right hand side in Figure 2.12, gives a better idea of the energy that can be provided monthly and yearly.

a)   b)
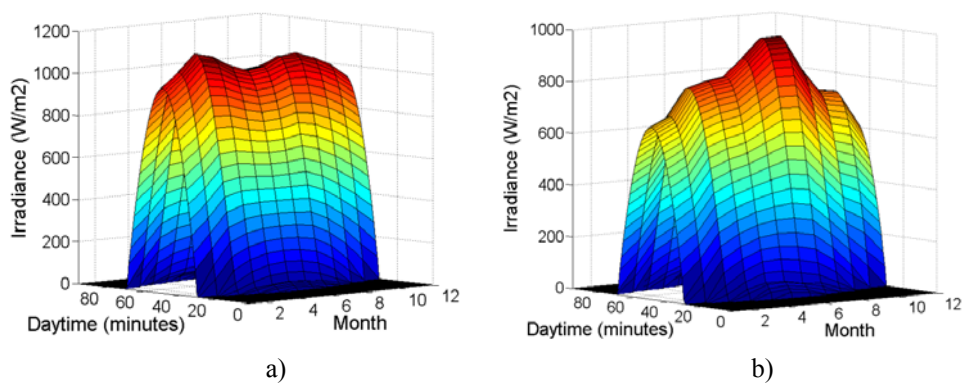
Figure 2.12 Standard irradiance for each month on a 34° tilted plane in the south of Spain. a) Clear sky conditions, ideal irradiance. b) Real sky conditions, average daily expected irradiance.

Clear difference on the monthly-averaged daily irradiance profiles for clear and real sky conditions can be appreciated among the two images. On one hand, the clear sky profiles are more similar among months. These achieve maximum irradiation values around the two equinoxes (March and April for spring, and September and October for autumn) due to the fact that the analyzed tilted plane is at the optimal angle of 34° (according to PVGIS), and present similar solar radiation patterns for the rest of the months, what is clearly associated to the Sun position equations. On the other hand, for the real sky profiles a big difference arises when comparing the average profile for winter and summer months, mainly due to the more frequent presence of clouds during the winter what reduces the overall, and hence the average, solar radiation during that period.

b) Real irradiation values data set

Apart from these two statistically calculated standard datasets extracted from PVGIS, actual irradiance values measured in the same location along the whole year 2009 have been used in the analysis presented in this thesis. These data contained a time-series of 365 days irradiance values sampled every two minutes (262800 samples). This is a sampling frequency accurate enough so as to estimate the effect of the passing clouds and the expected energy yield [106]. Figure 2.13 represents these data for the whole year long. Each of the spikes represented on it responds to one day.
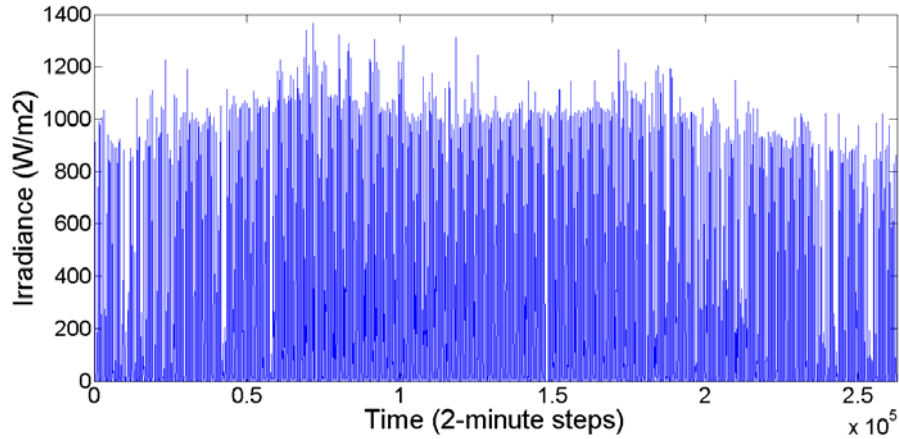
Figure 2.13 Annual solar irradiance with 2-minutes sampling for a location in the south of Spain.

This figure can be zoomed, Figure 2.14, in order to appreciate the variability of the solar radiation encountered during five days in a row, again sampled every 120 seconds.
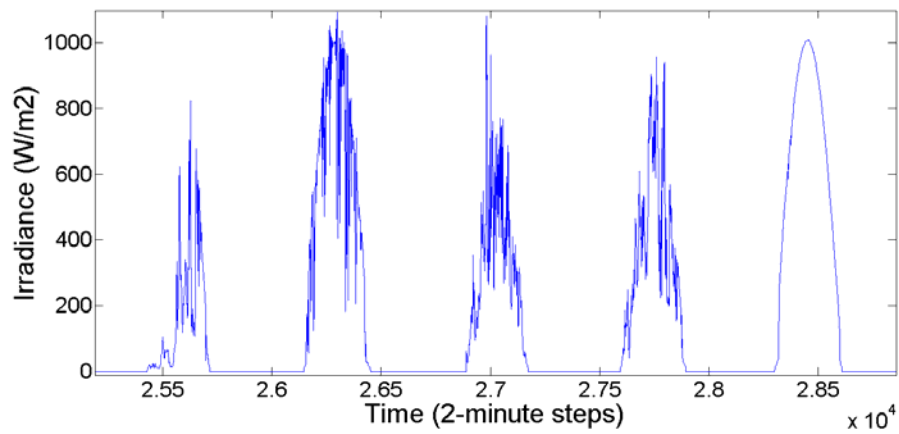
Figure 2.14 Five winter days solar irradiance with 2-minutes sampling.

97

From these real data measured in situ, the actual solar power spectrum registered can be extracted. Its outlook is shown in Figure 2.15 where the Fourier Transform, represented in the logarithmic scale, suggests a clear repetition pattern located around the 86400 seconds (24h). Hence, the spectrum perfectly depicts, as expected, the 24 hours solar cycle and its harmonics not showing any other remarkable behavior at any frequency apart of the stochastic nature of the variations due to clouds.
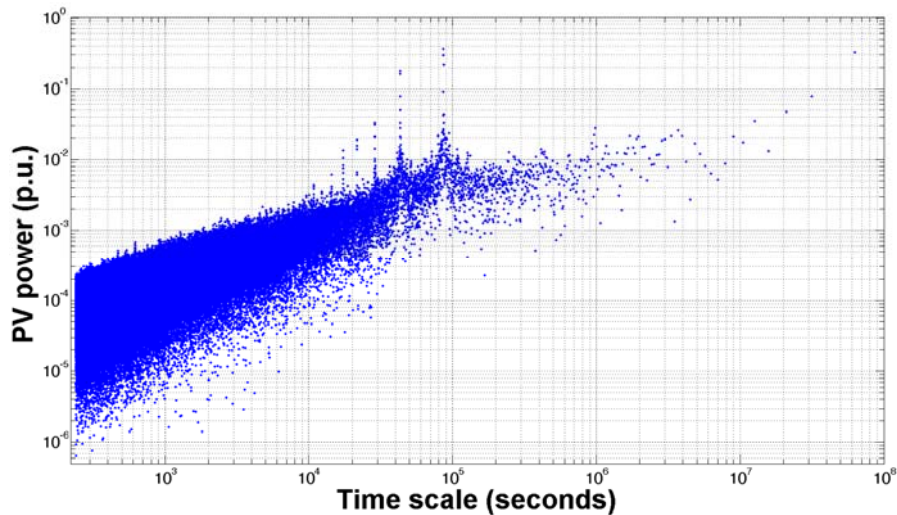
Figure 2.15 Annual solar radiation spectrum for a location in the south of Spain.

The outlook of this annual PV production spectrum can be greatly modified, as will be introduced in Chapter IV of the present thesis dissertation, by introducing an energy storage system (ESS) with a proper control strategy to rearrange or smooth the PV production. As a function of the ESS capacity and the energy management strategy implemented in a photovoltaic plant with storage, the spectrum will more or less modified at different frequencies.

c) *Matching degree between data sets*

To finish this section and the Chapter II, an analysis of the degree of matching between the two irradiation data sets introduced and used in this thesis are here introduced. Note that a good level of alignment between the real radiation values registered in situ for the year 2009 and the standard solar radiation values extracted from the PVGIS database is found, what can be observed in Figure 2.16 and Figure 2.18 and now analyzed.

On one hand, Figure 2.16 represents the accumulated daily energy (in the form of solar radiation) that would be received per square meter by the PV panels under both real measured radiation conditions (blue line) and the standard average solar radiation conditions provided by PVGIS (red line). One can appreciate how the real daily available irradiance evolved along that year 2009 according to, more or less (as a function of punctual overcast days), the profile of the monthly-averaged daily expected irradiance represented on Figure 2.12 b). The profiles on this last figure are, after all, what is reproduced with the red line in Figure 2.16. Regarding the equivalent energy production corresponding to both irradiation data sets, this can be compared by means of the capacity factor (C_f) of the PV power plant. The C_f can be defined as the quotient between the average power (P_{AVG}) in the period of time considered and the nominal power (P_N) of the plant, equation (2.5). Therefore, the C_f value provides the annually-averaged daily PV production per installed kW.

$$C_f = P_{AVG}/P_N \qquad (2.5)$$
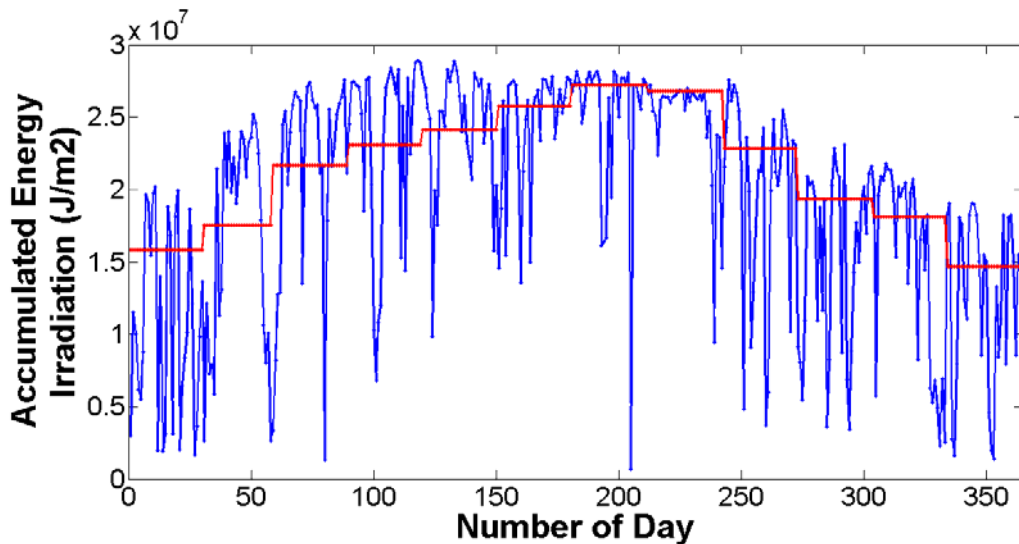
Figure 2.16 Daily energy for real and standard solar radiation curves.

The specific location in the south of Spain taken as a base for the analysis in this thesis is, according with the climatic European divisions already presented, within one of the highest potential regions for PV installations. Therefore, according to Figure 2.17, the annual capacity factor for this location is around 0.18, typical value for optimally tilted PV fix panels in that region, which returns around 4.3 kWh/kW$_{peak}$ of daily energy production

(around 1570 kWh/kW$_{peak}$ electricity generated yearly), value which will be used as base for the p.u. energy calculations along the whole thesis work. This can be compared with the C_f value offered by the real irradiation data along the year 2009 which produced an average energy yield of 4.1 kWh/kW$_{peak}$. Therefore, although not a perfect agreement among data sets for that year (2009 is classified below the average year in the number of clear days), an acceptable concordance is also found in the energy overall production. Still, an assimilation of the global annually-generated energy have been assumed, multiplying all the standard curves by the proper correction factor in order to annually balance the ideal and the real production. Conversely, the extra power (not received form the PV panels) the PV+ES power plant should provide to cope with the statistically calculated references should be provided by the ESS which would represent it to be most of the time completely discharged.
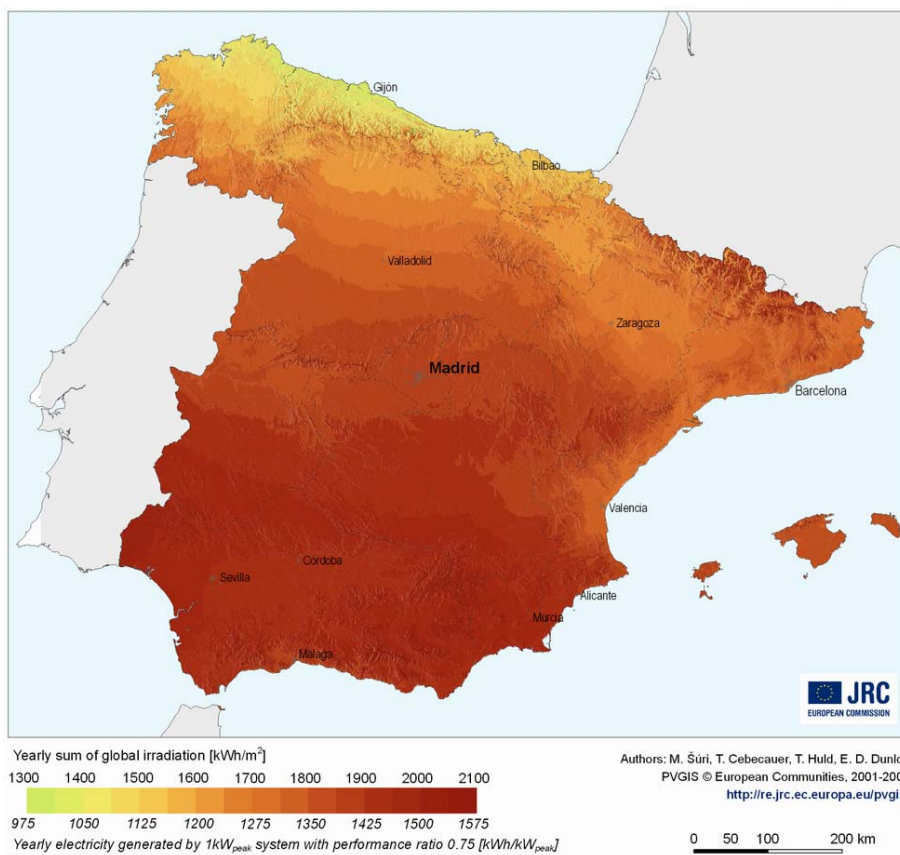
Figure 2.17 Global irradiation in Spain. Source: [100]**.**

On the other hand, Figure 2.18 represents a projection of the instants when solar radiation is detected for the first and the last time everyday along the year, i.e. the moment when the real daily irradiance (blue line) and the model or standard daily profiles (red line) are different to zero (lower part of the figure) and equal to zero once again (upper part). The time is represented in this figure on the "y" axis and is grouped again in 2-minutes steps (sampling frequency of the two sets of solar radiation curves).
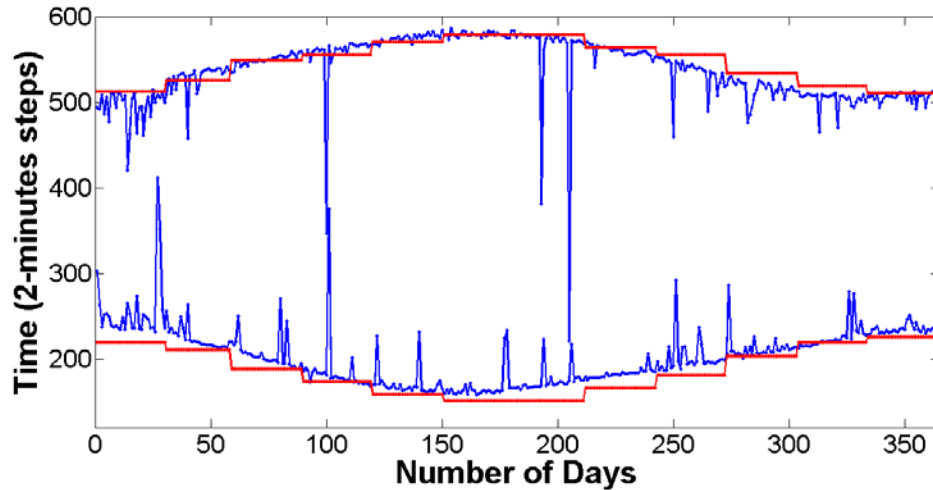
Figure 2.18 Daily dawn and sunset instants for real and standard solar radiation curves.

One can appreciate how the predicted and the actual moments for the aurora and the sunset do match everyday quite precisely with slight differences. These differences can be ascribed to two principal reasons:

- Firstly, the 15-minutes initial sampling period corresponding to all the standard daily curves provided by the PVGIS database. This could introduce same uncertainty when these curves are resampled to the 2-minutes sampling period to be compared and treated with the available real solar radiation.

- And secondly, the evolution of the solar time along the year. Note that the times in the daily radiation output from PVGIS are referred to the true solar time, meaning that the maximum is always at noon. To get to the local clock time, one should calculate the longitude distance from the point of interest to that point on our time zone where the Sun reaches the maximum height at the 12 o'clock local time. In addition, it is important to take into account that this distance varies along the year (±15 minutes)

according with the universal equation of time [2, 107]. Finally, the spring time hour change for daylight savings during the summer has to be also considered. All these consideration can be summarized with one example, e.g. to get the local time for the city of Sevilla (Spain) of the PVGIS provided standard solar radiation curves, one should add to the PVGIS output time one hour 24 minutes in winter and 2h 24m during the summer since approximately one hour must be added for every 15 degrees in longitude being this city about 6 degrees west and reaching the Sun its maximum at 15degrees east for this time zone.

Hence, taking into account the information represented on Figure 2.16 and Figure 2.18, the accuracy of the PVGIS database solar resource estimation with regard to real solar radiation measured during the year 2009 for the location under study can be concluded as quite precise.

2.4.   References

[1] C. A. Gueymard, "The sun's total and spectral irradiance for solar energy applications and solar radiation models," Solar Energy, vol. 76, pp. 423-453, 2004.
[2] T. Muneer, C. Gueymard and H. Kambezidis, Solar Radiation & Daylight Models. Butterworth-Heinemann, 2004.
[3] A. Angstrom, "Solar and terrestrial radiation." Q. J. R. Meteorol. Soc., vol. 50, pp. 121-126, 1924.
[4] A. Angstrom, "On the atmospheric transmission of sun radiation and on dust in the air," Geografiska Annaler, vol. 11, pp. 156-166, 1929.
[5] A. Angstrom, "On the atmospheric transmission of sun radiation. II," Geografiska Annaler, vol. 12, pp. 130-159, 1930.
[6] A. Angstrom, "On the computation of global solar radiation from records of sunshine," Arkiv Geophysik, vol. 3, pp. 551-556, 1956.
[7] A. Angstrom, "Techniques of Determinig the Turbidity of the Atmosphere1," Tellus, vol. 13, pp. 214-223, 1961.
[8] J. L. Monteith, "Attenuation of solar radiation: a climatological study," Q. J. R. Meteorol. Soc., vol. 88, pp. 508-521, 1962.
[9] R. E. Blankenship, D. M. Tiede, J. Barber, G. W. Brudvig, G. Fleming, M. Ghirardi, M. R. Gunner, W. Junge, D. M. Kramer and A. Melis, "Comparing Photosynthetic and Photovoltaic Efficiencies and Recognizing the Potential for Improvement," Science, vol. 332, pp. 805, 2011.
[10] J. P. Hennessey Jr, "Some aspects of wind power statistics," J.Appl.Meteorol.;(United States), vol. 16, 1977.
[11] L. Freris, Wind Energy Conversion Systems. Prentice Hall, 1990.
[12] L. Helle, Modeling and Comparison of Power Converters for Doubly Fed Induction Generators in Wind Turbines. Videnbasen for Aalborg Universitet, 2007.
[13] A. N. Celik, "Energy output estimation for small-scale wind power generators using Weibull-representative wind data," J. Wind Eng. Ind. Aerodyn., vol. 91, pp. 693-707, 4, 2003.
[14] C. Gueymard, "An anisotropic solar irradiance model for tilted surfaces and its comparison with selected engineering algorithms," Solar Energy, vol. 38, pp. 367-386, 1987.
[15] R. Perez, P. Ineichen, R. Seals, J. Michalsky and R. Stewart, "Modeling daylight availability and irradiance components from direct and global irradiance," Solar Energy, vol. 44, pp. 271-289, 1990.

[16] D. T. Reindl, W. A. Beckman and J. A. Duffie, "Evaluation of hourly tilted surface radiation models," Solar Energy, vol. 45, pp. 9-17, 1990.

[17] J. Duffie and A. Beckman, Solar Engineering of Thermal Processes. John Wiley and Sons, 1991.

[18] S. Coppolino, "A new correlation between clearness index and relative sunshine," Renewable Energy, vol. 4, pp. 417-423, 6, 1994.

[19] T. Muneer, S. Younes and S. Munawwar, "Discourses on solar radiation modeling," Renewable and Sustainable Energy Reviews, vol. 11, pp. 551-602, 5, 2007.

[20] B. Y. H. Liu and R. C. Jordan, "The interrelationship and characteristic distribution of direct, diffuse and total solar radiation," Solar Energy, vol. 4, pp. 1-19, 1960.

[21] M. S. Gul, T. Muneer and H. D. Kambezidis, "Models for obtaining solar radiation from other meteorological data," Solar Energy, vol. 64, pp. 99-108, 9, 1998.

[22] J. F. Orgill and K. G. T. Hollands, "Correlation equation for hourly diffuse radiation on a horizontal surface," Solar Energy, vol. 19, pp. 357-359, 1977.

[23] D. G. Erbs, S. A. Klein and J. A. Duffie, "Estimation of the diffuse radiation fraction for hourly, daily and monthly-average global radiation," Solar Energy, vol. 28, pp. 293-302, 1982.

[24] J. W. Spencer, "A comparison of methods for estimating hourly diffuse solar radiation from global solar radiation," Solar Energy, vol. 29, pp. 19-32, 1982.

[25] J. W. Bugler, "The determination of hourly insolation on an inclined plane using a diffuse irradiance model based on hourly measured global horizontal insolation," Solar Energy, vol. 19, pp. 477-491, 1977.

[26] E. L. Maxwell, "A quasi-physical model for converting hourly global horizontal to direct normal insolation," in Proc. Solar '87 Conf. Portland, OR, 1987, pp. 35-46.

[27] J. C. Lam and D. H. W. Li, "Correlation between global solar radiation and its direct and diffuse components," Build. Environ., vol. 31, pp. 527-535, 11, 1996.

[28] C. A. Gueymard, "Direct and indirect uncertainties in the prediction of tilted irradiance for solar engineering applications," Solar Energy, vol. 83, pp. 432-444, 3, 2009.

[29] R. Perez, P. Ineichen, K. Moore, M. Kmiecik, C. Chain, R. George and F. Vignola, "A new operational model for satellite-derived irradiances: description and validation," Solar Energy, vol. 73, pp. 307-317, 11, 2002.

[30] P. Ineichen and R. Perez, "A new airmass independent formulation for the Linke turbidity coefficient," Solar Energy, vol. 73, pp. 151-157, 9, 2002.

[31] C. Rigollier, O. Bauer and L. Wald, "On the clear sky model of the ESRA — European Solar Radiation Atlas — with respect to the heliosat method," Solar Energy, vol. 68, pp. 33-48, 1, 2000.

[32] M. Geiger, L. Diabaté, L. Ménard and L. Wald, "A web service for controlling the quality of measurements of global solar irradiation," Solar Energy, vol. 73, pp. 475-480, 12, 2002.

[33] F. Kasten, "The Linke turbidity factor based on improved values of the integral Rayleigh optical thickness," Solar Energy, vol. 56, pp. 239-244, 1996.

[34] R. Mueller, K. Dagestad, P. Ineichen, M. Schroedter-Homscheidt, S. Cros, D. Dumortier, R. Kuhlemann, J. Olseth, G. Piernavieja and C. Reise, "Rethinking satellite-based solar irradiance modelling:: The SOLIS clear-sky module," Remote Sens. Environ., vol. 91, pp. 160-174, 2004.

[35] R. Bird and R. L. Hulstrom, "Direct insolation models," Direct Insolation Models, 1980.

[36] R. Bird and C. Riordan. Simple solar spectral model for direct and diffuse irradiance on horizontal and tilted planes at the earth's surface for cloudless atmospheres. Solar Energy Research Inst., Golden, CO (USA). 1984.

[37] B. Molineaux and P. Ineichen, "Equivalence of pyrheliometric and monochromatic aerosol optical depths at a single key wavelength," Appl. Opt., vol. 37, pp. 7008-7018, 1998.

[38] C. Gueymard, "A two-band model for the calculation of clear sky solar irradiance, illuminance, and photosynthetically active radiation at the earth's surface," Solar Energy, vol. 43, pp. 253-265, 1989.

[39] C. A. Gueymard, "REST2: High-performance solar radiation model for cloudless-sky irradiance, illuminance, and photosynthetically active radiation – Validation with a benchmark dataset," Solar Energy, vol. 82, pp. 272-285, 3, 2008.

[40] F. Kasten, "A simple parameterization of two pyrheliometric formulae for determining the Linke turbidity factor," Meteorol. Rundsch., vol. 33, pp. 124-127, 1980.

[41] P. Ineichen, "Comparison of eight clear sky broadband models against 16 independent data banks," Solar Energy, vol. 80, pp. 468-478, 4, 2006.

[42] K. J. Kondratyev and M. P. Manolova, "Radiation balance of slopes," Solar Energy, vol. 4, 1960.

[43] M. Iqbal, An Introduction to Solar Radiation. Academic Press, Orlando, FL, 1983.

[44] J. L. Threlkeld, Solar Irradiation of Surfaces on Clear Days. ASHRAE, 1962.

[45] ASHRAE, "Handbook of fundamentals, SI edition," American Society of Heating, Refrigerating and Air-Conditioning Engineers, Atlanta, GA, 2005.

[46] R. C. Temps and K. L. Coulson, "Solar radiation incident upon slopes of different orientations," Solar Energy, vol. 19, pp. 179-184, 1977.

[47] T. M. Klucher, "Evaluation of models to predict insolation on tilted surfaces," Solar Energy, vol. 23, pp. 111-114, 1979.

[48] J. E. Hay, "Calculation of monthly mean solar radiation for horizontal and inclined surfaces," Solar Energy, vol. 23, pp. 301-307, 1979.

[49] A. Skartveit and J. Asle Olseth, "Modelling slope irradiance at high latitudes," Solar Energy, vol. 36, pp. 333-344, 1986.

[50] P. Moon and D. E. Spencer, "Illumination from a non-uniform sky," Illuminating Engineering, vol. 37, pp. 707-726, 1942.

[51] M. D. Steven and M. H. Unsworth, "The angular distribution and interception of diffuse solar radiation below overcast skies," Q. J. R. Meteorol. Soc., vol. 106, pp. 57-61, 1980.

[52] T. Muneer, "Solar radiation model for Europe," Building Services Engineering Research and Technology, vol. 11, pp. 153-163, November 01, 1990.

[53] T. Muneer, "Solar irradiance and illuminance models for Japan I: Sloped surfaces," Lighting Research and Technology, vol. 27, pp. 209, 1995.

[54] B. G. Akinoğlu and A. Ecevit, "Construction of a quadratic model using modified Ångstrom coefficients to estimate global solar radiation," Solar Energy, vol. 45, pp. 85-92, 1990.

[55] F. J. Newland, "A study of solar radiation models for the coastal region of South China," Solar Energy, vol. 43, pp. 227-235, 1989.

[56] M. R. Rietveld, "A new method for estimating the regression coefficients in the formula relating solar radiation to sunshine," Agricultural Meteorology, vol. 19, pp. 243-252, 6, 1978.

[57] K. K. Gopinathan, "Computing the monthly mean daily diffuse radiation from clearness index and percent possible sunshine," Solar Energy, vol. 41, pp. 379-385, 1988.

[58] A. S. S. Dorvlo and D. B. Ampratwum, "Modelling of weather data for Oman," Renewable Energy, vol. 17, pp. 421-428, 1999.

[59] J. Boland, "Time-series analysis of climatic variables," Solar Energy, vol. 55, pp. 377-388, 11, 1995.

[60] M. A. Herrero, "Harmonic analysis of the monthly solar radiation in Spain," Int J Ambient Energy, vol. 14, pp. 35-40, 1993.

[61] W. F. Phillips, "Harmonic analysis of climatic data," Solar Energy, vol. 32, pp. 319-328, 1984.

[62] M. E. Ghitany and N. F. El-Nashar, "Fitting Weibull distribution to ultraviolet solar radiation data," International Journal of Sustainable Energy, vol. 24, pp. 167-173, 2005.

[63] S. Rahman, M. A. Khallat and Z. M. Salameh, "Characterization of insolation data for use in photovoltaic system analysis models," Energy, vol. 13, pp. 63-72, 1, 1988.

[64] M. A. Khallat and S. Rahman, "A Probabilistic Approach to Photovoltaic Generator Performance Prediction," IEEE Transactions on Energy Conversion, vol. EC-1, pp. 34-40, 1986.

[65] A. Skartveit and J. A. Olseth, "The probability density and autocorrelation of short-term global and beam irradiance," Solar Energy, vol. 49, pp. 477-487, 12, 1992.

[66] D. L. King, W. E. Boyson and J. A. Kratochvil, "Analysis of factors influencing the annual energy production of photovoltaic systems," in Photovoltaic Specialists Conference, 2002. Conference Record of the Twenty-Ninth IEEE, 2002, pp. 1356-1361.

[67] R. A. Gansler, S. A. Klein and W. A. Beckman, "Investigation of minute solar radiation data," Solar Energy, vol. 55, pp. 21-27, 7, 1995.

[68] A. S. S. Dorvlo, J. A. Jervase and A. Al-Lawati, "Solar radiation estimation using artificial neural networks," Appl. Energy, vol. 71, pp. 307-319, 4, 2002.

[69] M. W. Gardner and S. R. Dorling, "Artificial neural networks (the multilayer perceptron)—a review of applications in the atmospheric sciences," Atmos. Environ., vol. 32, pp. 2627-2636, 8/1, 1998.

[70] M. Mohandes, S. Rehman and T. O. Halawani, "Estimation of global solar radiation using artificial neural networks," Renewable Energy, vol. 14, pp. 179-184, 8, 1998.

[71] H. K. Elminir, F. F. Areed and T. S. Elsayed, "Estimation of solar radiation components incident on Helwan site using neural networks," Solar Energy, vol. 79, pp. 270-279, 9, 2005.

[72] W. Marion and R. George, "Calculation of solar radiation using a methodology with worldwide potential," Solar Energy, vol. 71, pp. 275-283, 2001.

[73] M. Šúri, T. Huld, E. D. Dunlop and T. Cebecauer, "Geographic Aspects of Photovoltaics in Europe: Contribution of the PVGIS Website," Selected Topics in Applied Earth Observations and Remote Sensing, IEEE Journal of, vol. 1, pp. 34-41, 2008.

[74] Centre Energétique et Procédés - Ecole des Mines de Paris (France). HelioClim. [Online]. (Accessed: June 20, 2011), Available: http://www.helioclim.org/.

[75] German Aerospace Center. Solar energy mining database. [Online]. 2011). Available: http://www.solemi.com/home.html.

[76] Satel-Light. The european database of daylight and solar radiation. [Online]. 2011). Available: http://www.satellight.com/indexgS.htm.

[77] Atmosferic Science Data Center - National Aeronautics and Space Administration (NASA). Surface meteorology and solar energy (SEE). [Online]. (Accessed: June 21, 2011), Available: http://eosweb.larc.nasa.gov/sse/.

[78] European Centre for Medium-Range Weather Forecasts (ECMWF). ERA-interim. [Online]. (Accessed: June 21, 2011), Available: http://data.ecmwf.int/data/.

[79] Earth System Research Laboratory. [Online]. (Accessed: June 21, 2011), Available: http://www.esrl.noaa.gov/psd/data/gridded/.

[80] Japan Meteorological Agency. Irradiance data. [Online]. (Accessed: June 20, 2011), Available: http://www.data.jma.go.jp/obd/stats/etrn/index.php.

[81] Agencia Estatal de Meteorología (AEMET). Irradiance data. [Online]. (Accessed: June 20, 2011), Available: http://www.aemet.es/es/portada.

[82] UNESCO. World meteorological organization. [Online]. (Accessed: June 22, 2011), Available: http://www.wmo.ch/.

[83] H. Gilgen and A. Ohmura, "The Global Energy Balance Archive," Bull. Amer. Meteor. Soc., vol. 80, pp. 831-850, 05/01; 2011/06, 1999.

[84] A. Ohmura, E. G. Dutton, B. Forgan, C. Fröhlich, H. Gilgen, H. Hegner, A. Heimo, G. König-Langlo, B. McArthur and G. Müller, "Baseline Surface Radiation Network (BSRN/WCRP): New Precision Radiomerry for Climate Research," BULLETIN-AMERICAN METEOROLOGICAL SOCIETY, vol. 79, pp. 2115-2136, 1998.

[85] Russian Federal Service for Hydrometeorology and Environmental Monitoring. World radiation data center [Online]. (Accessed: June 22, 2011), Available: http://wrdc.mgo.rssi.ru/.

[86] International Lighting Commission. International daylight measurement program. [Online]. (Accessed: June 22, 2011), Available: http://idmp.entpe.fr/.

[87] European Comission. European solar radiation atlas (ESRA). [Online]. (Accessed: June 22, 2011), Available: http://www.helioclim.net/esra/.

[88] European Commission, Joint Research Centre. PVGIS database . [Online]. 2010). Available: http://re.jrc.ec.europa.eu/pvgis/index.htm.

[89] Meteotest. Meteonorm. [Online]. (Accessed: June 22, 2011), Available: http://meteonorm.com/.

[90] GeoModel Solar. Solargis database . [Online]. 2011). Available: http://solargis.info/.

[91] National Renewable Energy Laboratory (NREL). Solar maps. [Online]. (Accessed: June 22, 2011), Available: http://www.nrel.gov/gis/solar.html.

[92] SoDa. Solar radiation database . [Online]. 2010). Available: http://www.soda-is.com/eng/services/services_radiation_free_eng.php.

[93] United Nations Environment Programme (UNEP). Solar and wind energy resource assessment (SWERA) [Online]. (Accessed: June 20, 2011), Available: http://swera.unep.net/.

[94] M. Šúri, J. Remund, T. Cebecauer, D. Dumortier, L. Wald, T. Huld and P. Blanc, "First steps in the cross-comparison of solar resource spatial products in Europe," Proceeding of the EUROSUN, 2008.

[95] M. Šúri and J. Hofierka, "A New GIS-based Solar Radiation Model and Its Application to Photovoltaic Assessments," Transactions in GIS, vol. 8, pp. 175-190, 2004.

[96] M. Neteler and H. Mitasova, Open Source GIS: A GRASS GIS Approach. Kluwer Academic Pub, 2002.

[97] GRASS Development Team. Geographic resources analysis support system. [Online]. (Accessed: June 24, 2011), Available: http://grass.osgeo.org/.

[98] J. Remund, L. Wald, M. Lefèvre, T. Ranchin and J. Page, "Worldwide linke turbidity information," in Proccedings of ISES Solar World Congress, Goteborg, Sweden, 2003, .

[99] National Geospatial-Intelligence Agency (NGA) and National Aeronautics and Space Administration (NASA). Shuttle radar topography mission (SRTM). [Online]. (Accessed: June 20, 2011), Available: http://www2.jpl.nasa.gov/srtm/.

[100] M. Šúri, T. A. Huld, E. D. Dunlop and H. A. Ossenbrink, "Potential of solar electricity generation in the European Union member states and candidate countries," Solar Energy, vol. 81, pp. 1295-1305, 10, 2007.

[101] M. Šúri, T. A. Huld and E. D. Dunlop, "PV-GIS: a web-based solar radiation database for the calculation of PV potential in Europe," International Journal of Sustainable Energy, vol. 24, pp. 55-67, 2005.

[102] J. Monedero, J. García, F. Dobon, M. A. Yanes and F. Hernandez, "Calculation of PV potential maps in the Canary Islands," .

[103] T. Huld, M. Šúri and E. D. Dunlop, "Comparison of potential solar electricity output from fixed   inclined and two   axis tracking photovoltaic modules in Europe," Prog Photovoltaics Res Appl, vol. 16, pp. 47-59, 2008.

[104] T. Huld, T. Cebecauer, M. Šúri and E. D. Dunlop, "Analysis of one   axis tracking strategies for PV systems in Europe," Prog Photovoltaics Res Appl, vol. 18, pp. 183-194, 2010.

[105] T. A. Huld, M. Suri, R. P. Kenny and E. D. Dunlop, "Estimating PV performance over large geographical regions," in Photovoltaic Specialists Conference, 2005. Conference Record of the Thirty-First IEEE, 2005, pp. 1679-1682.

[106] B. Burger and R. Rüther, "Inverter sizing of grid-connected photovoltaic systems in the light of local solar resource distribution characteristics and temperature," Solar Energy, vol. 80, pp. 32-45, 1, 2006.

[107] Wikipedia. Equation of time. [Online]. (Accessed: April 22, 2011), Available: http://en.wikipedia.org/wiki/Equation_of_time.

Energy storage technologies

Energy Storage (ES) is the capability of storing energy for a period of time releasing it to be used at any moment when its usefulness or cost is more beneficial. When released, the energy can either be delivered in large amounts for commodity use, or in a controlled manner to optimize operation and enhance the reliability of the Electrical Power System (EPS). ES systems (ESS) have already been used for more than one century in our society, notably in the electric domain, and over that time a big variety of technologies have been developed. In fact, ES already became a dominant factor in the economic and industrial development with the widespread introduction of refined chemical fuels, such as gasoline, kerosene and natural gas in the late 1800s. Unlike other common ES systems used earlier, such as wood or coal, electricity is transmitted in a closed circuit and, for essentially any practical purpose, could not be stored as electrical energy. Actually, electricity has always been used when generated. This means that changes in demand could not be accommodated without either cutting supplies (as by brownouts or blackouts) or by storing the electric energy in another medium [1, 2].

As introduced in Chapter I, many Renewable Energy Sources (RES) present intermittent and stochastic power generation patterns due to their weather dependency (e.g. wind blows intermittently or solar energy depends clearly on clouds evolution). Hence, a further RES integration into the EPS requires storage in order to make this kind of power sources reliable and sustainable [3-8]. For the case of PV power, as for the wind power, it is clear nowadays that a more controllable and non-fluctuating production should be assured to increase its

sharing in the generation mix, offering ancillary services such as frequency and voltage control, power oscillations damping (POD), etc. This fact paves the way to implement hybrid generation technologies and integrate ES systems into PV power plants [4, 5, 9-12].

The first steps on ES integration into PV power plants date from 20 years ago [13]. However, the youngness of the ES technologies and the small size of the PV power plants at that time made this solution impractical. Subsequently, in the early 2000s, when the renewable experience aroused, this topic pushed hard again. As an example, note the creation of a European Network for research on storage technologies for intermittent renewable energies (INVESTIRE) [14], established between 2001 and 2003 under the 5th EU Framework Program, and which made a thorough study on the contribution of ES systems (ESS) to the integration of renewable generators. However, the main objective in that case was the evaluation of storage technologies maturity and the recommendation of R&D strategies to improve their use with renewables. It is not till recent years that a significant development on ES technologies (REDOX, Li-Ion and NaS batteries, supercapacitors etc.) has been carried out, combined with both, increasing demands on the operating conditions of large renewable generation systems and a huge increase in PV power plants ratings. This scenario, together with the huge increase on the installed PV power in many countries [15], makes the installation of ESS an increasingly interesting solution for improving grid-integration of PV power plants. [16]As a result, the possibility of implementing ESS in the evolving PV power plants is of particular relevance nowadays [16-21]. This research is further complemented by demonstration projects, like the one started in 2010 as part of the Eurogia+ cluster [22], in which a demonstration PV power plant with 1.1MW of Lithium-Ion batteries is being developed with the overall objective of reducing the cost of energy, provide ancillary services, improve network stability and offer back-up functions. And this trend is confirmed by the USA 2009 stimulus plan which enhances research on the application of ES to Smart Grids and microgrids [23].

3.1. ESS classification and characteristic parameters.

Different ESS classifications can be established nowadays [24-31], most of them normally dividing ES technologies between those storing energy in an electromagnetic way (direct storage) and those storing energy in a mechanical, thermal, chemical or electrochemical way (indirect storage). As can be appreciated in Figure 3.1, in the direct storage group, technologies such as ultracapacitors (UC) or superconducting magnetic

energy storage (SMES) can be highlighted, while in the other group, technologies such as pumped hydro (PHES), compressed air (CAES) or flywheels can be pointed out as mechanical systems on the one hand, and hydrogen and fuel cells (FC), batteries (BESS) and Flow Batteries as electrochemical systems on the other hand. Finally, thermoelectric energy storage (TEES) is the main one in the thermal group nowadays. These groups with their corresponding technologies can be are reviewed along this chapter.
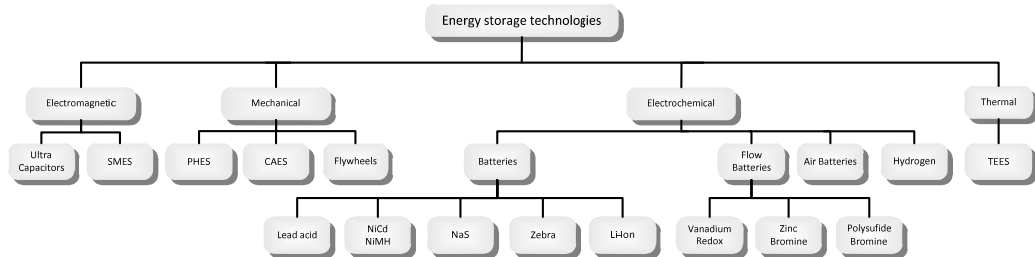
Figure 3.1 Classification of ES technologies. Source: [32]**.**

Once the different ES technologies have been classified and prior to describing each of them in detail, some characteristic parameters which are discussed in the following sections and apply to the different technologies must be defined for clarity:

- Power Capacity: is the maximum instantaneous output that an ES device can provide, usually measured in kilowatts (kW) or megawatts (MW).

- Energy Capacity: is the amount of electrical energy the device can store usually measured in kilowatt-hours (kWh) or megawatt-hours (MWh).

- Response Time: is the length of time it takes the storage device to start releasing power from the moment it is activated.

- Efficiency: indicates the quantity of electricity which can be recovered as a percentage of the electricity used to charge the device.

- Round-Trip Efficiency: indicates the quantity of electricity which can be recovered as a percentage of the electricity used to charge and discharge the device.

3.2. Mechanically based technologies.

As can be distinguished in Figure 3.1, energy can be mechanically stored mainly into three different ways: by elevating water into higher level tanks or reservoirs using revertible

pumps, by compressing air and storing it into artificial recipients or natural caves, or by speeding up spinning flywheels.

3.2.1. Pumped-Hydro Energy Storage (PHES).

This kind of energy storage technology can be firmly underlined nowadays as the most mature and the largest one with regards to energy capacity availability. Not for nothing, pumped-hydro is the oldest kind of large-scale ES technology since it was used from the beginning of the twentieth century being until 1970 the sole commercially available solution for large-scale ES. Nowadays, there are currently over 90GW installed around the world comprehending more than 240 PHES installations, which represents roughly the 3% of the global electric generating capacity [26, 33].

The main idea of the PHES technology is to take profit of some specific regional geographic features, places where two water reservoirs with different heights can be established, to even out the daily generating load. This is managed by, on the one hand, pumping water to the upper storage reservoir during off-peak hours and weekends using the excess base-load capacity in the EPS from coal, thermal or nuclear power plants. On the other hand, the water stored in this upper reservoir can be used during peak hours for hydroelectric generation, dropping it to the lower one.
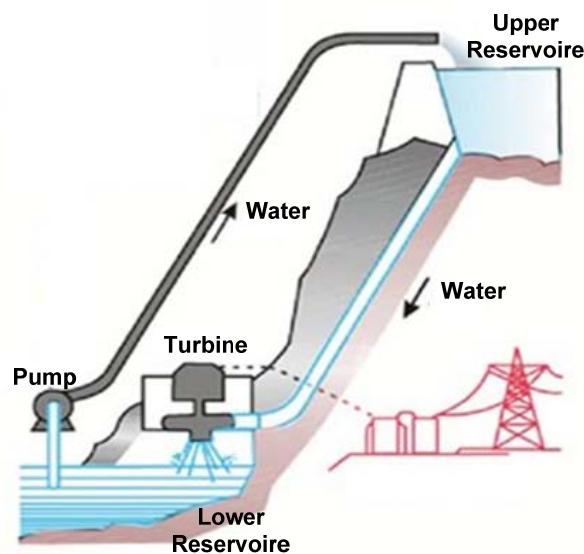
Figure 3.2 Simplified scheme of a PHES installation.

PHES recovers about 75% of the energy consumed, thus it is currently the most cost effective form of mass energy storage. Its efficiency is only limited by the pump/turbine group performance [26, 33, 34]. The power capacity of the plant depends on the flow rate and the hydraulic head, whilst the energy supply depends too on the hydraulic head as well as on the reservoir volume. In order to catch a glimpse on the potential of this kind of technology, only to remark that 1kg mass elevated 1km can store 9.8kJ of energy (equivalent to a 1kg mass accelerated to 140m/s or the temperature of 1kg of water incremented by 2.34ºC).

The key problem with PHES is that requires two nearby reservoirs at considerably different heights, as can be observed in Figure 3.3 and Figure 3.4, and often demands an initial considerable capital expenditure. However, its development perspectives are spectacular with some assessments estimating that there is currently a 200 GW extra latent opportunity for storage technologies concerning PHES around the world on cost, although geographically dependent. This is estimated to be equivalent to a $200 billion[1] market. The rest of the currently emerging storage technologies are nowhere close to this, and a typical target for PHES is 1000€ per kW / 100€ per kWh [1]. Other analyses are not so positive, mainly due to the high development costs, and focus its future development on underground PHES [26, 33, 35], which is designed with the upper reservoir at ground level and the lower reservoir deep below the earth's surface [36, 37].

Figure 3.3 Images corresponding to two different PHES installations.

---

[1] The USA $1 billion corresponds to 1.000 € millions in Europe.

Pumped water systems have high dispatchability, meaning they can come on-line very quickly, typically within 15 seconds [33]] which makes these systems very efficient at soaking up variability in electrical demand from consumers. These installations are very often considered by System Operators (SO) as a high value rapid-response reserve to cover transient peaks in demand. PHES can also be used for peak generation and black starts due to its large power capacity and sufficient discharge time. Moreover, PHES provides a load for base-load generating power plants during off-peak production, hence, cycling these low-dynamics generation units can be avoided, improving their lifetime as well as their efficiency.

Example of installations

Examples of these installations can be found in places such as Rocky Mountain (Georgia), Tenesse, Virginia, Colorado and New York in the USA, Tianhuangping (China) and Okinawa (Japan) in Asia, or Norway, Dinorwig power plant (Wales), Linth-Limmern hydropower plants (Switzerland), Ffestiniog power station (United Kingdom), and El Hierro or Cortes-La Muela (Spain), in Europe. In fact, it is in this latter where the currently biggest hydropower plant in Europe is under construction. It is located close to València, profiting the already existing PHES installation in the complex Cortes-La Muela, Figure 3.4. In this way, Spanish utility Iberdrola is broadening its ancient 630 MW power rated PHES installed system with the new group La Muela II. So, installed power is going to be increased up to 1720 MW producing some 1625 GWh annual estimated energy.

Another big example is the Tianhuangping PHES (China), which has a reservoir capacity of eight million cubic meters (the volume of water over Niagara Falls every 25 minutes) with a vertical distance of 600 m. The reservoir can provide about 13 GWh of stored gravitational potential energy (convertible to electricity at about 80% efficiency), or about 2% of China's daily electricity consumption.

It is to be noticed that most of these plants work with fresh water. However, some new facilities using seawater as storage medium are being developed lately, such as the PHES plant installed in Kunigami Village, Okinawa Prefecture, Japan in 1999 [33, 38]. It was the world's first seawater PHES and faced corrosion by using paint and cathodic protection.

Although variable speed pumping technology has already been studied and developed for decades [39-41], it is now being introduced in PHES. This can increase its efficiency by 5% to 10%. A further advantage when introducing variable speed pumps is to obtain PHES

systems which can be used for frequency regulation in both pumping and power generating modes. Lots of efforts on research and innovation of these facilities are being performed nowadays [42-49].

Figure 3.4 Cortes- La Muela PHES facility complex in València, Spain.

Moving one step forward, new PHES installations are being developed relating them to RES. This new concept in PHES comprehends utilizing wind energy or solar power to pump water. Wind turbines or solar cells that direct drive water pumps for an energy storing wind or solar dam can make it a more efficient process although limited, since those systems can only increase kinetic water volume during windy and daylight periods. That is the case of the green project being developed in the Spanish Canary Island of El Hierro [50]. The idea of this project is to power the entire island just from renewable energy resources. The power system under construction comprehends five windmills rated 2.3 MW each, and two water reservoirs with a 700 m height difference. Similar projects are being under study or development all around Europe: Greece [51], Feroe Islands [42] and Norway [43].

A daily curve of the overall hydraulic production in a country such as Spain can be observed in Figure 3.5 [52]. The PHES usage in the Spanish electric system can be appreciated on it, since there are periods of time along the day when the total hydraulic production is negative, meaning that this power is being used in pumping water to upper reservoirs.
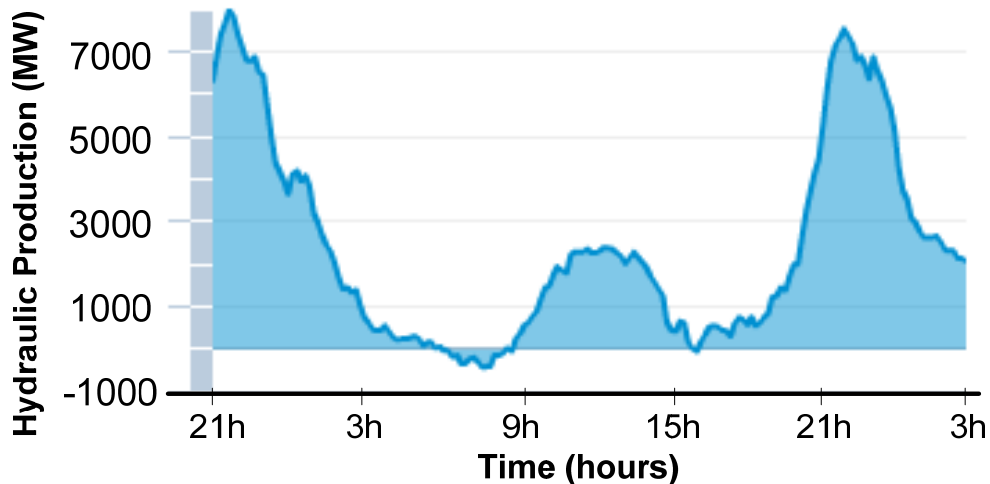
Figure 3.5 Daily curve of the hydraulic production in Spain. Source: [52]**.**

3.2.2. Compressed Air Energy Storage (CAES).

Compressed air energy storage (CAES) is also a mature storage technology for high-power long term load-leveling and demand side management applications [53, 54]. This technology can trace its roots already in the early 60s experiencing a great development along the 70s. As a result of this evolution a first installation was culminated in Germany in 1978. From then on, although all the technology needed in CAES installations has been continuously evolving and gas turbines are much more efficient nowadays, for different reasons only one of the subsequent projects, in Alabama (USA) in 1991 [33], came to fruition [55].

The functioning principle of this technology is that of storing low cost off-peak energy, in the form of compressed air in an underground reservoir, releasing the stored air during peak load hours, mixed with a fuel and used to power combustion turbines that produce environmentally friendly, dispatchable, and economical electricity. The underground reservoirs used in CAES facilities can be of different nature accounting from human-made rock to natural salt caverns, or even porous rocks created by water bearing aquifers or as a result of oil and gas extraction. Aquifer solutions are, by large, the least expensive solution [56], since water helps maintaining constant pressure levels in the reservoir. The structure and components of a CAES facility can be appreciated in Figure 3.6.

Furthermore, CAES can be integrated with cogeneration (CHP) since it has internal thermal processes associated to the gas compression and expansion [57], e.g. heated compressed air can be converted to energy through expansion turbines to produce electricity. In fact, in order to improve the efficiency in a CAES unit, the exhaust gas is passed through a recuperator to preheat the air coming from the high-pressure storage reservoir.
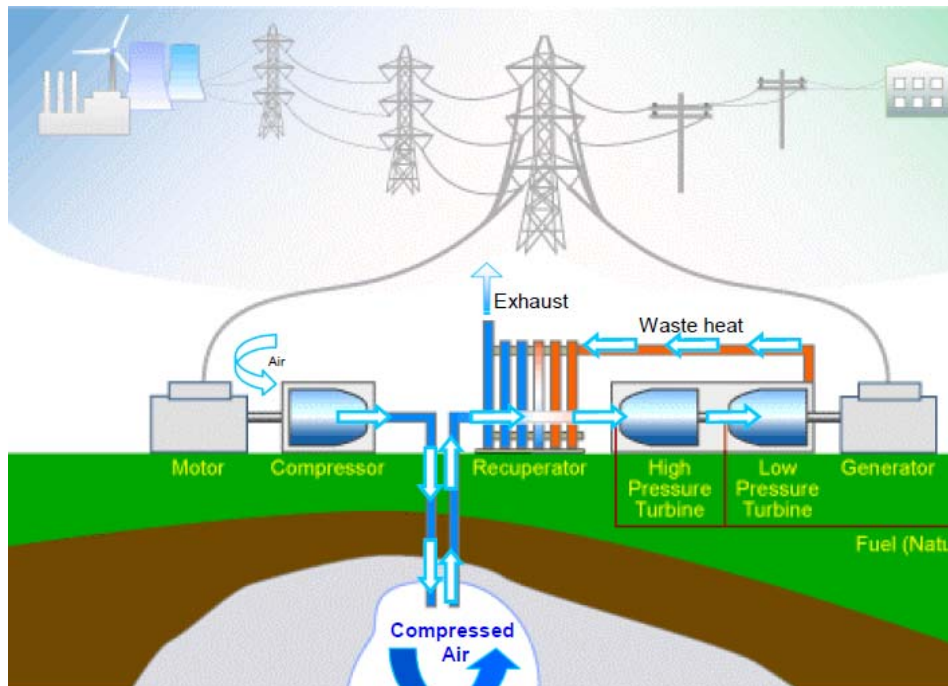
Figure 3.6 Schematic of CAES installation. Source: [58]

The most relevant components in a conventional CAES unit include [33]:

- A reservoir for the compressed air storage.

- A motor-generator with clutches on both ends, as a motor for driving the compressors or as a generator to produce electricity.

- Multi-stage compressors that condense the air into the reservoir.

- Intercoolers to reduce the power requirements during the compression cycle and an after cooler to reduce the storage volume requirements.

- A combustion chamber to heat the air via combustion of fuel before entering to the expansion system.

- An expansion system composed of high and low pressure expansion turbines which are connected to the generator mode when it is necessary to produce electricity.

- A control system for operating the turbine, the compressors and auxiliaries, and to switch from the motor mode to the generator mode.

- A thermal storage system that stores the heat produced during the compression phase in order to release it when the compressed air flows out of the reservoir for driving the turbine.

- Heat exchangers for capturing and releasing heat from/to air.

Finally, to conclude this section, some advantageous features which can be highlighted for CAES units are [57, 58]:

- The cost of the CAES units is low regarding to its ES capacities.

- CAES units offer quick response times and black start capability (The ramping rate of the CAES plants is around 30 % of the maximal load per minute).

- CAES units provide unlimited flexibility for load management tasks.

- CAES units can be nowadays constructed using commercially available equipment. And most of their components have estimated long life times (over 50 years).

Example of installations

So far, as previously stated, there are only two CAES plants in operation in the world which have been working for more than 15 years: the 290 MW plant belonging to E.N Kraftwerk in Huntorf, Germany, and the 110 MW plant of the Alabama Electric Corporation in McIntosh, Alabama, USA. Similar projects have been started elsewhere to look into the possibilities of CAES systems. For example, Italy has undergone some work in a small 25 MWe CAES research facility based on aquifer storage in Sesta. Research has been done too in Israel where a 3x100 MW CAES facility using hard rock aquifers was build. Equally, Luxembourg has undergone some level of development in a 100 MW unit, and Japan projected a 35 MW one. Finally, three bigger size units are under project: a 1 GW unit is currently under development in Russia and two more in the USA, a 0.5GW unit in Texas and a 2.7GW unit in Ohio. The latter, called Norton Energy Storage is being developed by the CAES Development Company (a Haddington Ventures LLC subsidiary). The site is a 10,000,000 m^3 limestone mine 700 m deep, in which they intend to compress air up to 100

bar before combusting it with natural gas. The first phase is expected to be between 200 MW and 480 MW costing $50 to $480 million. Another four phases are planned, to achieve in the site a possible capacity of 2700 MW, which would be able to operate for an entire 16-hour period and provide around 43200 MWh.

CAES was thought mainly for its integration into the EPS as a high power resource at the transport level. However, some of the new developments are nowadays being pushed forward by states and companies, such as the north American Ridge Energy Storage & Grid Services LP [58]. These new projects are applied to solve one of the main issues in a further RES integration, the intermittent production. This is fostering new CAES studies and development, as for the rest of the ESS, paving the way to new facilities [57, 59, 60]. In this regard, one project must be highlighted, the Iowa Stored Energy Project in the USA. It consists of 84 MW in wind turbines and a 200 MW CAES unit. Its cost is approximately $200 million and an underground aquifer located at around 370 m depth will be used as high pressure reservoir for both air and natural gas. The facility will operate between 12 and 16 hours per day, five days per week, combining wind power with power from CAES. This installation is expected to be cost competitive with other power plants in the same range of power located close to it. If few more wind turbines were added in the future, the combined power plant could evolve into a baseload facility in both scale and capacity.

Finally, other applications or possibilities do exist for CAES and the so-called micro-CAES systems. For instance, Walker Architects published the first CO_2 gas CAES application, proposing the use of sequestered CO_2 for Energy Storage on October 24, 2008. Furthermore, another future application which has just been published using units in a lower scale, considered as micro-CAES, is that of the compressed air vehicles [61]. Several companies have done preliminary design work for vehicles, mainly electric cars highlighting the case of the Indian Company Tata with its model called MiniCAT, using compressed air power as ESS in the electric vehicle industry.

3.2.3. Flywheel Energy Storage Systems (FESS).

Adding inertia to a motor or generator was the first method ever used in the electric domain in order to store energy and smooth out their variable speed operation, reducing or limiting in this way the power interruptions to critical loads. So, flywheels were already in use prior to the development of the present cost-effective power-conversion electronics which have widened their applications horizon.
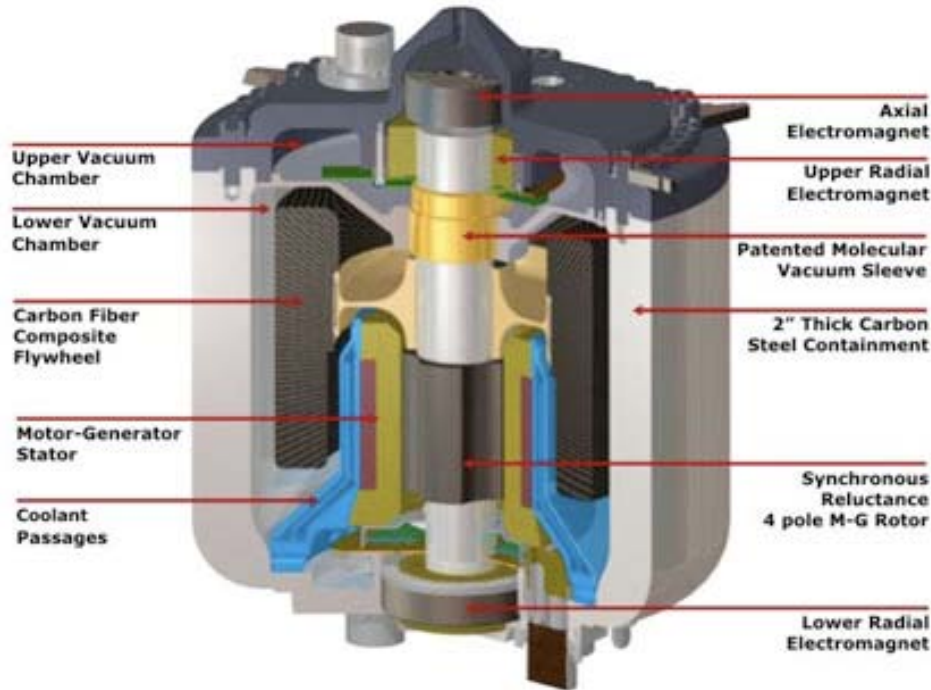
Figure 3.7 3D internal and external view of a FESS. Source: Pentadyne Power webpage.

Flywheels themselves present very simple physics. Their general structure can be observed in Figure 3.7. These are devices that permit ES in the form of a rotating wheel which can be accelerated to a very high speed. Therefore, the goal for this technology is to convert electrical energy into kinetic energy of a low-friction flywheel. This energy stored in the rotating flywheel can be subsequently released or recovered as electrical energy via a generator or power converter to provide energy when required, usually peak demand periods. Hence, this technology bases the amount of energy it can store, and the time it can provide the rated power, on the mass of the rotor and the rotating speed of the flywheel. Consequently, the most efficient way to store energy in a flywheel is to make it spin faster, and not to make it heavier. The energy stored in the flywheel is given by the formula:

$$E = \frac{1}{2}\,I\cdot\omega^2 \qquad\qquad\qquad \textbf{(3.1)}$$

Where E is the stored energy (in Joules), ω is the angular velocity (in radians per second) of the flywheel and I is the moment of inertia of the flywheel which can be calculated as:

$$I = \int \rho(x)r^2 dx \qquad \textbf{(3.2)}$$

Being $\rho(x)$ is the distribution of mass density around the rotating axis varying with the distance, and r the geometrical radius of the rotor. These equations can be rewritten as the energy per unit mass:

$$E_m = \frac{E}{m_f} = K\frac{\sigma}{\rho} \qquad \textbf{(3.3)}$$

Where E_m is the kinetic energy per unit mass, m_f is the mass of the flywheel (in kg), σ is the specific strength of the material (in Nm/kg), ρ is the density of the material in (kg/m^3) and K is the form factor or shape factor of the flywheel rotor. The value of this shape factor is a measure of the efficiency with which the flywheel geometry uses the material strength, and some characteristic values for the most common flywheel rotor shapes can be extracted from Table 3.1.
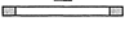
Flywheel type	Shape	K
Constant section		1.000
Constant stress-disk	-	0.931
Approx. Constant section		0.834
Conic disc		0.806
Flat non pierced disk		0.606
Thin rim		0.500
Rod or circular brush	-	0.333
Flat pierced disk		0.305

Table 3.1 Flywheel shape factor, *K*. Source: [62]**.**

Successful performance requires careful design and high-strength materials. Steel has been used for years, but modern composites, such as metal alloys, glass fiber, and polymer/carbon fiber, provide the strength required for coherence during extended duty cycles to prevent catastrophic failure of the flywheel at high rotation speeds. In fact, there are currently two types of FESS, the low speed flywheels (usually rotating below 10000 rpm) with a heavy rotor made from steel, and the high speed ones (rotating between 40000 and 80000 rpm) using carbon fiber rotors, magnetic bearings and usually contained within a

vacuum chamber to reduce aerodynamic drag losses. Regarding their ratings and capabilities, while the low speed ones can provide up to 1650 kW for up to 120 s, the high speed ones cannot provide more than 750 kW. However, the latter can operate during longer time periods up to one hour.

Although relatively high losses from the rotors have been a major issue for this technology, the new advances on all these complementary technologies [63] (new materials, magnetic levitation technologies, superconducting shaft bearing technologies, and variable-speed synchronous technologies) have permitted approaching the commercial stage. From the first models of flywheels, their efficiency has been improved continuously reaching 80 % [33] although some sources claim it can be as high as 90 %. Besides, since it is a mechanical device, the charge to discharge ratio is 1:1.

FESS units are quite competitive with alternative ESS for small power plants in terms of cost, but also in efficiency and storage energy density. Small flywheels that provide 30 to 1000 Wh for around $50-100/kWh have been developed. Moreover, according to [64] the initial capital cost, which is the main handicap for this technology, for a low speed FESS installation is in the range of $450/kWh, being around 50% more than that of lead-acid batteries[33], although when considering the whole lifetime of the facility, their total life-cycle cost can drop to, by far, less expensive costs thanks to FESS much lower operation and maintenance costs, together with a much longer life when compared to that of battery strings. On the other hand, costs for the high-speed flywheels is much more elevated, estimated around $25.000/kWh, what is typical for technologies still under development.

Example of applications

Already in the 70s, when advances in power electronics allowed the development of a new generation of flywheels, this technology was applied for centrifugal enrichment of uranium, with this application they were rediscovered as a potential new ESS [62].

From then on, thanks to their low maintenance needs and their availability to survive in harsh conditions, flywheels are suitable and suggested for applications which require very frequent and deep discharge-recharge cycles which are too demanding for example for batteries. Furthermore, when compared to batteries, FESS are also more compact and present hardly instantaneous response times. Consequently, flywheels are used for power quality enhancement [65]. That is why they already represent the 20% of the $1 billion energy storage market for uninterruptible power supplies (UPS) [35]. But other applications,

considering their power and energy commercial ratings, are possible. One of the most popular among them has been that of stabilizing frequency and voltage fluctuations in the electric grid [35, 66] and, lately, stabilizing the irregular power production from RES [67, 68].

The last flywheel developments which present extended capabilities (top high rotating speeds up to 100.000rpm and higher cycling capabilities), and especially, superconductor flywheel energy storage systems (SFESs) using high temperature superconductors (HTS) are capable of long term energy storage with very low energy loss [63]. These new developments can provide support to applications such as regenerative energy applications [26, 33] and to solutions for the electric vehicles industry [69, 70], or even in the aircrafts industry [71].

3.3. Electromagnetically based technologies.

On the contrary to mechanical systems, electromagnetically based technologies store the energy directly in the form of an electric field (ultracapacitors) or magnetic field (superconducting magnetic), that is why these are classified as direct storage technologies.

3.3.1. Superconducting Magnetic Energy Storage (SMES).

The Superconducting Magnetic Energy Storage (SMES) technology started its development with the apparition of the high-powered magnets at the beginning of the 60s, with a first serious proposal for SMES facility arising in 1969. From then on, several research projects were established in the USA (by the Department of Energy, the Department of Defense and others) as well as in Europe and in Japan. The goal was to develop a new large-scale ES technology capable to store hundreds of MWs and compete with CAES and PHES [72]. Nonetheless, research trends during the 80s focused the interest on smaller SMES, the so-called micro-SMES [27], with capacity to guarantee only industrial power quality and transmission system voltage stability [73, 74]. This has been the tendency up to now although recent studies propose extending their functionalities taking advantage of the power converters flexibility [75].

Nowadays, a SMES system consists mainly of five parts, which are the superconducting coil with the magnet (SCM), the power conditioning system (PCS), the cryogenic system for refrigeration (CS), the cryostat/vacuum vessel (VV) and the control unit (CU), as shown in Figure 3.8:
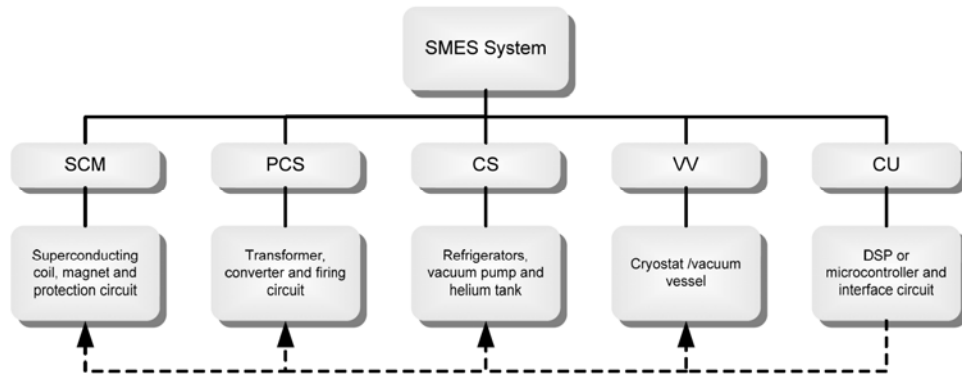
Figure 3.8 SMES classification of components.

The functioning principle of this technology is that of storing energy in the form of the magnetic field created when a constant current flows along the coil of cryogenically cooled superconducting material, usually made of Niobium-Titanium (NbTi) filaments that operate at very low temperature (around 4K). The energy stored by the SMES unit can be calculated from the following equation:

$$E_{SMES} = \frac{1}{2} L \cdot I^2 \qquad \qquad (3.4)$$

where L is the inductance of the coil, and I is the current passing through it. From this equation, it can be concluded that material properties are extremely important for this technology mainly due to the temperature dependence of the superconductive state. Generally, when current circulates through a wire, some energy is dissipated by Joule effect as heat due to the resistance of the wire itself. Nevertheless, if the wire is made from a superconducting material, resistance is reduced to approximately zero. In this way, energy can be stored with practically no losses.

To keep the superconducting state within a material, its functioning temperature must be kept at very low values. There are two types of superconductors:

- Low-temperature superconductors, as it is the case for the NbTi used in the coil, that conserve that particular characteristic at temperatures below 4.2 K which are achieved with liquid helium refrigeration.

- High temperature superconductors which present a temperature range of operation between 10 K to 150 K. In the SMES units, these materials are used in the interface

components between the cryogenic area of the SMES and the conductors to the PCS.

Although successful demonstration projects operating at 20K have been run in Germany, Finland, the USA and South Korea [27], high-temperature superconductor technology has received much less attention and SMES development have focused on NbTi technology.

One of the main advantages for SMES technology is their fast response time (under 100 ms) [76] providing very high output power levels (although only for a few seconds). Moreover, these systems are capable of discharging the near totality of the stored energy, as opposed to batteries. Discharging would be possible in milliseconds if it was economical for the application to have a PCS that is capable of supporting this. Another advantage is its cycling capability. SMES devices can run for thousands of charge/discharge cycles without any degradation to the magnet, what makes them very useful for applications requiring continuous operation with a great number of complete charge–discharge cycles, guaranteeing lifetimes over 20 years.

With respect to the efficiency of the SMES units, their values vary depending on the author but are always in the region between 90%, 95% upon [56, 75, 76] and 99% from [33].

Regarding its cost, it varies depending on the source of information. SMES units cost are accounted from $300/kW [74] to $509/kW[64], even higher up to $800/kW [75, 77] or, even in the range $1000–10,000/kW [34]. The reason for the wide variation in the cost of the power conversion system is its dependence on the configuration of the system. Main part of the investment, around 60%, is required by the SCM, a 30% correspond to PCS, and the lasting 10% to the rest of the equipment, mainly the cryostat [77]. Due to the peculiarities in the SMES applications and its scale it is difficult to compare the cost of SMES to other storage devices. Notably, SMES units are cost competitive when compared with FACTS or other transmission upgrade solutions, in both installation and operation costs. In terms of storing energy, SMES is not competitive yet but, since a reduction of about 30% in the components cost could be achieved, future advances could make SMES competitive in this domain, and even more attractive for network improvement solutions.

Example of installations

Thanks to the high power capacity and instantaneous charge and discharge rates of SMES, these units are very well suited for providing repeated short-interval discharges. So, the main application for this technology has been found to be to provide power quality

service to consumers vulnerable to power fluctuations [33, 75, 78]. The second main application is its capacity to provide transmission voltage support [75, 79, 80], connected to the network by means of high power converters with schemes as the one depicted in Figure 3.9. In this regard, it is a very useful network upgrade solution. Some sources claim it can help increasing the capacity of a local network by up to 15% [33].
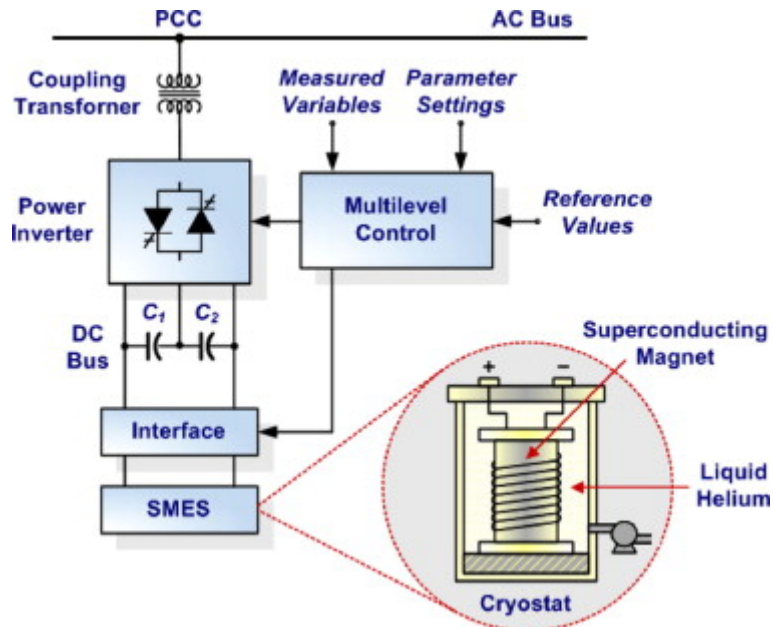
Figure 3.9 SMES unit diagram. Source: [79]

On the contrary, due to the high energy consumption level needed for its refrigeration units, which is one of the main drawbacks of this technology ([26, 75]), SMES facilities are unsuitable for daily cycling applications such as peak reduction, renewable applications, and generation and transmission deferral.

In all, more than 100MW of micro-SMES units (with a 3MW average power) are estimated to be currently installed in places such as Japan, Europe, South Africa or the USA. Among them, three examples of these installations to be noted are:

- The Wisconsin Public Service Corporation installation, in the USA [33]. This installation, formed by six SMES units from American Superconductor, is the one which helped increasing the power grid capacity, in the northern loop of the Wisconsin State, by a 15%. Voltage disturbances have been minimized with them

permitting the utility to assure a high power quality for the paper factories in the region.

- The Dortmunder Elektrizitats und Wasserwerke unit, in Germany [62]. This unit is designed to be able to provide 200 kW for around eight seconds, being connected to the grid of the plant via dc-link and the corresponding converter, with the goal to ensure power quality in the laboratory plant. The SMES unit is wound of NbTi mixed matrix superconductor cooled with Helium, with a two-stage cryo-cooler and a sophisticated quench protection system.

- The Sappi paper mill unit in Stanger, South Africa [33].This third installation consists on a 1 MVA Power Quality Industrial Voltage Regulator with SMES, from American Superconductor, at a Sappi paper mill. It was installed in 1997 with the goal to avoid voltage sags which forced to stop the whole fabrication procedure for ours with the corresponding economic impact. This installation is successful since only in the first year of operation avoided more than 30 potential shut downs.

3.3.2. Capacitors and UltraCapacitors (UC).

Traditional capacitors have been known since the very first beginnings of the electrical science development and used with the apparition of the first electric applications. Already in October 1745, Ewald Georg von Kleist of Pomerania, in Germany, found that electric charge could be stored by connecting a high voltage electrostatic generator by a wire to a volume of water glass [81]. Early capacitors were also known as "condensers", a term that is still occasionally used today and which was first used for this purpose by Alessandro Volta in 1782 with reference to the device's ability to store a higher density of electric charge than a normal isolated conductor [82].

Capacitors basically consist of two conductors separated by a non-conductive region. The electric energy is stored on them by accumulating positive and negative charges in two different plates separated by an insulating dielectric, creating an electric field in this region. The capacitance, C, represents the relationship between the stored charge, q, and the voltage between the plates, V, as shown in (3.5).

$$q = C \cdot V$$

$$(3.5)$$

The value of the capacitance depends on the permittivity of the dielectric, ε_d, the permittivity of the free space, ε_0 (8.854x10^{-12} F/m), the area of the plates, A, and the distance between the plates, d, as shown in (3.6).

$$C = \frac{\varepsilon_0 \cdot \varepsilon_d A}{d}$$

(3.6)

Furthermore, the energy stored on a capacitor, E_{CAP}, depends on the capacitance and on the square of the voltage, and it can be calculated by (3.7).

$$E_{CAP} = \frac{1}{2} C \cdot V^2$$

(3.7)

The amount of energy a capacitor is capable of storing can be increased by either increasing the capacitance or the operating voltage of the capacitor. This operating voltage is limited by the voltage-withstand-strength of the dielectric (which impacts the distance between the plates). Capacitance can be increased by increasing the area of the plates, increasing the permittivity, or decreasing the distance between the plates. As with batteries, the turnaround efficiency when charging/discharging capacitors is also an important consideration, as it is the response time. The effective series resistance (ESR) of the capacitor has a significant impact on both. The total voltage change when charging or discharging capacitors, dV, is shown in (3.8).

$$dV = i \cdot \frac{dt}{C_{tot}} + i \cdot R_{tot}$$

(3.8)

Where R_{tot} and C_{tot} are the result from a combined series/parallel configuration of capacitor cells to increase the total capacitance and the voltage level. The product $R_{tot} \cdot C_{tot}$ determines the response time of the capacitor for charging or discharging.

However, conventional electronic capacitors present clear limitations regarding power and energy capacities, what makes them non-profitable for ES applications at EPS level. That is why, a new technology known as electric double-layer capacitors with very large capacitance values has been developed. Those capacitors are frequently called supercapacitors, ultracapacitors (UC) or electrochemical capacitors [64]. Although the origins of this technology can be dated more than 100 years ago, it is not till the 1960s decade that serious research focused on them thanks to companies such as Standard Oil of Ohio (USA) or NEC and Matsushita Electric Industrial Company (both in Japan). It was finally in the 90s when UC were scaled up and commercialized, especially for pulsed power

applications and others such as engine starting, energy storage applications and the electric vehicle market.

UC are electrical storage devices comparable to conventional ones but with higher power and high energy densities, e.g. their energy density (between 5kWh/m^3 and 20kWh/m^3) is up to 100 times higher than that of conventional capacitors, and their power density is up to ten times higher than that of batteries. A comparison between the energy and power characteristics of these three technologies can be clearly appreciated in Figure 3.10.
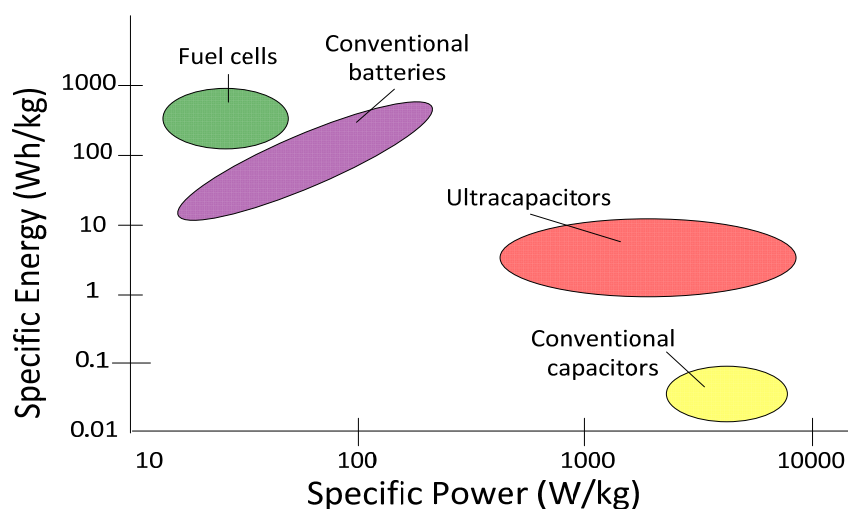
Figure 3.10 Energy and power comparison of capacitors with other technologies.

It can be considered that UC are half way between conventional capacitors and batteries. This could be true in both electric characteristics and physical internal structure. In fact, in the latter aspect, UC could be even closer to batteries since they have two electrodes immersed in an electrolyte (see Figure 3.11). One of the UC electrodes is porous, the active electrode, what makes it experience a large increase on its exchange surface area. This is the clue for the large improvement in ES capabilities referred to conventional caps. However, UC still have relatively low permittivity and voltage-withstand capabilities [83]. There are four different types of electric double layer capacitors, named types I to IV. None of them exceeds the 4 V per cell as voltage-withstand value. Hence, packs of UCs parallel and series connected have to be established in order to achieve high operation voltages and elevated power and energy values.

Though it is an electrochemical device, no chemical reactions are involved in UCs energy storage mechanism. The energy is accumulated via electrostatic charges on opposite surfaces of the double layer formed between each of the electrodes and the electrolyte ions. The amount they can store can be calculated with the same equation (3.7). Different combinations of electrodes and electrolyte materials have been used in UCs' development, with the different combinations resulting in varying values of capacitance, energy density, cycle-life, and cost characteristics. As a result, one can conclude that commercial UCs available nowadays present the following advantages: they can be completely discharged without damage, extremely long life (around 1 million complete cycles), do not suffer from memory effect, can be installed easily, are compact in size and can operate effectively in diverse aggressive environments (hot, cold and moist). At the moment, due to their still low values of ES density, they are most applicable for high peak-power/low-energy applications, while using them for large scale developments could lead to high costs.
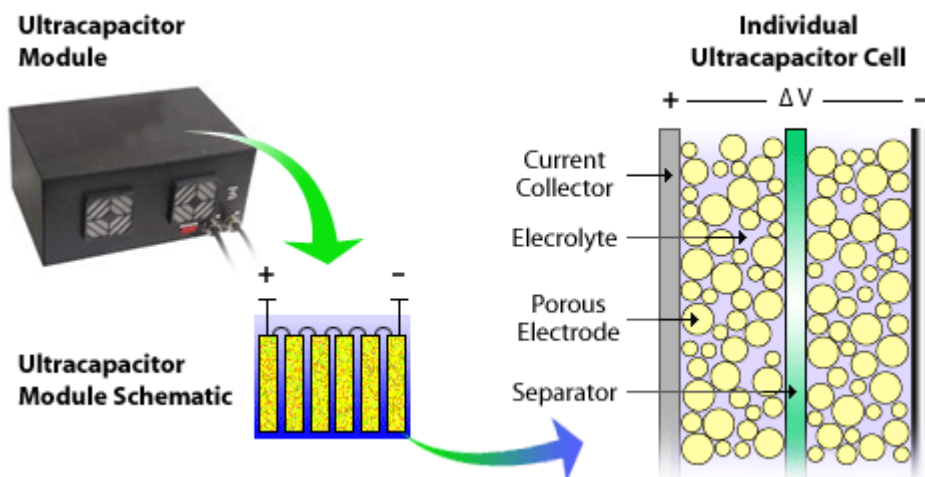
Figure 3.11 Ultracapacitors stack outlook and internal structure description. Source: NREL.

The estimated cost for this technology varies again depending on the source of information. While [84] states a prize around $28000/kWh, others such as [74] refer to around $12960/kWh, and [64] fixes a total system cost around $450/kW (in power) accounting 40% of this amount for the storage module itself. Assessments around the year 2006 estimated the price in $10260/kWh. And finally, some recent consultations to UC providers have resulted in a price of about 4095 € for Maxwell Technologies 125 V 63 F unit. Prices are dropping further and further but, in any case, they suppose unaffordable investments for large scale installations.

Example of installations

UC are used in many ac and dc applications in power systems, nowadays. They have long been used in pulsed power applications for high-energy physics and weapon applications. However, the present generation of UC still finds a limited use as large-scale ES devices for power systems, although proposed in the past for some grid applications such as load leveling [85]. As a developing technology, their capabilities must still be improved, their costs lowered and the reliability enhanced.

UC are often used for very short-term storage in power converters [86]. For example, additional capacitance can be added to the dc bus of motor drives and consumer electronics to provide added ability to ride through voltage sags and momentary interruptions [87-89]. The main transmission or distribution system application, where capacitors are used as large-scale energy storage, is in a distribution dynamic voltage restorer (DVR) presented in [90].

Figure 3.12 Ultracapacitor models from Maxwell Technologies. Source: Maxwell Technologies.

They are well positioned in other industries such as the automotive one [91], being already experienced in the hybrid electric vehicles (HEV) industry [92-95], and considered as ESS for the coming electric vehicle developments (EV) [33, 96, 97]. They have been used even in the Formula 1 where the FIA, the governing body, proposed in the Power-Train Regulation Framework for Formula 1 version 1.3 of 23 May 2007 that a new set of power train regulations be issued including a hybrid drive of up to 200 kW input and output power using "superbatteries" made with both batteries and ultracapacitors. In the transportation industry in general they have found application too, including UC units in trams (Spanish

company CAF), light railroad systems (Siemens' SITRAS SES System), electric buses [98] and even in elevators (Orona Group). Furthermore, they represent an important market in the mobile and communication systems industry as well as in some domestic electronics. In 2007, a cordless electric screwdriver that uses a UC unit for ES was produced.

Finally, just to point out some leading UC manufacturers around the world: Maxwell Technologies (USA), NESS Capacitor Co. (South Korea), Panasonic and Okamura (Japan), and SAFT in France and EPCOS in Germany.

3.4. Electrochemically based technologies.

Apart from mechanical and electrical ESS, there is a third group based on chemical and electrochemical technologies which is also very important. It includes the different families of batteries and the hydrogen technology. The common characteristic in this group of ESS is that they store the energy in the internal structure of some substance obtained by means of chemical reactions. The energy is recovered when desired by forcing the reversed reaction.

3.4.1. Batteries (BESS).

Batteries have been used for long and many different technologies have been developed [99]. The main families industrially developed and finally commercialized for some kind of ES application are presented in the coming sections.

a) Lead Acid Batteries.

Lead acid batteries (LA batteries) are the oldest type of rechargeable battery. They were invented in 1859 by the french physicist Gaston Planté. Some years later, this technology was used into pionering power-delivery systems to provide load leveling capability to meet peak demands. However, large expansion of generation systems together with the rapid development of internal combustion engines which took over the market for engines at the begining of the twentieth century, slew down their development for some time. As of the year 1920, they found new markets as electric motors for industrial traction applications or standby power systems in power plants and substations. Continuous research was performed along the century leading to manufacturing cost reductions and to a more reliable flooded LA technology. The valve regulated lead acid type of battery was developed in the seventies, presenting a lower manufacturing cost and easier maintenance, although shorter lifespan. From then, both technologies have subsisted in parallel, being improved continuosly till

present time to adapt them to multiple arising newer applications [100]. So, this is the most common worldwide ES device in use at present.

An LA battery cell consists of a negative electrode made of lead and a positive electrode made of lead dioxide, both of them immersed in diluted sulfuric acid electrolyte (35% acid and 65% water), being the lead the current collector which leads to low specific energy values. Furthermore, the lead is prone to corrosion when exposed to the sulfuric acid electrolyte. During the discharge, lead sulfate is produced on both electrodes. If the batteries are overdischarged or kept at a discharged state, the sulfate crystals become larger and are more difficult to break up during recharge. In addition, the large lead sulfite crystals disjoin the active material from the collector plates. Both, the power and energy capacities of LA batteries, are based on the size and geometry of the electrodes. The power capacity can be increased by increasing the surface area for each electrode, which means greater quantities of thinner electrode plates in the battery. However, to increase the storage capacity, the mass of each electrode must be increased, which means fewer and thicker plates. Consequently, a compromise must be met for each application. An example of internal LA battery structure can be appreciated in Figure 3.13.
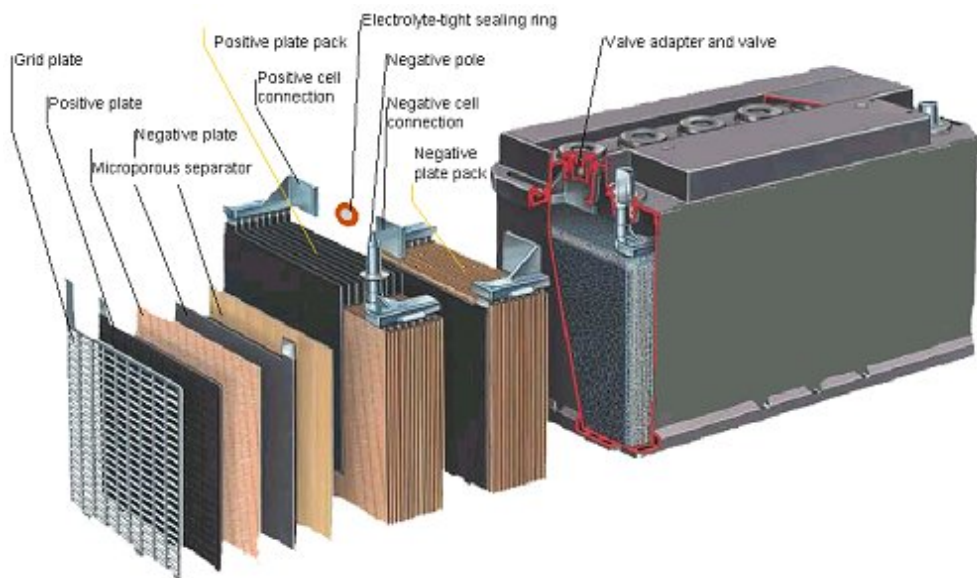
Figure 3.13 LA battery: list of components and structure. Source: Battery rejuvenator web site.

As previously stated, there are two types of LA batteries: flooded (FLA) and valve regulated (VRLA). The difference between them is that VRLA batteries are sealed and

contain a pressure regulating valve. This valve allows eliminating air from entering the cells and also prevents venting of the hydrogen produced in the chemical reactions that take place within the battery. This hydrogen production at the positive electrode involves the batteries experiencing a water loss during overcharge. That is why distilled water is sometimes added to FLA batteries (no needed in the VRLA type).

A lead-acid battery set of typical parameters is included in Table 3.2.

Specific energy	30-40 Wh/kg
Energy density	60-75 Wh/Liter
Specific power	About 250 W/kg
Nominal cell voltage	2 V
Electrical efficiency	About 80%, depending on recharge rate and temperature
Recharge rate	About 8 hours (possible to quick recharge 90%)
Self-discharge	1-2% per day
Lifetime	About 800 cycles, depending on the depth of cycle

Table 3.2 Lead acid battery main properties.

As it can be extracted from this table, the LA technology presents some advantages, but also disadvantages, when compared to other ES systems. On the positive side, they are very reliable and robust. They present strong surge capabilities and relatively high efficiency (65 – 80%). Furthermore, they are economical. Among them, VRLA batteries have lower maintenance costs, they weight less and occupy less space. However, these advantages are offset by higher initial costs and shorter lifetime.

On the negative side, LA batteries present low specific energy values (30 – 40 Wh/kg). They emit explosive gas and acid fumes, and have a poor cold temperature performance which suggests a thermal management system [101]. In fact, they are extremely sensitive to the environment. The typical operating temperature for a LA battery is roughly 27°C, but a change in temperature of 5°C or more can cut the life of the battery by 50%. In the same way, if the depth of discharge (DoD) exceeds 80% (battery normally designed to work with DoDs between this limit and 50% as lower limit) the life cycle of the battery will also be reduced [102], being already the designed lifespan quite short (500 –1000 cycles, poor for energy management purposes) [34]. In fact, the big issue for this technology is their unpredictable lifetime. They tend to have a nonlinear life and die suddenly; when their internal components corrode, their capabilities quickly deteriorate Hence there is need for constant monitoring and require regular maintenance [101]. Finally, a typical charge-to-discharge ratio of a LA battery is 5:1. At faster rates of charge, the cell will be damaged, what supposes a big handicap for applications which require fast recharge (case of electric vehicles). Although VRLA batteries require less maintenance, create less gaseous emissions

and present lower self-discharge than their non-valve regulated counterparts, they are primarily designed for back-up power supply and telecommunication applications due to their decreased cycle life [103].

The cost for this technology has been stated by many authors, varying as time goes by. Cost analyses of early large-scale installations developed during the last century estimate them over $1000/kW, including the power conversion system, with only half of it corresponding to the battery itself [104]. Recent studies reduce their cost, ranging from $200/kW to $300/kW [74]. Other authors value it higher up to the region from $300/kW to $600/kW [34], or more precisely $580/kW for [33, 64].

Despite having a very low energy-to-weight ratio and a low energy density, their ability to supply high surge currents means that the cells maintain a relatively large power-to-weight ratio. In fact, they have been traditionally used for applications where weight, volume, low energy density and limited cycle life are not an issue and where ruggedness and rough tolerance are required [105]. These features, along with their low cost and high reliability, make FLA attractive for use in conventional motor vehicles to provide the high current required by automobile starter motors [106]. This application represents the 70% of the LA batteries market in countries such as China [103]. They are also used for applications which require deep cycles with low steady power provided over a long time [35]. VRLA batteries are very popular for backup power (UPS systems) [101, 106], standby power supplies in telecommunications (21% of the LA batteries market in China [103]) and also for remote/off-grid renewable markets[107]. Again in China, LA batteries are being used for the 75% of new solar photovoltaic systems, which was 5% of the entire LA battery market in year 2007, and are expected to hold 10% by 2011 [103]. Nevertheless, due to LA batteries' technical limitations inherent in the technology, they are not expected to be the dominant ES system in the coming future [33, 108]. As environmental concerns continue to grow, standards and regulations on manufacturing and recycling of this technology will continue to increase, making difficult its expansion.

A huge number of big LA units were used at the beginning of the large-scale multifunctional ES facilities development. Some of them can be highlighted due to their significant characteristics [33, 104]. These are[33]:

- The 400 kW / 400 kWh installation developed for the Elektrizitatswerk in Hammermuehle (Germany) in 1980. This BESS was used for peak shaving and the

attendant reduction in demand charges. The system is of particular interest because of its longevity (operating till 2000).

- The 17 MW / 14 MWh BESS facility installed by BEWAG AG in Berlin (Germany) in 1986. Its goal was to provide frequency control and spinning reserve for the isolated, 'island' utility which served West Berlin. It operated during 9 years till the island was connected to the West European grid.

- The 1 MW / 4 MWh facility installed at the Kansai Power Co. in Tatsurni (Japan) in 1986. The goal of this project was to develop a multipurpose demonstration battery system.

- The 10 MW / 40 MWh FLA battery installed at a substation in Chino, California (USA), in 1988. It was an $ 18.2 million multifunctional test installation mainly oriented to evaluate load levelling operations [101, 109] which resulted successful and is still operated by Southern California Edison Company.

- The 4 MW / 7 MWh battery installed at Vaal Reefs Exploration and Mining Co. in (South Africa) in 1989 for peak shaving functionalities.

- The 20 MW / 14 MWh (40 minutes) battery installed at the Sabana Llana substation in Puerto Rico in 1994. The goal of this unit was to provide spinning reserve and voltage control to the entire island during normal operation.

- The 3 MW / 4.5 MWh VLRA battery installed at an LA battery recycling plant in Vernon, California (USA), in 1996. It has been working since then accomplishing the role of providing peak demand reduction and uninterruptible power.

- The 1.2 MW / 1.4 MWh VLRA battery installed by GNB Industrial Power for the MP&L Company in Metlakatla, Alaska (USA) in 1997. This project has been an example of extended RES integration into a weak grid thanks to the introduction of an ES system.

- And finally, the 40 MW / 14 MWh unit being promoted by the Golden Valley Electric Association (GVEA) in Golden Valley, Alaska (USA). It is foreseen as spinning reserve, for voltage regulation and frequency control, enhancing greatly the stability of the entire system and minimizing load shedding.

There are lots of manufacturers for this technology. Some of them are: Trojan Battery Company, C&D Technologies, Delco, Sunbright battery, Tudor Exide, EASTAR Batteries…

b) Nickel Cadmium and Nickel Metal Hydride Batteries.

Historically, the development of nickel based batteries started during the 1890s decade. The first Nickel-Cadmium (NiCd) battery was created by Waldemar Jungner (Sweden) in 1899. In 1901, Thomas Edison was awarded U.S. Patent 684,204 for a rechargeable nickel-zinc (NiZn) battery system. Both of them experimented with substituting iron for the cadmium in varying proportions obtaining some Nickel-Iron (NiFe) battery prototypes, some of them patented by Edison too, and implemented in some electric cars of the time as the Detroit Electric and the Baker Electric. Few applications were found for NiCd batteries at that time because of the high cost and difficulty in manufacture. Along the twentieth century some advances were obtained, as the sintered plate design in 1932 and the sealed NiCd cells in 1946. Continuous development allowed NiCd to finally become widely used in the portable industry market for consumer electronics beyond the 1970s. From then on, complete industrialization and commercialization of these different technologies has been worldwide achieved.

The NiCd battery technology uses nickel oxyhydroxide (NiOOH) for the positive electrode and metallic cadmium for the negative electrode. Both electrodes are separated by a polyamide or nylon divider. The electrolyte is a 30% aqueous solution of potassium hydroxide (KOH). During discharge, the NiOOH combines with water and produces nickel hydroxide and a hydroxide ion, generating at the same time Cadmium hydroxide at the negative electrode. To charge the battery the process can be reversed. However, during charging, oxygen can be produced at the positive electrode and hydrogen can be produced at the negative electrode. As a result some venting and water addition is required, but much less than required for a LA battery [35].

Nickel-Metal Hydride (NiMH) cell is another type of nickel rechargeable battery similar to the NiCd one. The NiMH battery uses a hydrogen-absorbing alloy for the negative electrode instead of cadmium. As in NiCd cells, the positive electrode is nickel oxyhydroxide (NiOOH). Other different technologies can be found in this family. Their particular characteristics, which vary with the different materials used in the anode, can be observed in the following Table 3.3.

As can be observed on this table, NiCd batteries do compete with LA batteries because they have a higher energy density (50–75Wh/kg) and have a longer life (2500 cycles). Furthermore, they can respond at full power within milliseconds. In this sense, they seem

appropriate for uninterruptible power supply and generator starting applications [103]. Also, NiCd batteries fail linearly and predictably (which helps predicting their state of health) and they have a quite longer lifespan than LA batteries (mainly at small depth-of-discharge rates, under 10%, where they can achieve even 50000 cycles), requiring only infrequent maintenance. Finally, they are the cheapest among the Nickel technologies, although more expensive than LA ones.

System	Ni-Cd Pocket plate	Ni-Cd sealed	Ni-MH	Ni-Zn	Ni-Fe Pocket plate	Ni-H$_2$
Nom. Voltage (V)	1.2	1.2	1.2	1.6	1.4	1.2
Energy Density (Wh/l)	40	100	75	60	55	105
Specific Energy (Wh/kg)	20	35	54	120	30	64
Power	Low	High	High	High	Low	Medium
Cycle life	2500	700	600	500	4000	6000
Discharge profile	Flat	Flat	Flat	Flat	Flat	Flat

Table 3.3 Properties for different types of Nickel based batteries. Source: SAFT batteries.

On the negative side, although NiCd batteries have a higher energy density and longer life cycle than lead-acid batteries, they are present lower properties than chemistries such as Li-ion and NiMH. Besides presenting low energy-density, NiCd batteries contain cadmium, hence are considered hazardous waste when disposed. In this sense, these batteries, together with NiMH ones, are recyclable and recycled for the recovery of nickel, iron, zinc and cadmium. But, the big handicap they present for large scale utility applications, requiring high investments, is the named memory effect [101]. If NiCd batteries are not fully discharged before being recharged, the battery will start losing its capacity [35]. Furthermore, NiCd batteries lose more energy than LA batteries due to selfdischarge, with an estimated 2% to 5% of their charge lost per month at room temperature in comparison to 1% per month for LA batteries [33].

For the rest of technologies, regarding NiMH, they are fully developed and can be considered safe. They have some advantages with regard to NiCd which include the following: a higher energy-density, relatively high power density, less pronounced "memory effect" and the fact of avoiding the use of cadmium. On the other hand, they present a more reduced lifespan, which can be improved with flat cycles obtaining an acceptable durability. In fact, last developments predict a very long life at a partial state of charge. Another big issue for this chemistry is its relatively high self-discharge rate, although this is being mitigated by introducing novel separators. Furthermore, NiMH batteries use excess energy to split and recombine water when overcharged. Therefore, the batteries are maintenance free. However, if the batteries are charged at an excessively high charge rate, hydrogen build up

can cause cell rupture. If the battery is overdischarged, the cell can be reverse-polarized, leading to capacity reduction [25]. Finally, a limiting problem for future applications is their low potential for cost reduction and increase in energy density (they are more expensive than NiCd and LA batteries).

With respect to Nickel-iron batteries, one important advantage is that they do not use neither lead nor or cadmium, which makes them a cleaner option on human and ecological health. Furthermore, they are able to survive frequent cycling due to the low solubility of the reactants in the electrolyte; hence they can have very long life even under harsh operation conditions (ability to withstand vibrations, high temperatures and other physical stress). However they have low specific energy, very low cell voltage (1.2V), poor charge retention, and high cost of manufacture. Finally, another chemistry of the family is Nickel-Zinc (NiZn). Compared to other secondary systems, NiZn cells have lower volumetric energy density and are also more costly then LA batteries due to market process of nickel and lead.

Focusing on the construction design, there are two main topologies for Ni based batteries:

- Sealed NiCd structured batteries (also "swiss roll" or "jelly-roll"). As appreciated in Figure 3.14, this design incorporates several layers of positive and negative material rolled into a cylindrical shape reducing internal resistance as there is a greater amount of electrode in contact with the active material in each cell. The charge gas is internally recombined and they do not release any gas unless severely overcharged or a fault develops. These are commonly used in commercial electronic products such as remote controls, where light weight, portability, and rechargeable power are important.
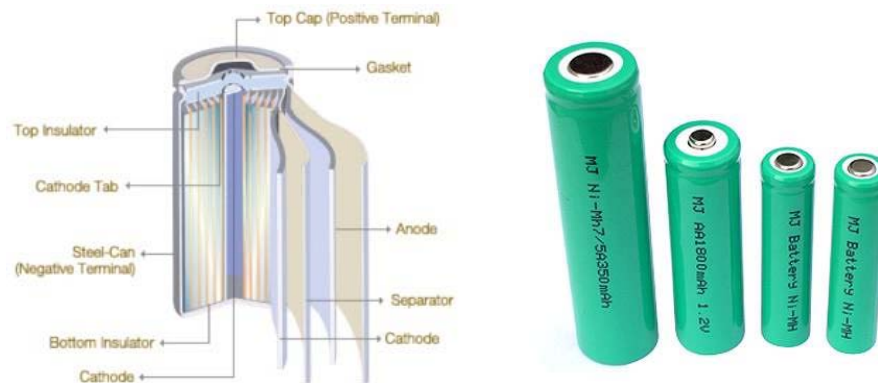
Figure 3.14 Sealed Nickel Cadmium batteries internal structure and external outlook.

- Vented NiCd batteries on the other hand have a vent or low pressure release valve that releases any generated oxygen and hydrogen gases when overcharged or discharged rapidly. Since the battery is not a pressure vessel it is safer, weights less and has a simpler and more economical structure. This also means the battery is not normally damaged by excessive rates of overcharge, discharge or even negative charge. These are used in aircraft and diesel engine starters, where large energy per weight and volume are critical and where large capacities and discharge rates are required.
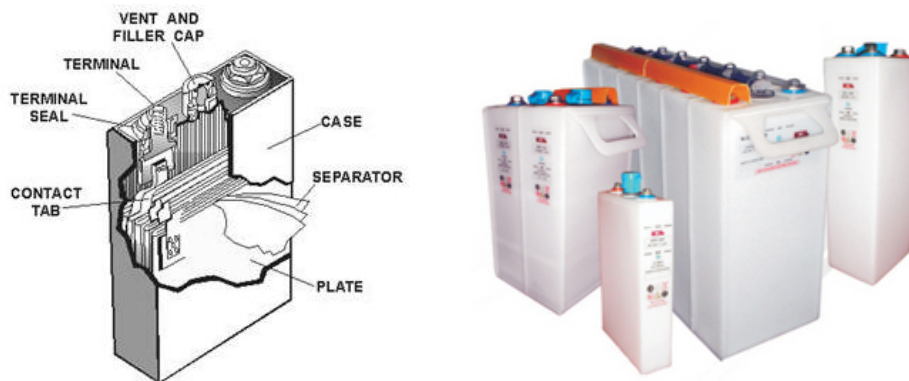
Figure 3.15 Vented Nickel Cadmium batteries internal structure and external outlook.

Advances reported in Nickel battery-manufacturing technologies throughout the second half of the twentieth century have made batteries increasingly cheaper to produce, although they keep being more expensive than LA batteries and will always remain for ES applications ($1000/kWh). According to [33, 64], a multi-MW multifunctional NiCd battery has a system cost of $600/kW, corresponding around 60% to the battery module. NiCd batteries were the chemistry of choice for a wide range of high-performance applications between 1970 and 1990. As of 2000, about 1.5 billion NiCd batteries were produced annually and up until the mid-1990s, NiCds had an overwhelming majority of the market share for rechargeable batteries in consumer electronics. However, their commercialization declined continuously from 1995 to 2003 [34]. This trend could be attributed to the increasing environmental concerns about toxic metals, such as cadmium [110], regulated now by the 2006 European Union's directive on batteries and accumulators. This directive banned NiCd batteries from September 2008 [111]. So, they have been recently replaced by Li-ion and NiMH chemistries in many applications [25] and it is unlikely that they will be used for future large-scale projects. However, some tests installations were developed in the

past, as an example of large scale installations using NiCd technology, the following can be highlighted:

- A 40MW/10MWh (supply for 15 minutes) installed by SAFT batteries in August 2003 for the Golden Valley Electricity Association of Fairbanks (Alaska, USA). This represents the world's second most powerful battery bank. Apart from covering the 15 minutes period it takes to the backup generation system to start-up (grid stabilization in an electrical island operation mode), the battery is also designed to provide frequency regulation (by repetitively cycling from charging to discharging) reducing the high spinning reserves needs in that region which are so typical in Alaska because of their independent and divided nature [33, 101].

- A NiCd battery installed by Alcad in the Lethabo power Station for the national power utility for South Africa, Eskom. They substituted a group of LA batteries which could not suffer the high operation temperatures registered in the region. NiCd can withstand 38ºC and have been providing since September 2000 the desired support to the local control of a generation unit located in the power station, ensuring a safe shutdown in case of unexpected tripping [33].

Concerning intermittent RES integration, although they could be considered due to their capability to withstand high temperatures, since wind and solar power are non-dispatchable and include forecast errors, NiCd batteries cannot operate economically without creating problems caused by the memory effect [34]. Furthermore, they do not perform well during peak shaving applications due to high selfdischarge ratio, and consequently are generally avoided for energy management systems.

Regarding NiMH batteries, for the reasons mentioned earlier, they have gained prominence over NiCd batteries in the recent past. They have been used in most available Hybrid Vehicles (Toyota Prius, Honda Insight, Ford Escape Hybrid, Chevrolet Malibu Hybrid, and Honda Civic Hybrid) during the 1990s and 2000s and compete with Lithium-ion batteries for the Electric Vehicle market [112], being already used in some prototypes (General Motors EV1, Honda EV Plus, Ford Ranger EV and Vectrix scooter). NiMH technology is used extensively in rechargeable batteries for consumer electronics (sealed type batteries), and it will also be used on the Alstom Citadis low floor tram ordered for Nice, France; as well as the humanoid prototype robot ASIMO designed by Honda.

Finally, the other nickel technologies are not used in high power applications. NiZn cells are available only in Sub C, AA and AAA battery types NiFe batteries have been displaced in most of their old applications (in European mining) by other types of rechargeable batteries. As a curiosity, note that a 50V NiFe battery was the main power supply in the World War II German V2 rocket (together with two 16V accumulators which powered the four gyroscopes), with a smaller version used in the V1 flying bomb. They are being examined again for use in wind and solar power systems and for modern electric vehicles, especially boats, where the weight of the batteries is not an issue.

Some of the main providers for industrial and electric power market applications are: SAFT batteries, Alcad Limited, Varta and Hoppecke Batterien GmbH.

c) *Sodium Sulfur Batteries.*

Ford Motor Company started the research and the development of this technology back in the sixties. For 20 years, different companies (such as General Electric, ABB and the New Energy and Industrial technology Development Organization from Japan) worked on it. But it was not till the late 80s that an agreement between TEPCO and NGK Insulators came to fruition. These two companies started the first demonstration projects in the early 90s, becoming commercial in Japan in 2002 [33].

NaS batteries are secondary batteries that charge/discharge electricity by exchanging sodium ions through a solid beta-alumina electrolyte. They are normally manufactured in a cylindrical shape, placing a molten-sodium negative electrode in the center and a molten-sulfur positive electrode in the outside. The electrolyte allows only the positive sodium ions to go through it and combine with the sulfur to form sodium polysulfide. During discharge, positive sodium ions flow through the electrolyte. These batteries operate at approximately 300°C in order to maintain the electrodes in a molten state and to obtain adequate electrolyte conductivity.

The main advantages of NaS batteries are [34, 113, 114]: high energy density (3 times higher than lead-acid batteries, up to 200 Wh/l), high efficiency (efficient ES due to high charge/discharge efficiency (around 85%) and minimum self-discharge), long lifetime (more than 2500 charge/discharge cycles), long-term durability (10-15 years), high response speed (only a few seconds) and capability to provide power over a long-time or in a pulsed mode (have a 600% rated pulse power capability that can last 30s [115, 116]). Furthermore, they

are environmental friendly since no pollutants are emitted in their operation (they are sealed) and present easy maintenance because there are no moving parts in the system [33, 117].

On the drawbacks side, mainly note the fact that NaS batteries retain the equipment during its operation at elevated temperatures of above 270°C. This is not only energy consuming but it also implies problems such as thermal management and safety regulations [118]. Furthermore, corrosion of the insulators can be a problem in the harsh chemical environment since they gradually become conductive and the battery self-discharge rate increases [35].
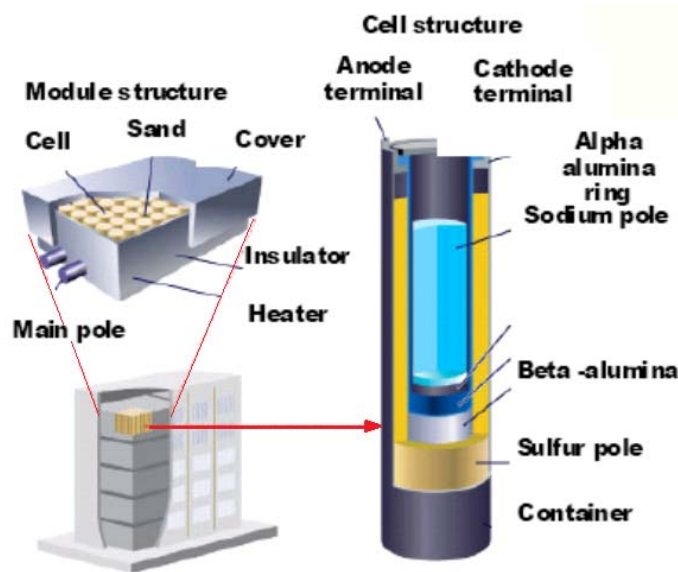
Figure 3.16 NaS battery cell and package.

Regarding the cost, these batteries are subjected to a high capital cost investments of around $2000/kW and $350/kWh comprehending the whole needed equipment, according to [34, 101]. However, the NaS batteries themselves are estimated to cost at around $810/kW [64]. Since this is only a recently commercialized product, the cost is likely to be reduced as mass production is achieved, with some predicting reductions upwards of 33% [33, 35].

Applications for NaS batteries include both demand-side applications (back up power source for emergencies, uninterrupted power supplies and electric load leveling) [117, 119] and grid side applications (improved grid power quality and energy management mainly associated with renewables). In fact, they are considered in [115] as the best ES battery type for the management of the energy generated by a wind farm.

In the last decade, NaS battery-based installations have grown exponentially from 10MWin 1998 to 305MW-2000MWh at the end of year 2008 [34]. Although they can be modular down to 50 kW, the general sizes are approximately 1 MW or even higher. Some examples can be highlighted:

- American Electric Power (AEP) installed the first NaS battery unit in North America at an office complex in Gahana, Ohio (USA), in September 2002. The installation is rated for 100 kW / 720 kWh (7 hours supply), with a 30 seconds 500 kW pulse capability in order to be able to provide power quality services [33].

- The same utility, AEP, installed a NaS battery demonstration project used in a substation update at Charleston, VA (USA) [120]. The batteries generate up to 1.2 MW of power for up to 7h, easing the strain by load leveling on an overloaded substation. Similar projects in substations were performed in Japan [119].

- TEPCO and NKG installed, in the Fujitsu semiconductor factory in Akiruno (Japan) in July 2002, a NaS battery unit capable to provide 1 MW for 7.2 hours under peak shaving operation mode, Figure 3.17. The goal of the ES unit is to provide this service together with power quality enhancement, for which the battery can to provide up to 3 MW during 13.5 s.

- Again in Japan, the Kyushu Electric Power Company installed a 2MW/14.4MWh unit with the goal to supply reliable and low cost power for lightning at a boat racing facility mainly used during the nights [33]. The goal was accomplished reducing the annual cost of the electric service by 28%.

Figure 3.17 NaS batteries installation at TEPCO site. Source: POWER Magazine.

Apart from these industrial and power grid applications, these batteries have been considered suitable for wind power generating systems and, in general, intermittent RESs integration [121, 122]. Some examples can be pointed out too. The largest worldwide ESS integrated within a wind farm (51 MW), not being a PHES or CAES installation, for stabilizing its power generation is the 34 MW / 245 MWh NaS battery installed in a northern Japan wind farm. Apart from that installation, the North American utility Xcel Energy is studying the viability of integrating a 1.2 MW / 7.2 MWh NaS battery unit with the 11.8 MW MinnWind wind project. Moreover, a 1.5 MW battery has been shown to work with 5 MW of solar power stabilization [123]. Finally, in May 2009, Electricité de France (EdF) and NGK have agreed on 150 MW of NaS batteries over the next five years to mitigate fluctuations in solar and wind energy production on various Mediterranean islands in order to reduce carbon emissions.

NGK Insulators Inc. is nowadays the only NaS battery supplier in the world although another company, Beta R&D, are trying to compete with them proposing a new sodium-nickel-chloride (NaNiCl) battery, popularly named as ZEBRA battery [124]. These are high-temperature electric batteries that use molten salts as an electrolyte and which present very similar characteristics to NaS batteries (120Wh/kg energy density and 150 W/kg power density, long lifetime), but can operate at temperatures from −40 to 70 °C [101]. They need a thermal management system (losses of about 100 W) and present high internal resistance. Proposed for use in busses, fleet vehicles and stationary applications [125], they are manufactured in large cells (up to 500 Ah) and their cost is estimated around 500 €/kWh.

Figure 3.18 Zebra battery external outlook. Source: RWTH Aachen University.

A comparison of characteristics among conventional NaS and new Zebra batteries can be observed in the following table in which battery models for electric vehicles applications (25 -40 kWh), where 360 cells are used on each battery, have been considered.

	Energy density	Specific Energy	Power density	Specific Power
NaS	151 Wh/l	105 Wh/kg	234 W/l	200 W/kg
NaNiCl2	183 Wh/l	118 Wh/kg	270 W/l	180 W/kg

Table 3.4 Comparison of properties between Sodium Sulfur and Zebra batteries.

d) Lithium Ion Batteries.

Lithium ion (Li-ion) batteries are quite a recent technology. In fact, it was not till the 1970s that they were first proposed by M.S. Whittingham at Binghamton University, at Exxon. He used titanium (II) sulfide as the cathode and lithium metal as the anode. Advances on the electrochemical properties of lithium, focusing on its property to intercalate in graphite, were obtained in the 1980s [126, 127]. Furthermore, parallel research on cathode materials provided very good results [128, 129]. These efforts led to the first commercial lithium ion battery released by Sony in 1991. Their cells used layered oxide chemistry, specifically lithium cobalt oxide. From then on, multiple developments and improvements have been achieved.

There are nowadays mainly four different Li-ion battery groups which are reflected in the table below.

Specifications	Li-cobalt $LiCoO_2$ (LCO)	Li-manganese $LiMn_2O_4$ (LMO)	Li-phosphate $LiFePO_4$ (LFP)	NMC $LiNiMnCoO_2$
Voltage	3.60V	3.80V	3.30V	3.60/3.70V
Charge limit	4.20V	4.20V	3.60V	4.20V
Cycle life	500–1,000	500–1,000	1,000–2,000	1,000–2,000
Operating temperature	Average	Average	Good	Good
Specific energy	150–190Wh/kg	100–135Wh/kg	90–120Wh/kg	140-180Wh/kg
Specific power	1C	10C, 40C pulse	35C continuous	10C
Safety	Average. Require protection circuit and cell balancing of multi cell pack. Requirements for small formats with 1 or 2 cells can be relaxed		Very safe, need cell balancing and V protection.	Safer than Li-cobalt. Need cell balancing and protection.
Thermal. Runaway	150°C (302°F)	250°C (482°F)	270°C (518°F)	210°C (410°F)
In use since	1994	1996	1999	2003
Researchers, manufacturers	Sony, Sanyo, GS Yuasa, LG Chem Samsung Hitachi, Toshiba	Hitachi, Samsung, Sanyo, GS Yuasa, LG Chem, Toshiba Moli Energy, NEC	A123, Valence, GS Yuasa, BYD, JCI/Saft, Lishen	Sony, Sanyo, LG Chem, GS Yuasa, Hitachi Samsung
Notes	Very high specific energy, limited power; cell phones, laptops	High power, good to high specific energy; power tools, medical, EVs	High power, average specific energy, elevated self-discharge	Very high specific energy, high power; tools, medical, EVs

Table 3.5 Properties for different types of Lithium based batteries. Source: Battery University web site.

144

The former battery groups move lithium ions between the anode and cathode to produce a current flow [130] and the differences among them lie on the cathode and anode materials. Figure 3.19 depicts the functioning mechanism. The main characteristics of the basic cell in a Li-ion battery, its density and voltage, depend on the chemistry used. The specific energy density is between 100Wh/kg and 200Wh/kg, so they can double the energy density of nickel metal hydride or nickel–cadmium battery. Furthermore, the cell of this battery can be operated with higher current level than other cells, but some problems have to be solved. The internal resistance can produce internal heat-up and failure. Therefore, to ensure safe operation, it is mandatory to use a battery management system to, at least, provide over-voltage, under-voltage, over-temperature and over-current protection [131]. In addition, more advanced systems provide cell voltage balancing that ensures that all batteries operate at the same voltage and, therefore, state of charge [25].
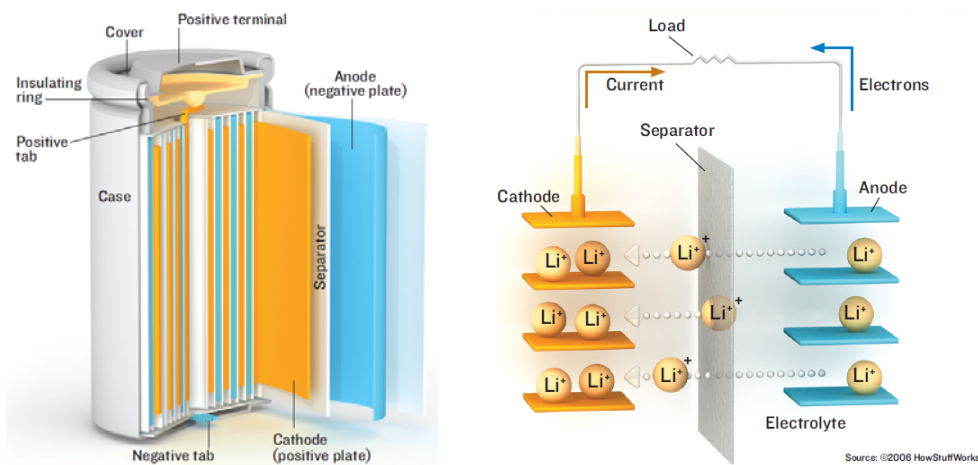
Figure 3.19 Lithium ion batteries internal structure and external outlook. Source: [132]

The main advantages of this battery technology are the high energy-to-weight ratios, a fast discharge capability, a relatively low self-discharge (less than half that of NiCd and NiMH), no need of periodic discharges since they do not present memory effect, they are much lighter than other energy-equivalent secondary batteries and also need low maintenance. Moreover, they present nowadays a wide variety of shapes and sizes efficiently fitting the devices they power. They can be found as cylindrical cells (long years of experience with this cells' design, and have high lifetime expectations although cooling is difficult), as pouch cells (with very good cooling properties and high energy density although

tightness of foils is still in question), and as prismatic cells (presenting a simple system design and combining several advantages of cylindrical cells and pouch cells).

Figure 3.20 Different cell concepts for Li-ion batteries. Sources: SAFT catalogue, eLithion web site and Lithium Energy Japan catalogue, respectively.

On the contrary, Li-ion batteries present some drawbacks too. As already indicated, they require a protection circuit to limit voltages and avoid overcurrents, which is one of their main drawbacks. Besides that, they are subjected to aging even when not being used (aging occurs with all batteries and modern Li-ion systems have a similar life span to other chemistries).

The price of Li-ion batteries is still quite high, although costs are expected to be largely reduced as the technology ages and its commercialization matures. This should happen in brief thanks to the fostering they are receiving from the automotive industry in order to be used within the future electric vehicles (EV). Specialist on this domain estimate that the current price of the Li-ion batteries installed in the latest EV prototypes oscillates around the 500 €/kWh.

An issue may arise with the the worldwide limited lithium resources [133, 134]. Creating 800 million EV that use in average a 15 kWh lithium-ion battery each would deplete 30% of world's lithium reserves which could lead to an increase in lithium and batteries costs [25, 34, 135].

Finally, Li-ion batteries have been used according to their advantages in applications where weight and volume are very important; i.e. mainly portable equipment (tools, laptops, cameras, mobile telephones) but also, thanks to their high energy density and as already introduced, they are nowadays the most promising option for ES in plug-in hybrid and

electric vehicle (EV) applications [96], substituting the Nickel Metal Hydride batteries which were the chemistry of choice in automotive till now [106, 112]. Many car manufacturers have already used them in their new EV prototypes. That is the case of models such as: Transit BEV, Transit Connect BEV and Focus BEV Prototype models from Ford, the Mitsubishi iMiev, the Nissan Leaf, the Daimler Smart, the BMW Active E, the Tesla Roadster and S models, the Stromos, the Renault Fluence Z.E., the Volvo C30, etc.

It should be noted that there are projects to integrate large scale Li-ion batteries with RES, like the 60 MWh installation being constructed in Kansas (USA) to store wind energy by the company EaglePicher Technologies [136], or the Li-ion battery type currently under development by the company A123 Systems for reserves, frequency regulation and grid stabilization [137]. These projects pave the way for future application of Li-ion batteries in PV power plants, as it is proposed in this PhD thesis.[136]

Some of the many companies that are developing lithium-ion battery technology for the power systems industry are: SAFT Batteries, AltairNano, EEMB Batteries, Everspring and the two aforementioned, A123 Systems and EaglePicher Technologies.

e) Flow Batteries.

Flow batteries are a promising technology that stores and releases energy through a reversible electrochemical reaction produced between two electrolytes, which are stored in different tanks (avoiding the characteristic self-discharge typical in other types of batteries), and through a microporous membrane that separates both electrolytes but allows selected ions to cross through, creating the electrical current flow. In this sense, they are somehow a special type of batteries difficult to compare with the rest of conventional battery technologies. In fact, they are considered half way between them and hydrogen fuel cells (technology presented in the next subsection).

There are many potential electrochemical reactions, usually called reduction-oxidation reaction or REDOX, but only a few of them are useful in practice. In this sense, the main four groups of flow batteries which are being commercially developed are: vanadium redox flow batteries (VR), zinc bromine flow batteries (ZnBr), polysulfide bromide (PSB) flow batteries and cerium zinc (CeZn) flow batteries.

The historical development for each of them presents some similarities and although VR were the first to be developed, in part thanks to inspiration on the work performed by the NASA on iron-chromium batteries during the 70s, all of them have experienced the main

technological development in the last 15-20 years. In fact, they are so recent that the cerium zinc type is still under the demonstration projects phase.

These batteries are usually composed of three subsystems which are observed in Figure 3.21: the cell stack or flow reactor, the electrolytes tanks system and the control and power system. Most of them are designed in a modular way, so they are easy to expand (just by adding cell stacks) and present the big advantage of decoupling the total stored energy from the rated power. The rated power depends on the reactor size, while the stored capacity depends on the volume of the electrolyte tanks. This flexibility makes them capable to support a wide variety of applications including from seasonal storage to, thanks to a sub-millisecond response time and a pulse capability, intermittent RES integration and energy retail or power quality applications.
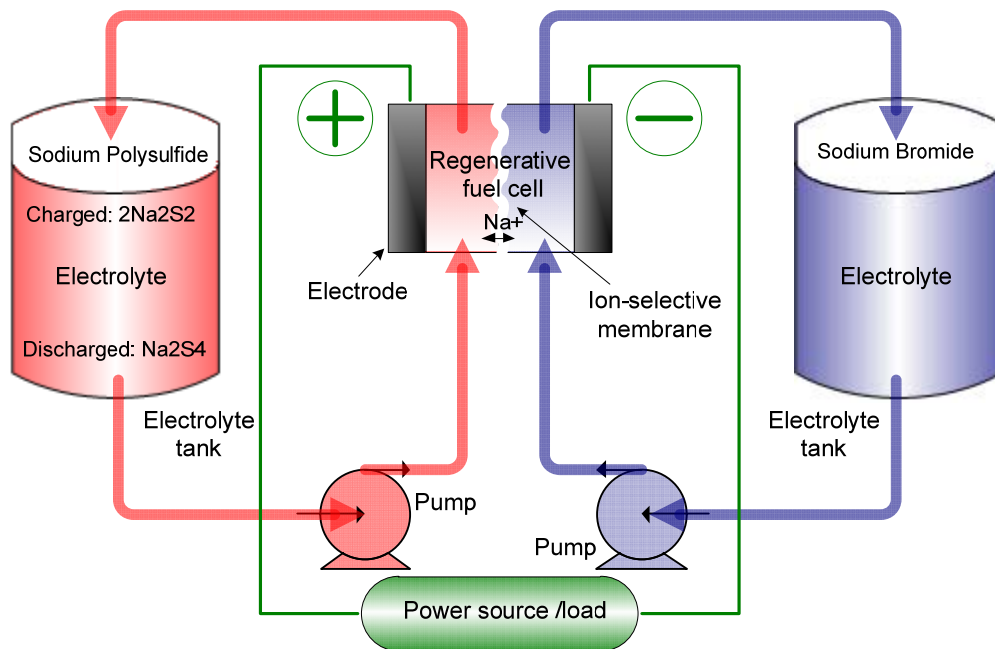
Figure 3.21 Flow battery cell scheme.

With respect to their technical characteristics, an individual analysis must be introduced for each of the technologies. VR flow batteries combine two types of vanadium ions in a sulphuric acid electrolyte at each electrode; with V^{2+}/V^{3+} in the negative electrode, and V^{4+}/V^{5+} in the positive electrode. When battery discharges, electrolytes flow into the reactor and H^+ ions are exchanged through the microporous membrane. This exchange modifies the ionic content of the vanadium mixtures generating electrical energy. During recharge this process

is reversed. They present a 75% round trip efficiency with a cycle life of at least 10000 complete charge/discharge cycles, being the most critical component their proton exchange membrane. For the case of ZnBr flow batteries, energy is stored in an aqueous solution of zinc and bromine ions that only differ in their concentration of elemental bromine. Both ions are allowed to migrate through the microporous polyolefin membrane to the opposite electrolyte, equalizing the charge and converting potential chemical energy to electrical energy. Unlike other flow batteries, the electrodes in a ZnBr flow battery act as substrates to the reaction. In this sense, they are somehow similar to conventional batteries. They present slightly lower characteristics with an estimated 70% round trip efficiency for a cycle life of around 2000 complete charge/discharge cycles, being the most critical component for them the microporous exchange membrane too. PSB flow batteries are very similar to VR although the electrolytes are sodium bromide as the positive one, and sodium polysulfide as the negative one. During the discharge, there are now sodium ions passing through the membrane. They present, although still acceptable, even lower characteristics, with an estimated 65% round trip efficiency but for a cycle life of again around 10000 complete charge/discharge cycles, being the most critical component again the cation-selective membrane. And, finally, CeZn flow batteries contain zinc (negative electrode) and cerium (positive electrode) ions suspended in a methane sulfonic acid. They present an estimated 70% round trip efficiency for a cycle life of around 10000 complete charge/discharge cycles too, being the most critical component once again its membrane.

Some advantages and disadvantages can be summarized for flow batteries in general. As compared to solid-state batteries, there are the following potential advantages: essentially, the immediate recharge capability achieved just by replacing the exhaust electrolyte; no self-discharge during the storage period; no solid-state phase changes during charge and discharge; and the state-of-charge can be determined easily [138]. Furthermore, on the positive side, it is noteworthy that they present high power and energy capacities with decoupled dimensioning[138]. In addition, as the same reversible chemical reaction is responsible for charging and discharging the battery, their charge/discharge ratio is 1:1; moreover, they can fully discharge without damaging the system; also they use nontoxic materials; and finally, note that the operate at low-temperatures. On the contrary, their main disadvantage is the need for moving mechanical parts (such as pumping systems) which complicates the maintenance and the system size reduction, and notably, their commercialization.

Regarding the costs, these vary as a function of the application desired since each application will require different energy and power ratings. Equally, since energy and power dimensioning are decoupled, two costs have to be pointed out. Reference costs provided in [33, 64] are:

- For VR, the power cost is $1828/kW, and the energy cost is $100/kWh to $1000/kWh, depending on the battery design, attributing 80% to the storage module too [138].

- For ZnBr, the power capacity cost is $639/kW and the energy capacity cost is $400/kWh, attributing 60% to the storage module.

- For PSB, the power capacity cost is $1094/kW and the energy capacity cost is around $170/kWh, attributing 80% to the storage module too.

- Finally for CeZn, the power capacity cost ranges from $750/kW to $1000/kW and the energy capacity cost is around $60/kWh, attributing 50% to the storage module too.

Installation costs would have to be added to the previous costs. In this sense, the worst part is for PSB batteries which are the only one, among them, which needs to be constructed on-site, increasing the turnkey costs. The rest of them, being completely modular, do not need any construction on-site.

Finally, to review the existing installations and some possible future applications for flow batteries, the different technologies have to be analyzed separately once again. For example, to start with VR technology, note that there are currently over 20 MWh installed around the world, which take profit of their unique versatility in the MW range to be used for load leveling, remote area power systems, renewable energy stabilization [138] but also for uninterruptible power supply, back-up power and power quality. Notable examples are the 3 MW VR battery in the Totorri Sanyo Electric Company (Osaka, Japan), the 250 kW-520 kWh at the University of Stellendosch (Cape Town, South Africa) or the 250 kW-2000 kWh at the PacificCorp building in Moab (Utah, USA) {{{}}. But the largest example is a 4 MW/6 MWh unit installed by Sumitomo Electric Industries in Tomamae Wind Villa (Japan) in 2005, which has been cycled over 270,000 times to various depths of charge within 3 years to stabilize a 32 MW wind farm [34].

Apart from VR batteries, ZnBr batteries are currently entering the market and are aimed for renewable energy applications. It is estimated that, by the end of 2009, there were 4 MW of installed capacity in the world, with storage capacity of 8 MWh. Some developers have already proposed 1.5 MW ZnBr battery developments to back up a 20 MW wind farm for several minutes. Thus, it is expected to keep the wind farm operational for another 200 extra hours a year [74]. In low levels of wind penetration, flow battery systems deliver the lowest cost per energy stored in a study that compares lead-acid batteries, flow batteries, flywheel, superconducting magnetic energy storage, CAES, hydrogen and PHS, with a profitable price of 41 to 45 cents/kWh [115, 139]. Three initial pilot installations which can be stand out [33]: a 200 kW-400 kWh ZnBr battery installed by ZBB Energy in a suburban shopping center in Melbourne (Australia), another 200kW-400 kWh battery from ZBB Energy installed at the Detroit Edison Substation (Michigan, USA) and a 500 kW ZnBr battery installed, again by the same developer, at a refurbished solar generation station in New South Wales (Australia).

PSB batteries, like for the case of VR batteries, can scale into the MW region and therefore must have a future within energy storage. However, only demonstration facilities were projected, note the 12MW-100MWh battery system installed at the Little Barford Power Station in Cambridgeshire (UK), and the same size facility at the Tennessee Valley Authority in Columbus (Mississippi, USA), but they were cancelled sine die.

Only a 2kW testing facility in Glenrothes (Scotland) is known for Cerium Zinc flow batteries, since they are under commercial development.

Different developers can be found nowadays in the market for each of the technologies except for the CeZn type which is being developed by the British company Plurion Inc.

f) Metal Air Batteries.

The metal air battery concept is not new. It has been known for long and used, in the form of non-rechargeable Zn-air button-cell batteries for hearing-aid devices or for film cameras that previously used mercury batteries. In contrast, rechargeable metal-air batteries, and particularly Li-air batteries, remain in the initial research phase but continue to attract new researchers because of their promising characteristics. They get their name from reactants that provide energy by undergoing electrochemical reactions. In zinc-air cells, for instance, energy is released by oxidizing zinc (which is held within the battery case) with oxygen from the air. Since the oxidizer is not stored in the battery but supplied continuously

from an external source (air) these kinds of batteries are similar to fuel cells, in which neither the oxidizer nor the fuel is packaged inside the cell.
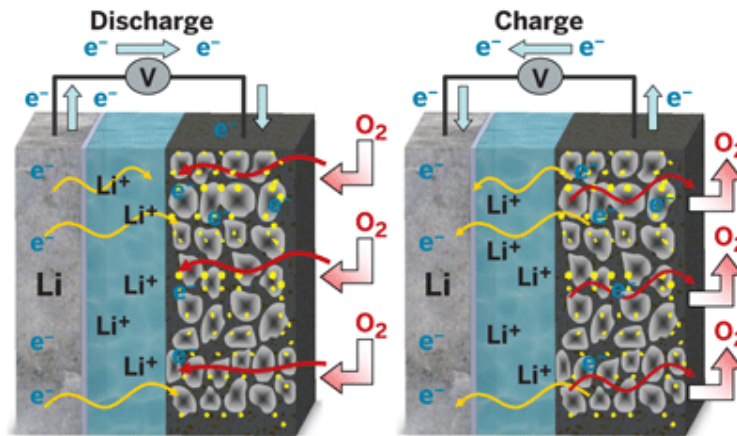
Figure 3.22 Functioning scheme of a Li-air battery. Source: [140]**.**

As can be appreciated in Figure 3.22, a metal-air electrochemical cell is type of battery cell whose anode is made of a pure metal material, lithium in this case, and the porous carbon cathode is connected to an inexhaustible supply of air. These batteries typically rely on water-based electrolytes and gel polymer electrolyte membranes that served as both the separator and ion-transporting medium. These electrolytes usually flood the porous electrodes. Oxygen from ambient air is drawn in through the porous "air" electrode and produces hydroxyl ions in contact with the electrolyte. These ions reach the anode and begin to oxidize the metal material (e.g. In a lithium-air battery's porous carbon cathode Li+ ions react with oxygen molecules at catalyst sites to form lithium oxides). This is a reaction that produces current through the release of electrons.

There are multiple combinations of metal-air electrochemical cells being under research: lithium-air, zinc-air, aluminum-air, calcium-air, magnesium-air, iron-air, titanium-air, beryllium-air, etc. The main characteristics for some of them can be observed in Table 3.6.

Metal	Electroch. Equivalent Ah/g	Theoretical voltage versus O_2	Oxidation state change	Theoretical specific energy kWh/kg	Actual operating voltage V
Li	3.86	3.40	1	11.14	2.4-3.1
Zn	0.82	1.65	2	1.35	1.0-1.2
Al	2.98	2.70	3	8.10	1.1-1.4
Ca	1.34	3.40	2	4.18	2.0
Mg	2.20	3.10	2	6.46	1.2-1.4
Fe	0.96	1.30	2	1.20	1.0

Table 3.6 Properties for different types of air-metal batteries.

Among the various metal-air battery chemical couples in Table 3.6, the Li-air battery is the most attractive since the cell discharge reaction between Li and oxygen has a high open-circuit voltage and a theoretical specific energy of 5200 Wh/kg. In practice, oxygen is not stored in the battery, and the theoretical specific energy excluding oxygen is 11140 Wh/kg, a value comparable to the 12200 Wh/kg assigned to the gasoline [140]. Hence, a Li-Air ionic liquid battery presents up to 11 times the energy density of the top lithium-ion technologies for less than one-third of the cost. This is achieved thanks to a lighter cathode and to the fact that oxygen is freely available in the environment and does not need to be stored in the battery. Theoretically, with oxygen as an unlimited cathode reactant, the capacity of the battery is only limited by the Li anode. So, it stands out that the main advantage that they present is that they have huge energy densities. Theoretical values can be observed in Table 3.6.

On the contrary, they present in general many drawbacks and technical issues which have to be overcome such as their dependence on environmental conditions (when keeping free access to air they should minimize the water evaporation and they need to remove CO_2 from the air to prevent formation of carbonates in the electrolyte). Furthermore, they have nowadays a very limited operative temperatures range, short lifespans, low numbers of charging cycles and low round-trip efficiencies. In addition, they develop a non-uniform distribution of anode material as results of the dissolution and precipitation of the reaction products. Nowadays, they have a very low cycle life performance.

Three main technologies (Lithium, Zinc and Aluminum) are currently under development but are not yet commercially available. Some specific handicaps can be pointed out for each of them. Regarding Air-Lithium batteries with solid electrolyte, they present limited output power and low current densities due to electrolyte conductivity. Furthermore, their current lifespans are very short not achieving more than 50 cycles [141]. During discharge, oxygen is reduced at the cathode as it reacts with lithium from the anode to form lithium oxides. But that process proceeds too slowly for possible applications such as electric-vehicle propulsion [140]. For the case of the Zn-air batteries, they are mainly primary batteries, i.e. non-rechargeable, to the moment. A possible formation of dendrites which could create short-circuits in the cells has been detected. Rechargeable prototypes have very few cycles' life (although primary Zn-air batteries can achieve 2000cycles). And finally, regarding Al-air batteries, they cannot be neither considered rechargeable nowadays. Once the aluminum anode is consumed by its reaction with atmospheric oxygen at a cathode immersed in a

water-based electrolyte to form hydrated aluminum oxide, the battery will no longer produce electricity. However, it may be possible to mechanically recharge the battery with new aluminum anodes made from recycling the hydrated aluminum oxide. Such recycling will be essential if aluminum-air batteries are to be widely adopted. Furthermore, although they have one of the highest energy densities among all the types of batteries, they are not widely used because of other problems such as cost, life cycle and start-up time, which have restricted their use to mainly military applications. Hence, many difficulties have to be solved in all the technologies.

It can be concluded that these electrochemical cells promise big opportunities, but their industrial production is still years away.

g) *Comparison of battery technologies*

To summarize this section, some comparatives can be established among the different types of batteries presented. The following Table 3.7 reviews some of the main characteristics for the most important and developed technologies among those presented here. Flow batteries have not been introduced in the comparison due to their different operating nature which makes them being considered half way between batteries and hydrogen fuel cells. In this sense, they are somehow a special type of batteries difficult to compare with the rest of conventional battery technologies.

	Lead-acid	NiCd	NiMH	NaS	Zebra	Li-ion	Zinc air
Specific Energy (Wh/kg)	30-40	45-80	60-120	150	100-190	110-250	470
Energy density (Wh/liter)	60-75	80	150	50-200	150	250-620	1300
Specific Power (W/kg)	180-250	150	200	150-240	150	250-340	105
Nom. Cell voltage (V)	2.105	1.2	1.2	2	HV (stack)	3.6	1.65
Life cycles	500-1000	2500	600	2500	500-3000	500-2000	500-2000
Fast charge time (h)	8-16	1	2-4	2-4	2-4	2-4	2-4
Energy discharge per month (%)	3-20	20	30	5	10	10	10

Table 3.7 Properties comparison among different battery technologies.

A graphical representation of the specific energy versus the energy density of the different technologies can provide a clear picture of the energetic characteristics evolution, which helps identifying each technology with its possible ES applications. And similarly, the specific energy for the different technologies can be represented versus their corresponding specific power. These comparisons are represented in Figure 3.23 and Figure 3.24 respectively.
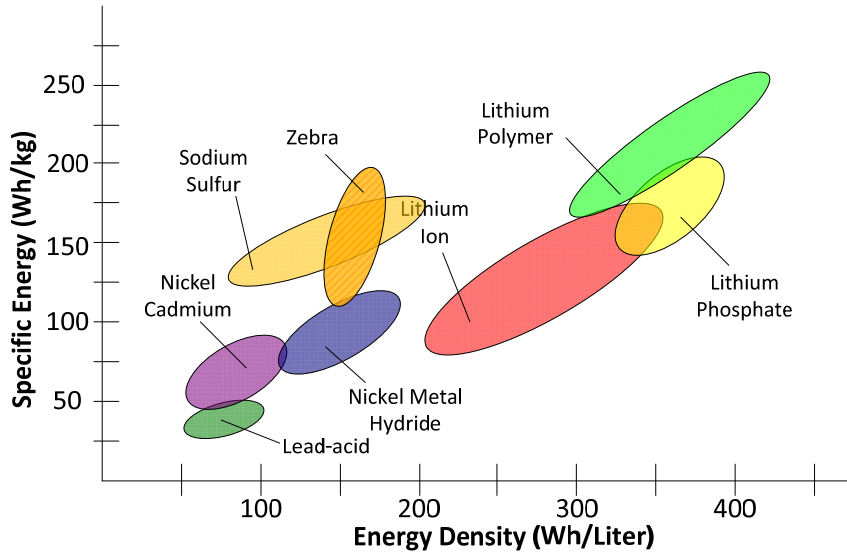
Figure 3.23 **Specific energy vs. energy density for the different battery technologies.**
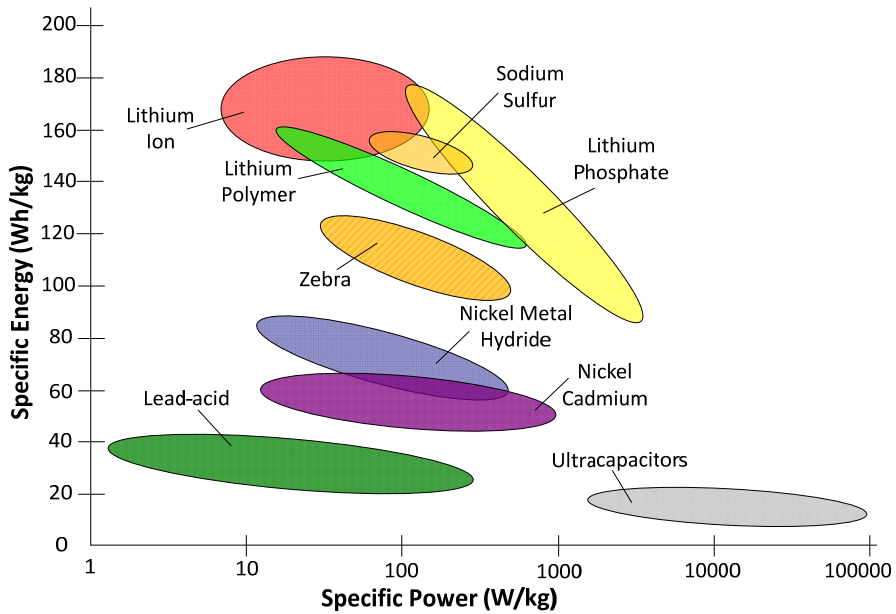
Figure 3.24 **Specific energy vs. specific power for the different battery technologies. Source:**

[142]

To conclude the BESSs comparison, it can be stated that LA and Ni based batteries will probably remain being used for their current applications and that further breakthroughs are

unlikely. Hence, the main clear candidates for future large-scale projects and RES integration among BESSs are NaS batteries, Flow batteries which are currently already competing in the renewable energy market and, maybe, the sole doubt is on the Li-Ion family of batteries which rely on the current technological advancements achieved thanks to their possible use within the electric vehicle industry. Therefore, some of the BESSs families are likely to be used although some uncertainties over the future of this sector can be the noted as various technologies continue to develop and it is not clear yet which one will get its way.

3.4.2. Hydrogen and Fuel Cells (FC).

Going back in science history, the first time Hydrogen is referred in bibliography is in 1671, when Robert Boyle discovered and described the reaction between iron filings and dilute acids, which results in the production of hydrogen gas. Just some years later, in 1766, Henry Cavendish was the first to recognize hydrogen gas as a discrete substance, by identifying the gas from a metal-acid reaction as "phlogiston", meaning "flammable air" and further finding in 1781 that the gas produced water when burned. In 1783, Antoine Lavoisier gave the element the name hydrogen (from the Greek ὕδρω (hydro) meaning water and (γενῆς) genes meaning creator) when he and Laplace reproduced Cavendish's findings [143]. From then on, hydrogen has been used in multiple applications normally related with transports. Some of them finished tragically, as its application to the Zeppelin's industry which was abandoned when the Hindenburg Zeppelin LZ was destroyed by fire in the air in 1937. Others resulted more positive, like the spaceflights case which, after liquid hydrogen was tested successfully as rocket fuel at Ohio State University in 1943, it has been successfully used through the Gemini project, which used hydrogen as fuel for the first time, and till now concluding with the NASA space shuttles program.

Hydrogen is now being developed also as an ES medium, although it differs from the conventional idea of ESS because it uses different processes for hydrogen production, storage, and use, which are the 3 stages in the hydrogen as Energy Storage System. In this sense, hydrogen is not a primary energy source, but an energy carrier, because it must first be manufactured by other energy sources in order to be used. As a storage medium, it may play a significant role for RES integration [74, 76, 144]. If this kind of energy sources is used to make hydrogen instead of tripping whenever the EPS cannot accept any more power due to low instantaneous demand, then RES can be utilized fully whenever they are available [4,

145]. Broadly speaking, it does not matter when they cut in or out, the hydrogen is simply stored and used as required for electric production or as a fuel.

So, to talk about the hydrogen economy, term coined in 1970 by John Bockris proposing a system of delivering energy worldwide using hydrogen and which is still prevailing [146], means to develop the three stages previously introduced and to overtake the issues still present.

a) Producing Hydrogen

Three different methodologies can be highlighted to produce hydrogen: to obtain it by steam reformation of natural gas, to extract it from fossil fuels or to generate it by water electrolysis. Among them, steam reformation produces pollutants, and extracting hydrogen from fossil fuels turns to be four times more expensive than using the hydrogen as fuel itself, hence, electrolysis has become the most promising way for hydrogen production.

An electrolyser generates hydrogen and oxygen from water by introducing an electric current which produces electrolysis. Due to the high cost of using electricity in this process, note that about 50kWh of energy are required to produce one kilogram of hydrogen [34], electrolysers are desired to present high efficiencies [35, 74] although they hardly achieve at best nowadays an 85% efficiency in the electrolysis procedure. For that reason, it seems logical to assume that the only attractive option for future Hydrogen production is integrating electrolyser units with RES and use their surplus production. As an estimation, at common off-peak high-voltage line rate in the USA of around $0.03/kWh, hydrogen costs $1.50 a kilogram, equivalent to $1.50 a US gallon for gasoline if used in a fuel cell vehicle [34]. Furthermore, electrolyser costs have to be added.

b) Storing Hydrogen

There are some different systems, strategies and technologies which are developed to store hydrogen in the most efficient way, although none of them has achieved high round trip efficiencies yet (between 65% and 70% efficient). They can be classified into the following three groups:

- Liquid hydrogen, which can be obtained by pressurizing and cooling. However liquid hydrogen requires cryogenic storage and boils around 20.268K (–252.882°C). Hence, its liquefaction imposes a large energy loss and tanks must also be well insulated to prevent boil off, adding more costs. Liquid hydrogen presents

lower energy density by volume than hydrocarbon fuels such as gasoline by approximately a factor of four, which can be understood by analyzing the density problem for pure hydrogen: there is actually about 64% more hydrogen in a liter of gasoline (116 grams hydrogen) than there is in a liter of pure liquid hydrogen (71 grams hydrogen). Furthermore, the carbon in the gasoline also contributes to the energy of combustion. This type of storage is the one used in the space shuttle.

- Compressed hydrogen can be stored in different media. Hydrogen compressed in hydrogen tanks at 350bar and 700bar have been tested and used for the transport industry. Car manufacturers have been developing this solution, such as BMW, Honda or Nissan. On the contrary, some researchers have investigated underground hydrogen storage in reservoirs to provide grid energy storage for intermittent energy sources, like wind power [147], although wind power has already been integrated with hydrogen tanks, e.g. the Danish Lolland Hydrogen Community. The estimated costs for tanks storage is 6 times that of underground installations ($12/kWh vs. $2/kWh) but is the only option for mobile applications. The main disadvantage for compressed hydrogen is related to the mechanical compression. The round trip efficiency of the process is low (around 70%) and to get acceptable energy densities by volume (and smaller tanks), high pressures must be applied. Even though, this storage methodology is the most extended nowadays.

- Chemical hydrogen storage, methodology based in forcing the hydrogen to react with some types of materials forming a wide range of substances (such as Metal hydrides, Carbohydrates, Ammonia, Synthesized hydrocarbons, Formic acid and others) which facilitate the transport and storage of hydrogen. When required, the hydrogen is removed from the parent material. The energy density obtained with this methodology is similar to that obtained for liquefied hydrogen. The extra material required to store the hydrogen is a major problem with this technique as it creates extra costs and mass. All of the strategies based on chemical storage are being investigated nowadays, being in the early stages of development, so, they cannot be applied commercially yet.

c) Using Hydrogen

The third stage within a Hydrogen economy represents the way hydrogen can be used in order to extract its energy and generate electric power. There are two main drivers for doing that: internal combustion engines (ICE) and fuel cells (FC).

ICE have traditionally been fuelled with petrol derivatives but they can be adapted easily to the use of hydrogen. Hence, they are considered nowadays as a temporary solution for the hydrogen technology deployment while FC technologies are getting enough level of maturity so as to be commercially available. In this sense, due to the great expected efficient and reliable characteristics (they have no moving parts) and their virtually emission-free operation, FCs are expected to be the generator of choice for future hydrogen powered energy applications.

FCs were invented about the same time as batteries although, for many reasons, they were not well-developed until the advent of manned spaceflight (Gemini Program) when lightweight, non-thermal (and therefore efficient) sources of electricity were required in spacecraft. This was the first commercial use of a FC.

There are many different FC technologies with their corresponding specific characteristics (varying in the operation temperature, the type of fuel and catalyst used …); however, they all work in the same general manner. They are made up of three segments (two electrodes: anode and cathode, and the electrolyte) which are sandwiched together (with similar structure to flow batteries).Two chemical reactions occur at the interfaces of the three different segments. The net result of the two reactions is that fuel (H_2) is consumed, water or carbon dioxide is created, and an electric current is generated. A simplified scheme can be appreciated in Figure 3.25.
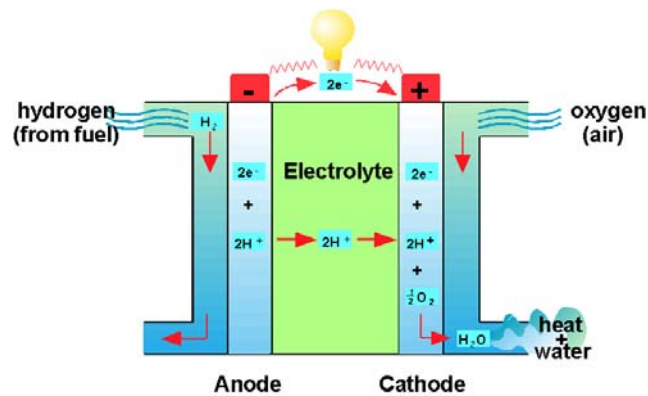
Figure 3.25 Fuel cell general operation scheme.

Among the different FC technologies which have been proposed, there are five major types that have been developed to varying degrees which can be highlighted. They are differentiated and named according to the electrolyte used in the cells: polymer-electrolyte membrane or proton exchange membrane fuel cells (PEMFC), alkaline fuel cells (AFC), phosphoric-acid fuel cells (PAFC), molten-carbonate fuel cells (MCFC), and solid-oxide fuel cells (SOFC). The electrolyte also determines the operating temperatures of the cells, as shown in Table 3.8.

Fuel cell	Electrolyte	Catalyst	Fuel	Efficiency (%)	Operating temp (°C)	Power output (kW)
PEMFC	Solid organic polymer	Platinum	H_2	45	60 to 100	50-250
AFC	Potassium Hydroxide	Platinum/Palladium Platinum/Gold	H_2	70	80 to 100	0.3-12
PAFC	Phosphoric Acid	Platinum	H_2	40	150-200	200
MCFC	Potassium, Sodium or Lithium Carbonate	Mostly Nickel	H_2/CO_2	60	600-1000	10-2000
SOFC	Solid Zirconium Oxide	Variety of nonprecious metals	H_2	60	600-1000	1000

Table 3.8 Main characteristics for the different technologies of Fuel Cells.

In view of the properties compiled in Table 3.8, each technology can be subsequently used, or being proposed, for different applications which profit their advantages taking into account their limitations. These considerations are collected in Table 3.9.

Electrolyte	Advantages	Disadvantages	Applications
PEMFC	• Highest power density • Reduced corrosion and electrolyte-management problems • Rapid start-up time	• Relatively expensive catalysts required • High sensitivity to fuel impurities	• Portable application to electric vehicles
AFC	• High power density • Demonstrated in space applications	• High sensitivity to fuel impurities, intolerant to CO_2 which furthermore can easily poison the water produced by cell which is drinkable.	• Widely used in the space industry (NASA)
PAFC	• High quality waste heat (for co-generation applications) • Demonstrated long life Can use impure H_2 such as H_2 from fossil fuels	• Relatively expensive catalysts required • Relatively low power density	• Large stationary generation. • Also Cogeneration (increases efficiency to 85%)
MCFC	• High quality waste heat • Inexpensive catalysts • Tolerant to fuel impurities	• High operating temperature and corrosive electrolyte result in short cell lifetime • Relatively low power density	• Cogeneration (increases efficiency to 85%)
SOFC	• High quality waste heat • Inexpensive catalysts • Tolerant to fuel impurities • Solid electrolyte	• High temperature enhances corrosion and breakdown of all cell components and causes slow start-up • Sealing of stacks	• Utility applications. • Prototype for cogeneration exists with overall an 85% efficiency

Table 3.9 Advantages, disadvantages and applications for the different Fuel Cell types.

In general, FCs present the clear energy capacity advantages with regard to batteries and environmental advantages with regard to ICEs. However, their efficiency must be still improved. When hydrogen is consumed nowadays in a FC car, a power plant, or a CHP unit, the efficiency of this transformation stage varies from 40% to 70%, depending on the type of FC, as can be observed in Table 3.8. Furthermore, their dynamic response is not very fast (being even worse for high power FC which operate at high temperatures, MCFC and SOFC) which represents a handicap for applications with rapidly changing power demands. Their cost varies largely depending on the type of FC (from €500/kW to €8,000/kW) [35], although the cost may drop to $15–145/kW by 2020 as technology gets mature and commercial developments are launched [34, 148].

d) Hydrogen technologies balance

As can be extracted from the previous section concerning the state of art of the technologies involved in the hydrogen economy, the main drawback for these systems is their overall efficiency which can finally range, as a function of the technology considered, from 25% to 45%. These low efficiency levels result in very high energy costs due to the low degree of utilization of limited and expensive energy resources such as solar, wind or biomass. Even like that, and although hydrogen storage costs approximately 4.5 times more than natural gas [149, 150] hydrogen is a serious contender for future ES applications due to its huge flexibility or versatility. Once hydrogen transformations will be produced effectively, it will be adaptable to practically any application required and will probably replace conventional fuels. Consequently, producing hydrogen from RES using electrolysis to consume peak exceeding production periods seems the clearest strategy nowadays.

The changeover towards the "hydrogen economy" is envisaged before the peak oil strangles the global economy, that is, in less than fifty years [74, 146].

e) Example of installations and applications

The number of applications using hydrogen is already large although its introduction in the electrical system is still low. Nevertheless, it is expected to grow rapidly as related technologies become commercially available.

As a matter of fact, different research and promotion hydrogen programs are being developed in the USA, the EU, and Japan. Both public institutions and private companies are pushing hard to promote the way towards the hydrogen economy and a further wind power integration, and although electrolyzer/storage/FC systems are either inoperable or

uneconomical at low levels of wind penetration, several examples of pilot installations are already registered [34]. In the first place, a community based pilot program using wind turbines and hydrogen generators is being undertaken from 2007 for five years in the remote community of Ramea, Newfoundland and Labrador. Similar projects have been going on places such as Utsira, a small Norwegian island municipality, since 2004 (project developed by Norsk Hydro and Enercon which operates as an isolated power system with 90% availability), or the town of Nakskov, Denmark, where a wind-hydrogen project has been successfully producing hydrogen since May 2007. In the first of them, a 600 kW wind turbine is coupled with a 48 kW electrolyzer and a 10 kW fuel cell. Hydrogen is stored in a $12m^3$ tank, providing power enough to 10 houses for 2–3 days without wind. Grid stability and back-up are provided by a flywheel and a battery bank. The second project, Nakskov, uses an 8 kW electrolyzer, a 10.5 kW fuel cell, and a $25m^3$ hydrogen storage tank. The hydrogen is used to produce electricity when demand exceeds generation, and the excess oxygen is used for a waste water cleaning projects. Furthermore, Iceland is attempting to become the first 'hydrogen country' in the world by producing hydrogen from surplus renewable energy and converting its transport infrastructure from fossil fuels to hydrogen [35]. Ireland is analyzing large scale wind power integration made possible to ESS using hydrogen [74]. The same is taking place in the Netherlands [150]. Germany is in the gap too with Siemens and P&T Technologies working on new wind-hydrogen engines [34]. As it is the case in the UK, where a company called Wind Hydrogen Limited intends to develop large scale wind-hydrogen schemes to be possibly applied in off-shore wind farms.

Besides the electric generation industry, hydrogen has found applications in the automotive and transport industries as an emissions-free alternative to gasoline [151]. In this sense, a number of prototype vehicles implementing hydrogen technologies have already been presented. The list is long an comprehend, among others, car manufacturers and models such as: Chrysler Natrium, Fiat Panda Hydrogen, Peugeot Quark, Mercedes-Benz F-Cell, Morgan LIFEcar, Honda with models FCX and FCX Clarity, BMW with models H2R and Hydrogen 7 or General Motors with the Hy-wire or the Sequel model.

Finally, hydrogen could find another application and become a competitor for seasonal storage of intermittent RES [74] together with PHES, flow batteries, CAES which are those ESS technically viable for this application nowadays. But for that, it still requires to increase efficiency and reduce the self-discharge rate. A study in this way shows that hydrogen would become an attractive option if wind penetration was increased to 18% in Southern California

by 2020 [139]. In fact, this American state is experiencing a big movement in this domain thanks to the HyGen Company which is developing a multi megawatt hydrogen generating and distribution network with the idea of applying that philosophy.

3.5. Other technologies.

Some other ES technologies, which are not purely ES systems, such as electric vehicles (EVs), biofuels, biogas or liquid nitrogen could be considered as possible candidates to contribute with the EPS operation by means of some intermediate electric power system. Nonetheless, there is one ES technology left which must be pointed out since it is already mature, commercially installed and offering ancillary services to the EPS in different countries. This technology, detailed in the following, is the Thermoelectric Energy Storage.

3.5.1. Thermoelectric energy storage (TEES)

Thermal or thermoelectric energy storage (TEES) has not been generally considered when discussing ES technologies although it is a mature industry, cost-competitive and counts with a large number of commercial installations already in operation around the world. In fact, TEES development started in the late 70s and has advanced steadily since then. Unlike the hydrogen ESS which enable interactions between the electricity, heat and transport sectors, TEES technology only combines the electricity and heat sectors [35].

TEES technology is based on storing energy in the form of heat in a thermal reservoir so that it can be recovered at a later time converting it back into electric power. The initial source of energy can be electricity or, on the contrary, heat which can be extracted from a number of different thermal applications, industrial processes or generation techniques. So, TEES covers a great variety of installations which can be grouped into three main categories:

- On the one hand, end-use TEESs which are designed to work integrated in a building's cooling system and provide the air-conditioning. These systems use electricity, preferably from off-peak periods although they can be integrated with a combined heat and power (CHP) unit. Then, through the use of hot or cold storage media (chilling either water or an ethylene glycol solution) which are kept in underground aquifers, ice tanks, or other storage materials, they reduce the electricity consumption of the building's heating or air conditioning systems by providing heat, cold and electric power respectively. These installations can be

profited to cover peak demand hours and balance the energy demand curve of the building improving its energy efficiency [25, 33].

- On the other hand, TEES applied to solar thermal power plants. This type of TEES installation uses synthetic oil or molten salts that store the energy in the form of heat collected by concentrating solar power (CSP) plants which can make these plants semi dispatchable. The TEES can allow generation to be shifted to periods without solar resource, extending power production for 1–10h after sunset [152], and to provide backup energy to smooth the plant power output during periods with reduced sunlight which can be typically caused by cloud cover. Different CSP technologies are being used together with TESS, but their analysis is beyond the scope of this Thesis. Just to point out the Parabolic Trough Systems which is the most implemented one and that can be appreciated in Figure 3.26.

- Finally, a third group would comprehend those installations relating RES with CHP units. The TEES technology, as the rest of ESS, can be very effective to improve EPS flexibility allowing a further integration of RES. The clear example for this is Denmark where this has been applied. They have achieved a big wind power penetration thanks to a very flexible EPS obtained by integrating a large number of CHP units which provide, apart from electric power, district heating in most of the cities. So, both electricity and heat can be provided from these units in a combined and complementary form. During times of low wind power, lots of electricity must be generated by the CHP units to accommodate for the shortfall power production. Consequently, lots of hot water is produced although there is no demand for it, thus the exceeding hot water is sent to the thermal storage tank. On the contrary, during high wind power periods, the CHP units produce very little electricity and the corresponding hot water which can be not enough for the instantaneous demand. Therefore, there is in that situation a shortage in hot water and hence the thermal storage is used to supply that shortfall.

Figure 3.26 Prototype Parabolic Trough Systems in Almeria (Spain).

According to [33], the cost for end-use TEES ranges from $250 to $500 per peak kW shifted and the payback period is affirmed to oscillate, depending on each specific project, from one to three years. Nevertheless, it is noteworthy that if TEES installation is integrated during the building construction, the cost can be drastically reduced by using smaller ducts (20% to 40% reduction), chillers (40% to 60% smaller), fan motors, air handlers and water pumps. In this sense, [64] has estimated the overall air conditioning cost can be reduced by 20% to 60%.

Regarding TEES applied to CSP, exact costs are difficult to establish although, according to some studies and projects being developed [153, 154], can be estimated around $315 per peak kW, cost which are expected to drop till $315 per peak kW in 2015 [154].

The cost for the EPS balancing TEES, applied in Denmark, cannot be stated. It is huge, requires large investments and a National Policy thought to facilitate this electric structure.

Example of installations

Being a mature technology on its end-use application, TEES presents in this domain more than 7000 installations already installed worldwide, replacing nearly 5GW of peak load requirements [33]. They are implemented in places such as Hospitals, Schools, Malls, Universities, Museums, and Auditoriums…

Regarding TEES in CSP plants, the largest group of installations which implement Parabolic Trough Systems in the world were the Solar Energy Generating Systems (SEGS). These are nine plants, named I through IX, located in the Mohave Desert in southern

California, which were built in the 1985 to 1991 time frame. The characteristics of the different plants can be appreciated in Table 3.10. Only the first one implemented TEES.

Plant Name	Location	First Year of Operation	Net Output (MW$_e$)	Solar Field Outlet Temp (°C)	Solar Field Area (m^2)	Solar Turbine Effic.(%)	Power Cycle	Dispatchability provided by:
SEGS IX	Harper Lake, CA	1991	80	390	483,960	37.6	100 bar, reheat	HTF heater
SEGS VIII	Harper Lake, CA	1990	80	390	464,340	37.6	100 bar, reheat	HTF heater
SEGS VI	Kramer Junction, CA	1989	30	390	188,000	37.5	100 bar, reheat	Gas boiler
SEGS VII	Kramer Junction, CA	1989	30	390	194,280	37.5	100 bar, reheat	Gas boiler
SEGS V	Kramer Junction, CA	1988	30	349	250,500	30.6	40 bar, steam	Gas boiler
SEGS III	Kramer Junction, CA	1987	30	349	230,300	30.6	40 bar, steam	Gas boiler
SEGS IV	Kramer Junction, CA	1987	30	349	230,300	30.6	40 bar, steam	Gas boiler
SEGS II	Daggett, CA	1986	30	316	190,338	29.4	40 bar, steam	Gas boiler
SEGS I	Daggett, CA	1985	13.8	307	82,960	31.5	40 bar, steam	3-hrs TES

Table 3.10 SEGS plants list: technology, net output, project type, and funding. Source: NREL.

Some more prototype TEES with CSP plants were developed in that period of time. A summary of the most important prototypes is introduced in Table 3.11.

Project	Type	Storage Medium	Cooling Loop	Nominal Temperature Cold Hot (°C)		Storage Concept	Thermal Capacity (MWht)
Irrigation pump Coolidge, AZ, USA	Parabolic Trough	Oil	Oil	200	228	1 Tank Thermocline	3
IEA-SSPS Almería, Spain	Parabolic Trough	Oil	Oil	225	295	1 Tank Thermocline	5
SEGS I Daggett, CA, USA	Parabolic Trough	Oil	Oil	240	307	Cold-Tank Hot-Tank	120
IEA-SSPS Almería, Spain	Parabolic Trough	Oil Cast Iron	Oil	225	295	1 Dual Medium Tank	4
Solar One Barstow, CA, USA	Central Receiver	Oil/Sand/ Rock	Steam	224	304	1 Dual Medium Tank	182
CESA-1 Almería, Spain	Central Receiver	Liquid Salt	Steam	220	340	Cold-Tank Hot-Tank	12
THEMIS Targasonne, France	Central Receiver	Liquid Salt	Liquid Salt	250	450	Cold-Tank Hot-Tank	40
Solar Two Barstow, CA, USA	Central Receiver	Liquid Salt	Liquid Salt	275	565	Cold-Tank Hot-Tank	110

Table 3.11 Firstly developed TEES installations in CSP technology worldwide.

In addition to the SEGS and to the other prototype plants presented in Table 3.11, there are several commercial projects planned or already under construction stage. Still in the USA, a 1MW experimental plant has been constructed in Arizona implementing an Organic Rankine Cycle (ORC) as power cycle. Furthermore, a 64 MW plant is under construction in Nevada reproducing the SEGS technology. With the same technology, several 50 MW plants have been constructed in Spain in the last five years. Note that the early Spanish plants include seven hours of thermal storage. Other projects in various stages of planning include integrated solar combined cycle systems (ISCCS) in southern California, India, Egypt, Morocco, Mexico, and Algeria. Finally, there are some SEGS plants with ES type planned to be constructed in Israel.

3.6. Comparison of ES technologies.

Among the different technologies introduced in this chapter, it is very difficult to establish a logical and pondered global comparative. Each of them is, individually, more or less appropriate for certain applications but no technology is perfect for everything and although some ESS can function in all application ranges, most options would not be economically viable. The choice for using a certain ESS for a determined application, or even for different scale projects conceived within the same application domain, will depend on various factors such as the punctual application power and energy ratings, the response time required, the weight and the volume limitations, the operating environment and the operating temperature among others. Furthermore, factors such as the commercial availability, the expected lifetime and, of course, the estimated cost for providing the expected services will be crucial for the economic viability of the project.

Consequently, clear information on the different values of the design parameters and operation characteristics for the various ESS must be available and known previous to the investment decision. In this sense, Table 3.12 pretends to be a summary reference for evaluating the various ESS. Hence, although comparison seems not possible among these technologies, at least some ideas about the scale and characteristic differences are provided.

For decision-making, all the information presented in Table 3.12 must be separated. In this way, although the global comparison is impossible some kind of confrontation among them can be done. Various charts which combine the different columns and other factors are presented in [155]. Those more representative are explained in the following.

ES technology	Power capacity	Energy capacity	Response time	Efficiency (%)	Lifetime	State of development
Pumped Hydro	30MW – 4000MW	500 – 8000MWh	Sec. to min.	70 – 85	Even 50 years	Commercial
Compressed Air	50MW – 300MW	500 – 2600MWh	Sec. to min.	64 – 75	Even 40 years	Commercial/prototypes for vessels
Flywheel	Up to 2MW	Up to 15 min	Milliseconds	90	20 years	Commercial/prototypes Depends on spin speed
Superconducting Magnetic	0.01 – 10MW	Up to 30 min	Immediately	95	30 years	Commercial/research Depends on range
Ultracapacitors	Up to 1MW	Up to 1 min	Immediately	85 – 98	10 years	Commercial
Lead Acid Battery	0.001 – 40MW	Up to 40MWh	Milliseconds	75 – 85	1000 cycles	Commercial
Nickel Cadmium Battery	0.001 – 40MW	Up to 10MWh	Milliseconds	60 – 70	1000 – 3500 cycles 10 – 15 years	Commercial
Sodium Sulfur Battery	0.05 – 50MW	Several 100MWh	Few seconds	75 – 89	2500 cycles Up to 15 years	Commercial
Lithium Ion Battery	0.001 – 0.5MW	Several MWh	Milliseconds	90 – 95	20000 cycles	Commercial/under development
Vanadium Redox Flow Battery	0.05 – 3MWs	Several MWh	Milliseconds	70 – 85	10000 cycles, 7 – 10 years	Improved prototypes in test/ Commercial
ZnBr Flow Battery	Up to 1MW	Less than 4h	Milliseconds	75	2000 cycles	Improved prototypes in test/ Commercial
PSB Flow Battery	Up to 15MW	Less than 20h	Milliseconds	60 – 75	2000 cycles	Improved prototypes in test/ Commercial
Air-metal Batteries	Limited to the moment	Limited only by anode's life	Milliseconds	60-70	50 cycles	Under primary research and development
Fuel Cells	Up to 250kW	Rechargeable with H_2	Milliseconds	35 – 45	10 to 20 years	Improved prototypes in test/ Commercial
Thermoelectric systems	1MW – 100MW	2 – 800MWh	Sec. to min.	30-70	20 years	Commercial

Table 3.12 General comparison of different ES technologies for EPS applications.

Firstly, a diagram combining power ratings and discharge time at rated power for EES systems installed as of November 2008 is introduced Figure 3.27. This is a representation of the two first columns in Table 3.12 and provides an idea about what ES applications could be provided by each of the technologies according to their capacities. It is clear and relevant on it that the most implemented ESS for large–scale applications to present are PHES and CAES.

In the second place, other two important parameters to consider before selecting an ESS are efficiency and cycle life, Figure 3.28. Both of them affect significantly the overall ES cost. Low efficiency increases the effective energy cost as only a fraction of the stored energy will be utilized. Low cycle life also increases the total cost as the storage device needs to be replaced more often. Thus, these additional costs need to be considered along with others such as the capital cost and the operating expenses to obtain a proper picture of the total investment.
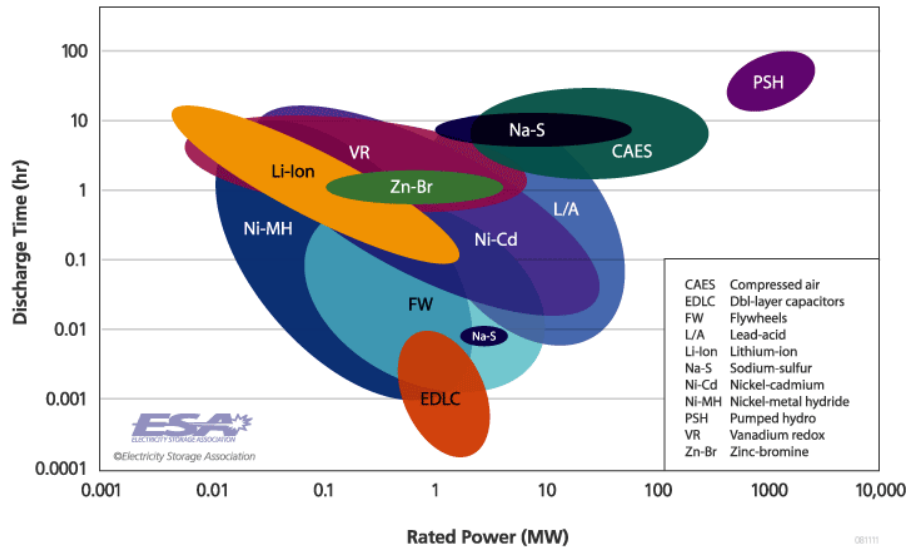
Figure 3.27 **Discharge time versus rated power for the different ES technologies. Source:** [155]**.**
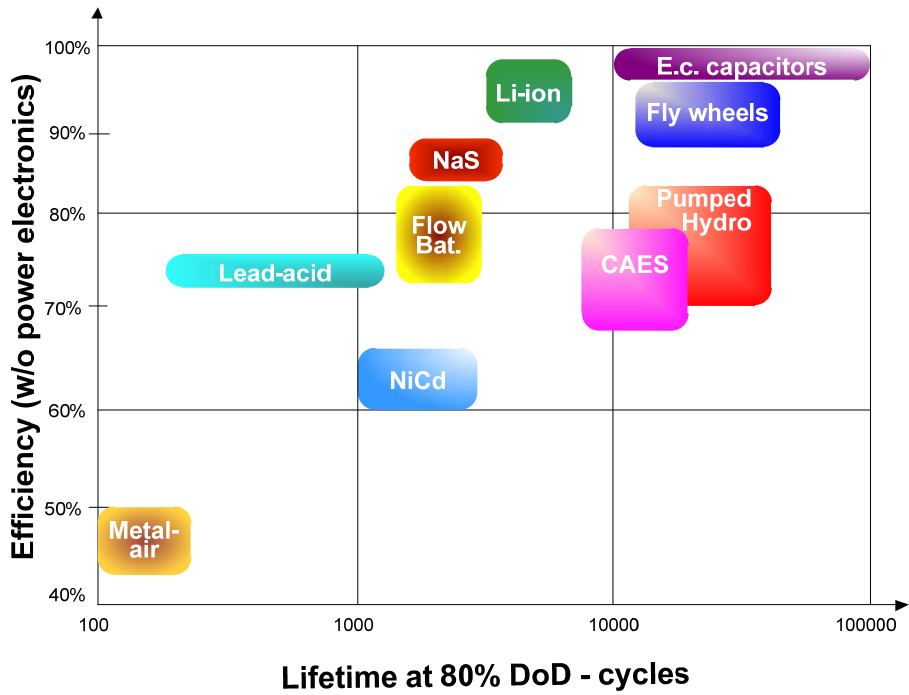
Figure 3.28 **Efficiency vs. lifetime for the different ES technologies. Source:** [155]**.**

Thirdly, another interesting comparison which can be represented is the state of development for each of the technologies represented versus the various power ratings, Figure 3.29. This figure provides a clear idea about the technologies commercially available nowadays for the different levels of power, which indicates what ES technology options can be used right now for a determined application.
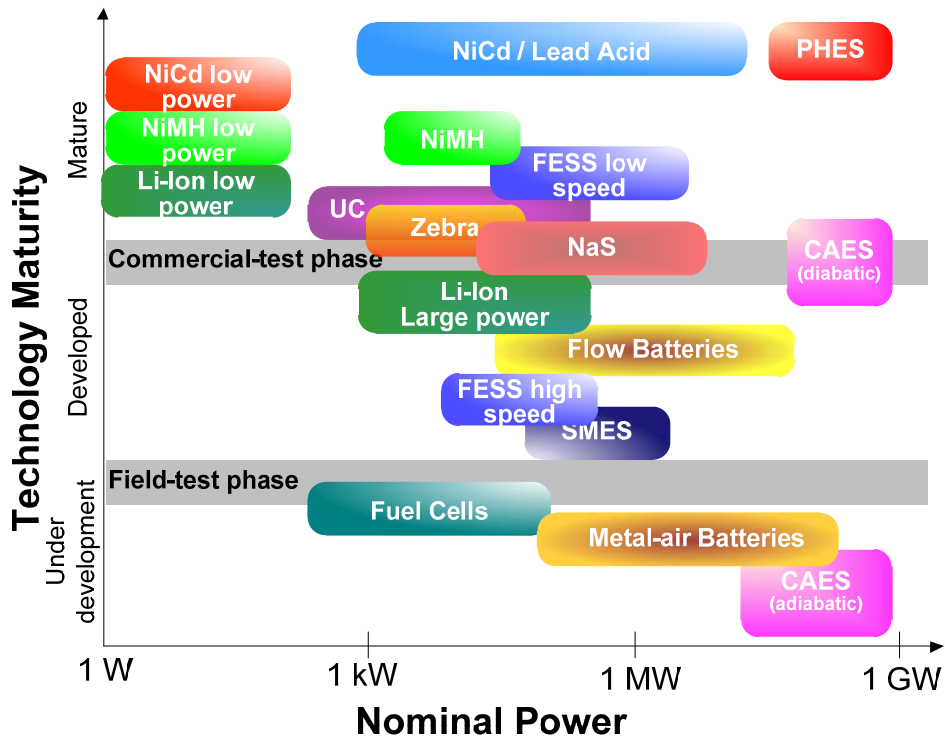
Figure 3.29 State of development vs. nominal power for the various ES technologies. Source:
[155]**.**

In addition, considering again the lifetime column, a good way to evaluate the cost of the ESS for frequent cycling applications, such as load leveling, it has to take into account the per-cycle cost, i.e. how much the ESS costs compared to the number of charge/discharge cycles it can experience. Figure 3.30 shows the capital component of this cost, taking into account the impact of cycle life and efficiency. For a more complete per-cycle cost analysis, one should also consider O&M, disposal, replacement and other ownership expenses, which may not be known for the emerging technologies. It should be noted that per-cycle cost is not an appropriate criterion for peak shaving or energy arbitrage where the application is less frequent or the energy cost differential is large and volatile [155].
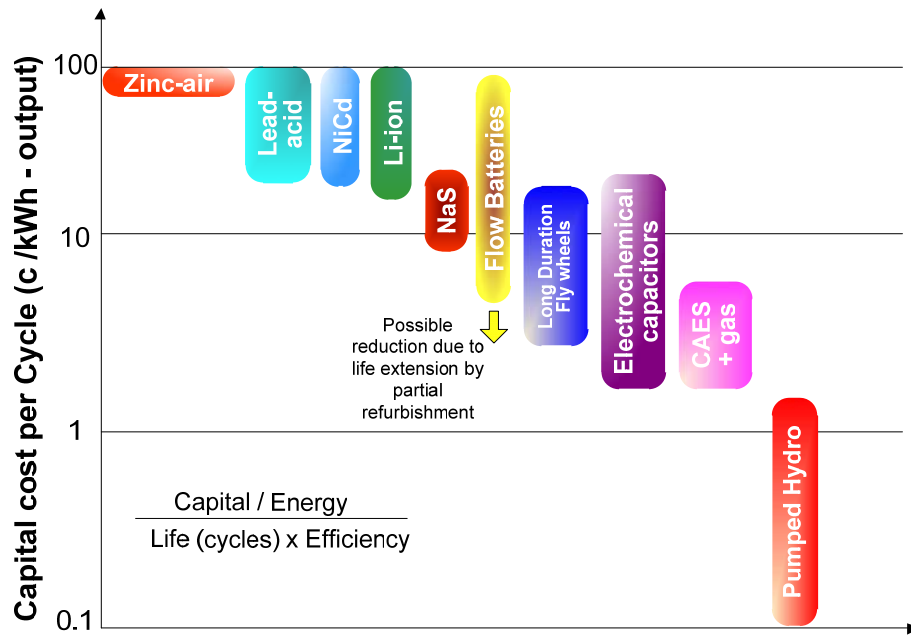
Figure 3.30 Capital cost per cycle for the different ES technologies. Source: [155]**.**
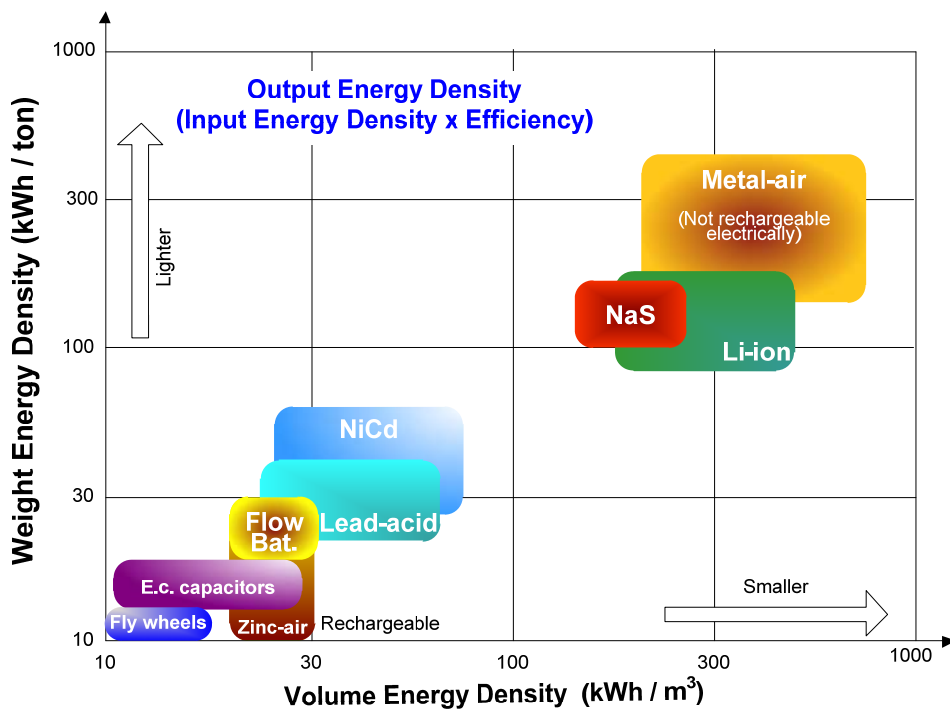
Figure 3.31 Specific vs. volume energy density for the different ES technologies. Source: [155]**.**

On the other hand, as previously introduced and although not presented in Table 3.12, the size and weight characteristics of the ESS are important factors for certain applications. Another chart is represented for comparing these two factors for the various ESS, Figure 3.31.

Metal-air batteries have the highest energy density in Figure 3.31. However, the electrically rechargeable types, such as Lithium-air or Zinc-air batteries, have a relatively small cycle life and are still in the development stage, Figure 3.29. On the other hand, it is noteworthy that the energy density ranges reflect the differences among manufacturers, product models and the impact of packaging.

Following with costs analysis, while capital cost is an important economic parameter, it stands out that the total cost of the ESS (including the impact of equipment life and O&M costs) is a much more meaningful index for a complete economic analysis. For example, while the capital cost of lead-acid batteries is relatively low, they may not necessarily be the least expensive option for load leveling due to their relatively short life for this type of application, Figure 3.30. In this sense, the following assumptions must be done to represent Figure 3.32: the battery costs have been adjusted to exclude the cost of power conversion electronics and the cost per unit energy has also been divided by the ESS efficiency to obtain the cost per output (useful) energy. Furthermore, note that the ES technologies costs change as frequently as they evolve. The cost ranges represented in Figure 3.32 include approximate values obtained by the Electricity Storage Association (ESA) in 2002 and the expected mature values in a few years.
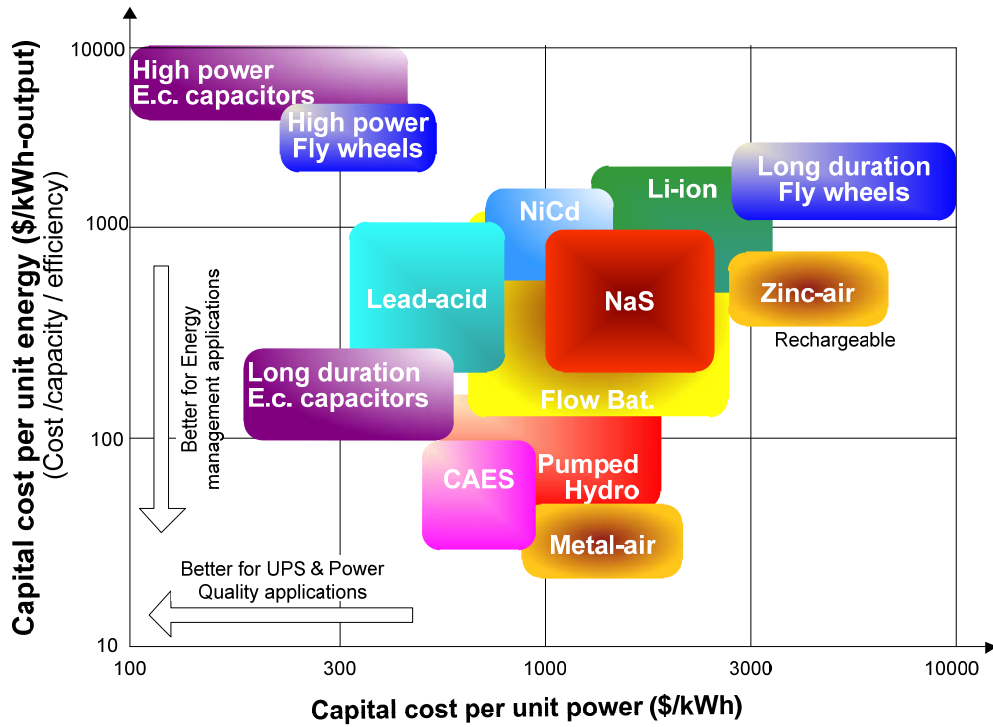
Figure 3.32 Energy cost vs. power cost for the different ES technologies. Source: [155]**.**

Finally, and to summarize the information about the costs of the different ES technologies compared in the previous figures, one last table is presented here which introduces the different costs of these technologies (both capital and O&M) for each of the technologies compiling the information provided by different authors [5, 26, 33, 35, 62, 64, 74, 156, 157].

Technology	Capital cost			O&M cost		Cost certainty
	Power related cost ($/kW)	Energy related cost ($/kWh)	BOP ($/kWh)	Fixed ($/kW-y)	Variable (c$/kWh)	
Pumped hydro	600 - 2000	0 – 20	Included	3.8	0.38	Price list
Underground pumped hydro	n/a	n/a	n/a	3.8	0.38	Estimate
Compressed air (in reservoirs)	425 - 480	3 - 10	50	1.42	0.01	Price quotes
Compressed air (in vessels)	517	50	40	3.77	0.27	Estimate
Lead-acid battery	200 - 580	175 - 250	~50	1.55	1	Price list
Nickel-cadmium battery	600 – 1500	500 – 1500	n/a	n/a	n/a	Estimate
Sodium-sulphur battery	259 - 810	245	~40	n/a	n/a	Project specific
Li-ion battery	n/a	750 – 1000	n/a	n/a	n/a	Project specific
Vanadium-redox flow battery	1250 – 1800	175 - 1000	n/a	n/a	n/a	Project specific
Polysulphide-bromide flow battery	1000 - 1200	175 - 190	n/a	n/a	n/a	Project specific
Zinc-bromine flow battery	640 - 1500	200 - 400	Included	n/a	n/a	Project specific
Low-speed flywheel	300	200 - 300	~80			Price list
High-speed flywheel	350	500 - 25000	~1000	7.5	0.4	Project specific
Supercapacitor	300	82000	10000	5.55	0.5	Project specific
Superconducting magnetic (Micro)	300	72000	~10000	26	2	Price quotes
Superconducting magnetic	300	2000	~1500	8	0.5	Estimate
Hydrogen (fuel cell)	1100 - 2600	2 - 15	n/a	10	1	Price quotes
Hydrogen (engine)	950 – 1850	2 - 15	n/a	0.7	0.77	Price list

Table 3.13 Costs comparison for the different ES technologies.

3.7. Discussion on ES Technology selection.

As it was introduced in Chapter I, ESS can be used for a large number of grid applications. Various research works already with the suitability of the different ES technologies for each of these applications [24, 25, 28, 33, 34, 74, 109, 158, 159]. In fact, some authors even provide interesting tables where grid applications are crossed with ESS and some RES [5, 35]. In this sense, Table 3.14 represents one of these tables extracted from [5].

Nevertheless, for the sake of the clarity and simplicity in the conclusions presented in this section, all the possible applications can be classified just into the following three categories, grouping into coarse time intervals applications with similar energetic requirements:

- Power Conditioning. These applications, (also known as end user peak shaving), require the energy stored to be used for seconds or less to assure the continuity of the power supply (avoid blackouts), to skip short-period interruptions (voltage sags), to reduce voltage peaks, and mitigate variable fluctuations (flicker).

- Bridging Power. This type of applications requires the energy stored to be used for seconds to minutes to assure continuity of service when switching from one source of energy generation to another. Some applications are primary frequency regulation, distribution network upgrade deferral, back up and transmission and distribution stabilization.

Full Power Duration of Storage	Applications of Storage and Possible Replacement of Conventional Electricity System Controls	Large Hydro	Biomass	Hydrogen Electrolysis + Fuel Cell	Compressed Air Energy Storage (CAES)	Heat or Cold Store + Heat Pump	Pumped Hydro	Redox Flow Cells	New And Old Battery Technologies	Flywheels	Superconducting Magnetic Energy Storage (SMES)	Ultracapacitor	Conventional Capacitor or Inductor
4 Months	Annual smoothing of loads, PV, wind and small hydro.	X	X	X									
3 Weeks	Smoothing weather effects: load, PV, wind, small hydro.	X	X	X									
3 Days	Weekly smoothing of loads and most weather variations	X	X	X	X	X	X	X					
8 Hours	Daily load cycle, PV, wind, Transmission line repair	X	X	X	X	X	X	X	X				
2 Hours	Peak load lopping, standing reserve, wind power smoothing. Minimization of NETA or similar trading penalties.	X	X	X	X	X	X	X	X				
20 Minutes	Spinning reserve, wind power smoothing, clouds on PV	X		X	X	X	X	X	X	X			
3 Minutes	Spinning reserve, wind power smoothing of gusts.			X			X	X	X	X			
20 Seconds	Line or local faults. Voltage and frequency control. Governor controlled generation.							X	X	X	X	X	X

Table 3.14 Technical suitability of ESS technologies to different applications. Source: [5]

- Energy Management. For these applications, the ESS is used to decouple the timing of generation and consumption of the electric energy. Typical applications comprehend load leveling, load following, energy arbitrage, and transmission network upgrade deferral.

So, applications are mainly grouped as a function of the power and energy they require. Hence, apart from them one last application has to be outlined: the cooperation to an extended RES integration. This cannot be incorporated to any of the previous groups since it is somehow transversal and does not present a precise range of ppwer and energy needs. The RES integration requirements depend on many factors such as the type of RES technology and the current degree of penetration [6].
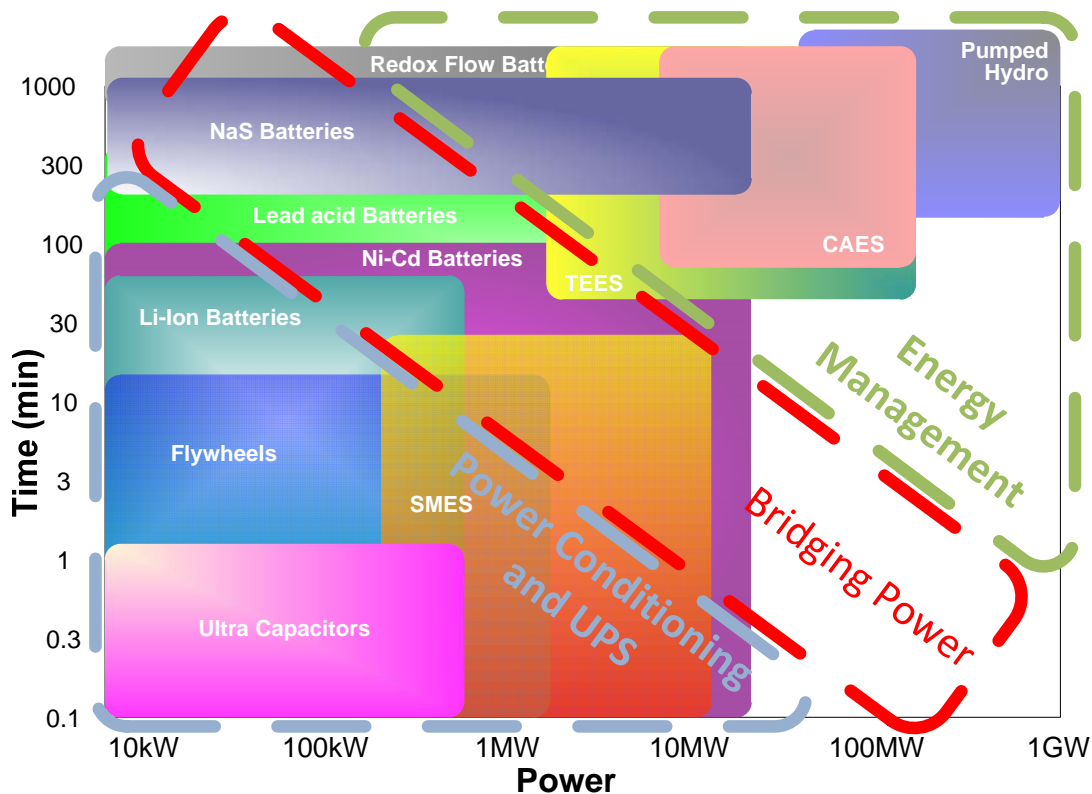
Figure 3.33 Time vs. power operational range of the different ES technologies.

Then, the grid applications energy requirements can be compared with the various technologies analyzed along this chapter (power and energy ratings for each technology in this figure have been introduced according to Table 3.12). It can be clearly appreciated in

Figure 3.33 that the ESS that would fit the best for each type of grid application would be. However, note that the energy requirement borders among the applications are not always strictly defined.

Thus, some conclusions can be noted about the ES technology to use on each case.

a) Conclusions over ES technologies for power quality applications.

According to Figure 3.33, power quality applications are covered by low capacity ES technologies such as UC [87-89, 160, 161], SMES [80, 162], FESS [65-67, 163] and different types of batteries [24, 104, 125, 164-166], managing the active power plus additional reactive power control. All of these technologies present different states of development although most of them already enjoy some commercial model, Figure 3.29. Thus, any of them could be used in the near future for power quality applications.

b) Conclusions over ES technologies for bridging power applications.

In the same way, many different ES technologies could be used for bridging power applications highlighting among them some types of batteries and, in a second term, SMES and high power FESS. Regarding the different types of batteries, NaS seems the the most interesting candidate for large scale projects nowadays [114, 117, 120, 167, 168], although both flow batteries (which are already implemented in some prototype RES integration projects [35, 138]) and Li-ion batteries [169] (the big gamble for the electric vehicle automotive industry [96]) are evolving very fast and could be expected to be suitable for that range of applications soon [34]. Demonstration results for these batteries will be decisive for bridging applications too in the near future. LA and NiCd will probably remain to be used for their existing applications since no important breakthroughs are expected. It is noteworthy that flow batteries are much more complex than conventional batteries, what is the reason why conventional batteries still remain an attractive alternative to them in some applications.

c) Conclusions over large-scale technologies for energy management

For the case of energy management applications, these have been traditionally associated to large scale projects which require high power (>50 MW) and enormous energy capacities (>100 MWh) to the ESS. So, only a few technologies are identified as suitable: notably PHES and CAES. In fact, energy arbitrage has been traditionally performed by PHES because it can be constructed at large capacities (over 100 MW range) and can discharge over periods of time ranging from 100 to 1000 min. Furthermore, PHES is a mature

technology with more than 240 facilities worldwide currently in operation (over 90 GW) as well as 7 GW of additional plants planned in Europe alone over the next years. CAES has been used for energy arbitrage too although (as indicated on its section) only few installations are in operation nowadays [25]. Underground PHES together with CAES using vessels are still only concepts and thus commercially unproven for grid applications. The third large scale technology already introduced in the market which can also be applied for energy arbitrage but for load leveling too is the TEES, which is not restricted by geographic limitations inherent to both CAES and PHES. In fact, this is a key issue for both of them having found problems to determine new suitable locations. Furthermore, large battery units (including flow batteries and maybe future metal-air batteries) could be considered for energy management applications too [168, 170]. And even more, associated to PV plants were power and energy capacity requirements are not so high [13, 16]. In this sense, both NaS and Li-ion batteries could be analyzed for medium power energy management applications.

Finally, note a new idea which is producing a singularly intense echo among engineers because it could represent a revolution at the EPS level: to use the capacity offered by the electrical vehicles' batteries for both load leveling and energy arbitrage (V2G philosophy) [171].

d) Conclusions on specific technologies for PV power plants.

It is clearly stated in Chapter I that intermittent RESs, mainly solar and wind, will need to be supported with other conventional utility power plants and ESS for a further penetration because when high integration degrees will be achieved the system operation will become more complex and will require additional balancing power [8, 9, 17, 156]. Hence, large ES capacities will allow a high percentage of wind [29, 172, 173], photovoltaic [11, 16, 19, 174, 175], and other RES in the electrical mix contributing to fulfill the objectives for a more sustainable distributed structure for the EPS. Thus, in order to integrate RESs, it is necessary to propose ESS that can offer energy capacities of several hours (as many as possible) and various power levels (depending on the RES to integrate, PV or wind…). Note that research and development on different ES technologies integrated into wind power plants are already under way [176-181].

Regarding PV power plants, amongst the different ES technologies presented in Table 3.12, few are able to meet the requirements of PV power plant applications. These

requirements include: fast reaction time, high efficiency, physical size to be placed on the location, easiness of maintenance, long life cycle and, preferably, possibility to independently sizing storage power and capacity and maturity of the technology [26, 32, 106, 123, 157, 182]. According to them, batteries are referred to as the key technology to operate integrated with them [123]. On the one hand, among the different battery technologies, lead-acid battery systems have been mostly used in past applications [103, 107, 174], mainly due to their maturity and low cost, but performance limitations, short life cycles, and high maintenance demands have limited their adoption in new large scale PV applications. On the other hand, breakthroughs in a new generation of Lithium-Ion based BESS are entering the market meeting most of the PV power plants operation requirements. Furthermore, their dynamical properties seem to fit perfectly for solar variations and some experience has already been gained with them in the field of wind power [29]. Finally, a further significantly improvement in Lithium based batteries performances is expected in the near future due to large research effort that is being developed on them, especially focused on its potential application to electric vehicles [28, 94, 96, 157, 183, 184].

Therfore, batteries are defined as the major contender for PV integration and as the technology which will provide PV plants with capability for grid applications. The selection of one or other types of batteries among Li-ion, NaS or flow batteries will depend on the power and energy requirements (both from the PV plant and the grid application desired) and on the commercial evolution (costs) for these three technologies.

3.8. References

[1] J. Howes, "Energy storage: renewable energy's missing link," Power Engineering International Issue, February 2010, 2010.

[2] G. Marsh, "RE storage: The missing link," Refocus, vol. 3, pp. 38-41, 2002.

[3] R. M. Dell and D. A. J. Rand, "Energy storage--a key technology for global energy sustainability," J. Power Sources, vol. 100, pp. 2-17, 2001.

[4] C. Hoffmann, M. Greiner, L. Bremen, K. Knorr, S. Bofinger, M. Speckmann and K. Rohrig, "Design of transport and storage capacities for a future european power supply system with a high share of renewable energies," in 3rd International Renewable Energy Storage Conference IRES, Berlin, 2008, pp. 24-25.

[5] J. P. Barton and D. G. Infield, "Energy storage and its use with intermittent renewable energy," IEEE Transactions on Energy Conversion, vol. 19, pp. 441-448, 2004.

[6] A. Nourai, "Large-scale electricity storage technologies for energy management," in Power Engineering Society Summer Meeting, 2002 IEEE, 2002, pp. 310-315 vol.1.

[7] A. Nourai, V. I. Kogan and C. M. Schafer, "Load Leveling Reduces T&D Line Losses," IEEE Transactions on Power Delivery, vol. 23, pp. 2168-2173, 2008.

[8] Z. A. Styczynski, P. Lombardi, R. Seethapathy, M. Piekutowski, C. Ohler, B. Roberts and S. C. Verma, "Electric energy storage and its tasks in the integration of wide-scale renewable

resources," in Integration of Wide-Scale Renewable Resources into the Power Delivery System, 2009 CIGRE/IEEE PES Joint Symposium, 2009, pp. 1-11.

[9] M. Liserre, T. Sauter and J. Y. Hung, "Future Energy Systems: Integrating Renewable Energy Sources into the Smart Power Grid Through Industrial Electronics," IEEE Industrial Electronics Magazine, vol. 4, pp. 18-37, 2010.

[10] J. T. Bialasiewicz, "Renewable Energy Systems With Photovoltaic Power Generators: Operation and Modeling," IEEE Transactions on Industrial Electronics, vol. 55, pp. 2752-2758, 2008.

[11] P. Denholm and R. M. Margolis, "Evaluating the limits of solar photovoltaics (PV) in electric power systems utilizing energy storage and other enabling technologies," Energy Policy, vol. 35, pp. 4424-4433, 9, 2007.

[12] J. M. Carrasco, L. G. Franquelo, J. T. Bialasiewicz, E. Galvan, R. C. P. Guisado, M. A. M. Prats, J. I. Leon and N. Moreno-Alfonso, "Power-Electronic Systems for the Grid Integration of Renewable Energy Sources: A Survey," IEEE Transactions on Industrial Electronics, vol. 53, pp. 1002-1016, June, 2006.

[13] B. H. Chowdhury, "Central-station photovoltaic plant with energy storage for utility peak load leveling," in Energy Conversion Engineering Conference, 1989. IECEC-89., Proceedings of the 24th Intersociety, 1989, pp. 731-736 vol.2.

[14] A. Ruddell. Investigation on storage technologies for intermittent renewable energies: Evaluation and recommended r&d strategy. 2003.

[15] International Energy Agency (IEA) - Photovoltaic Power Systems Programme. Cumulative installed PV power . [Online]. Available: http://www.iea-pvps.org/.

[16] M. Lafoz, L. Garcia-Tabares and M. Blanco, "Energy management in solar photovoltaic plants based on ESS," in Power Electronics and Motion Control Conference, 2008. EPE-PEMC 2008. 13th, 2008, pp. 2481-2486.

[17] S. Teleke, M. E. Baran, S. Bhattacharya and A. Q. Huang, "Rule-Based Control of Battery Energy Storage for Dispatching Intermittent Renewable Sources," Sustainable Energy, IEEE Transactions on, vol. 1, pp. 117-124, 2010.

[18] A. Nourai and D. Kearns, "Batteries Included," Power and Energy Magazine, IEEE, vol. 8, pp. 49-54, 2010.

[19] R. Carbone, "Grid-connected photovoltaic systems with energy storage," in Clean Electrical Power, 2009 International Conference on, 2009, pp. 760-767.

[20] G. Petrone, G. Spagnuolo, R. Teodorescu, M. Veerachary and M. Vitelli, "Reliability Issues in Photovoltaic Power Processing Systems," IEEE Transactions on Industrial Electronics, vol. 55, pp. 2569-2580, 2008.

[21] S. J. Chiang, K. T. Chang and C. Y. Yen, "Residential photovoltaic energy storage system," IEEE Transactions on Industrial Electronics, vol. 45, pp. 385-394, 1998.

[22] EUROGIA+. [Online]. 2011). Available: http://www.eurogia.com/.

[23] E. Lightner and S. Director, "Evolution and progress of smart grid development at the department of energy," in DOE Presentation at FERC-NARUC Smart Grid Collaborative Workshop, Washington, DC, 2008, .

[24] K. C. Divya and J. Østergaard, "Battery energy storage technology for power systems--An overview," Electr. Power Syst. Res., vol. 79, pp. 511-520, 2009.

[25] S. Vazquez, S. M. Lukic, E. Galvan, L. G. Franquelo and J. M. Carrasco, "Energy Storage Systems for Transport and Grid Applications," IEEE Transactions on Industrial Electronics, vol. 57, pp. 3881-3895, 2010.

[26] O. Luimnigh and D. Connolly, "An investigation into the energy storage technologies available, for the integration of alternative generation techniques," University of Limerick, 2009.

[27] P. J. Hall and E. J. Bain, "Energy-storage technologies and electricity generation," Energy Policy, vol. 36, pp. 4352-4355, 12, 2008.

[28] P. F. Ribeiro, B. K. Johnson, M. L. Crow, A. Arsoy and Y. Liu, "Energy storage systems for advanced power applications," Proc IEEE, vol. 89, pp. 1744-1756, 2001.

[29] J. McDowall, "Integrating energy storage with wind power in weak electricity grids," J. Power Sources, vol. 162, pp. 959-964, 11/22, 2006.

[30] J. M. Guerrero, L. G. De Vicuna and J. Uceda, "Uninterruptible power supply systems provide protection," Industrial Electronics Magazine, IEEE, pp. 28-38, 2007.

[31] S. Lemofouet and A. Rufer, "A Hybrid Energy Storage System Based on Compressed Air and Supercapacitors With Maximum Efficiency Point Tracking (MEPT)," IEEE Transactions on Industrial Electronics, vol. 53, pp. 1105-1115, 2006.

[32] M. Swierczynski, R. Teodorescu, C. N. Rasmussen, P. Rodriguez and H. Vikelgaard, "Overview of the energy storage systems for wind power integration enhancement," Vestas Power Program, Denmark, 2010.

[33] R. Baxter, Energy Storage: A Nontechnical Guide. PennWell Corp., 2005.

[34] M. Beaudin, H. Zareipour, A. Schellenberglabe and W. Rosehart, "Energy storage for mitigating the variability of renewable electricity sources: An updated review," Energy for Sustainable Development, 2010.

[35] D. Connolly, "A review of energy storage technologies," 2009.

[36] N. Uddin and M. Asce, "Preliminary design of an underground reservoir for pumped storage," Geotech. Geol. Eng., vol. 21, pp. 331-355, 2003.

[37] I. H. Wong, "An underground pumped storage scheme in the Bukit Timah granite of Singapore," Tunnel. Underground Space Technol., vol. 11, pp. 485-489, 1996.

[38] T. Fujihara, H. Imano and K. Oshima, "Development of pump turbine for seawater pumped-storage power plant," Hitachi Review, vol. 47, pp. 199-202, 1998.

[39] R. J. Kerkman, T. A. Lipo, W. G. Newman and J. E. Thirkell, "An Inquiry into Adjustable Speed Operation of a Pumped Hydro Plant Part 1-Machine Design and Performance," Power Apparatus and Systems, IEEE Transactions on, pp. 1828-1837, 1980.

[40] R. J. Kerkman, T. A. Lipo, W. G. Newman and J. E. Thirkell, "An Inquiry into Adjustable Speed Operation of a Pumped Hydro Plan Part II-System Analysis," Power Apparatus and Systems, IEEE Transactions on, pp. 1838-1844, 1980.

[41] W. B. Gish, J. R. Schurz, B. Milano and F. R. Schleif, "An adjustable speed synchronous machine for hydroelectric power applications," Power Apparatus and Systems, IEEE Transactions on, pp. 2171-2176, 1981.

[42] P. A. Mikladal, "Sustainable energy in the Faroe Islands–the role of hydropower," Ministry of the Interior, 2008.

[43] J. A. Suul, K. Uhlen and T. Undeland, "Wind power integration in isolated grids enabled by variable speed pumped storage hydropower plant," in Sustainable Energy Technologies, 2008. ICSET 2008. IEEE International Conference on, 2008, pp. 399-404.

[44] J. A. Suul, K. Uhlen and T. Undeland, "Variable speed pumped storage hydropower for integration of wind energy in isolated grids–case description and control strategies," in IEEE, NORPIE/2008, Nordic Workshop on Power and Industrial Electronics, 2008, pp. 9-11.

[45] T. Kuwabara, A. Shibuya, H. Furuta, E. Kita and K. Mitsuhashi, "Design and dynamic response characteristics of 400 MW adjustable speed pumped storage unit for Ohkawachi power station," Energy Conversion, IEEE Transactions on, vol. 11, pp. 376-384, 1996.

[46] C. Nicolet, Y. Pannatier, B. Kawkabani, A. Schwery, F. Avellan and J. J. Simond, "Benefits of variable speed pumped storage units in mixed islanded power network during transient operation," in HYDRO 2009 Conference, Processing World Hydro Development, Lyon, France, 2009, .

[47] A. Bocquel and J. Janning, "Analysis of a 300 MW variable speed drive for pump-storage plant applications," in Proc. of the 11th European Conference on Power Electronics and Applications, Dresden, Germany, 2005, .

[48] T. Gjengedal, "Application of adjustable speed hydro (ASH) machines in the norwegian power system," in Power Tech Proceedings, 2001 IEEE Porto, 2001, pp. 6 pp. vol. 2.

[49] J. A. Suul, "Control of Variable Speed Pumped Storage Hydro Power Plant for Increased Utilization of Wind Energy in an Isolated Grid," Control of Variable Speed Pumped Storage Hydro Power Plant for Increased Utilization of Wind Energy in an Isolated Grid, 2006.

[50] C. Bueno and J. Carta, "Wind powered pumped hydro storage systems, a means of increasing the penetration of renewable energy in the Canary Islands," Renewable and Sustainable Energy Reviews, vol. 10, pp. 312-340, 2006.

[51] G. Caralis and A. Zervos, "Analysis of the combined use of wind and pumped storage systems in autonomous Greek islands," Renewable Power Generation, IET, vol. 1, pp. 49-60, 2007.

[52] Red Eléctrica de España (REE). Demanda de energía en tiempo real. [Online]. 2011). Available: http://www.ree.es/operacion/curvas_demanda.asp.

[53] Sang-Seung Lee, Young-Min Kim, Jong-Keun Park, Seung-Il Moon and Yong-Tae Yoon, "Compressed air energy storage units for power generation and DSM in korea," in Power Engineering Society General Meeting, 2007. IEEE, 2007, pp. 1-6.

[54] Y. S. H. Najjar and M. S. Zaamout, "Performance analysis of compressed air energy storage (CAES) plant for dry regions," Energy Conversion and Management, vol. 39, pp. 1503-1511, 10, 1998.

[55] S. Succar, Compressed Air Energy Storage. CRC, 2010.

[56] S. M. Schoenung, "Characteristics and technologies for long-vs. short-term energy storage," Sandia National Laboratories, 2001.

[57] P. Lombardi, P. Vasquez and Z. A. Styczynski, "Optimised autonomous power system," in Integration of Wide-Scale Renewable Resources into the Power Delivery System, 2009 CIGRE/IEEE PES Joint Symposium, 2009, pp. 1-13.

[58] Ridge Energy Storage & Grid Services LP, "The economic impact of CAES on wind in TX, OK, and NM," Department of Energy, Texas, USA, 2005.

[59] P. Denholm and R. Sioshansi, "The value of compressed air energy storage with wind in transmission-constrained electric power systems," Energy Policy, vol. 37, pp. 3149-3158, 2009.

[60] J. Mason, V. Fthenakis, K. Zweibel, T. Hansen and T. Nikolakakis, "Coupling PV and CAES power plants to transform intermittent PV electricity into a dispatchable electricity source," Prog Photovoltaics Res Appl, vol. 16, pp. 649-668, 2008.

[61] Wikipedia. Compressed-air vehicle. [Online]. 2010). Available: http://en.wikipedia.org/wiki/Compressed_air_vehicles.

[62] F. A. Farret and M. G. Simões, Integration of Alternative Sources of Energy. Wiley-IEEE Press, 2006.

[63] T. Ichihara, K. Matsunaga, M. Kita, I. Hirabayashi, M. Isono, M. Hirose, K. Yoshii, K. Kurihara, O. Saito and S. Saito, "Fabrication and evaluation of superconducting magnetic bearing for 10ákWáh-class flywheel energy storage system," Physica C: Superconductivity, vol. 426, pp. 752-758, 2005.

[64] S. Eckroad and I. Gyuk, Handbook of Energy Storage for Transmission & Distribution Applications. EPRI-Department of Energy, 2003.

[65] Z. Jiancheng, H. Lipei, C. Zhiye and W. Su, "Research on flywheel energy storage system for power quality," in Power System Technology, 2002. Proceedings. PowerCon 2002. International Conference on, 2002, pp. 496-499 vol. 1.

[66] Z. Jun-xing and W. Tong-xun, "A novel dynamic voltage restorer with flywheel energy storage system," Journal of Mechanical & Electrical Engineering, vol. 2, 2010.

[67] H. Liu and J. Jiang, "Flywheel energy storage-An upswing technology for energy sustainability," Energy Build., vol. 39, pp. 599-604, 2007.

[68] G. O. Cimuca, C. Saudemont, B. Robyns and M. M. Radulescu, "Control and performance evaluation of a flywheel energy-storage system associated to a variable-speed wind generator," Industrial Electronics, IEEE Transactions on, vol. 53, pp. 1074-1085, 2006.

[69] R. Hebner, J. Beno and A. Walls, "Flywheel batteries come around again," Spectrum, IEEE, vol. 39, pp. 46-51, 2002.

[70] L. Ulrich, "Top 10 Tech Cars 2011," Spectrum, IEEE, vol. 48, pp. 28-39, 2011.

[71] M. Strasik, J. R. Hull, J. A. Mittleider, J. F. Gonder, P. E. Johnson, K. E. McCrary and C. R. McIver, "An overview of Boeing flywheel energy storage systems with high-temperature superconducting bearings," Superconductor Science and Technology, vol. 23, 2010.

[72] C. S. Hsu and W. J. Lee, "Superconducting magnetic energy storage for power system applications," Industry Applications, IEEE Transactions on, vol. 29, pp. 990-996, 1993.

[73] X. D. Xue, K. W. E. Cheng and D. Sutanto, "Power system applications of superconducting magnetic energy storage systems," in Industry Applications Conference, 2005. Fourtieth IAS Annual Meeting. Conference Record of the 2005, 2005, pp. 1524-1529 Vol. 2.

[74] A. Gonzalez, B. Gallachóir, E. McKeogh and K. Lynch, "Study of electricity storage technologies and their potential to address wind energy intermittency in ireland," University of Limerick, Ireland, 2004.

[75] M. H. Ali, Bin Wu and R. A. Dougal, "An Overview of SMES Applications in Power and Energy Systems," Sustainable Energy, IEEE Transactions on, vol. 1, pp. 38-47, 2010.

[76] H. Ibrahim, A. Ilinca and J. Perron, "Energy storage systems—Characteristics and comparisons," Renewable and Sustainable Energy Reviews, vol. 12, pp. 1221-1250, 6, 2008.

[77] V. Karasik, K. Dixon, C. Weber, B. Batchelder, G. Campbell and P. Ribeiro, "SMES for power utility applications: a review of technical and cost considerations," Applied Superconductivity, IEEE Transactions on, vol. 9, pp. 541-546, 1999.

[78] A. Abu-Siada and S. Islam, "Application of SMES Unit in Improving the Performance of an AC/DC Power System," Sustainable Energy, IEEE Transactions on, vol. 2, pp. 109-121, 2011.

[79] M. G. Molina, P. E. Mercado and E. H. Watanabe, "Static synchronous compensator with superconducting magnetic energy storage for high power utility applications," Energy Conversion and Management, vol. 48, pp. 2316-2331, 8, 2007.

[80] L. Ji-ru, Y. Zhong-dong and Y. Quan-qing, "Research on Superconducting Magnetic Energy Storage Based on Dynamic Voltage Restorer," High Voltage Engineering, vol. 3, 2008.

[81] R. C. Dorf and J. A. Svoboda, Introduction to Electric Circuits. New York: Wiley, 2010.

[82] A. Volta, "Sketch of Alessandro Volta," The Popular Science Monthly, pp. 118-119, May-Oct 1892.

[83] G. L. Bullard, H. B. Sierra-Alcazar, H. L. Lee and J. L. Morris, "Operating principles of the ultracapacitor," Magnetics, IEEE Transactions on, vol. 25, pp. 102-106, 1989.

[84] K. Y. Cheung, S. T. Cheung, R. G. De Silva, M. P. Juvonen, R. Singh and J. J. Woo. Large-scale energy storage systems. Imperial College London, ISE2 [Imperial College London]. 2003.

[85] M. H. Rahman, K. Nakamura and S. Yamashiro, "A grid-connected PV-ECS system with load leveling function taking into account solar energy estimation," in Electric Utility Deregulation, Restructuring and Power Technologies, DRPT. Proceedings of the IEEE International Conference on, 2004, pp. 405-410 Vol.1.

[86] N. Kakimoto, H. Satoh, S. Takayama and K. Nakamura, "Ramp-Rate Control of Photovoltaic Generator With Electric Double-Layer Capacitor," Energy Conversion, IEEE Transactions on, vol. 24, pp. 465-473, 2009.

[87] M. Corley, J. Locker, S. Dutton and R. Spee, "Ultracapacitor-based ride-through system for adjustable speed drives," in Power Electronics Specialists Conference, 1999. PESC 99. 30th Annual IEEE, 1999, pp. 26-31 vol.1.

[88] Y. R. L. Jayawickrama and S. Rajakaruna, "Ultracapacitor based ride-through system for a DC load," in Power System Technology, 2004. PowerCon 2004. 2004 International Conference on, 2004, pp. 232-237 Vol.1.

[89] P. Pillay, R. M. Samudio, M. Ahmed and R. T. Patel, "A chopper-controlled SRM drive for reduced acoustic noise and improved ride-through capability using supercapacitors," Industry Applications, IEEE Transactions on, vol. 31, pp. 1029-1038, 1995.

[90] N. Abi-Samra, C. Neft, A. Sundaram and W. Malcolm, "The distribution system dynamic voltage restorer and its applications at industrial facilities with sensitive loads," in Proc. 8th Int. Power Quality Solutions, Long Beach, CA, 1995, .

[91] A. F. Burke, "Batteries and Ultracapacitors for Electric, Hybrid, and Fuel Cell Vehicles," Proceedings of the IEEE, vol. 95, pp. 806-820, 2007.

[92] M. Conte, P. P. Prosini and S. Passerini, "Overview of energy/hydrogen storage: state-of-the-art of the technologies and prospects for nanomaterials," Materials Science and Engineering B, vol. 108, pp. 2-8, 4/25, 2004.

[93] P. Rodatz, G. Paganelli, A. Sciarretta and L. Guzzella, "Optimal power management of an experimental fuel cell/supercapacitor-powered hybrid vehicle," Control Eng. Pract., vol. 13, pp. 41-53, 1, 2005.

[94] E. Schaltz, A. Khaligh and P. O. Rasmussen, "Influence of Battery/Ultracapacitor Energy-Storage Sizing on Battery Lifetime in a Fuel Cell Hybrid Electric Vehicle," IEEE Transactions on Vehicular Technology, vol. 58, pp. 3882-3891, 2009.

[95] E. Schaltz, A. Khaligh and P. O. Rasmussen, "Investigation of battery/ultracapacitor energy storage rating for a fuel cell hybrid electric vehicle," in Vehicle Power and Propulsion Conference, 2008. VPPC '08. IEEE, 2008, pp. 1-6.

[96] S. M. Lukic, J. Cao, R. C. Bansal, F. Rodriguez and A. Emadi, "Energy Storage Systems for Automotive Applications," IEEE Transactions on Industrial Electronics, vol. 55, pp. 2258-2267, 2008.

[97] M. Ortuzar, J. Moreno and J. Dixon, "Ultracapacitor-Based Auxiliary Energy System for an Electric Vehicle: Implementation and Evaluation," Industrial Electronics, IEEE Transactions on, vol. 54, pp. 2147-2156, 2007.

[98] S. S. Williamson, A. Khaligh, S. C. Oh and A. Emadi, "Impact of energy storage device selection on the overall drive train efficiency and performance of heavy-duty hybrid vehicles," in Vehicle Power and Propulsion, 2005 IEEE Conference, 2005, pp. 10 pp.

[99] D. Linden, Handbook of Batteries. Elsevier, 1995.

[100] Shuo Tian, Munan Hong and Minggao Ouyang, "An Experimental Study and Nonlinear Modeling of Discharge I–V Behavior of Valve-Regulated Lead–Acid Batteries," Energy Conversion, IEEE Transactions on, vol. 24, pp. 452-458, 2009.

[101] H. Chen, T. N. Cong, W. Yang, C. Tan, Y. Li and Y. Ding, "Progress in electrical energy storage system: A critical review," Progress in Natural Science, vol. 19, pp. 291-312, 2009.

[102] D. U. Sauer and H. Wenzl, "Comparison of different approaches for lifetime prediction of electrochemical systems—Using lead-acid batteries as example," J. Power Sources, vol. 176, pp. 534-546, 2/1, 2008.

[103] Y. Chang, X. Mao, Y. Zhao, S. Feng, H. Chen and D. Finlow, "Lead-acid battery use in the development of renewable energy systems in China," J. Power Sources, vol. 191, pp. 176-183, 2009.

[104] C. D. Parker, "Lead–acid battery energy-storage systems for electricity supply networks," J. Power Sources, vol. 100, pp. 18-28, 11/30, 2001.

[105] J. Larminie, J. Lowry and I. NetLibrary, Electric Vehicle Technology Explained. Wiley Online Library, 2003.

[106] S. Vazquez, S. M. Lukic, E. Galvan, L. G. Franquelo and J. M. Carrasco, "Energy Storage Systems for Transport and Grid Applications," IEEE Transactions on Industrial Electronics, vol. 57, pp. 3881-3895, 2010.

[107] D. U. Sauer, M. Bächler, G. Bopp, W. Höhe, J. Mittermeier, P. Sprau, B. Willer and M. Wollny, "Analysis of the performance parameters of lead/acid batteries in photovoltaic systems," J. Power Sources, vol. 64, pp. 197-201, 2, 1997.

[108] H. Blanke, O. Bohlen, S. Buller, R. W. De Doncker, B. Fricke, A. Hammouche, D. Linzen, M. Thele and D. U. Sauer, "Impedance measurements on lead-acid batteries for state-of-charge, state-of-health and cranking capability prognosis in electric and hybrid electric vehicles," J. Power Sources, vol. 144, pp. 418-425, 2005.

[109] R. B. Schainker, "Executive overview: Energy storage options for a sustainable energy future," in Power Engineering Society General Meeting, 2004. IEEE, 2004, pp. 2309-2314 Vol.2.

[110] F. Ferella, I. De Michelis and F. Vegliò, "Process for the recycling of alkaline and zinc-carbon spent batteries," J. Power Sources, vol. 183, pp. 805-811, 2008.

[111] The European Parliament and the Council of the European Union, "Directive 2006/66/EC on batteries and accumulators and waste batteries and accumulators," 2006.

[112] S. R. Ovshinsky, M. A. Fetcenko and J. Ross, "A nickel metal hydride battery for electric vehicles," Science, vol. 260, pp. 176, 1993.

[113] A. Bito, "Overview of the sodium-sulfur battery for the IEEE stationary battery committee," in Power Engineering Society General Meeting, 2005. IEEE, 2005, pp. 1232-1235 Vol. 2.

[114] Lee Wei Chung, M. F. M. Siam, A. B. Ismail and Z. F. Hussien, "Modeling and simulation of sodium sulfur battery for battery-energy storage system and custom power devices," in Power and Energy Conference, 2004. PECon 2004. Proceedings. National, 2004, pp. 205-210.

[115] R. Dufo-López, J. L. Bernal-Agustín and J. A. Domínguez-Navarro, "Generation management using batteries in wind farms: Economical and technical analysis for Spain," Energy Policy, vol. 37, pp. 126-139, 1, 2009.

[116] R. Walawalkar, J. Apt and R. Mancini, "Economics of electric energy storage for energy arbitrage and regulation in New York," Energy Policy, vol. 35, pp. 2558-2568, 2007.

[117] Z. Wen, "Study on energy storage technology of sodium sulfur battery and it's application in power system," in Power System Technology, 2006. PowerCon 2006. International Conference on, pp. 1-4.

[118] Electropaedia. High temperature batteries. [Online]. Accessed: May 22, 2011Available: http://www.mpoweruk.com/high_temp.htm.

[119] E. Kodama and Y. Kurashima, "Development of a compact sodium sulphur battery," Power Engineering Journal, vol. 13, pp. 136-141, 1999.

[120] K. Mattern, A. Ellis, S. E. Williams, C. Edwards, A. Nourai and D. Porter, "Application of inverter-based systems for peak shaving and reactive power management," in Transmission and Distribution Conference and Exposition, 2008. T&D. IEEE/PES, 2008, pp. 1-4.

[121] Bo Yang, Y. Makarov, J. Desteese, V. Viswanathan, P. Nyeng, B. McManus and J. Pease, "On the use of energy storage technologies for regulation services in electric power systems with significant penetration of wind energy," in Electricity Market, 2008. EEM 2008. 5th International Conference on European, 2008, pp. 1-6.

[122] O. M. Toledo, D. Oliveira Filho and A. S. A. C. Diniz, "Distributed photovoltaic generation and energy storage systems: A review," Renewable and Sustainable Energy Reviews, vol. 14, pp. 506-511, 1, 2010.

[123] R. Hara, H. Kita, T. Tanabe, H. Sugihara, A. Kuwayama and S. Miwa, "Testing the technologies," Power and Energy Magazine, IEEE, vol. 7, pp. 77-85, 2009.

[124] Electropaedia. Zebra batteries. [Online]. Accessed: May 22, 2011Available: http://www.mpoweruk.com/zebra.htm.

[125] L. Gaillac, D. Skaggs and N. Pinsky, "Sodium nickel chloride battery performance in a stationary application," in Telecommunications Energy Conference, 2006. INTELEC'06. 28th Annual International, 2006, pp. 1-4.

[126] J. J. Smith, "International meeting on lithium batteries," Rome, Tech. Rep. 84, 1982.

[127] R. Yazami and P. Touzain, "A reversible graphite-lithium negative electrode for electrochemical generators," J. Power Sources, vol. 9, pp. 365-371, 1983.

[128] M. M. Thackeray, W. I. F. David, P. G. Bruce and J. B. Goodenough, "Lithium insertion into manganese spinels," Mater. Res. Bull., vol. 18, pp. 461-472, 1983.

[129] A. Manthiram and J. B. Goodenough, "Lithium insertion into Fe2 (SO4) 3 frameworks," J. Power Sources, vol. 26, pp. 403-408, 1989.

[130] G. A. Nazri and G. Pistoia, Lithium Batteries: Science and Technology. Springer Verlag, 2009.

[131] I. Bloom, S. A. Jones, V. S. Battaglia, G. L. Henriksen, J. P. Christophersen, R. B. Wright, C. D. Ho, J. R. Belt and C. G. Motloch, "Effect of cathode composition on capacity fade, impedance rise and power fade in high-power, lithium-ion cells," J. Power Sources, vol. 124, pp. 538-550, 11/24, 2003.

[132] J. Voelcker, "Lithium batteries take to the road," Spectrum, IEEE, vol. 44, pp. 26-31, 2007.

[133] I. Råde and B. A. Andersson, "Requirement for metals of electric vehicle batteries," J. Power Sources, vol. 93, pp. 55-71, 2/1, 2001.

[134] W. Tahil, "The trouble with lithium," Meridian International Research, 2007.

[135] M. Armand and J. M. Tarascon, "Building better batteries," Nature, vol. 451, pp. 652-657, 2008.

[136] A. Ostmeyer. Eaglepicher plans batteries to store wind-farm energy. [Online]. (Accessed: May 20, 2011), Available: http://www.joplinglobe.com/joplin_metro/local_story_133210903.html.

[137] A123. A123 systems. [Online]. (Accessed: May 20, 2011), Available: www.a123systems.com/applications/grid-stabilization.

[138] L. Joerissen, J. Garche, C. Fabjan and G. Tomazic, "Possible use of vanadium redox-flow batteries for energy storage in small grids and stand-alone photovoltaic systems," J. Power Sources, vol. 127, pp. 98-104, 2004.

[139] T. E. Lipman, R. Ramos and D. M. Kammen, "An assessment of battery and hydrogen energy storage systems integrated with wind energy resources in california," California Energy Commission, California, Tech. Rep. CEC-500-2005-136, 2005.

[140] G. Girishkumar, B. McCloskey, A. C. Luntz, S. Swanson and W. Wilcke, "Lithium-Air Battery: Promise and Challenges," The Journal of Physical Chemistry Letters, vol. 1, pp. 2193-2203, 07/15, 2010.

[141] B. Kumar, J. Kumar, R. Leese, J. P. Fellner, S. J. Rodrigues and K. Abraham, "A solid-state, rechargeable, long cycle life lithium–air battery," J. Electrochem. Soc., vol. 157, pp. A50, 2010.

[142] P. Van den Bossche, F. Vergels, J. Van Mierlo, J. Matheys and W. Van Autenboer, "SUBAT: An assessment of sustainable battery technology," J. Power Sources, vol. 162, pp. 913-919, 11/22, 2006.

[143] L. W. Jones, "Toward a liquid hydrogen fuel economy," University of Michigan, Tech. Rep. Engineering Technical Report UMR2320, 1970.

[144] Caisheng Wang, "Fuel cells and load transients," Power and Energy Magazine, IEEE, vol. 5, pp. 58-63, 2007.

[145] D. Heide, L. von Bremen, M. Greiner, C. Hoffmann, M. Speckmann and S. Bofinger, "Seasonal optimal mix of wind and solar power in a future, highly renewable Europe," Renewable Energy, vol. 35, pp. 2483-2489, 11, 2010.

[146] Rifkin Jeremy, La Economía Del Hidrógeno La Creación De La Red Energética Mundial y La Redistribución Del Poder En La Tierra. Paidós, .

[147] S. A. Sherif, F. Barbir and T. N. Veziroglu, "Wind energy and the hydrogen economy--review of the technology," Solar Energy, vol. 78, pp. 647-660, 2005.

[148] H. Tsuchiya and O. Kobayashi, "Mass production cost of PEM fuel cell by learning curve," Int J Hydrogen Energy, vol. 29, pp. 985-990, 2004.

[149] M. Aguado, E. Ayerbe, C. Azcárate, R. Blanco, R. Garde, F. Mallor and D. M. Rivas, "Economical assessment of a wind-hydrogen energy system using WindHyGen® software," Int J Hydrogen Energy, vol. 34, pp. 2845-2854, 2009.

[150] N. J. Schenk, H. C. Moll, J. Potting and R. M. J. Benders, "Wind energy, electricity, and hydrogen in the Netherlands," Energy, vol. 32, pp. 1960-1971, 2007.

[151] M. Korpaas and C. J. Greiner, "Opportunities for hydrogen production in connection with wind power in weak grids," Renewable Energy, vol. 33, pp. 1199-1208, 2008.

[152] A. Oudalov, T. Buehler and D. Chartouni, "Utility scale applications of energy storage," in Proc. IEEE ENERGY Conf. Atlanta, GA, 2008, pp. 18-25.

[153] R. Sioshansi and P. Denholm, "The Value of Concentrating Solar Power and Thermal Energy Storage," Sustainable Energy, IEEE Transactions on, vol. 1, pp. 173-183, 2010.

[154] L. Stoddard, J. Abiecunas and R. O'Connell, "Economic, energy, and environmental benefits of concentrating solar power in california," National Renewable Energy Laboratory, Sandia National Laboratories, 2006.

[155] Electricity Storage Association. [Online]. 2010). Available: http://electricitystorage.org.

[156] A. Zervos, C. Lins, T. Ackermann, E. Tröster, R. Short and S. Teske, "[R]enovables 24/7, la infraestructura necesaria para salvar el clima," Greenpeace International, European Renewable Energy Council (EREC), Madrid, Noviembre 2009. 2009.

[157] Electricity Storage Association. Lithium ion batteries technology. [Online]. 2010). Available: http://www.electricitystorage.org/site/technologies/li-ion_batteries/.

[158] A. Joseph and M. Shahidehpour, "Battery storage systems in electric power systems," in Power Engineering Society General Meeting. IEEE, 2006, pp. 8.

[159] I. Hadjipaschalis, A. Poullikkas and V. Efthimiou, "Overview of current and future energy storage technologies for electric power applications," Renewable and Sustainable Energy Reviews, vol. 13, pp. 1513-1522, 9, 2009.

[160] A. Virtanen and H. Tuusa, "Power compensator for high power fluctuating loads with a supercapacitor bank energy storage," in Power and Energy Conference, 2008. PECon 2008. IEEE 2nd International, 2008, pp. 977-982.

[161] Chong Han, A. Q. Huang, S. Bhattacharya, L. W. White, M. Ingram, S. Atcitty and W. Wong, "Design of an ultra-capacitor energy storage system (UESS) for power quality improvement of electric arc furnaces," in Industry Applications Society Annual Meeting, 2008. IAS '08. IEEE, 2008, pp. 1-6.

[162] Lin Cui, Dahu Li, Jinyu Wen, Zhenhua Jiang and Shijie Cheng, "Application of superconducting magnetic energy storage unit to damp power system low frequency oscillations," in Electric Utility Deregulation and Restructuring and Power Technologies, 2008. DRPT 2008. Third International Conference on, 2008, pp. 2251-2257.

[163] S. Samineni, B. K. Johnson, H. L. Hess and J. D. Law, "Modeling and analysis of a flywheel energy storage system for Voltage sag correction," Industry Applications, IEEE Transactions on, vol. 42, pp. 42-52, 2006.

[164] M. E. Glavin, P. K. W. Chan, S. Armstrong and W. G. Hurley, "A stand-alone photovoltaic supercapacitor battery hybrid energy storage system," in Power Electronics and Motion Control Conference, 2008. EPE-PEMC 2008. 13th, 2008, pp. 1688-1695.

[165] J. Cao, N. Schofield and A. Emadi, "Battery balancing methods: A comprehensive review," in Vehicle Power and Propulsion Conference, 2008. VPPC '08. IEEE, 2008, pp. 1-6.

[166] F. Giraud and Z. M. Salameh, "Steady-state performance of a grid-connected rooftop hybrid wind-photovoltaic power system with battery storage," IEEE Transactions on Energy Conversion, vol. 16, pp. 1-7, 2001.

[167] Y. Iijima, Y. Sakanaka, N. Kawakami, M. Fukuhara, K. Ogawa, M. Bando and T. Matsuda, "Development and field experiences of NAS battery inverter for power stabilization of a 51 MW wind farm," in Power Electronics Conference, IPEC, International, 2010, pp. 1837-1841.

[168] B. P. Roberts, "Sodium-sulfur (NaS) batteries for utility energy storage applications," in Power and Energy Society General Meeting - Conversion and Delivery of Electrical Energy in the 21st Century, 2008 IEEE, 2008, pp. 1-2.

[169] A. Nourai, B. P. Martin and D. R. Fitchett, "Testing the limits [electricity storage technologies]," Power and Energy Magazine, IEEE, vol. 3, pp. 40-46, 2005.

[170] D. K. Nichols and S. Eckroad, "Utility-scale application of sodium sulfur battery," in Proceedings of the IEEE International Stationary Battery Conference (Battcon'03), pp. 1–9.

[171] A. Y. Saber and G. K. Venayagamoorthy, "Optimization of vehicle-to-grid scheduling in constrained parking lots," in Power & Energy Society General Meeting, 2009. PES '09. IEEE, 2009, pp. 1-8.

[172] T. Tanabe, T. Sato, R. Tanikawa, I. Aoki, T. Funabashi and R. Yokoyama, "Generation scheduling for wind power generation by storage battery system and meteorological forecast," in Power and Energy Society General Meeting - Conversion and Delivery of Electrical Energy in the 21st Century, 2008 IEEE, 2008, pp. 1-7.

[173] S. W. Mohod and M. V. Aware, "Energy storage to stabilize the weak wind generating grid," in Power System Technology and IEEE Power India Conference, POWERCON. Joint International Conference on, 2008, pp. 1-5.

[174] Y. Riffonneau, S. Bacha, F. Barruel and S. Ploix, "Optimal power flow management for grid connected PV systems with batteries," Sustainable Energy, IEEE Transactions on, vol. PP, pp. 1-1, 2011.

[175] Yun Zhong, Jiancheng Zhang, Gengyin Li and Xindi Yuan, "Mathematical model of new bi-directional DC-AC-DC converter for supercapacitor energy storage system in photovoltaic generation," in Electric Utility Deregulation and Restructuring and Power Technologies, 2008. DRPT 2008. Third International Conference on, 2008, pp. 2686-2690.

[176] D. J. Swider, "Compressed Air Energy Storage in an Electricity System With Significant Wind Power Generation," IEEE Transactions on Energy Conversion, vol. 22, pp. 95-102, 2007.

[177] C. Abbey and G. Joos, "Supercapacitor Energy Storage for Wind Energy Applications," IEEE Transactions on Industry Applications, vol. 43, pp. 769-776, 2007.

[178] A. Arulampalam, M. Barnes, N. Jenkins and J. B. Ekanayake, "Power quality and stability improvement of a wind farm using STATCOM supported with hybrid battery energy storage," IEE Proceedings - Generation, Transmission and Distribution, vol. 153, pp. 701-710, 2006.

[179] J. S. Anagnostopoulos and D. E. Papantonis, "Pumping station design for a pumped-storage wind-hydro power plant," Energy Conversion and Management, vol. 48, pp. 3009-3017, 11, 2007.

[180] E. D. Castronuovo and J. A. P. Lopes, "On the optimization of the daily operation of a wind-hydro power plant," IEEE Transactions on Power Systems, vol. 19, pp. 1599-1606, 2004.

[181] S. Faias, P. Santos, F. Matos, J. Sousa and R. Castro, "Evaluation of energy storage devices for renewable energies integration: Application to a portuguese wind farm," in Electricity Market, 2008. EEM 2008. 5th International Conference on European, 2008, pp. 1-7.

[182] Intertek, "The future of battery technologies – part II: Focus on lithium-ion batteries," Intertek Group plc, 2009.

[183] B. Kennedy, D. Patterson and S. Camilleri, "Use of lithium-ion batteries in electric vehicles," J. Power Sources, vol. 90, pp. 156-162, 10/1, 2000.

[184] M. Broussely, J. P. Planchat, G. Rigobert, D. Virey and G. Sarre, "Lithium-ion batteries for electric vehicles: performances of 100 Ah cells," J. Power Sources, vol. 68, pp. 8-12, 9, 1997.

Control strategies for PV power plants with energy storage

A fter introducing the solar resource nature and the different energy storage (ES) technologies available on the markets, as well as their possible applications, in previous chapters, it is now time to relate them to the distributed generation (DG), and more precisely to the solar generation industry. It has been noted that, thanks to the increasing financial stimulus experienced by renewable energies across the planet during the last decade, photovoltaic (PV) systems have emerged as an important power source. Nowadays, solar power is a rapidly growing and very promising renewable source of electric energy [1]. This expected evolution will face the problem of large PV power penetration into the Electrical Power System (EPS) due to the stochastic nature of the solar resource, as it was introduced along Chapters I and II in this Thesis dissertation. In fact, this is an issue for most of the renewable energy sources (RES) which usually present intermittent production. For PV, and other intermittent RES (highlighting wind power), a more controllable and non-fluctuating production should be assured in order to increase its participation of the power production mix. In this sense, it has been also introduced that some ES systems (ESS) will have to be integrated and combined with RES [2-4]. It should be noted that, given its power levels, economical importance and level of penetration, the research and development on different ES technologies integration into wind power plants are already on the way [5-11].

As regards to the PV domain, some studies have already been performed combining PV with other distributed generation (DG) technologies and integrating some kind of ES [12-18]

but, these proposals are mainly focused on microgrids or small stand-alone networks where supply for local loads is to be guaranteed and network balance wants to be assured [19-24]. However, not much research has been executed on large combined PV+ES power plants pursuing to modify the pattern of the power injected into the EPS as well as the plant operational capabilities, which could convert it into a virtual plant offering even some ancillary services to the EPS. Examples of these applications can be also found, e.g. a grid-connected PV generator was combined with a fuel cell in [25], a SMES in [26] or a battery bank in [27, 28] to effectively level its output, or even some applications using UCs to smooth the output [29].

One of the main goals in this Thesis was set to determine the improvement in the power production quality, in terms of controllability and predictability, which can be obtained by incorporating some ES unit into the PV grid-tied power plants. As presented in Chapter I, ES technologies present many interesting applications when combined with RES which generally depend upon the ES system characteristics and upon the control strategy implemented.

Thereupon, this chapter is devoted to the introduction and analysis of some possible energy management strategies (EMS) to be implemented in PV power plants with ES. Each of the strategies pursues a different goal in terms of improved operability of the PV power plant. For doing so, the power plant model proposed for the analysis which combines PV with energy storage is first introduced. Then, the different EMS which can be used to control such a plant are presented. Following the various EMS, some complementary control options which could be superimposed over any of the main EMS are also highlighted. Finally, some simulation results derived from the application of these EMS to the PV power plant with ES are set out. The simulation results presented in this chapter are focused mainly on PV production cumulative probability distribution and on the PV production frequency spectrum modifications when introducing the ES unit.

4.1. Introduction to the PV+ES power plant model.

According to the introduction to this chapter, some ES system will have to be integrated within future PV power plants to reduce their power production variability and provide them with extended operation capabilities. This will be a key issue in the coming future for a further deployment of PV installations and to pave the way to an increased degree of penetration for solar installations. However, the stochastic nature of the solar radiation

concerns all kind of PV technologies (even those solar installations not based on the PV effect) and this fact, together with the still uncertain commercial trends for ES technologies associated to renewables (although some candidates are already starting to stand out thanks to the impulse from the electric vehicle industry and some prototypes in wind power plants), is the reason why a generic PV power plant with ES (PV+ES) is analyzed in this Thesis. The proposed PV power plant can be observed in Figure 4.1. It represents a grid connected PV power plant which contains a variable number of multi-string PV inverters, typically ac-dc converters commercial models, and an ES system. All of these components are radially distributed and connected in parallel to the plant point of common coupling (PCC).
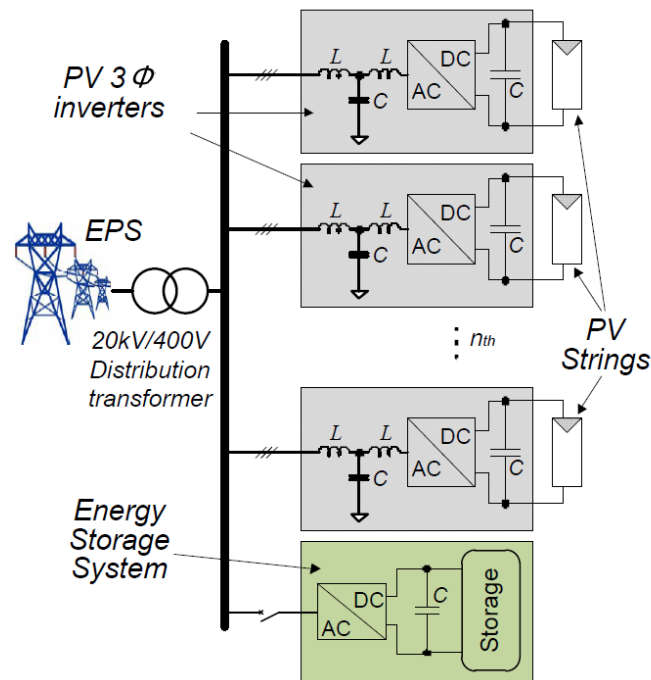
Figure 4.1 Schema of the PV+ES power plant topology.

Therefore, the overall production of this kind of PV+ES power plant will be that combining the instantaneous PV power generated by the panels (thanks to the incident solar radiation) plus the power balance exchanged by the ES unit with the rest of the system at the PCC. So, the operation of the ES system as an energy buffer which, by being charged and discharged continuously according with a controlled EMS, will complement the PV instantaneous production. Hence, a defined power value at the PCC can be assured with a certain degree of confidence, far away from the already cited solar radiation highly stochastic

behavior. A more predictable and controllable production is achieved in this way thanks to the ES unit, a possibility not available nowadays in standard PV plants. In addition, some other ES applications, among those summarized in Chapter I, can be adopted (integrated within the EMS control) to optimize the economic income of the ES unit.

Regarding the storage unit which can be appreciated at the bottom of the Figure 4.1 this can be identified to any of the different technologies presented in Chapter III. In this sense, as previously mentioned, a generic ESS has been normally considered for the different analysis performed in this Thesis, i.e. no specific technology has been modeled or introduced in the annual energy analysis software developed in this work. In this sense, only those parameters corresponding to the ES unit which influence on the PV+ES power plant behavior are taken into account during the simulations. Those parameters are: charging and discharging efficiencies (round trip efficiency), power exchange limitations (related and according to the hypothetical ES unit connection converter rated power), energy capacity, initial and reference state-of-charge (SOC) values and, finally, reference SOC recovery time (τ_{SOC}). Apart from the charging and discharging efficiencies, which have been normally fixed to 90%, the rest of parameters have been changed along the different sets of simulations adapting their values to the different analysis and situations encountered. In fact, in some cases the goal of the analysis has been just to define an optimal value for some of them (mainly the energy capacity), hence they could not be initially established and had to be variable to allow the analysis.

However, for some of the specific analysis presented along the Chapter V a certain ES technology has been adopted. More precisely, among the different technological options presented in Chapter III, Lithium Ion batteries (Li-ion) and ultracapacitors (UC) have been used. The first have been simulated in order to proceed with an ageing analysis when operating this type of batteries within such a power plant. On the contrary, UC have been modeled for simulation analysis too, but also to obtain certain experimental results.

Finally, note that the irradiation data sets used along the different simulations and tests correspond to those already introduced in the last section of Chapter II. As there mentioned, these comprehend standard irradiation profiles, downloaded from the PVGIS database [30, 31], and actual irradiation values measured in situ in the Spanish southern location where the various analysis have been concentrated. Both sets of data were adapted to the PV power plant rated power in order to get a coherent production, although all the analysis was finally performed in the per unit system with the target of generalizing the results.

4.2. Energy management strategies.

The fact of introducing ES capacity on a PV power plant provides it with extended functionalities, as it was introduced in Chapter I. However, among all of the different possibilities, only the PV+ES power plant operation improvement related to the capability to control the plant power production has been analyzed in this Thesis. This capability implies to be able to modify the time when the power is exchanged with the EPS as well as the amount of power itself at any moment regardless of the PV instantaneous production, improving in this way the predictability of the PV+ES plant production.

This dispatchable production is achieved by defining a power reference, which can respond to different EMS, to be injected by the PV+ES plant into the grid at every moment. This power reference is then accomplished by a combination of the PV instantaneous production and the power exchanged by the ESS, as can be appreciated in Figure 4.2. The basic equation which drives the operation of the power plant production is (4.1).

$$P_{ref} = \left(P_{pv} + P_{ES}\right) \tag{4.1}$$

Where P_{ref} is the power reference, P_{pv} the instantaneous power provided by the PV panels (depending mainly on time, location and weather) and P_{ES} the current power delivered by the ES, the one to be controlled. This is, in turns:

$$\text{Discharge:} \qquad P_{ES} > 0 \rightarrow dE_{ES}\big/dt = -P_{ES}\big/\varepsilon_d \tag{4.2}$$

$$\text{Charge:} \qquad P_{ES} < 0 \rightarrow dE_{ES}\big/dt = -P_{ES} \cdot \varepsilon_c \tag{4.3}$$

Where E_{ES} is the stored energy (available energy), ε_c the charging efficiency and ε_d the discharging efficiency. The E_{ES} can be permanently accounted by means of the state-of-charge (SOC) of the ESS control.

In this manner, the ES power (P_{ES}) is the one controlled in order to complement the instantaneous PV production, according to the defined power reference and improving in this way the production predictability. This reference tracking is done taking into account the ESS energy and power limitations. Therefore, the extended operation functionalities that a PV power plant with ES can offer to the System Operator (SO) depend on both its power and energy ratings and on the EMS implemented on the plant.
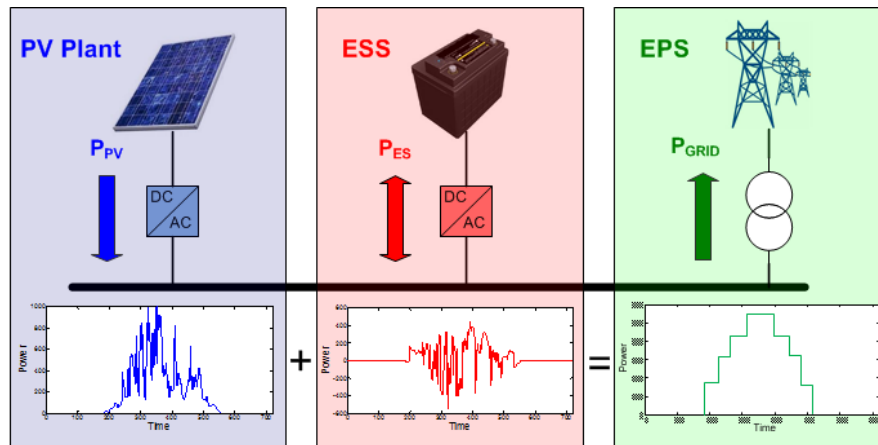
Figure 4.2 Functioning principle of the PV+ES power plant under an EMS.

In this Thesis, different EMS which provide the corresponding power references to the PV+ES power plant are presented and analyzed. These strategies have been implemented and tested by simulation using Matlab/Simulink® in order to study their corresponding power and energy requirements. The various strategies proposed, together with some complementary controls which can be equally implemented in the system, are introduced in the following.

4.2.1. Constant power steps control strategy.

This first EMS is basically centered on setting constant power references for the PV power plant during certain periods of time. It was already introduced in Chapter I as one of the mid-term renewables' energy management strategies (Renewables Availability & Predictability Improvement). The main target of this strategy stands out to be converting the PV power plant into a more stable and more predictable power generator (dispatchability) which could be better traded in electricity markets similarly to conventional generators [32].

Different works or proposals have already been published using a constant power step type control strategy for PV plants with some kind of ES integrated [26-28, 33-35]. However, none has addressed the problem of sizing the ESS so that the PV+ES plant can track the power reference without saturations for a certain period of time. This is one of the final goals pursued in this PhD Thesis.

The block diagram which represents the control structure of the PV+ES power plant when the constant power steps EMS is implemented can be observed in Figure 4.3. The power references for the plant are generated with the "constant power steps" block, which

usually receives the real sky irradiation conditions reference PV production dataset provided by PVGIS as input. However, the clear sky conditions production dataset can also be used as will be described for some of the different proposals presented in this chapter. Note that, as it was defined in Chapter II, clear sky corresponds to ideal sky conditions with no clouds at all, while real sky conditions take into account statistically determined periods of time with clouds combined with clear periods along each month to determine the average.
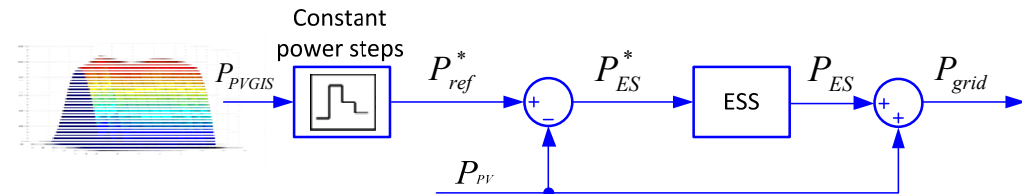
Figure 4.3 Constant power steps EMS block diagram.

The constant power step EMS seems initially more appropriate for clear days when the total irradiance can be easily forecasted and, in this way, the power plant constant output power which can be accomplished straight calculated. However, for some of the yearly analysis whose results are introduced in Chapter V, this EMS has been applied in both clear and cloudy days. In fact, some of the complementary control options presented later in this chapter can enable an acceptable operation also during cloudy days, what is also analyzed in Chapter V.

Different procedures can be considered when defining the constant power references. In a general way, one first procedure is to calculate the constant reference values in such a manner that the energy produced by the PV+ES power plant is the same that would be produced by the PV panels alone taking into account the losses of the system (charge and discharge, self-discharge of the ES system…). The goal of that procedure is to keep the SOC value when finishing each day as close as possible to the initial SOC for that day although economic reasons could suggest a different operation or control of the daily final SOC. A second proposal is to adapt the value of the constant power step reference to that power value which optimizes the efficiency of the PV grid-tie inverter, according to [36]. This second procedure searches to reduce system losses although it has not been analyzed in this Thesis. Other procedures do pretend to maximize the daily power injected by the PV+ES power plant or minimize the deviation of the SOC with regard to a reference value. These are quite more complex procedures which have been also analyzed and are further described below.

It is important to note that the constant power steps reference defined to be tracked by PV+ES power plants will be probably traded on power markets and communicated, or negotiated, in advance with the system operator in future scenarios. This production forecast will have to be done the day before or, in case of trading on the intraday electricity markets, with some hours in advance. Deviations in the final production with regard to the power compromised will involve economic penalties [37]. Therefore, a good accuracy in the energy yield estimates will be required, what will be harder to achieve during cloudy days.

In this sense, although constant annual references have been considered in some of the ESS requirement analysis performed in this Thesis, the duration, the number and the value of the constant power steps can be modified every day along the year, adapting them relatively frequently (every day, every hour…). Therefore, different parameters which define and modify the expected PV energy yield can be considered. Some of the most important are:

- The initially expected average irradiation estimated for each month, which can be obtained from solar databases in order to optimize the yearly overall production.

- The weather forecast, which obtained from meteorological agencies, can help estimating the daily expected irradiation with some hours or days in advance.

- The evolution of PV solar energy produced along the day, which can be measured in situ and can provide valuable information to estimate the production in the coming hours and correct the constant energy yield compromise for that day.

The assumption of one or various among these considerations can lead to different variants of the same EMS, as will be explained along this chapter. As a result, one single constant step or multiple different-level constant steps (in both cases while optimizing or just balancing the SOC at the final of the day) can be introduced as constant power references along the day in order to adapt the reference to the estimated PV production. Therefore, among these different options, several have been used in the different analysis performed in this Thesis. They will be identified when describing each of the corresponding analysis.

An example of the first procedure balancing PV production with reference production has been introduced in Figure 4.4. Five different power curves have been represented on it. The initial PV instantaneous power production along a sunny summer day has been represented in blue. The energy produced by the PV power plant along that day can be redistributed into different constant power step references. A four-level constant steps reference has been

represented in red, while three different one single constant step references, lasting respectively 6, 10 and 14 hours, have been represented in different grey scales.
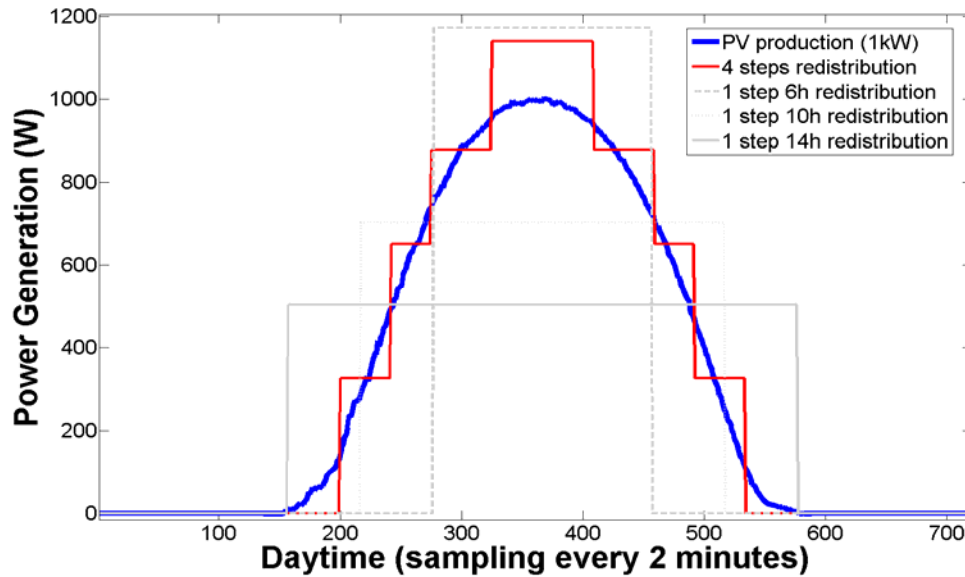
Figure 4.4 Constant power step strategy possibilities in a sunny day.

A more detailed description on the different constant power EMS variants that can be considered and whose ESS requirements have been analyzed in this Thesis is here introduced.

a) One single constant step

For the case of the one single constant step strategy, only one different level of power is required to the PV+ES plant each day, i.e. the power plant will inject no power till a certain moment when the step reference is activated, injecting from then on a constant power value for a certain period of time.

In a general way, the starting time and the duration of the step (which define in this way the stop time) can vary. As regard to the starting time, it will be normally defined such that, taking into consideration the step duration, the step will be centered with regard to the Sun maximum radiation hour which, considering solar time, is always achieved at around noon. Hence, the local starting time (clock time) has to be properly calculated considering the time differences between local and solar times along the year. To use a starting time, different from that calculated in this way, would signify a PV production shifting which corresponds

to another EMS also introduced in Chapter I as a mid-term strategy. However, this production shifting is more energy demanding and is beyond the scope of the analysis performed in this PhD Thesis.

Regarding the step durations, they are straight related to the step power levels since both parameters define the energy provided by the plant. Different strategies assimilating the energy provided by the single step reference to that energy which would be provided by the panels in a PVGIS real sky standard day or to that energy forecasted as real for the day have been analyzed.

An example of daily energy redistribution with different one single constant step references can be appreciated in Figure 4.5. All the steps in that figure will inject the same energy to the EPS that will be provided by the PV panels (blue continuous line). That is, their steps power values have been calculated so as to provide the same energy that the PV panels would produce during that clear day, accomplishing in this way the first of the possible operation goals previously introduced: keeping the SOC at the final of the days as close as possible to that of the dawn.
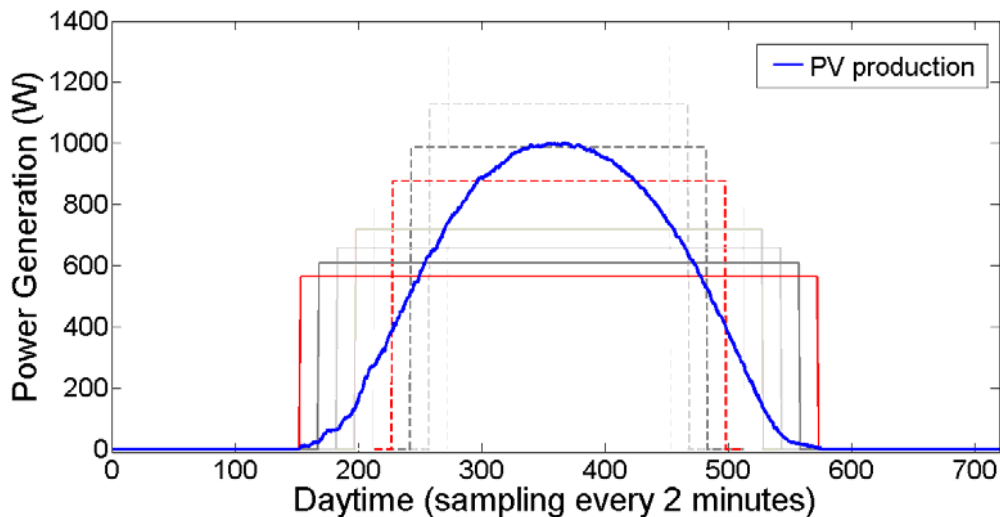
Figure 4.5 Different constant power step possibilities.

Therefore, a first analysis of the ESS power and energy rating needs to operate the PV+ES power plant tracking each of the references represented in Figure 4.5 and with different degrees of confidence (percentage of time along the year when the ESS would saturate) has been performed. Results to this analysis are presented in Chapter V.

In order to do those analyses, constant power single step references, for each of the step lengths considered (2, 4, 5, 6, 7, 8, 9, 10, 11, 12, 13, 14, 16 and 18 hours), have been developed along the whole year (one step per day). These annual references have been divided by months, i.e. 12 different step power values have been defined along the year. This can be clearly observed in Figure 4.6 where the whole annual reference for the case of an eight-hours-length constant power daily single step reference is represented.

Zoom of the transition from
November to December
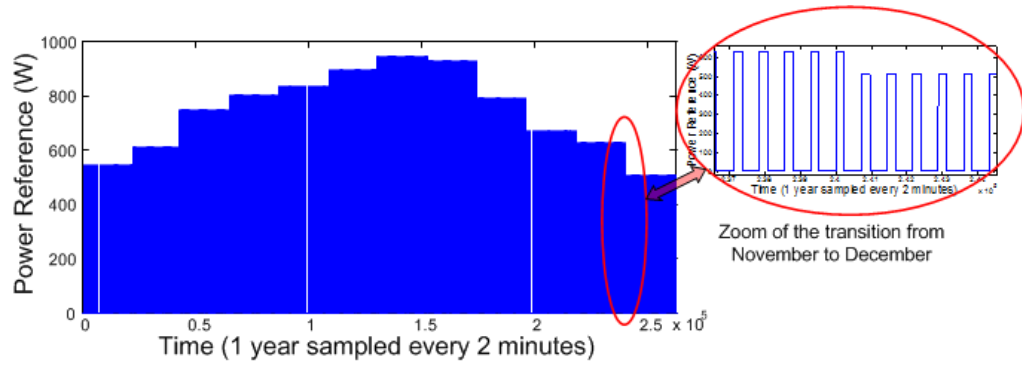
Figure 4.6 Annual constant power step references.

As for the case presented in Figure 4.5, the daily single step power values assigned here to each of the monthly periods corresponds to the level of power which would provide the same energy as the daily average energy production estimated by PVGIS for a generic PV power plant along that month under real sky conditions and for the location under study, correspondence which can be observed in Figure 4.7. Though, these are now overlapped in Figure 4.7 to the 12 different daily equivalent constant steps applied along the year which generate by concatenation the overall reference represented in Figure 4.6.

Hence, the power value of the steps is obtained by dividing the expected daily energy production among the number of hours the single step reference is desired to last every day:

$$Step\_power\_value(month) = \frac{Daily\_energy\_yield(month)}{number\_of\_hours\_step}, \text{in (kW/kW}_{peak}) \qquad \textbf{(4.4)}$$

The estimated PV production values, or daily energy yield, were already presented in Chapter II where the corresponding standard solar radiation curves under these real sky conditions for the location under study on a surface tilted 34º (optimal inclination) were introduced, Figure 2.12. In fact, an energy comparison and identification between the power profile evolution along the 12 months in the Figure 4.6 or Figure 4.7 and the power standard irradiation profiles in Figure 2.12 can be easily performed. Now, the average daily irradiance

values for each month, derived from those irradiation curves represented in Figure 2.12 are introduced in Table 4.1.
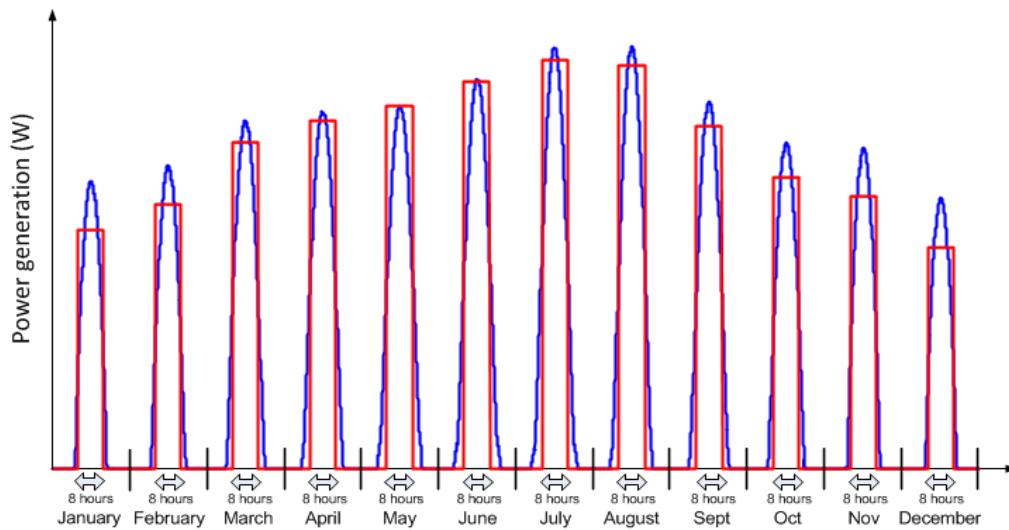
Figure 4.7 Monthly-energy adapted daily constant power step references.

From the real sky (RS) irradiance values in Table 4.1, an average daily irradiance along the year of 5.97 kWh/m^2 is derived. This value, combined with a general approximation of the PV system losses equal to 26.4% (also according to PVGIS for a crystalline silicon installation where losses corresponding to cables, inverter, temperature, reflectance, etc. are considered) generates an annually averaged daily energy yield of 4.38 kWh/kW$_{peak}$. Note that this value is in accordance with the typical PV plant capacity factor (C_f) assumed to be 4.3 for the south of Spain. Similarly, a PV daily production value averaged for each month can be calculated. These monthly-averaged daily energy yields will be those introduced in equation (**4**.4) in order to obtain the corresponding monthly step power values, which can be appreciated in Figure 4.7.

Month	Jan.	Feb.	Mar.	Apr.	May	Jun.	Jul.	Aug.	Sept.	Oct.	Nov.	Dec.
RS	4397	4882	6022	6421	6706	7162	7560	7452	6344	5376	5040	4092
CS	6284	7049	8039	8128	7970	7855	7891	8017	7787	7313	6731	6087

Table 4.1 Monthly-averaged daily irradiance values, in Wh/m^2, for real sky (RS) and clear sky (CS) conditions in the south of Spain.

Therefore, this is the way how these constant step references were defined to be used for one of the main analysis performed in this Thesis. The goal of this analysis was to provide a range of magnitude of the ESS needs and operability possibilities to PV plant designers and

operators which could pretend to operate their PV power plant under a constant power steps strategy. The analysis is therefore performed "a priori" since the real PV energy yield along the year cannot be accurately forecasted.

However, another more complex study of the ESS ratings needed under a single step constant power strategy when the real PV production forecast is very accurate has been also performed. High production forecast accuracy allows defining a constant power step value adapted to the daily real PV energy yield, keeping more or less constant the length of the daily step but not its power value, as can be clearly appreciated in Figure 4.8. A daily one single constant step reference lasting seven hours per day has been introduced in that figure, injecting with that power profile so much energy as the PV panels would produce that day. By doing this, a lower energy capacity than that estimated for the previous analysis is required in this case to track the reference since the real daily PV production rarely coincides with its corresponding month's average production, which has been only statistically estimated.
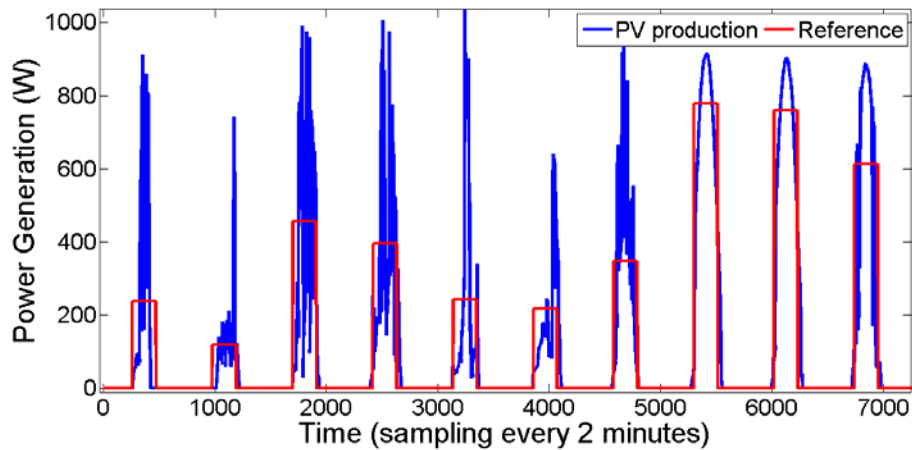
Figure 4.8 Daily real energy adapted constant power single steps reference.

That assumption, considering that the real PV production along the month would not largely differ from the statistically estimated one, is what was expected in those analyses introduced previously. That fact may not be realistic for some very wet or very dry years although it can be accepted for a general sizing which pretends to be some kind of ESS sizing reference. Anyway, the goal of this last and advanced study presented here is to try to determine an optimal size ESS to be installed in a PV power plant minimizing its energy requirements. This minimization can be obtained by means of an accurate weather forecast

combined with an on-line surveillance of the power generated along the day and an analysis of the expected production trend. This can be achieved with the complementary controls presented later in this chapter and, as for the rest of analyses previously introduced, results for this latter case are also presented in Chapter V.

b) Multiple constant steps

Another constant power EMS option has been developed and simulated. It implements different steps with varying levels of power adapted to the evolution of the estimated radiation along the day. The outlook of one of this multiple constant step references can be observed in Figure 4.4 where a four-level constant step power reference was represented in red.

The case of the multiple constant steps strategy presents the clear advantage, with regard to the previous constant power single step strategy, of reducing the capacity of the ES needed to assure the power production commitment. This can be understood from the fact that the permanent difference in the instantaneous value between the PV production curve and the reference curve in Figure 4.4 is smaller. Hence, the areas between both curves, which represent the amount of energy that the ESS must store to accomplish a proper operation, are then much smaller for this case than for the single constant step strategy.

Furthermore, although these constant-level multiple-step references do reduce the constancy of the final PV power plant output (the production is going to vary along the day following the different power steps), the predictability of the generated power is not affected since it will still track a previously defined reference.

Therefore, as explained in the previous section for the single constant step case, a set of 12 reference days, adapted to the monthly-averaged estimated daily PV production, were developed. The operation goal when defining the references was again to keep the SOC at the final of the day as close as possible to that of the dawn. The starting and stop times were also conceived so as to be symmetrical with regard to the Sun's zenith time. Finally, the value of the different steps (also symmetrical in time) was calculated to accomplish with the mentioned daily energy production requirements.

Among the various possibilities of multiple-step combinations, only the four-level possibility was considered. That reference establishes four different levels of constant power to be tracked by the plant along the day. The 12 monthly-adapted daily constant-power multiple-step profiles obtained in this case are represented in Figure 4.9. This figure presents

the evolution of the 12 monthly profiles along the daytime as function of the month in which the plant is operating. This representation emulates that of the standard irradiation profiles represented in Figure 2.12 for CS and RS conditions.

From these 12 profiles, an annual reference has been constructed, concatenating daily profiles for each day of the year, to proceed with the evaluation of the PV+ES energy needs against the real radiation along the year 2009. This annual reference has not been introduced in any figure since its global outlook is very similar to that or the single step references represented in Figure 4.6.
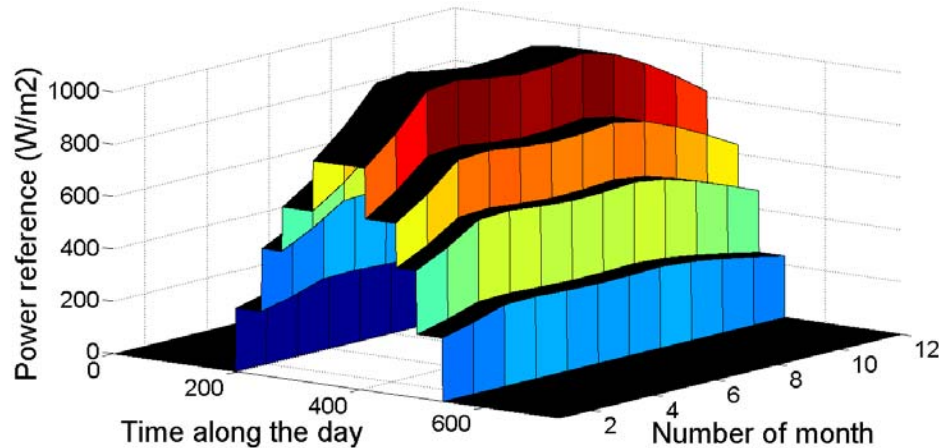
Figure 4.9 Constant power step strategy possibilities in a sunny day.

c) Hourly-adapted constant steps

This third strategy could be considered the extreme case of the previous one since it produces one different step value every hour along the day. The main goal of this strategy would be to allow the PV plant to operate in a very flexible way along the whole day while reducing even more the ESS' needs. Note that the reference and the initial PV real production are even closer at any moment in this strategy than in any other before.

The fact of being able to vary the production every hour along the day would qualify the PV+ES power plants to participate in the daily and intraday electricity markets which, as introduced in Chapter I, require one hour length constant power commitments to the different generators. Examples of two different hour-by-hour defined references can be observed in Figure 4.10 and Figure 4.11, corresponding to the optimal 24h constant steps power production for a sunny and a cloudy day respectively.
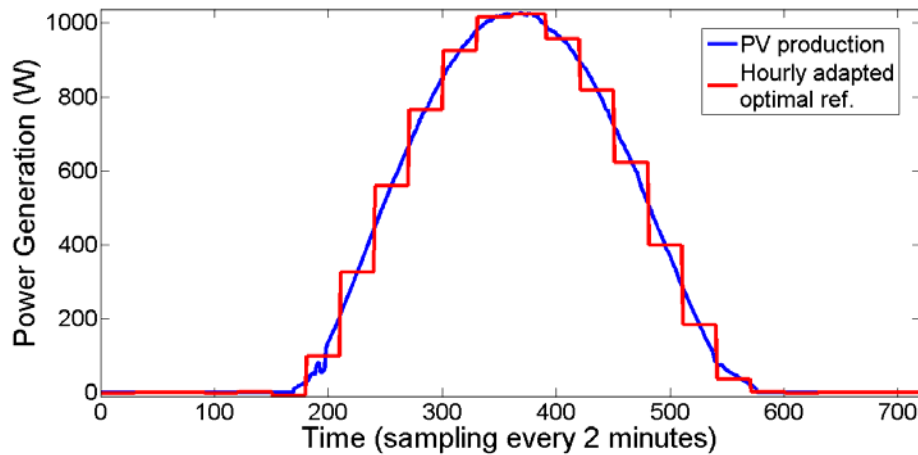
Figure 4.10 An hourly-adapted constant steps reference in a sunny day.

Normally, the initial daily 24 hours reference is calculated the day before. Since real instantaneous irradiation cannot be known in advance, the weather forecast is taken into account again and the clear sky irradiation profile, provided by PVGIS for those days (depending on the month), is used as the most representative averaged information source. An optimization of the power production steps is then performed in order to minimize the ESS' needs to be able to supply that reference subjected to certain restrictions (one hour length steps as minimum for the case of Spain). This action yields to an ideal daily reference with quite a regular form, as that in Figure 4.10, which the system would properly reproduce under clear day conditions but, on the contrary, would easily induce ESS saturations during overcast days. This is due to the fact that, since ESS' ratings to ideally cope with this strategy are smaller, any unexpected deviation (more or less clouds than expected) will saturate the system very quickly by overcharging or completely discharging the ESS.

However, the existence of 6 different intraday electricity markets paves the way to these PV+ES certainly dispatchable power plants to offer power commitments organized by hours in the diary electricity market. In case of need due to weather forecast errors, which would conduct to an energy yield deviation, these could be corrected successively in the different intraday electricity markets as the day goes on in order to avoid penalties. This target would be achieved with some advanced control techniques which have been considered in this Thesis too and which are introduced later in the complementary control actions section (4.3.3, 4.3.4 and 4.3.5).
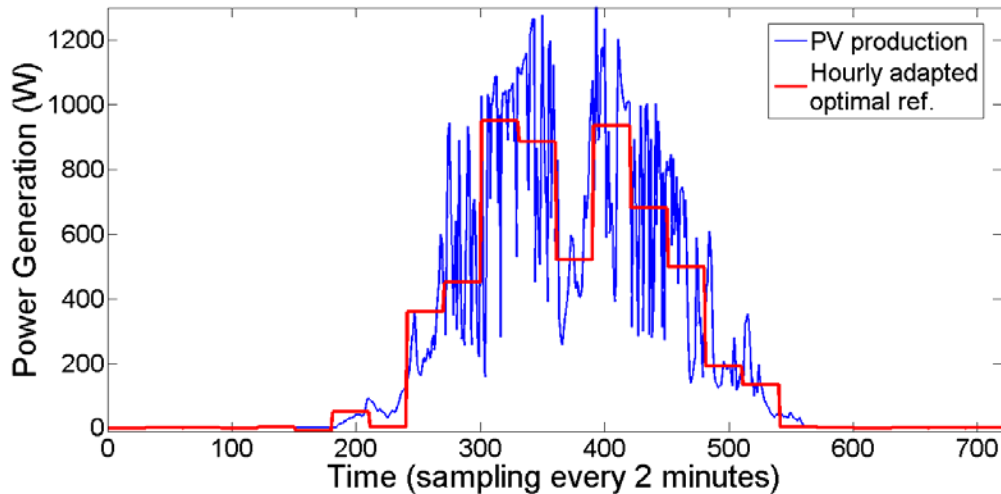
Figure 4.11 An hourly-adapted constant steps reference in a cloudy day.

4.2.2. Fluctuations reduction control strategy.

A second control strategy philosophy has been developed and simulated. This EMS has been called fluctuations reduction or smoothening control strategy. This type of EMS was also introduced within the ESS applications related to renewables in Chapter I, as it was the previous EMS. There, it was classified as one of the possible short-term renewables' energy management strategies, which comprehended: production leveling, smoothening and regulation.

Different works or proposals have already been published using this type of control strategy for PV plants integrating some kind of ES [22, 29, 38, 39]. However, as for the previous strategy, none has addressed the problem of quantifying the ESS' energy and power requirements to allow the PV+ES plant tracking the power reference without saturations during a certain period of time. This is, again, one of the final goals of the analyses performed in this PhD Thesis.

The block diagram for this EMS can be observed in Figure 4.12. As can be appreciated on it, contrary to the constant power steps control strategy, this EMS is not based on fixing a constant power value to be tracked by the PV+ES power plant but just on filtering the frequent power variations which are usually registered in the PV production caused by the instantaneous solar irradiation variations, mostly experienced during cloudy days. Therefore, the fluctuations reduction control strategy flattens the power delivered by the PV power plant

to the EPS by using the ESS capacity as a real energy filter or energy buffer. In this sense, this strategy tends to decouple the power injected by the power plant to the EPS from the solar energy received on the PV panels. Therefore, while the previous strategy would ideally work better under sunny conditions, when the energy yield can be easily forecasted, this strategy will scarcely modify the PV production on clear days being much more effective on cloudy ones when PV production fluctuates significantly.
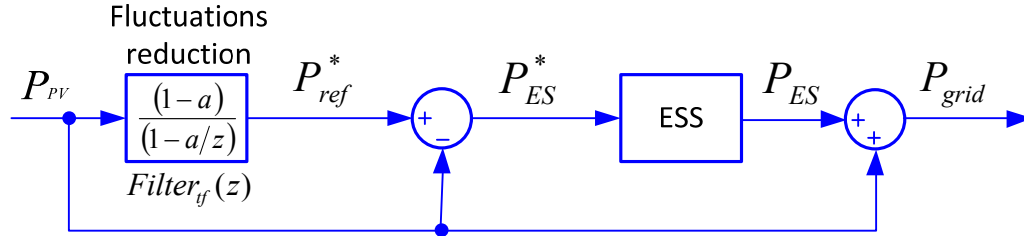
Figure 4.12 Fluctuations reduction EMS block diagram.

According to Figure 4.12, the input to the control block for this EMS is not anymore a standard radiation dataset (P_{PVGIS}) but the instantaneous real PV production (P_{pv}) which is fed to a low-pass first-order standard discrete filter, equation (4.5), which generates the smoothed reference (P_{ref}).

$$Filter_{tf}(z) = \frac{(1-a)}{(1-a/z)} \tag{4.5}$$

Being the cutting frequency of this discrete filter calculated as:

$$\omega_c = \frac{1}{\tau} = -\frac{\log(a)}{T} \tag{4.6}$$

Where ω_c is the cutting frequency, τ is the filter's time constant and T the sampling period of the input signal (T=120s along all the simulations performed in this Thesis).

The resulting references produced by the filter when a cloudy day radiation curve is introduced can be observed in Figure 4.13 for different levels of filtering.

These levels are defined by the filter parameter "a", which is straightly related to the filtering time constant by means of the equation (4.6). The equivalence among their values can be extracted from Table 4.2 which has been calculated for a T=120s.
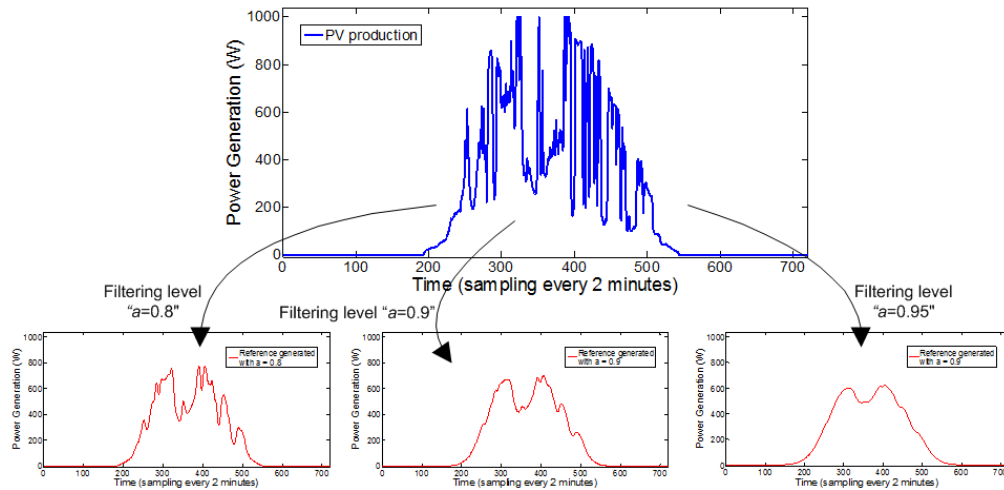
Figure 4.13 PV production versus PV+ES reference defined by the control system.

In the case the ESS is already installed in the power plant, the filtering level could be adapted by choosing the time constant according to the power and energy characteristics of the available ES, optimizing to them the smoothening of the input signal which could be performed by the PV+ES power plant. In this sense, high frequency (very short term variations) power components can be filtered with low energy capacities while low frequency power components are related to high energy requirements and, therefore, a high ES energy capacity is needed to compensate them and obtain a predominantly flat curve.

Filter parameter value	Filter time constant
a = 0.7	$\tau \approx 5.5$ minutes
a = 0.8	$\tau \approx 9$ minutes
a = 0.85	$\tau \approx 12.3$ minutes
a = 0.9	$\tau \approx 19$ minutes
a = 0.95	$\tau \approx 39$ minutes
a = 0.97	$\tau \approx 66$ minutes
a = 0.99	$\tau \approx 199$ minutes
a = 0.995	$\tau \approx 399$ minutes

Table 4.2 Production variability evolution as filtering level is incremented.

As an example, a simulation using three days with high presence of clouds is presented in Figure 4.14. Two different sets of curves are represented on it. On one hand, Figure 4.14a) presents the power waveforms corresponding to the power generated by a 1kW PV power plant (once again in blue) overlapping to it the three resulting power curves which could inject into the EPS a PV+ES power plant operating under the fluctuations reduction EMS. Three different levels of filtering ("*a*" equal to 0.95, 0.99 and 0.995, respectively) have been

represented. On the other hand, Figure 4.14b) compiles the corresponding evolution of the ESS instantaneous energy reserve availability along the same three days taken considering the three filtering levels. Note the different energy evolutions as "*a*" is incremented. An identical 10kWh ESS has been considered in the three cases.

a)

b)
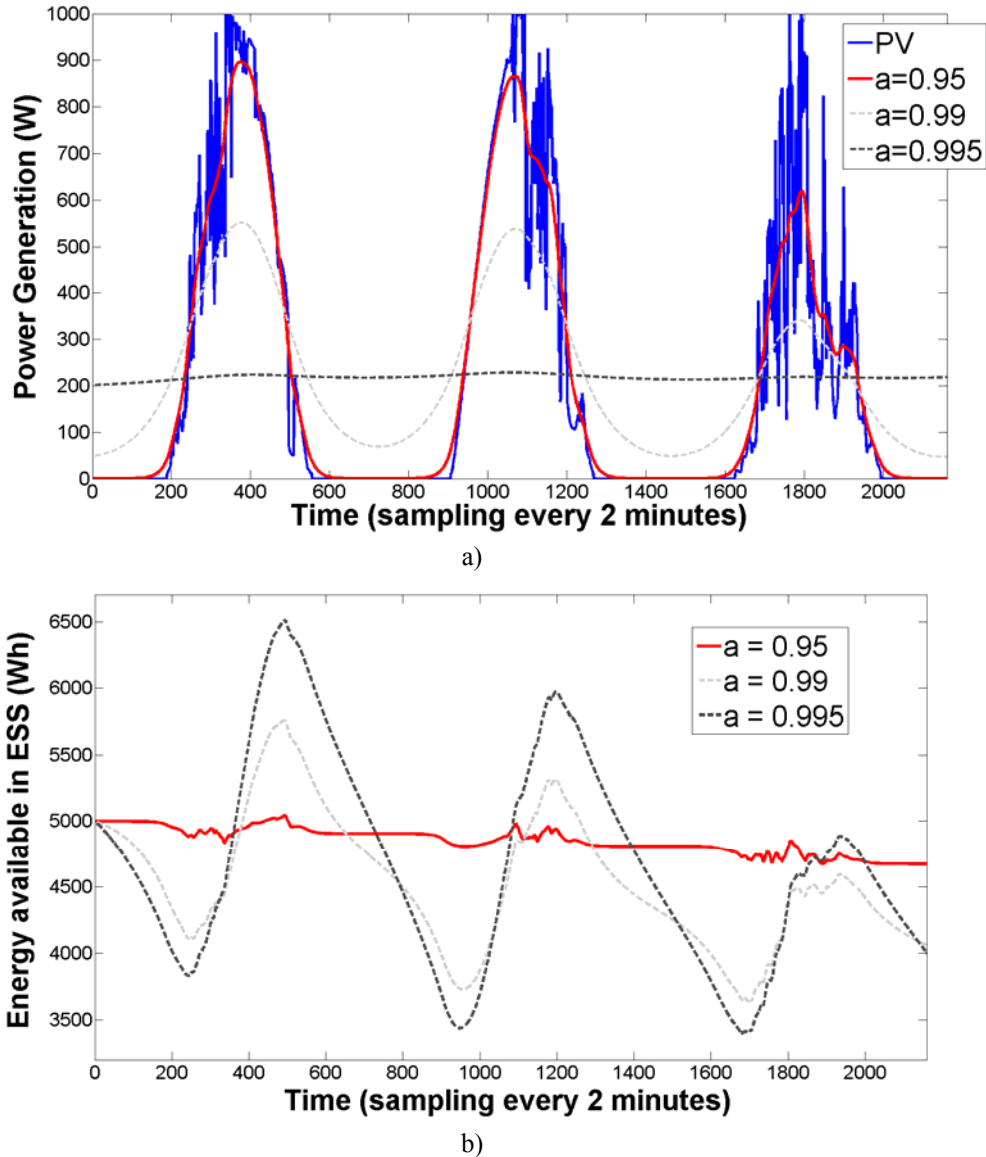
Figure 4.14 Fluctuations reduction strategy performance along three cloudy days: a) power evolutions, b) energy capacity in the ESS, for different filtering levels.

Therefore, it can be clearly concluded from Figure 4.14 how by increasing the degree of smoothening (increasing the value of parameter *"a"*), a more constant generation can be offered from the PV+ES power plant to the system operation but, that functioning mode entails larger ESS energy requirements, as previously mentioned.

To conclude with this section, one will verify with the results presented in Chapter V that this second EMS will normally allow operating under much smaller ESS capacity demanding conditions (mainly when considering filtering time constant values below 40 minutes) than those obtained for the constant power EMS. This fact makes it more achievable in economic and technologic terms, according with the different ES technologies state-of-the-art presented in Chapter III. This could qualify PV power plants with ES to operate, with the same amount of energy capacity they would require to properly operate under a constant power steps EMS, under the fluctuations reduction EMS being able to provide, at the same time, some ancillary services (primary and secondary reserves…). Thus, an improved economic operation could be achieved. Conversely, the main handicap for this strategy is that, although reducing the PV production variability and being this reduction very significant for high frequency power oscillations (as will be presented in Section 4.4.2), the PV+ES production will keep being stochastic to a large degree. Therefore, PV power plants with ES implementing this EMS will not be able to access electricity markets and participate in the pool, which will limit their incomes to the corresponding feed-in-tariffs.

4.3. Complementary control options.

Different complementary control actions can be overlapped to the previously presented EMS in order to improve the control of the PV+ES power plant, optimizing at the same time the ESS utilization. A slightly more complex scheme than those represented in Figure 4.3 and Figure 4.12 can be defined in order to compile and integrate the different complementary control actions. This extended scheme in presented in Figure 4.15.

Thus, two different programmable stages are found now in the control scheme in Figure 4.15, identified respectively as EMS and Control blocks. The first one is related to the EMS and, therefore, to the generation of references for the PV+ES power plant. On the contrary, the second one is related to the reference tracking. While the first stage will present a large refresh period (being updated in the range of hours or even once a day), the second stage will present a small refresh period since the reference tracking is subjected to instantaneous variations of the operation variables and conditions.
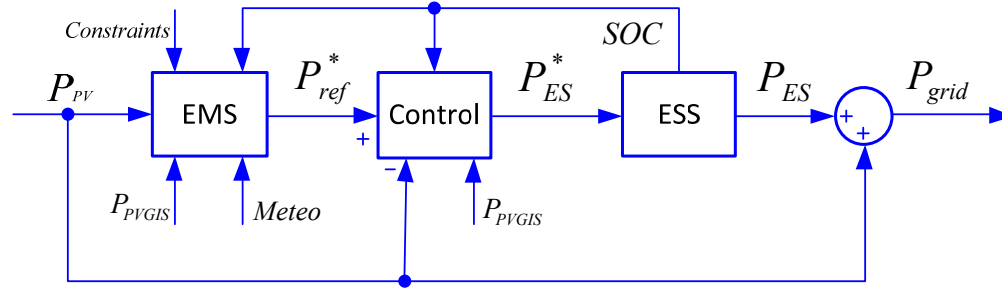
Figure 4.15 Global control system block diagram including optional controls.

Some of the complementary actions here introduced are more related to the reference generation stage, and some others concentrate on the reference tracking one. Their relation with one stage or the other, as well as the place where these are represented scheme in Figure 4.15, is explained in the following within each of the corresponding sections.

4.3.1. Preferred state-of-charge.

A first complementary control action that could be integrated within any of the previous EMS is simply the control of the ES current energy reserve available, monitored by means of its SOC. A target for this SOC control would be to keep it around a certain value in order to avoid saturations and tripping of the system due to successive days of large deviations between the real radiation and the average statistically estimated radiation. If no control on the SOC of the system is performed, these estimated/real radiation deviations would be added up hour after hour and day after day till the moment when the deviation tendency turns around or the ESS system saturates. Thus, enormous energy capacities would be required in order to avoid these ESS capacity saturations.

The main goal for introducing this complementary action is then to be able to reduce or limit the ESS energy power requirements by forcing the system to automatically recover a defined SOC after some time, largely decoupling in this way the storage capacity from the radiation deviations.

Thereby, if a level for the SOC is defined as preferred or reference (SOC_{ref}), meaning that the system will always pretend to remain around that SOC_{ref}, once the ESS is required for some power exchange with the rest of the power plant (deviating temporarily the SOC from the SOC_{ref}) the ESS will tend to recover that SOC level within a programmable and defined period of time, which is usually named as reference SOC recovery time (τ_{SOC}).

This complementary control action is defined in the block diagram of Figure 4.15, represented by the feedback arrow in the upper part of the diagram, which returns the current SOC (or equivalently the ESS energy reserve level) to the control block. That control block uses in this case that SOC level information, evolving from a simple addition block, like it was in Figure 4.3 and Figure 4.12, towards an addition block which integrates now two terms. These terms correspond to the equation governing the PV+ES plant operation when this SOC_{ref} control mechanism is activated. Equation which can be written as:

$$P_{ES} = \left(P_{ref} - P_{pv}\right) + \frac{\left(E_{ES} - E_{ES\,max} \cdot SOC_{ref}\right)}{\tau_{SOC}}$$ (4.7)

Where:

- P_{ref} – current power required at the PCC

- P_{pv} – current solar photovoltaic power

- E_{ES} – current ESS energy

- E_{ESmax} – capacity of ESS

- SOC_{ref} – preferred state of charge

- τ_{SOC} – storage charge time constant

The first part in the equation (4.7) is responsible for the output power reference tracking, in agreement with equation (4.1), while the second part accounts for keeping the SOC as close as possible to the SOC_{ref}. The tradeoff between those two tasks is determined by the τ_{SOC} value which establishes how fast the control makes the ES to regain that SOC_{ref}. Nonetheless, this second term is relevant for the dynamics of the system since it modifies the ideal response of the power plant to keep the current energy reserve close to the SOC_{ref}. That is the big handicap that arises when activating this complementary control. Its performance implies the ESS to suffer a modification on its functioning since it will not exchange all the power required by the reference but the power theoretically demanded minus the power that its control system estimates the ESS needs to recover its SOC_{ref} within the defined τ_{SOC}. The effect of this distortion can be observed in the two examples, one for each of the EMS introduced, represented in Figure 4.16.

Figure 4.16a) shows the distortion introduced by the τ_{SOC} on the overall PV plant generated power when using a 10 hours constant power step reference. It can be appreciated how, instead of the expected squared-shape production along the day (following

corresponding one single step reference), the PV+ES plant injects the power curves represented in different grey scales, which vary as a function of the specified τ_{SOC} value. Similarly, Figure 4.16b) shows the same distortion when τ_{SOC} is activated but operating with the fluctuations reduction control strategy. A clear deformation on the power injected by the PV+ES power plant can be also appreciated (different grey curves) with regard to the plant reference (red curve) when the τ_{SOC} assumes values which approach that of the filter time constant. This happens for values of τ_{SOC} below 24 hours when "a =0.98".

a)   b)
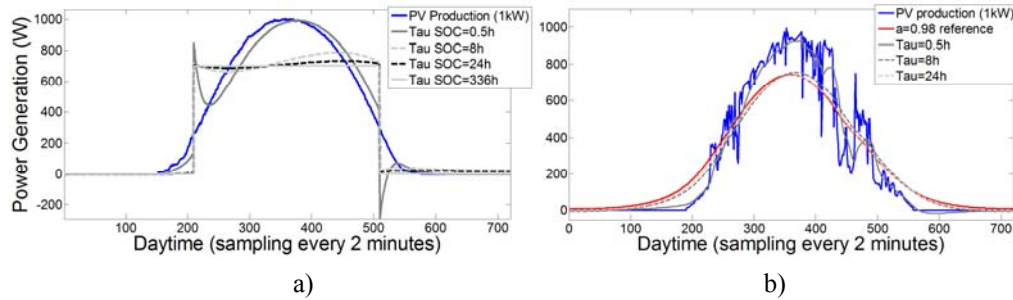
Figure 4.16 Deformations due to the τ_{SOC} effect for: a) a 9 hours constant step reference, b) a smoothening reference with a = 0.98 as filtering parameter value.

A compromise between this undesirable effect and the reduction obtained in the profitable ESS size when the τ_{SOC} is introduced must be achieved. A detailed analysis on that topic, studying the effect on the ESS energy requirements produced by different possible values of the τ_{SOC} is described in Chapter V.

4.3.2. Power change rate limitations.

A second complementary control action is the power gradient limitation control. This action is equally adaptable to in any of the previously introduced EMS. The functioning principle of this action would be focused on limiting the power change rates in the reference provided to the PV+ES plant power (limiting dP_{ref}/dt). Thus, these power gradient limitations could be applied with two main goals: to protect the equipment against violent instantaneous reference step changes (programmed or instantaneously required by the SO) during the constant power strategy operation on one hand, and to limit high power reference changes due to quick variations in weather conditions (which are desired to be smoothed) during the fluctuations reduction strategy operation on the other hand.

For the case of this complementary control action, it could be integrated as a constraint in any of the two programmable blocks of Figure 4.15. In case of being introduced in the

"EMS" block, it would be assumed as a limitation in the possible references to be generated, while in case of being introduced in the "Control" block, it would be considered as a correction implemented by the high frequency online control performed in this block to the references provided by the EMS. In any case, the target of the action would be the same.

Some proposals have already been published on this topic regarding photovoltaic generators [29]. However, since it is more related to the power converter technical limitations (which have not been analyzed in this PhD Thesis) than to the ESS ratings themselves, this complementary control option has not been considered in any of the simulation analysis presented in Chapter V. Therefore, this is a door which remains open for future works with a higher presence of experimental content. Note that only in the experimental tests performed using UCs, that are presented in Chapter V, some power change rate limitations have been introduced. In that case, of course, these were used for the sake of power electronic components protection.

4.3.3. Meteorologically-based adjustments.

In a third place, a complementary control action based on the weather forecast and, hence, on the daily energy yield that can be expected for that day can be considered to improve the performance of the system. This complementary control action has been highlighted in Figure 4.15 by means of the arrow called "*Meteo*" and, according to that block diagram, it impacts the "EMS" block, that is, it influences the system references generation.

In fact, the main contribution achieved by using this complementary control action would be the possibility of adapting the power references, defined with some hours of advance, to the weather conditions expected for the hours of active PV+ES operation. Furthermore, some type of meteorologically-based adjustment over the initial *SOC* of the ESS at the moment of starting those active hours can also be contemplated. These two options are described below.

a) System references adjustment.

The meteorologically-based complement which allows modifying the initial standard system references could be applied to any of the two EMS presented in this chapter.

For the case of the fluctuations reduction EMS, a proper weather forecast could help the PV power plant operator to calculate and decide in advance the filtering degree that can be apply that day to the expected PV production as a function of the ESS capacity installed in the plant.

On the other hand, for the case of the constant power steps EMS, which uses by default averaged-standard irradiation curves extracted from PVGIS for real sky conditions to estimate the daily PV energy yield, the weather forecast information updated for each specific day could allow modifying those standard irradiation profiles. This adjustment implies a change in the expected PV energy yield and, hence, in the constant step reference for that day should be consequently adapted to the new expected energy production. When using this daily or even hourly meteorologically-based adjustment, the standard PVGIS dataset proposed to be used as base to generate the initial constant references is the clear sky conditions one. This will represent the ideal day which will more precisely correspond to any of the clear days in the month, being modified only modified when weather forecast is not the optimal. If the PVGIS real sky conditions dataset was used, rarely any of the days in the month would exactly correspond with the standard averaged-model day.

Note that, regardless of the type of constant power steps strategy (one single step or multiple steps per day) selected for operating the power plant, a meteorologically-based daily adjustment of the power references (energy redistribution) will be always beneficial. As a matter of fact, this will help avoiding saturations of the ESS in case that the real weather conditions drive the PV production far away from its PVGIS-based expected production values. Note that, since standard irradiation profiles offered by PVGIS are monthly-averaged radiation curves, an overcast day in summer can differ on its energy yield, with regard to the statistical monthly average, as much as 90% of the overall expected production. Thus, if no adjustment is done in the constant power step reference for that day, a complete discharge of the ESS is likely to occur.

For the sake of clarity, a simple scheme representing this meteorologically-based complementary control has been developed. This is shown in Figure 4.17.
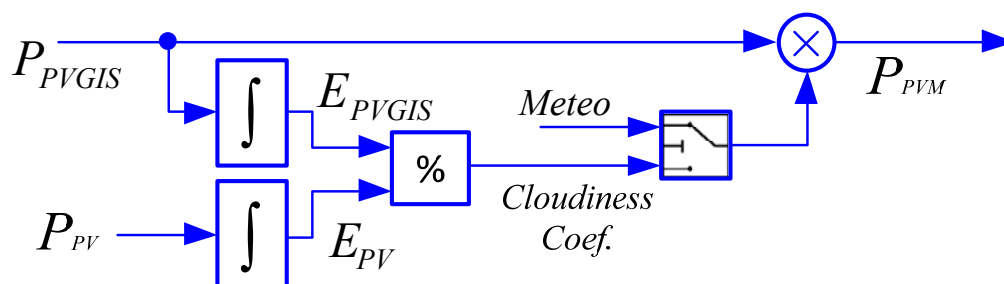
Figure 4.17 Meteorologically-based reference generation adjustment scheme.

This scheme may be understood together with the block diagram in Figure 4.15. The EMS block in that diagram is fed with different inputs which are mostly used in the adjustment here presented. In fact, the meteorologically-based complementary control consists of two parameters, integrated within the EMS block, which can be clearly observed in Figure 4.17: the C*loudiness coefficient* and the *Meteo coefficient*.

Two of the inputs, the current power provided by the PV panels each day (P_{PV}) and the standard power production profile expected for that day, according to PVGIS (P_{PVGIS}), are integrated as time goes by along each day. Thus, an instantaneous comparison can be done at any moment between the real energy that has been generated (E_{PV}) and the ideal energy that should have been generated according to the PVGIS model (E_{PVGIS}). The quotient among these two energy values provides an instantaneous weather dependent coefficient which will vary along the daytime and is the first of the two cited parameters: the *Cloudiness coefficient (CC)*. This *CC* provides information on how cloudy each day has been till the moment of the analysis. This coefficient can be useful given that, following the PV production trend till that moment (value of *CC*), the energy yield which should be expected in the coming hours can be estimated. This is done by taking into account that the energy yield along the daytime keeps always a similar evolution regardless of the specific weather conditions encountered each day, phenomenon which can be appreciated in Figure 4.18.

a)   b)
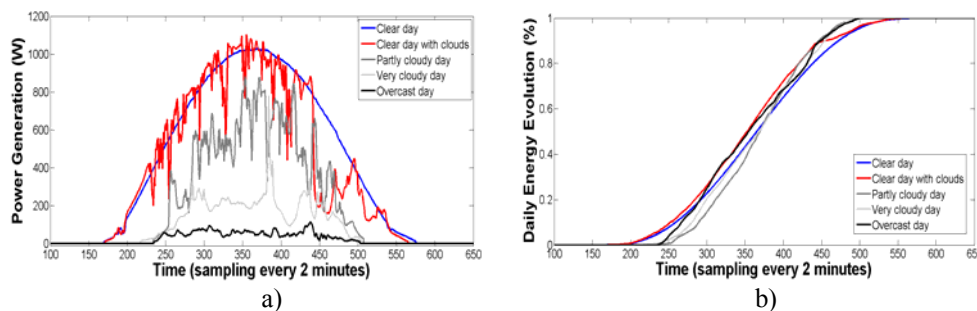
Figure 4.18 Power (a) and energy (b) evolutions along different weather-conditioned days.

It can be observed in that figure how the PV energy yield evolution along any of the five different days represented (a clear day, a clear day with clouds, a partly cloudy day, a very cloudy day and an overcast day), measuring it as a percentage of the final total energy daily production, follows a very cubic polynomial-like shape. This shape can be understood from the much approximated quadratic shape of the solar radiation or the daylight along the day (geometric relations of the relative positions Sun-earth surface). Therefore, the following

mathematical relation can be used to estimate an approximated accumulated energy yield at any future instant.

$$E_{estimated}(t+k) = \frac{E_{measured}(t)}{E_{PVGIS}(t)} \cdot E_{PVGIS}(t+k) = CC(t) \cdot E_{PVGIS}(t+k) \qquad \textbf{(4.8)}$$

Where *CC* is the previously mentioned *Cloudiness coefficient*, $E_{PVGIS}(t)$ and $E_{PVGIS}(t+k)$ are the generated energy values (according to the PVGIS model) at instants "*t*" and "*k*" respectively, $E_{measured}(t)$ is the energy produced by the PV power plant till that moment "*t*" and $E_{estimated}(t+k)$ is the energy that the evolution model estimates that will be approximately generated at the time "*k*". Therefore, an estimation of the PV energy yield in the coming hours can be obtained, and hence the power references adapted to it.

And the second parameter which can be used in this system references' meteorologically-based adjustment consists on, apart from calculating the *CC* based on the past evolution of the production, introducing in parallel to the previous one another coefficient which models the expected energy yield prediction (calculated for the rest of the day) as a function of the updated weather forecast. This coefficient, which has been called "*Meteo*", is also depicted in Figure 4.17. Therefore, while the CC takes into account the past production dynamics to project the future final energy production in the day, the *Meteo* only considers the weather forecast for the coming ours to estimate the final energy production in the day.

The global meteorologically-based references adjustment, taking into account one coefficient (with past information projecting future estimations) or the other (with only weather forecasts) but never both of them at a time (Figure 4.17), multiplies the initial PVGIS real sky standard power profiles (P_{PVGIS}), producing a new set of expected power profiles which represent the new standard production model (P_{PVM} in Figure 4.17). This is the one being fed to the EMS itself (mainly for the case of the constant steps EMS) to generate the new references adjusted to the daily and progressively updated meteorological conditions.

This adjustment can be done several times per day if the PV+ES power plant is desired to operate in the electricity intraday markets. Then, the first time to be executed would be when initially defining the 24 hours production program which, as introduced in Chapter I, is for the Spanish market before midday of the day before. At that moment, no information for past PV production is available since daylight hours of the day on schedule are yet to come. Therefore, the *Meteo* coefficient will be the one used in that occasion being the references

exclusively adapted according to the weather forecast. From then on, six different occasions can be identified to readjust the references which should usually coincide with the six different scheduled intraday electricity market periods. The finishing time of the periods when power offers and modifications are accepted for management on each of the intraday markets are, in Spain: 17:44 hours of the previous day (first intraday market), 21:44 hours of the previous day (second intraday market), 01:44 hours of the current day (third intraday market), 04:44h of the day on schedule (fourth intraday market), 07:44 hours of the day on schedule (fifth intraday market) and 11:44 hours of the day on schedule (sixth intraday market). Among those six occasions, the *CC* adjustment term based on the day-on-schedule real past production will be only available in the last two and in the first one of the next day's schedule (which interferes on the current day production), being then the *Meteo* coefficient the sole adjustment parameter available in the rest of the intraday markets. Furthermore, the *CC* existing information will still be little significant in the fifth one, hence it will be really helpful only for the sixth and first intraday recalculations, as can be appreciated in Figure 4.19. An evolution of the *CC* coefficient value along each of the five prototype days in Figure 4.18 together with the time when the fifth and the sixth intraday bids' matching periods do finish have been represented in that figure. Note that the different evolutions confirm that the estimated *CC* value can only be relied on from the sixth intraday onwards.
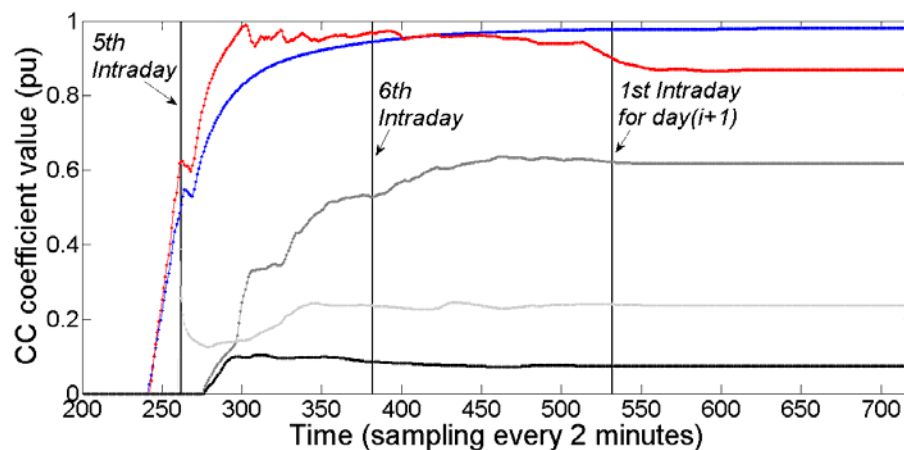
Figure 4.19 CC value evolution along the prototype days with regard to the intraday times.

For both sixth and first intraday markets, although the *CC* coefficient adjustment should prevail given that it implicitly incorporates the day production trend, the variability of the weather has to be always taken into account and the updated weather forecast always

considered. In fact, if the weather forecast indicates the irradiation conditions, and hence the production tendency, are going to be severely modified in the coming hours, the *CC* coefficient should be neglected, maintaining the *Meteo* with an updated value according to the forecast as the parameter which modifies the power profiles.

Thereupon, according with that specified in the previous paragraphs, a good weather forecast turns to be a key issue for the proper operation of the PV+ES plant, especially for the first hours of the day whose power production has been decided at moments when no feedback on the current daily production was available (before the dawn). In this sense, the five prototype days corresponding to five different representative weather panoramas (yielding to power production profiles as those which have been depicted in Figure 4.18a)) have been defined.

The classifications of days into the five prototype categories was based on comparing the energy yield for each of the 365 real measured available days during the year 2009 with their corresponding monthly-averaged standard PVGIS power profiles, comparison defined by:

$$Daily\_Energy\_Quotient = \frac{E_{real}}{E_{PVGIS\_clear\_sky}} \cdot 100 \tag{4.9}$$

The annual evolution of daily energy relations can be observed in Figure 4.20, where the values of the daily quotients have been represented.
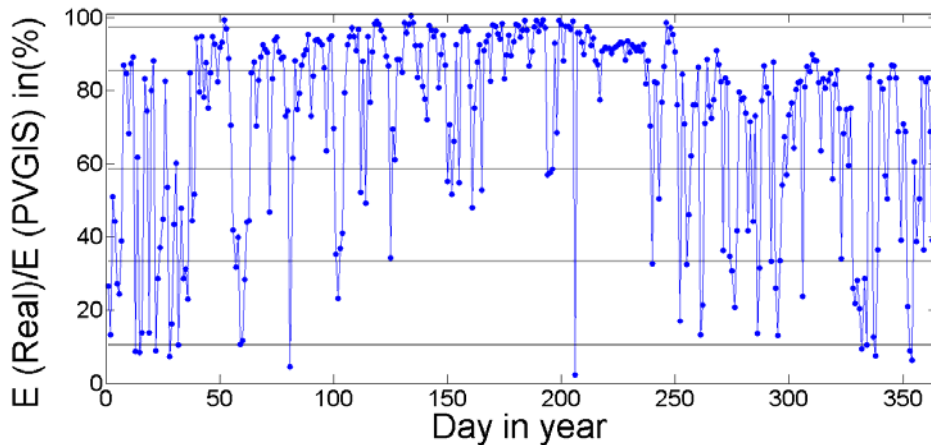
Figure 4.20 Daily energetic relation between real and PVGIS model for clear sky conditions.

As a function of the energy relations calculated for each day and represented in Figure 4.20, these have been grouped according with the following rules:

- $E_{real}/E_{PVGIS\ CLEAR\ SKY}$ greater than 95% - considered a clear day.

- $E_{real}/E_{PVGIS\ CLEAR\ SKY}$ in between 70 and 95% - considered a clear day with some clouds.

- $E_{real}/E_{PVGIS\ CLEAR\ SKY}$ in between 45 and 70% - considered a partly cloudy day.

- $E_{real}/E_{PVGIS\ CLEAR\ SKY}$ in between 20 and 45% - considered a very cloudy day.

- $E_{real}/E_{PVGIS\ CLEAR\ SKY}$ under 20% - considered an overcast day.

A total number of 52, 196, 43, 51 and 23 days in that year are included, according to these rules, within each of the five different representative weather panoramas, respectively.

For each of these five prototype-day groups, a value of the *Meteo* coefficient has been established and compiled in Table 4.3. The corresponding values have been calculated as the average of the energy quotient values for those days which have been included on each of the five meteorological groups. These averaged values defining the *Meteo* coefficient are also represented in Figure 4.20 means of horizontal lines. The mean value for each range has been also introduced in Table 4.3 (in parentheses) for each of the five groups. Although the average value calculated for the real days whose information is available fits better for that specific year and placement (hence for the analysis performed in this Thesis), the mean values in parenthesis could better represent a general value for a generic location.

Weather forecast	Meteo (Referred to PVGIS clear sky)
Clear day	0.98 (1)
Clear day with some clouds	0.85 (0.825)
Partly cloudy day	0.58 (0.575)
Very cloudy day	0.33 (0.325)
Overcast day	0.1 (0.1)

Table 4.3 Values of the *Meteo* coefficient as a function of the expected weather conditions.

Thus, a progressive update of the weather forecast and the more and more representative information of the past PV production will help adjusting the references for the last hours of the day, refining the initial power production schedule. Also, it will help improving the production with regard to the situation when no weather forecast information is available, case in which, according to that previously introduced in this chapter, the production schedule is defined with the sole information of the PVGIS real sky model. This, together with taking into account the *SOC* at the moment when redefining the references, will help avoiding saturations in the functioning on the power plant what would undesirably represent economic penalties.

b) Initial SOC adjustment.

A second possible contribution can be identified for this meteorologically-based action. Although it has not been stood out in the block diagram of Figure 4.15, the weather forecast can be also used to modify the SOC reference value at the beginning of the daily functioning programmed hours. By default, the system will be initialized at around the 50% of the SOC to allow an initial correct operation in both senses (charging and discharging). As a function of the weather forecast and the estimated irradiance for the day, a certain level different from that 50% for the initial SOC will be fixed. Thus, if an overcast day is expected, meaning that irradiance should be normally below the PVGIS monthly-averaged value for real sky conditions, a SOC approaching the unit will be established so that the system can start operating during the first hours of the day minimizing the risk to run out of energy. Conversely, if a clear day is expected the daily irradiance may be determined with certain accuracy, hence, the initial SOC will be adapted to the programmed EMS to avoid saturations. This is a control action which, on the contrary to the previous one using the *CC* and the *Meteo* coefficients, would only be used once a day, that is, when initially defining the 24 hours power production program.

Finally, note that the initial *SOC* adjustment makes sense for the two EMS presented in this chapter while the system references adjustment, although also adaptable to any of them, will be better profited by the constant power steps EMS as can be understood from the description introduced above.

4.3.4. Steps optimization.

Apart from the meteorologically-based complement, some further adjustments can be taken in order to try guaranteeing an even more accurate PV production avoiding ESS saturations and resultant penalties. According to that introduced in Section 4.2.1.c), the hourly defined constant power steps EMS is the clear candidate strategy which will allow PV plant operators to participate in electric markets. Therefore, an optimization of this hourly-adapted constant power steps reference is here proposed using quadratic programming (QP), which is the problem of optimizing (minimizing or maximizing) a quadratic function of several variables subject to linear constraints on these variables. The quadratic programming problem can be formulated as:

Minimize (with respect to x) $$f(x) = \frac{1}{2} x^T Q x + c^T x$$ **(4.10)**

- Subject to one or more constraints of the form:

$$Ax \le b$$ *(linear inequality constraint)*   **(4.11)**

$$Ex = b$$ *(linear equality constraint)*   **(4.12)**

The main advantage of quadratic programming is that it is a very well-known problem in the convex optimization field and, as long as Q is a positive definite matrix, there are quite a lot of available methods which allow solving it efficiently in polynomial time.

The simple block diagram in Figure 4.21 represents this optimization stage. This diagram shows schematically both input parameters (such as the SOC or the P_{PVM}) and output signals (the references) which are generated by the quadratic programming (QP) block where the optimization is performed.
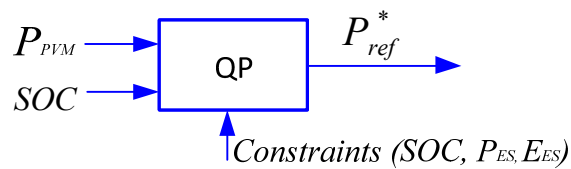
Figure 4.21 Steps optimization system for generation of references block diagram.

Note how the optimization here presented takes into account the meteorologically-based adjustment (P_{PVM} from Figure 4.17) although these actions are independent one from each other and a step reference optimization could be done without meteorological information, being then based exclusively on the PVGIS models. However, the meteorological adjustment has been introduced in order to profit the different intraday periods (presented in the previous section) so as to refine, once and again along the day, the optimally compromised power steps using an updated weather forecast, the current SOC value and the measured accumulated PV production.

The goal of the optimization is then to produce, according to the updated values of the input parameters at the moment when each optimization is recalculated, the hourly-adapted constant power steps reference which will allow redistributing the PV panels production into

an hourly-constant PV+ES production while keeping the SOC level of the ESS as close as possible to a reference value. This optimization is defined by the following equation:

$$\min \sum_{0}^{720} \left(SOC_i - SOC_{ref} \right)^2 \tag{4.13}$$

Being SOC_i the ESS state-of-charge at any sampled moment during the analysis and SOC_{ref} the same favorite value of the SOC that was defined in 4.3.1. This is normally defined as 50% of the capacity with the goal of avoiding energy saturations. Therefore, it is a quadratic optimization type which is subject to the following constraints:

$$P_{ref}(t) = \begin{cases} p_1 & t = 0.....30 \\ p_2 & t = 31....60 \\ .... & \\ p_{24} & t = 691....720 \end{cases} \tag{4.14}$$

$$P_{ref}(t) = P_{PV}(t) + P_{ES}(t) \qquad\qquad t = 0,...,720 \tag{4.15}$$

$$P_{min} < P_{ES}(t) < P_{max} \qquad\qquad t = 0,...,720 \tag{4.16}$$

$$E_{ES}(t) = E_{ES}(t-1) - T \cdot P_{ES} \qquad\qquad t = 0,...,720 \tag{4.17}$$

$$E_{min} < E_{ES}(t) < E_{max} \qquad\qquad t = 0,...,720 \tag{4.18}$$

The total number of samples considered in the optimization ($N = 720$) corresponds to the number of 2-minute periods in 1 day, time used as sampling period for the analysis performed in the present Thesis. Therefore, each of the hourly power step references which are defined with the optimization lasts 30 samples, equation (4.14). However, it is important to note that, along the daytime, different optimizations can be performed and, hence, not all the 24 hours will have to be contemplated on them. Thus, the counter value in equation (4.13), together with the corresponding number of samples, will be adapted to the time of the day when the optimization is carried on. Furthermore, four additional restrictions are introduced. Those in equations (4.15) and (4.16) establish the value of the power that must be exchanged by the ESS (P_{ES}) in order to accomplish the P_{ref} demanded to the PV+ES plant and also some limitations in the power value that can be assigned to the ESS, respectively. On the other hand, restrictions in equations (4.17) and (4.18) are focused on how the ESS'

state-of-charge evolves along the daytime and what are the limits to these variations in the SOC level. Finally, note also that no charging or discharging efficiency coefficients have been introduced in the model, which would interfere in equation (4.17), since these involve a non-linear behavior of the system. Nonetheless, these efficiencies do have been included in the annual simulation performed to determine ESS ratings presented in the next chapter.

As an example of functioning of this optimization method, the hourly references for two different days have been represented in Figure 4.22 and Figure 4.23.
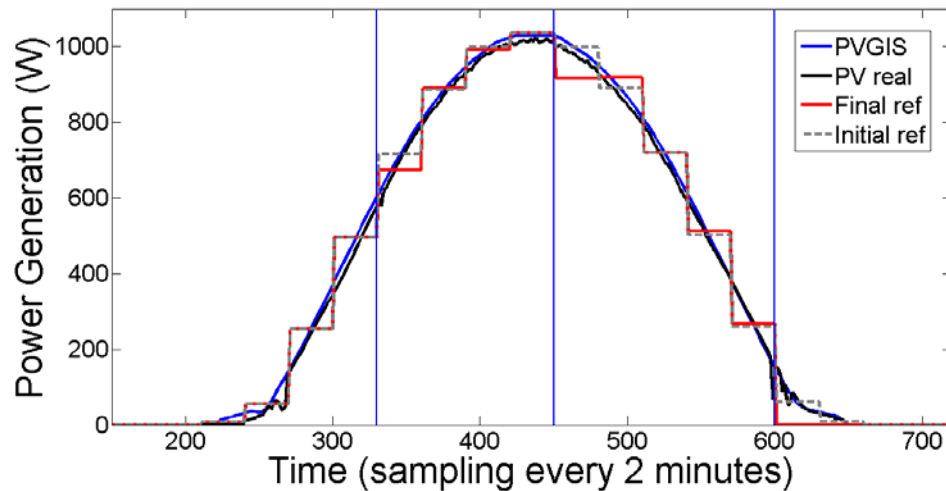
Figure 4.22 Successive optimizations performed to generate updated hourly constant power steps references during a clear sunny day.

The different adjustments that the P_{ref} experiences along the days as the optimizations are refreshed can be observed. The optimizations have been defined during the last minutes of the intraday trading periods although their corresponding new updated references are not activated till each intraday scheduled operation starting time (5th at 11am, 6th at 3pm and 1st at 8pm). These times are also represented by vertical blue lines in both figures.

Note how during the clear day in Figure 4.22 the PV production is similar to that modeled by PVGIS, thus, the hourly-defined references are hardly modified in the different intraday times (red line with regard to the grey-dashed one). Only during the 6th operation hours, the power reference values are somehow reduced along the first hour in order to compensate the previous measured differences between the model and the reality. Similarly, the first intraday (from the day+1 schedule) comprehends an adjustment which forces the plant to inject quite a lot of energy during one hour so as to regain the SOC_{ref} as soon as

possible. This final compensation in the evening hours could be modified to inject the same energy among different hours.

Conversely, much more severe adjustments can be identified in Figure 4.23 for the cloudy days. Since the real PV production for that day differs from the predicted model quite a lot more than for clear days, and although not being a critical day because good levels of production are still accounted, recalculated references (red line) modify significantly the initial production schedule calculated the day before (grey-dashed line). Therefore, while high production levels will be demanded when starting the sixth intraday period, no power will be demanded after the first one (day+1). In one case and the other, adjustments are made in order to keep the SOC level as close as possible to its reference value trying to compensate deviations between the predicted model and the real PV production experienced during the hours previous to each intraday period.
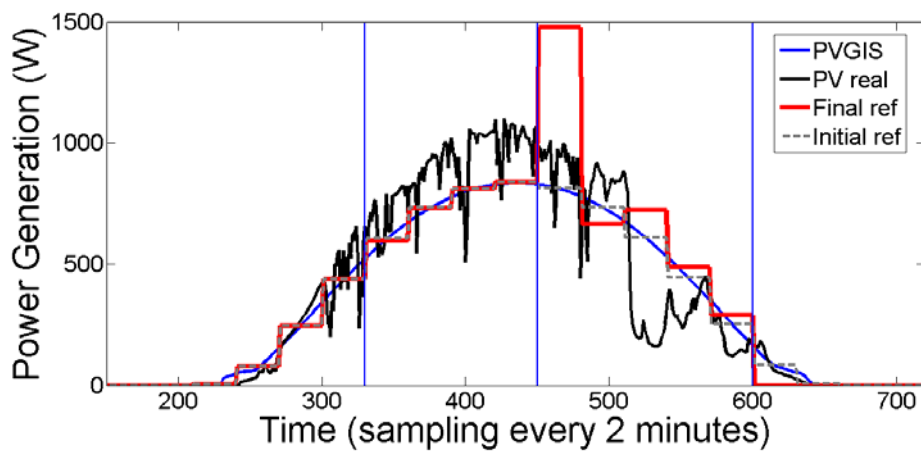
Figure 4.23 Successive optimizations performed to generate updated hourly constant power steps references during a cloudy day.

4.3.5. Predictive control for constant steps value.

Even with an optimally-defined constant power step strategy and a good energy forecast, ESS saturations can be achieved due to unforeseen changes in the instantaneous meteorological conditions. This is also valid for the fluctuations reduction EMS. If a filtering level has been defined, according to certain estimated weather conditions, and these vary suddenly, saturations of the system will be achieved. Thus, although both EMS do work correctly for days with favorable meteorological conditions and properly calculated and

adapted PV+ES power demands (using the two complementary control actions just introduced), there is no way to avoid filling or emptying the ES system when these conditions do not hold. Therefore, some extra control action should be taken to be able to modify the PV+ES production prior to achieving a saturated state, avoiding in this way getting out of the production control and returning to a solar radiation-dependent stochastic production mode.

This extra control action is introduced within the "Control" block in Figure 4.15 in order to improve the accuracy of the reference tracking. It adapts or modifies the power references assigned to the PV+ES power plant by the EMS to avoid future saturations in a continuous mode. The control action considered to watch over the ESS' instantaneous SOC, and estimate future evolutions of the system, is based on the predictive control philosophy. More precisely, it is a control design technique, known as Model Predictive Control (MPC), which is based on the following three-step strategy [40]:

1. The future outputs for a given horizon N, called the prediction horizon, are predicted at each instant t using the process model. These predicted outputs $y(t + k|t)$ depend on the known values up to instant t (past inputs and outputs) and on the future control signals $u(t + k|t)$, which are those to be sent to the system and calculated.

2. The set of future control signals is calculated by optimizing a determined criterion dependent on the predicted future trajectory and control signals. This criterion usually includes a quadratic term of the error between the predicted output signals and the reference trajectories.

3. Although a complete sequence of N future control signals is computed, only $u(t|t)$ is effectively sent to the process, because at the next sampling instant $y(t + 1)$ is already known (instead of predicted) and step 1 is repeated. This is the receding horizon concept.

MPC presents a series of advantages over other control methods, amongst which the following stand out [40, 41]:

*   The multivariable case can be systematically designed. Furthermore, all inputs and outputs can be given different relative importance, making the tuning of the controller intuitive even with a limited knowledge of control.

- Constraints, such as the actuators limited field of action or some limits in the process variables due to constructive or safety reasons, can automatically be taken into account by the controller, allowing a better performance.

- When future references or disturbances are known, this information can be used by the controller to improve performance.

On the contrary, the main drawbacks of MPC are the necessity to count with an accurate prediction model of the controlled outputs and a great computational effort needed to solve a constrained optimization problem, which can be too consuming for fast process applications.

In the context of PV plants integrating ES and controlled according to any of the EMS presented in Section 4.2, these drawbacks can be overcome because refresh time is not critical and some radiation models can be found. Thus, a novel or complementary control methodology based on this predictive control approach is also proposed in this PhD Thesis. The goal of this methodology designed is to control the production and the SOC in order to progressively modify the reference to the plant, before the next reference change is imposed by the global EMS, so as to keep the SOC far from saturation as much time as possible.

The block structure of this predictive control approach, which would be integrated within the "Control" block in Figure 4.15, can be observed in Figure 4.24.
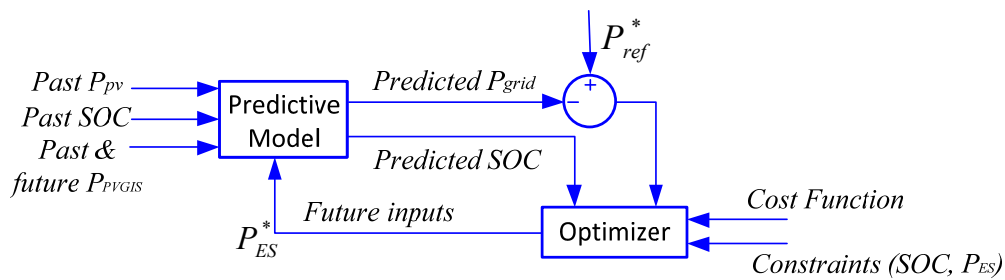
Figure 4.24 Predictive control system block diagram.

In this manner, the PV+ES system is defined with one control signal (the power exchange with the ESS, named P_{ES}) and two different outputs: the power exchange with the grid, named P_{grid}, and the energy stored in the ESS (controlled by means of the SOC). Furthermore, there are limitations on the operation of the system, as it is the fact that E_{ES} can only vary from 0 to the system capacity (SOC from zero to one), and that P_{ES} is limited by the ESS grid-connection converter rated power. The MPC formulation of the problem is characterized by the following optimization:

226

$$J_N = \min \sum_{k=o}^{N} \alpha \cdot \left(P_{ref}(t+k) - P_{grid}(t+k) \right)^2 + \beta \cdot \left(E_{ref}(t+k) - E_{ES}(t+k) \right)^2 + \gamma \cdot P_{ES}^2(t+k) \qquad \textbf{(4.19)}$$

subject to:

$$P_{grid}(t+k) = P_{PV}(t+k) + P_{ES}(t+k) \qquad\qquad k = 0,...,N \qquad \textbf{(4.20)}$$

$$E_{ES}(t+k+1) = E_{ES}(t+k) + T \cdot P_{ES}(t+k) \qquad\qquad k = 0,...,N \qquad \textbf{(4.21)}$$

$$P_{ES,\min} \le P_{ES} \le P_{ES,\max} \qquad\qquad k = 0,...,N \qquad \textbf{(4.22)}$$

$$E_{ES,\min} \le E_{ES} \le E_{ES,\max} \qquad\qquad k = 0,...,N \qquad \textbf{(4.23)}$$

where J_N is the value function, α, β and γ are the system variables weightings, P_{PV} is the prediction of the power generated by the PV panel and T_C is the control period.

The MPC advantages become apparent when it is applied to the analyzed problem. First, the problem has clearly a multivariable nature: the power fed into the grid is the main output to be controlled, but the SOC and power exchange of the ESS have to be considered too. P_{ES} is important because of the power losses and the ESS deterioration due to its usage. On the other hand, the ESS' SOC becomes increasingly important at the end of the day, as an empty or full system would compromise the flexibility of the system for the following day. Note that different behaviors for all these variables can be easily achieved by changing parameters α, β and γ. Furthermore, the ability of considering constraints in the controller is the main advantage of this proposal. Lastly, in the most usual case of using the constant power EMS, as the system is expected to track a constant power setpoint, future power references are known and can therefore be used from the beginning. The main difficulty found to apply the proposed strategy comes from the fact that the power produced by the PV panel in the future, which is used in previous equations, P_{PV}, is not perfectly known, but has to be estimated. To do so, ideal models extracted from PVGIS, and adjusted by the real power measured at the moment of calculation can be used.

According to the previous considerations, it can be concluded that, if a long enough horizon N is chosen, the controller will avoid the filling or emptying of the ESS and therefore it will improve significantly the performance of the PV+ES system.

An example of functioning of this control approach is presented in Figure 4.25. A whole clear day has been considered and a one single constant power step reference of 10 hours per day (red curve) has been introduced. A comparison in the performance of a 1 kW PV power plant with 0.5 kWh of ESS capacity with and without the activation of the MPC can be carried on.

a)

b)
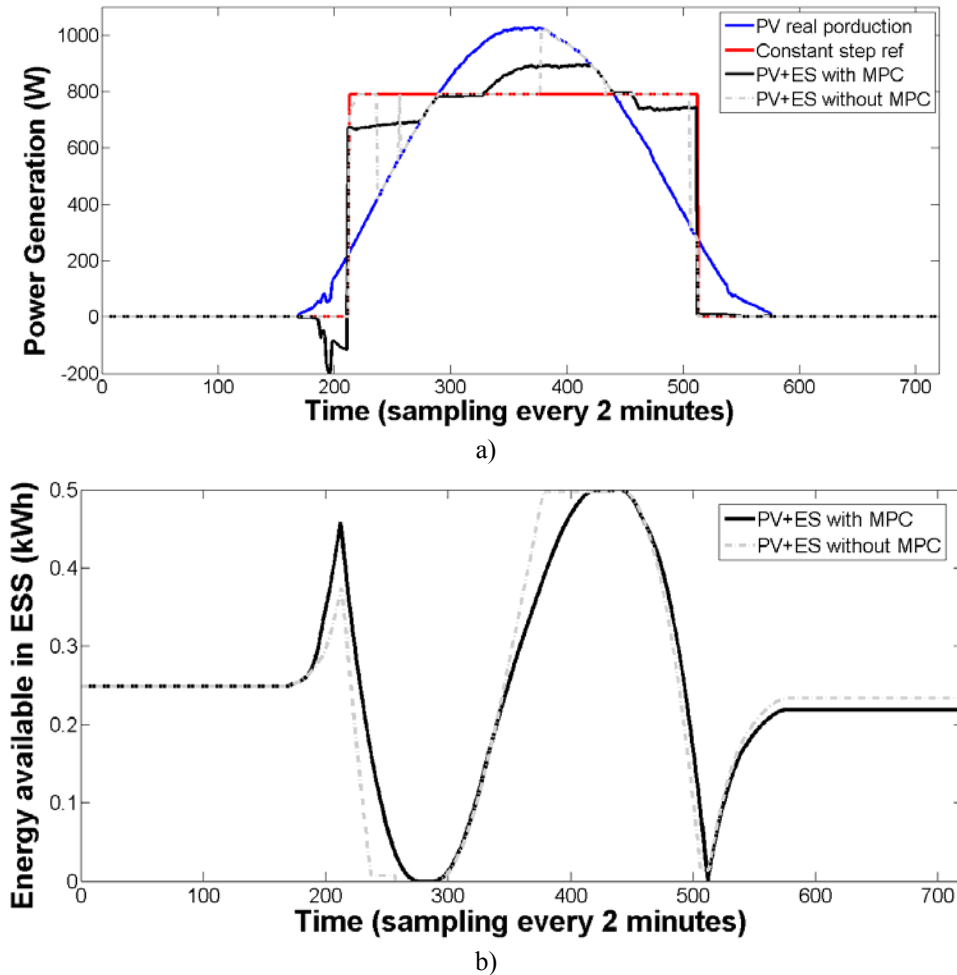
Figure 4.25 Example of functioning of the MPC approach in a PV+ES power plant: a) powers evolution, b) energy evolutions.

While the gray curves depict respectively the power injected by the PV+ES power plant into the grid, curve in upper Figure 4.25a), and the ESS energy reserve evolution along the

day, curve in lower Figure 4.25b), when the MPC is not implemented, the black curves represent the same variables (P_{grid} and SOC) but for the case when the MPC is incorporated.

It can be clearly appreciated how in the first case, the PV+ES tracks the reference till the moment the SOC is saturated. From then on, the control over the power plant production is lost and depends completely on the instantaneous PV production. Conversely, in the case MPC is incorporated, it anticipates the SOC coming saturation and modifies the PV+ES production trying to keep it as constant and as close as possible to the plant reference. ESS saturation time is therefore minimized although the initial reference is not reliably tracked.

The results obtained for days with different meteorological conditions (sunny, cloudy and partly cloudy days) and several ESS sizes when implementing this control technique are also presented in Chapter V, comparing them with the simpler controller obtained by substraction of the power reference and the PV real production presented in equation (4.1). Discussion about the advantages of the MPC strategy is also stated in that chapter.

4.4.   Summary and simulation results.

The two main EMS which have been simulated and analyzed in this PhD Thesis, together with some advanced complementary control options which can be integrated with any of them to improve their performance, have been presented in this chapter. The different ESS sizing results corresponding to each of the EMS are presented in Chapter V though.

However, some initial analyses on the resulting performance of the PV plants with ES when implementing these EMS are introduced here. These analyses correspond to the variations experienced into the PV production cumulative probability distribution and into the PV production frequency spectrum thanks to the ESS integration.

4.4.1. PV production cumulative probability redistribution.

A first clear result that can be highlighted when integrating ES into a PV power plant is the possibility to modify its cumulative distribution function (CDF). This function, usually used in probability theory or statistics is applied here to the PV production field. It describes the probability that the PV power, which follows an unknown probability distribution, will be found at a value less than or equal to a certain value of power P. Intuitively, this function is also referred in statistics as the "area so far" function of the probability distribution since it measures the area under the probability distribution function till the value equal to P.

Therefore, given that the power production of the PV can be modified according to the different EMS, so will be the corresponding CDF.

Figure 4.26 represents some changes that can be obtained in the CDF of the annual power production. The initial PV power CDF, based on the current radiation, is represented in blue while the other curves in grey and red colors represent CDF for the resulting power productions with the different strategies and parameters presented in Figure 4.4 and Figure 4.14. These have been obtained considering an ideal behavior of the PV+ES system (no losses on one hand and capacity large enough so as to track any reference without saturations on the other hand). Therefore, since the round trip efficiency of the ESS has been considered to be equal to 100% along the simulations performed to get the redistribution on Figure 4.26, the average power produced by the system along the year scarcely changes for the different ideal redistributions. However, this is not completely real because energy losses in the charging and discharging process of the ESS will be always faced. Either way, what can be observed in this figure is how the fractions of time when very high or very low power levels are generated are modified as a function of the EMS implemented.
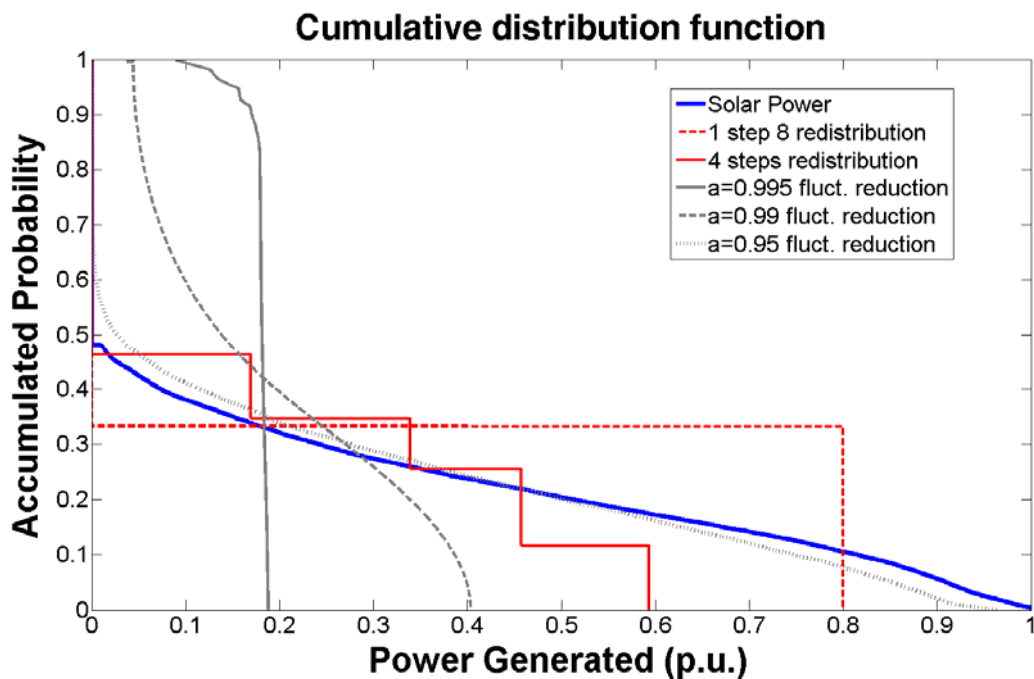
Figure 4.26 Change in power output CDF when introducing ES under different control strategies.

Therefore, Figure 4.26 shows that, with enough ES capacity, the PV power plant production statistical distribution can be enormously modified, comprehending from a constant power production along the whole time (case of injecting the average power, P_N x C_f = 0.18p.u., and which corresponds approximately to the fluctuations reduction strategy with "*a = 0.995*" in the figure) to an elevated power production level assured along approximately the 35% of the calculated time (case of using the constant power strategy with an 8 hours step of 0.8 p.u.).

This big variability and flexibility of the power plant operation is the main advantage of the ES introduction. A key point whose interest is completed with the ES energy requirements analysis presented in the next chapter for the two strategies.

4.4.2. PV production spectrum change.

A second immediate result when introducing an ES unit into a PV power plant is the elimination of the short-term instantaneous fluctuations in the power production, what is reflected on its frequency spectrum. Although this effect may seem more associated to the fluctuations reduction control strategy (as its name indicates and after observing its performance in Figure 4.14), it is valid for the two strategies presented before. Note that while the fluctuations reduction strategy eliminates them just for being its goal, the constant power strategy eliminates fluctuations by default when establishing a constant power reference to track regardless of the input noise. However, the effect of the two strategies on the frequency spectrums differs quite a few as can be appreciated in Figure 4.27. This figure represents the annual single-sided amplitude spectrum (represented versus frequency) for each of the strategies, comparing the real PV spectrum (named "solar power" in the legend and represented in blue) with the total PV+ES power (represented in red). As can be observed, the constant power strategy (Figure 4.27a)) modifies the spectrum in the whole frequency range although introduces some noise corresponding to the harmonics or multiples of the low frequency fundamental component representing the 24 hours step repetition. Conversely, for the fluctuations reduction strategy (Figure 4.27b)) the frequency response is largely modified in the high frequency range (as desired to avoid with this strategy) although the effect is minimum in the low frequency range.

a)   b)
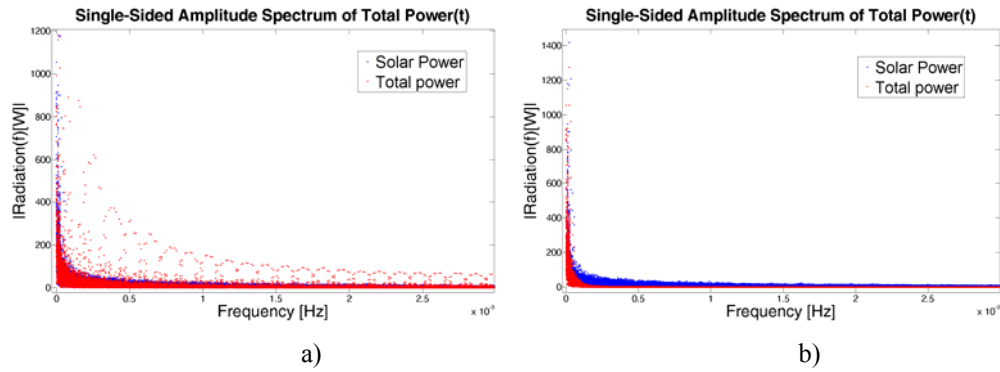
Figure 4.27 Annual power spectrum for the PV+ES power plant operating under: a) constant output power strategy, b) fluctuations reduction strategy.

For the sake of clarity, the reduction in the high frequency domain variability obtained by operating the power plant under the fluctuations reduction strategy for a filtering value of "*a* = 0.95" can be more clearly appreciated in Figure 4.28. This figure has been represented in the same format as it was done for the solar spectrum in Chapter II, Figure 2.15. But now in Figure 4.28, the PV+ES power plant production spectrum (in red) is represented against the initial real PV annual production spectrum (in blue). A clear reduction in the high frequency region (left side of the graph) can be observed. This figure is represented on a logarithmic scale using the time per cycle (or repetition) in the abscissa axis instead of the frequency. As Figure 2.15, this one here also shows a clear repetition pattern located around the 86400 seconds (24h) for both spectra, perfectly depicting the 24 hours solar cycle and its corresponding harmonics. This 24 hours repetition pattern is not modified by the EMS, as expected, since its generated reference presents the same fundamental component periodicity.

Furthermore, the EMS filters performance can be observed for all those fluctuations beyond its cutting frequency or, what is the same, its corresponding filter time constant which, according to Table 4.2 is 39 minutes for the value of "*a*" considered. This filter time constant represents a reduction of 3 dB in the amplitude for those values in Figure 4.28 located around the equivalent time per cycle (magnitude in abscissa). This is:

39 minutes = 2340 seconds → multiplied by 2·*π* = 14702 seconds/rad   (4.1)

Where the amplitude attenuation can be verified.

Finally, note that no saturations have been either identified in this case since a large enough ESS has been considered. Saturations in power or energy would have modified the frequency spectrum of the PV+ES power plant in the high or low frequency range, respectively.
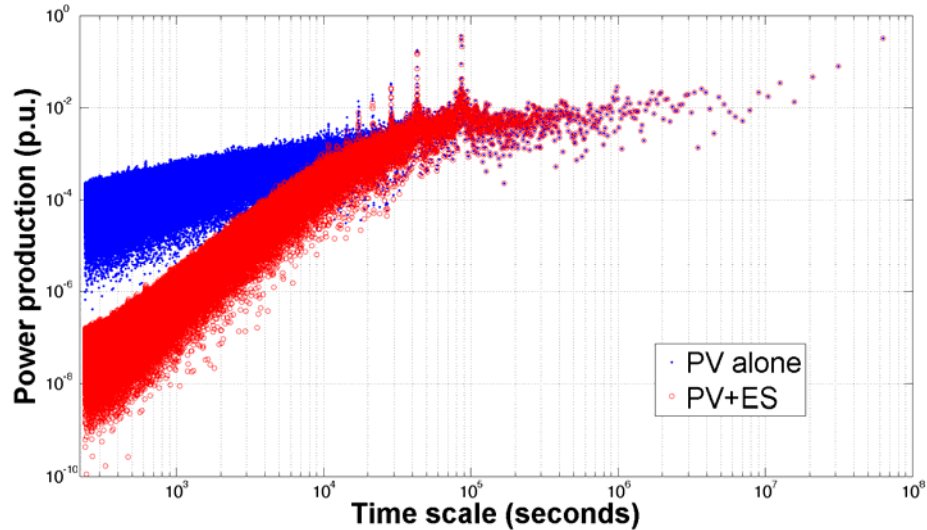
Figure 4.28 Annual power spectrum for the PV power plant with ES under fluctuations reduction strategy, "*a = 0.95*".

Moreover, the amount of yearly variability reduction can be accounted by calculating the standard deviation of the power plant production, working under different values of the "*a*" parameter and comparing them with the initial PV production. This comparison is presented in Table 4.4 where it can be observed how the variability is reduced as the filtering level (value for "*a*") is augmented. In this case, since the ES storage time constant influences the system response too (as presented in 4.3.1), a value τ_{SOC} = 24 hours has been fixed. In the same way, the timeframe considered in order to account the standard deviation is the whole year 2009, when the mean production value is calculated as 0.2256 p.u.

Therefore, by introducing any of the EMS to the PV+ES a smoothening can be obtained, comprehending a general reduction in the fluctuations of the current PV output power, i.e. reducing the variability of the power production referred to an average value over a period (its standard deviation). Variability reduction which is reflected in the frequency spectrum of the PV+ES combined production.

Filter parameter value	Standard deviation (p.u.)
a = 0 (PV alone)	0,3392
a = 0.7	0,3350
a = 0.8	0,3336
a = 0.85	0,3322
a = 0.9	0,3291
a = 0.95	0,3171
a = 0.97	0,2959
a = 0.99	0,1866
a = 0.995	0,1112

Table 4.4 Production variability evolution as filtering level is incremented.

Once the strategies implemented and its initial operation results have been introduced in this chapter, the next chapter will be devoted to the global ESS dimensioning results.

4.5. References

[1] International Energy Agency (IEA) - Photovoltaic Power Systems Programme. Cumulative installed PV power . [Online]. Available: http://www.iea-pvps.org/.

[2] J. P. Barton and D. G. Infield, "Energy storage and its use with intermittent renewable energy," IEEE Transactions on Energy Conversion, vol. 19, pp. 441-448, 2004.

[3] P. Denholm and R. M. Margolis, "Evaluating the limits of solar photovoltaics (PV) in electric power systems utilizing energy storage and other enabling technologies," Energy Policy, vol. 35, pp. 4424-4433, 9, 2007.

[4] C. Hoffmann, M. Greiner, L. Bremen, K. Knorr, S. Bofinger, M. Speckmann and K. Rohrig, "Design of transport and storage capacities for a future european power supply system with a high share of renewable energies," in 3rd International Renewable Energy Storage Conference IRES, Berlin, 2008, pp. 24-25.

[5] D. J. Swider, "Compressed Air Energy Storage in an Electricity System With Significant Wind Power Generation," IEEE Transactions on Energy Conversion, vol. 22, pp. 95-102, 2007.

[6] C. Abbey and G. Joos, "Supercapacitor Energy Storage for Wind Energy Applications," IEEE Transactions on Industry Applications, vol. 43, pp. 769-776, 2007.

[7] A. Arulampalam, M. Barnes, N. Jenkins and J. B. Ekanayake, "Power quality and stability improvement of a wind farm using STATCOM supported with hybrid battery energy storage," IEE Proceedings - Generation, Transmission and Distribution, vol. 153, pp. 701-710, 2006.

[8] J. S. Anagnostopoulos and D. E. Papantonis, "Pumping station design for a pumped-storage wind-hydro power plant," Energy Conversion and Management, vol. 48, pp. 3009-3017, 11, 2007.

[9] E. D. Castronuovo and J. A. P. Lopes, "On the optimization of the daily operation of a wind-hydro power plant," IEEE Transactions on Power Systems, vol. 19, pp. 1599-1606, 2004.

[10] K. Yoshimoto, T. Nanahara and G. Koshimizu, "New control method for regulating state-of-charge of a battery in hybrid wind Power/Battery energy storage system," in Power Systems Conference and Exposition, 2006. PSCE '06. 2006 IEEE PES, 2006, pp. 1244-1251.

[11] S. M. Muyeen, R. Takahashi, T. Murata, J. Tamura and M. H. Ali, "Application of STATCOM/BESS for wind power smoothening and hydrogen generation," Electr. Power Syst. Res., vol. 79, pp. 365-373, 2, 2009.

[12] B. S. Borowy and Z. M. Salameh, "Methodology for optimally sizing the combination of a battery bank and PV array in a wind/PV hybrid system," IEEE Transactions on Energy Conversion, vol. 11, pp. 367-375, 1996.

[13] L. Joerissen, J. Garche, C. Fabjan and G. Tomazic, "Possible use of vanadium redox-flow batteries for energy storage in small grids and stand-alone photovoltaic systems," J. Power Sources, vol. 127, pp. 98-104, 2004.

[14] E. Schaltz, A. Khaligh and P. O. Rasmussen, "Influence of Battery/Ultracapacitor Energy-Storage Sizing on Battery Lifetime in a Fuel Cell Hybrid Electric Vehicle," IEEE Transactions on Vehicular Technology, vol. 58, pp. 3882-3891, 2009.

[15] M. E. Glavin, P. K. W. Chan, S. Armstrong and W. G. Hurley, "A stand-alone photovoltaic supercapacitor battery hybrid energy storage system," in Power Electronics and Motion Control Conference, 2008. EPE-PEMC 2008. 13th, 2008, pp. 1688-1695.

[16] C. Wang and M. H. Nehrir, "Power Management of a Stand-Alone Wind/Photovoltaic/Fuel Cell Energy System," IEEE Transactions on Energy Conversion, vol. 23, pp. 957-967, 2008.

[17] D. B. Nelson, M. H. Nehrir and C. Wang, "Unit sizing and cost analysis of stand-alone hybrid wind/PV/fuel cell power generation systems," Renewable Energy, vol. 31, pp. 1641-1656, 8, 2006.

[18] E. M. Nfah and J. M. Ngundam, "Feasibility of pico-hydro and photovoltaic hybrid power systems for remote villages in Cameroon," Renewable Energy, vol. 34, pp. 1445-1450, 6, 2009.

[19] A. Chaurey and S. Deambi, "Battery storage for PV power systems: An overview," Renewable Energy, vol. 2, pp. 227-235, 6, 1992.

[20] C. J. Rydh and B. A. Sandén, "Energy analysis of batteries in photovoltaic systems. Part I: Performance and energy requirements," Energy Conversion and Management, vol. 46, pp. 1957-1979, 2005.

[21] C. J. Rydh and B. A. Sandén, "Energy analysis of batteries in photovoltaic systems. Part II: Energy return factors and overall battery efficiencies," Energy Conversion and Management, vol. 46, pp. 1980-2000, 2005.

[22] T. Monai, I. Takano, H. Nishikawa and Y. Sawada, "A collaborative operation method between new energy-type dispersed power supply and EDLC," Energy Conversion, IEEE Transactions on, vol. 19, pp. 590-598, 2004.

[23] F. Valenciaga and P. F. Puleston, "Supervisor control for stand-alone hybrid power system using wind and photovoltaic energy," IEEE Transaction on Energy Conversion, vol. 20, pp. 398-405, 2005.

[24] F. Valenciaga, P. F. Puleston and P. E. Battaiotto, "Power control of a photovoltaic array in a hybrid electric generation system using sliding mode techniques," Control Theory and Applications, IEE Proceedings -, vol. 148, pp. 448-455, 2001.

[25] S. Rahman and K. S. Tam, "A feasibility study of photovoltaic-fuel cell hybrid energy system," Energy Conversion, IEEE Transactions on, vol. 3, pp. 50-55, 1988.

[26] K. S. Tam, P. Kumar and M. Foreman, "Enhancing the utilization of photovoltaic power generation by superconductive magnetic energy storage," Energy Conversion, IEEE Transactions on, vol. 4, pp. 314-321, 1989.

[27] F. Giraud and Z. M. Salameh, "Analysis of the effects of a passing cloud on a grid-interactive photovoltaic system with battery storage using neural networks," IEEE Transactions on Energy Conversion, vol. 14, pp. 1572-1577, 1999.

[28] F. Giraud and Z. M. Salameh, "Steady-state performance of a grid-connected rooftop hybrid wind-photovoltaic power system with battery storage," IEEE Transactions on Energy Conversion, vol. 16, pp. 1-7, 2001.

[29] N. Kakimoto, H. Satoh, S. Takayama and K. Nakamura, "Ramp-Rate Control of Photovoltaic Generator With Electric Double-Layer Capacitor," Energy Conversion, IEEE Transactions on, vol. 24, pp. 465-473, 2009.

[30] M. Šúri, T. A. Huld and E. D. Dunlop, "PV-GIS: a web-based solar radiation database for the calculation of PV potential in Europe," International Journal of Sustainable Energy, vol. 24, pp. 55-67, 2005.

[31] European Commission, Joint Research Centre. PVGIS database . [Online]. 2010). Available: http://re.jrc.ec.europa.eu/pvgis/index.htm.

[32] E. Hirst and B. Kirby, "Separating and measuring the regulation and load-following ancillary services," Utilities Policy, vol. 8, pp. 75-81, 6, 1999.

[33] R. Hara, H. Kita, T. Tanabe, H. Sugihara, A. Kuwayama and S. Miwa, "Testing the technologies," Power and Energy Magazine, IEEE, vol. 7, pp. 77-85, 2009.

[34] M. H. Rahman, K. Nakamura and S. Yamashiro, "A grid-connected PV-ECS system with load leveling function taking into account solar energy estimation," in Electric Utility Deregulation, Restructuring and Power Technologies, DRPT. Proceedings of the IEEE International Conference on, 2004, pp. 405-410 Vol.1.

[35] R. Om, S. Yamashiro, R. K. Mazumder, K. Nakamura, K. Mitsui, M. Yamagishi and M. Okamura, "Design and Performance Evaluation of Grid Connected PV-ECS System with Load Leveling Function." Trans. Inst. Electr. Eng. Jpn, vol. 121, pp. 1112-1119, 2001.

[36] B. Burger and R. Rüther, "Inverter sizing of grid-connected photovoltaic systems in the light of local solar resource distribution characteristics and temperature," Solar Energy, vol. 80, pp. 32-45, 1, 2006.

[37] P. S. Georgilakis, "Technical challenges associated with the integration of wind power into power systems," Renewable and Sustainable Energy Reviews, vol. 12, pp. 852-863, 4, 2008.

[38] H. Beltran, M. Swierczynski, A. Luna, G. Vazquez and E. Belenguer, "Photovoltaic plants generation improvement using li-ion batteries as energy buffer," in Industrial Electronics, Proc. of the IEEE International Symposium on GDansk, Polland, 2011, .

[39] Xiangjun Li, Dong Hui, Li Wu and Xiaokang Lai, "Control strategy of battery state of charge for wind/battery hybrid power system," in Industrial Electronics (ISIE), 2010 IEEE International Symposium on, 2010, pp. 2723-2726.

[40] E. F. Camacho and C. Bordons, Model Predictive Control. Springer Verlag, 2004.

[41] J. A. Rossiter, Model-Based Predictive Control: A Practical Approach. CRC, 2003.

Results for the different control strategies and applications

A fter the introduction to the PV power plants' production limitations exposed in Chapter I, the solar resource availability and characteristics analysis performed in Chapter II which completes the understanding of the limitations due to the solar resource nature, and the ES technologies review presented in Chapter III as a possible solution to those PV limitations, Chapter IV is focused on the multiple control methodologies that can be implemented in PV power plants with ES to overcome those limitations taking profit of the ES integration. Therefore, different energy management strategies (EMS) which can be optionally modified by some complementary adjustments are presented in that chapter. However, although describing the different strategies and adjustments no results on the sizing of the ESS needed to be able to accomplish the reference or behavior established by the different EMS have been introduced yet. This is the final goal of this Thesis. However, only some initial simulation results derived from the direct application of these EMS to the PV power plant with ES, focused mainly on PV production cumulative probability distribution and on the PV production frequency spectrum modifications when introducing the ES units, are set out in Chapter IV.

Therefore, Chapter V is devoted to the presentation of these ESS' sizing results. In this sense, ES capacity requirements are introduced here for each of the different analyses carried out for a PV+ES power plants operating under the various EMS previously introduced. To do

that, the Matlab programs which have been developed and used to perform the analyses are first introduced. Then, each of the analyses is described pointing out its goal and its characteristics as well as introducing the main results obtained for it. Finally, some partial conclusions related to each of the analyses are also highlighted. It can be noted in the different sections of the chapter how, since each of the EMS pursues a different goal in terms of improved operability of the PV power plant, and there are different adjustments which can be activated or not in the control, quite different levels of ES capacity are required in the various analyses. This will pave the way to the economic viability of some control strategies, closing the door to the others.

5.1. Analysis of the different programs used.

In order to perform the different analyses presented in this chapter, different Matlab programs have been developed. Among them, four can be highlighted: a general program used to perform the global annual analyses, an ageing analysis program developed to study the ageing associated to some type of ESS (batteries) when operating in a PV power plant, a power steps optimization program used to calculate the optimal hourly-constant power steps according to certain input state variables and, finally, a predictive control program developed to analyze the reference correction possibilities in the intra-hour range in order to avoid saturations. Each of them is explained in detail in the following, leaning on their corresponding developed flow chart.

5.1.1. General PV+ES program.

As previously introduced, the first program introduced in this section has been developed to perform the annual analyses of the PV+ES power plants operating under the two main EMS introduced in Chapter IV: the constant power and the fluctuations reduction. This program provides information on the time along the year when a defined ESS saturates if operated in a PV plant under those EMS. The flow chart summarizing the general structure of the program is observed in Figure 5.1. According to it, this can be divided into three differentiated stages:

- the configuration stage where many input parameters are demanded to the user. These parameters (ESS power and energy ratings, PV plant rated power, sampling time of the vectors, preferred state-of-charge of the ESS, use of real or ideal irradiation profiles and others…) do define the conditions of the analysis to be performed.
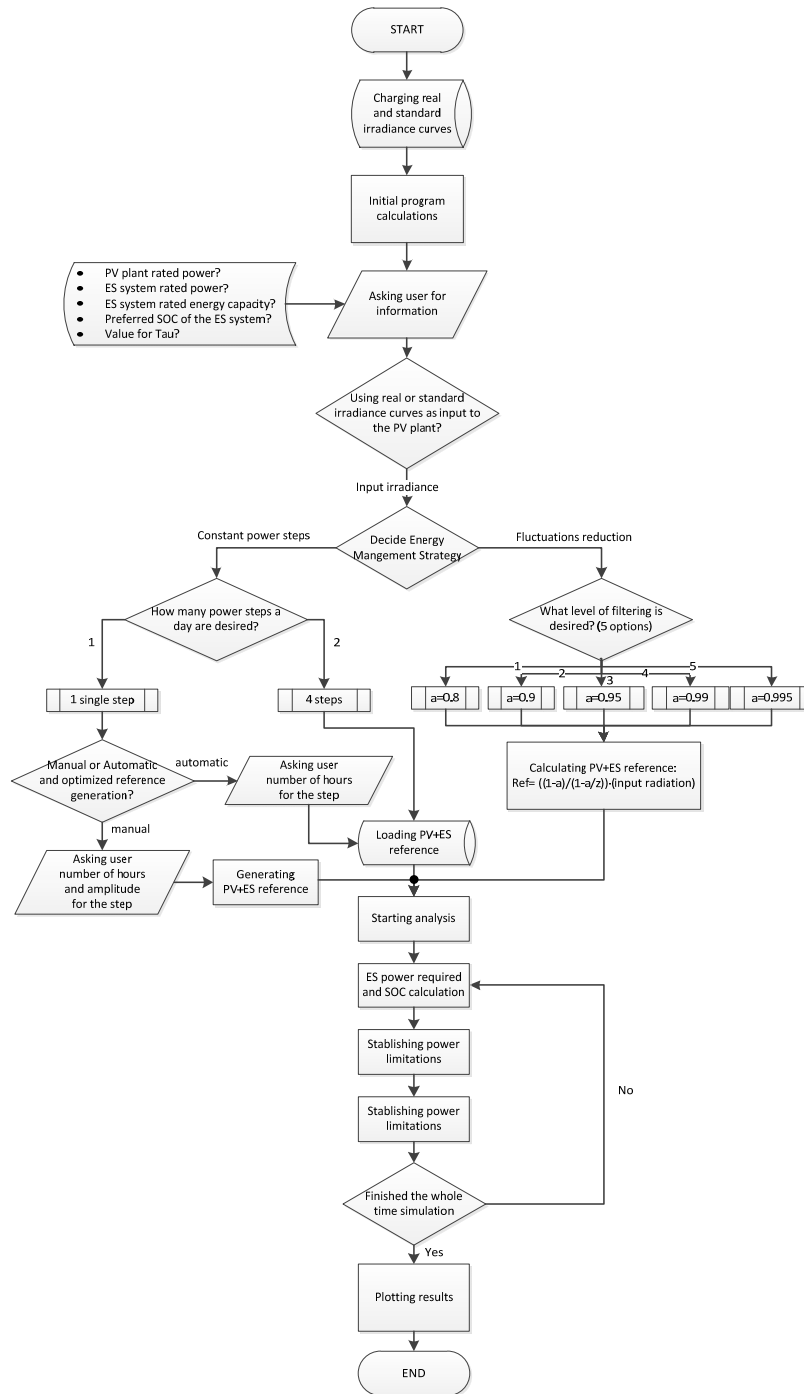
Figure 5.1 Schema of the PV+ES general program.

- an EMS selection stage where the user can select what is the type of strategy that is wanted to be analyzed according to the power plant configuration previously defined. Among all the possibilities that can be found in the two cited EMS, only some of them have been programed and analyzed. These can be appreciated in Figure 5.1 and correspond to five different levels of filtering for the fluctuations reduction EMS, and the case of one single step or four-level steps for the constant power steps EMS.

- the calculation stage itself. The program runs the simulation for the defined period of time, normally one year for the analysis performed in this Thesis. It calculates at every step of simulation (sampling time of the input vectors) the evolution of powers (that produced by the PV plant and that required to the ESS) and the evolution of the SOC. Meanwhile, the program controls the system all the time in order it does not surpass the power and energy capacity values defined as operation limits. In this sense, it registers those periods of time when the system ratings are overpassed identifying them as saturations of the system.

From the resulting power, energy and saturated time vectors obtained for the different ESS ratings analyzed, interesting conclusions over ESS sizing needs can be extracted. Results obtained with this program for the different configurations implemented and analyzed are introduced in Sections 5.2 and 1.1.

5.1.2. Ageing analysis program.

A second program which has been developed along this Thesis comprehends the code which allows studying the ageing process experienced by a certain ESS when used within a PV power plant operating under any of the two main EMS presented in Chapter IV. In this sense, it is complementary to the previous program. In all, only one specific ES technology has been analyzed in this Thesis: a Lithium ion battery. A set of characteristics corresponding to those of the SAFT corporation [1] "Intensium Flex Medium Power" battery commercial model have been adopted in order to calculate by simulation the ageing of a real battery model. The results for this study are introduced in Section 1.1.

The functioning and structure of the ageing analysis program used in this study can be more easily understood with the help of the flow chart represented in Figure 5.2.

The lifetime of the battery depends on different parameters, i.e. temperature, number of peak currents, number of charge and discharge cycles and depth of those cycles [2]. For the

sake of simplicity in the study, only the number of charge and discharge cycles has been taken into account. It can be appreciated in Figure 5.2 how the ageing program only receives the SOC evolution along the whole time period simulated with the general program presented in 5.1.1. Because the battery SOC does not typically follow a regular cycling pattern along the period of time under analysis, a cycle-counting algorithm is used to identify the equivalent complete charge-discharge cycles (full cycles) in that evolution curve. The algorithm used is known as the "rain flow counting" (RFC), method which is a type of cycle-counting technique traditionally used in mechanical engineering for the fatigue analysis of structures under cyclic stresses [3, 4]. Fatigue analysis requires a decomposition of the loading sequence into elementary cycles characterized by their mean value and amplitude [5]. Later versions of the algorithm have been developed searching to improve the fatigue life prediction when compared with calculations using the classical RFC method [5-8]. Some of these proposals have already been used in the renewables domain, but still focusing in the fatigue/fracture analysis of mechanical components. This is the case of the LIFE2 computer code which is a program developed by the SANDIA National Laboratories (USA) specialized in the fatigue analysis of wind turbine components [9]. Nevertheless, in the last few years, the RFC algorithm has already been applied by different authors for estimating batteries lifespan [10-13], which is the final goal in this study. Therefore, the RFC algorithm is also implemented in Matlab and used in the ageing analysis of the Li-ion battery.

According with that introduced in the previous paragraph, this algorithm is programed as a function which is executed while sending to it a SOC evolution. It returns: the SOC evolution transformed into a distilled signal with drops which allows the cycle-counting, the number of cycles experienced with that SOC evolution for the different depths of discharge, a histogram representing that number of cycles for each cycle's depth and the number of equivalent full cycles. This can be observed in Figure 5.3 which represents a simple diagram establishing the main input and outputs exchanged by this RFC algorithm with the rest of the ageing program.
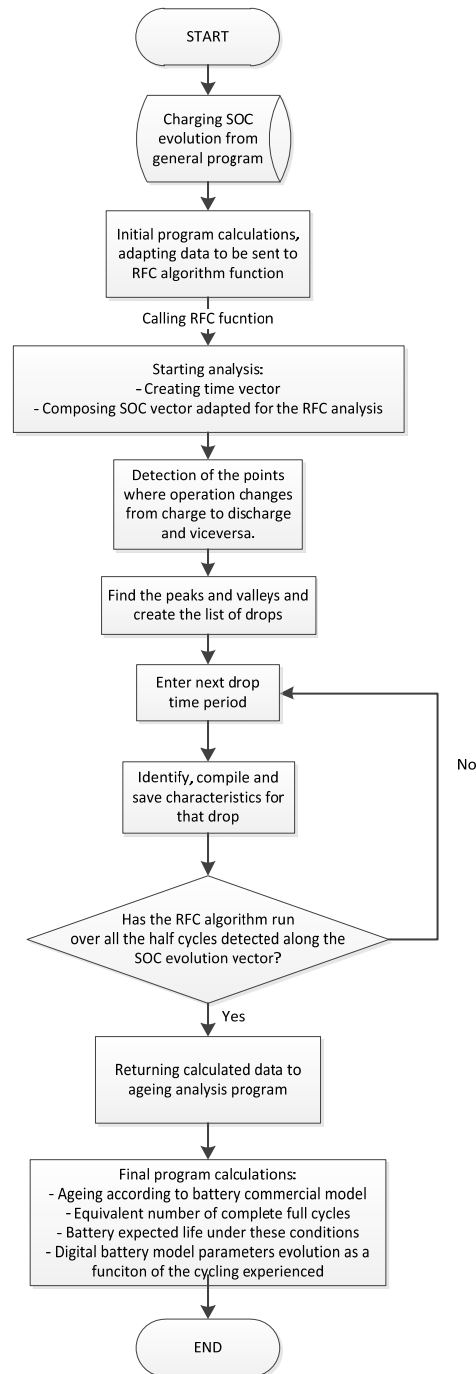
Figure 5.2 Schema of the ageing analysis program.
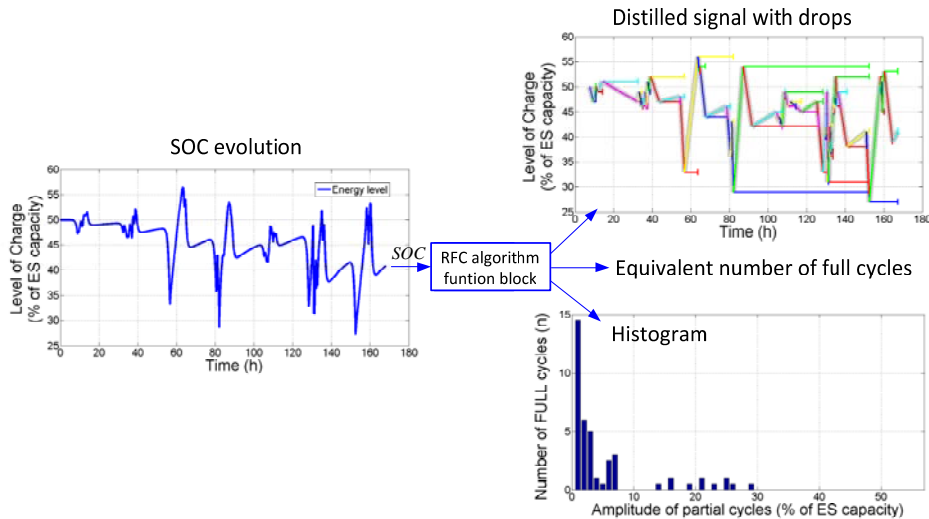
Figure 5.3 Rainflow counting algorithm input and output information.

To get a more precise understanding of the internal functioning of the RFC algorithm, Figure 5.4 should be observed. This figure illustrates how the RFC method is applied using the "distilled signal with drops" that the algorithm generates. The case of a battery operating in a PV power plant under the fluctuations reduction EMS has been represented. Two types of lines can be observed: the thick gray line represented on the back which corresponds with the discretely-adapted SOC of the battery, which is desired to be analyzed, and the thinner colored lines, overlapped to the previous one, which are the charging or discharging half cycles (HC) generated by the RFC algorithm. These HC are those used to count the number of full cycles for each specific cycle depth-of-discharge (*DoD*). Note that each HC starts either at a peak or at a trough. When rotating 90∘ clockwise Figure 5.4, the adapted SOC curve resembles a pagoda roof. By letting a raindrop start at each peak and trough, the half cycle belonging to a specific drop can be obtained by following the drop's path down the roof. However, the drop flow is stopped, finishing that half cycle, when one of the following conditions is met:

- It reaches the end of the time history, e.g. half cycles 2, 7 and 9.

- It faces a peak/trough of opposite sense and greater magnitude than its starting peak/trough, e.g. half cycle 1, 3, 5 and 8.

- It merges with a drop that started at an earlier peak/trough, e.g. half cycles 4 and 6.

243

From the colored lines in Figure 5.4, the algorithm accounts the number of HC performed by the ESS for each demanded *DoD*, being the amplitude of those half cycles the difference between the *DoD* at its starting and ending points. That means, for instance, that half cycle number 1 presents an amplitude equal to 15% (from 50% to about 65%). To complete the number of full cycles, two half cycles of the same amplitude and different direction have to be accounted. In this manner, the number of full cycles for each depth is obtained.
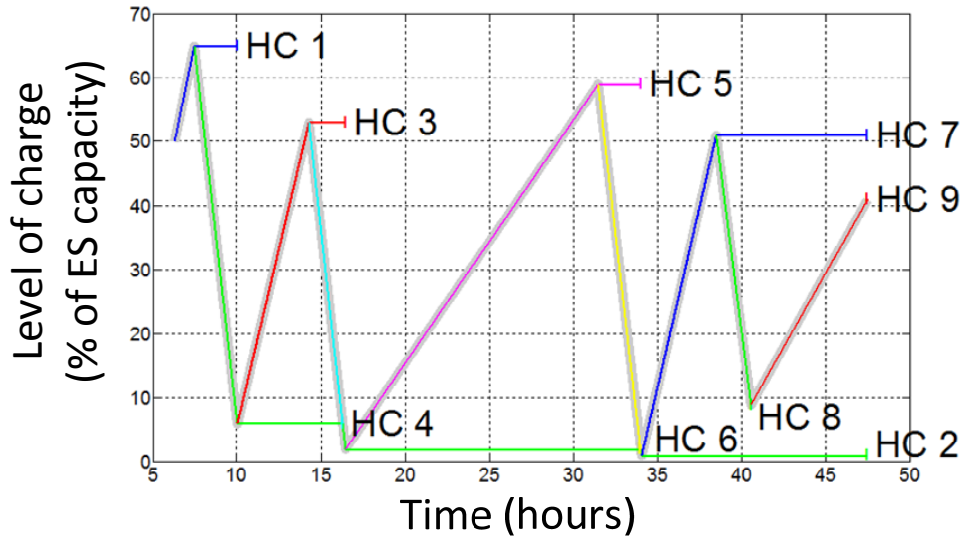
Figure 5.4 RFC resulting cycles curves (drops in colors).

Moreover, the algorithm performs an estimation of the equivalent number of complete cycles (with 100% of charge and discharge) that can be extracted from the calculated HC.

To validate the liability of the obtained results, this technique has be compared with a simpler one which is normally valid for simpler charge and discharge evolution curves. This is based on an approximated full-cycle calculation straightly obtained from the values of: rated energy capacity of the battery and power demanded to it on each step of simulation. The number of full cycles is hence calculated comparing them along the whole time period considered by using the expression in equation (5.1).

$$N^\circ \text{ of cycles} = \frac{\sum_{n=1}^{simu:steps} abs(P_{ES}) \cdot dt}{2 \cdot Capacity} \tag{5.1}$$

Both techniques differ by less than 1% in a simple SOC evolution curve, what validates the use of the RFC technique for the complex evolutions analyzed in this Thesis work.

Once the number of cycles counted by the RFC algorithm is known, and continuing with the ageing program, this is used to estimate the ageing of the battery according with that cycling behavior. The ageing analysis program combines that resulting information with the batteries' manufacturer cycle life curve. This curve is, for the case of the SAFT "Intensium Flex Medium Power" model, the one represented in Figure 5.5.

From that point onwards, the ageing evolution the battery suffered along the period of time analyzed, and how the battery capacity and its open circuit voltage are modified, are obtained. For doing so, a weighted sum is calculated in order to obtain the overall consumed life (in percentage) along the time period considered. This is calculated according to the following equation defined in [2] and [10]:

$$\text{Battery Aging} = \sum_{DoD=1}^{DoD=100} \frac{N_{cyc}(DoD)}{N_{max}(DoD)} \cdot 100 \tag{5.2}$$

Where N_{cyc} is the number of full cycles for each possible amplitude or depth (defined by the *DoD* variable) and N_{max} is the number of cycles the battery can handle for each specific *DoD*, according to Figure 5.5.
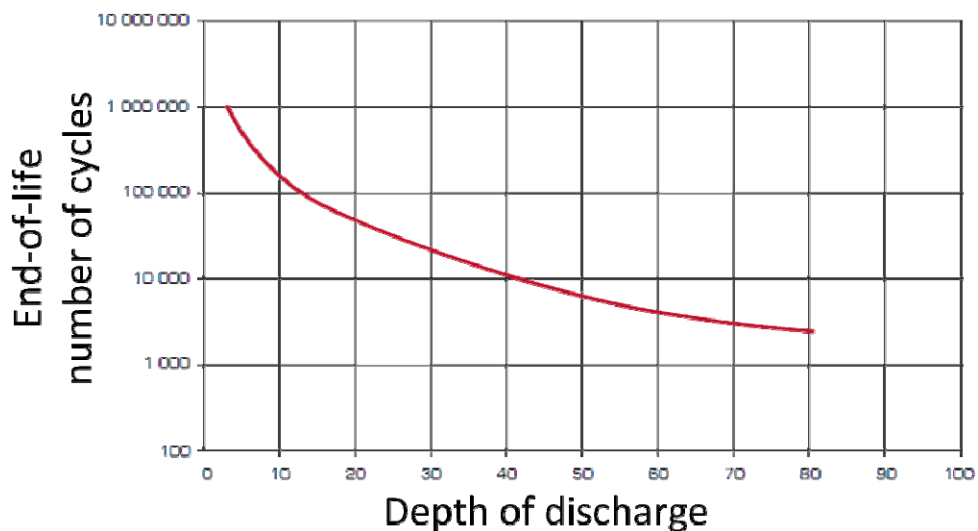
Figure 5.5 Cycle life curve at 25ºC for the Intensium Flex model. Source: SAFT Batteries [1]**.**

Moreover, a simple estimation of the time the battery could be used according to that control strategy (considering that the operation behavior is going to be kept the same) can be projected. This is done taking into account that the battery is considered to be dead when

"Battery Ageing" is equal to 1 (100 % in equation (5.2)). In this sense, the battery expected lifetime can be calculated, using the period of time which has been simulated, by means of the following equation:

$$\text{Life expectancy} = \frac{\text{Length of simulated period}}{\text{Battery Aging (in pu)}} \tag{5.3}$$

Finally, some calculations are done in the program in order to get an approximation on the influence of the number of cycles experienced on some battery characteristic parameters as can be: the total instantaneous capacity and the cycling resistance (which modifies the battery output voltage). These two parameters have been implemented in a battery model, developed in the Matlab/ Simulink® environment adapting the SAFT battery model under consideration. This model is presented in Annex B and implements those Li-ion battery's characteristic equations stated in [14-16]. Among those equations, (5.4) and (5.5) represent the dependence of the two previously cited parameters on the number of complete full cycles already performed by the battery.

$$\text{Capacity} = 1 - \left(4.5 \cdot 10^{-3} \cdot \sqrt{\text{Nº of cycles}}\right) \tag{5.4}$$

$$\text{Cycling resistance} = 1.5 \cdot 10^{-3} \cdot \sqrt{\text{Nº of cycles}} \tag{5.5}$$

5.1.3. Power steps optimization program.

The third analysis program which has been developed for this Thesis is devoted to the generation of hourly-optimized power steps. This program implements those complementary control actions introduced in Sections 4.3.3 and 4.3.4. Therefore, it offers the option to take into account current meteorological conditions and also to update the power plant reference along the day in order to adjust the production continuously. PV power plants can profit the existence of six intraday markets along which their production plan can be modified. In summary, the power steps optimization program paves them the way to participate in the electric market.

Similarly to the two previous programs, a flow chart representing the functioning structure has been developed for this one, Figure 5.6. As can be observed in this flow chart, this program also presents different stages. Mainly, it presents a configuration and a

calculation stage. While the first one is only used during the initialization, the second one is accessed once and again as long as the simulation is on.

In the configuration stage, both the PV power plant and the ESS characteristics are defined. As done for the case of the general program in 5.1.1, parameters such as the sampling time, the charging and discharging efficiencies and a preferred SOC are also introduced. In the same way, the user defines different operation options as those described below:

- For instance, if the meteorological adjustment presented in 4.3.3 is active or not. In case it is activated, does the user give priority to the *Meteo* or to the *CC* coefficient? Or maybe a combination of both depending on the intraday market?

- In case the meteorological adjustment is off, the user must define if the program must recalculate the reference along the different intraday market periods in order to adapt this reference to probable current deviations in the daily production. These can be detected by means of the SOC instantaneous level when compared to the expected one.

- In both cases, the user has the option to define how many and what intraday markets the program has to take into account to recalculate the reference. Normally, if the user desires the PV+ES plant to participate in the intraday markets, all of them will logically be profited and hence the reference adapted in all of them.

- Finally, there is the option to avoid profiting the intraday market opportunities and operate with a fix reference defined 24 hours in advance but also hourly-optimized. The fact of presenting this reference optimization which modifies its value every hour according to the expected PVGIS production model is the only difference for this operating option with regard to the constant power steps EMS simulated with the general program.

In the calculation stage, the hourly-adapted reference is processed for each day along the time considered. Depending on the configuration options introduced, the optimization introduced in 4.3.4 is performed once, twice, three or even four times per day (the initial one plus another for each of the three intraday markets taking place during sunlight hours).
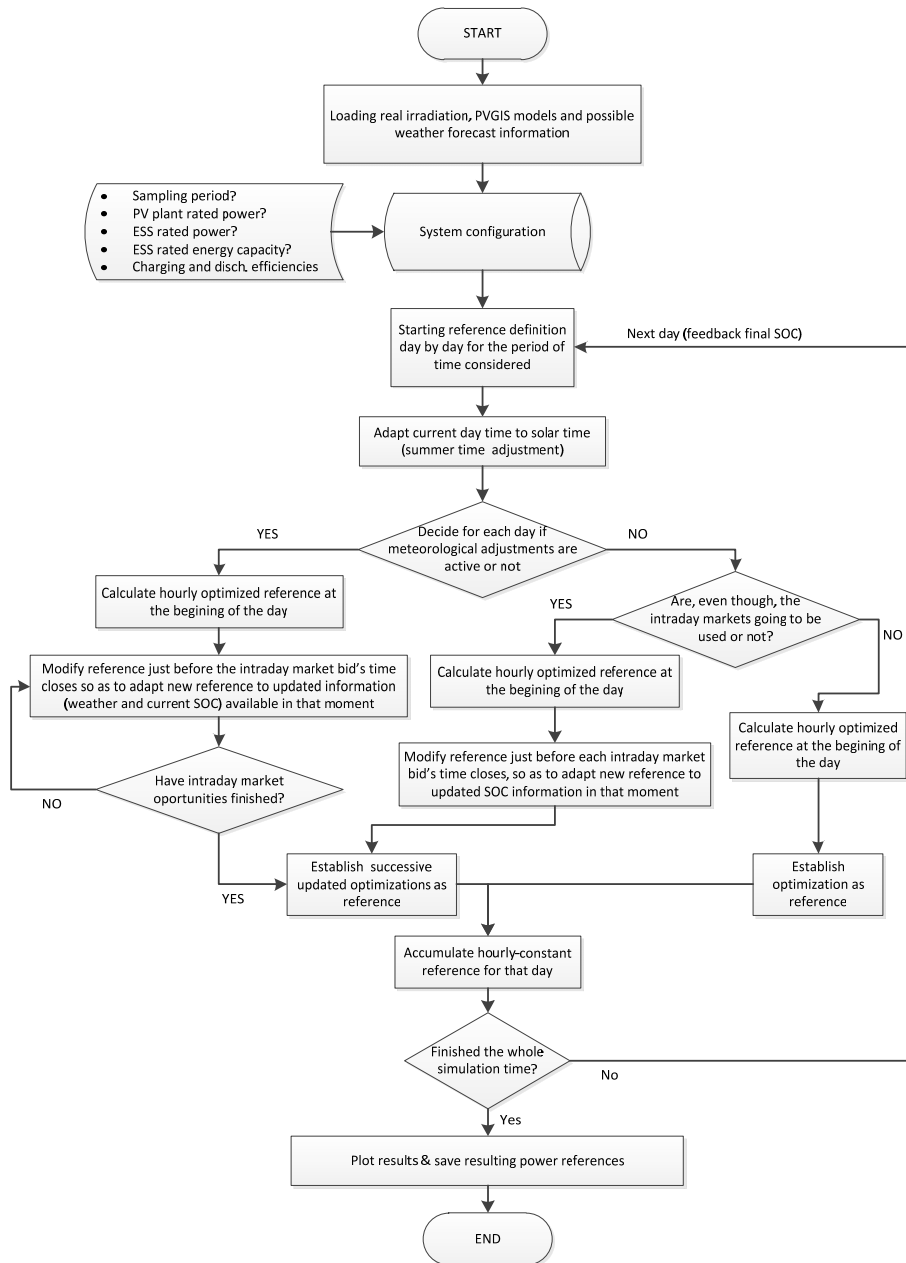
Figure 5.6 Scheme of the power steps optimization program.

All the different operation options, here introduced as possibilities of the program, are analyzed in the Thesis. The corresponding results obtained using the different configurations, in combination with the general program in 5.1.1, are presented in Section 1.1.

248

5.1.4. Predictive control program.

Finally, a fourth program has been developed to implement the predictive control philosophy applied to PV+ES power plants. Similarly to the ageing program presented in 5.1.2, this one is also complementary to those in 5.1.1 and 5.1.3. In fact, it does not generate any reference but only performs the power plant operation's surveillance in order to avoid ESS saturations. Then, it modifies the existing references at any moment in case of need, being in this sense, a higher frequency control (intra-hour) implemented in a programming layer below the two main programs cited before. Its general structure can be appreciated in Figure 5.7.

According to this flow chart, the predictive control program also presents two stages: the initialization stage and the surveillance stage. During the first one the system is configured and some important parameters under study of the power plant as well as some parameters of the predictive control system are defined. Conversely, once configured, the program enters the surveillance stage along which the control system tries to predict if any saturation state (loss of plant production control) is likely to occur as a function of the current SOC and the future modeled power plant reference. In case a saturation success is detected within the prediction horizon, the program tries to anticipate that situation in order to avoid it. For doing so, it modifies the PV+ES power reference in the sense to counteract the tendency so that the saturation state is postponed or even completely avoided. Therefore, this program introduces new control options that can be also modified to improve the power plant behavior.

5.2. Sizing results for the two basic EMS.

The first important analysis performed in this Thesis corresponds to the sizing estimation required to know what ESS characteristics are needed to operate a PV+ES power plant under any of the two EMS introduced in the previous chapter, Sections 4.4.1 and 4.2.2. Therefore, this section establishes the ES ratings that will enable PV plants to operate according to two of the desired characteristics presented in Chapter I: with a power availability and predictability improvement or with a power production smoothening. In order to face this ESS sizing challenge, a set of parameters for both the generic PV+ES power plant characteristics, as that presented in 4.1, and in the EMS have to be defined. The set of parameters defining the case study analyzed in this Thesis is presented in Table 5.1.
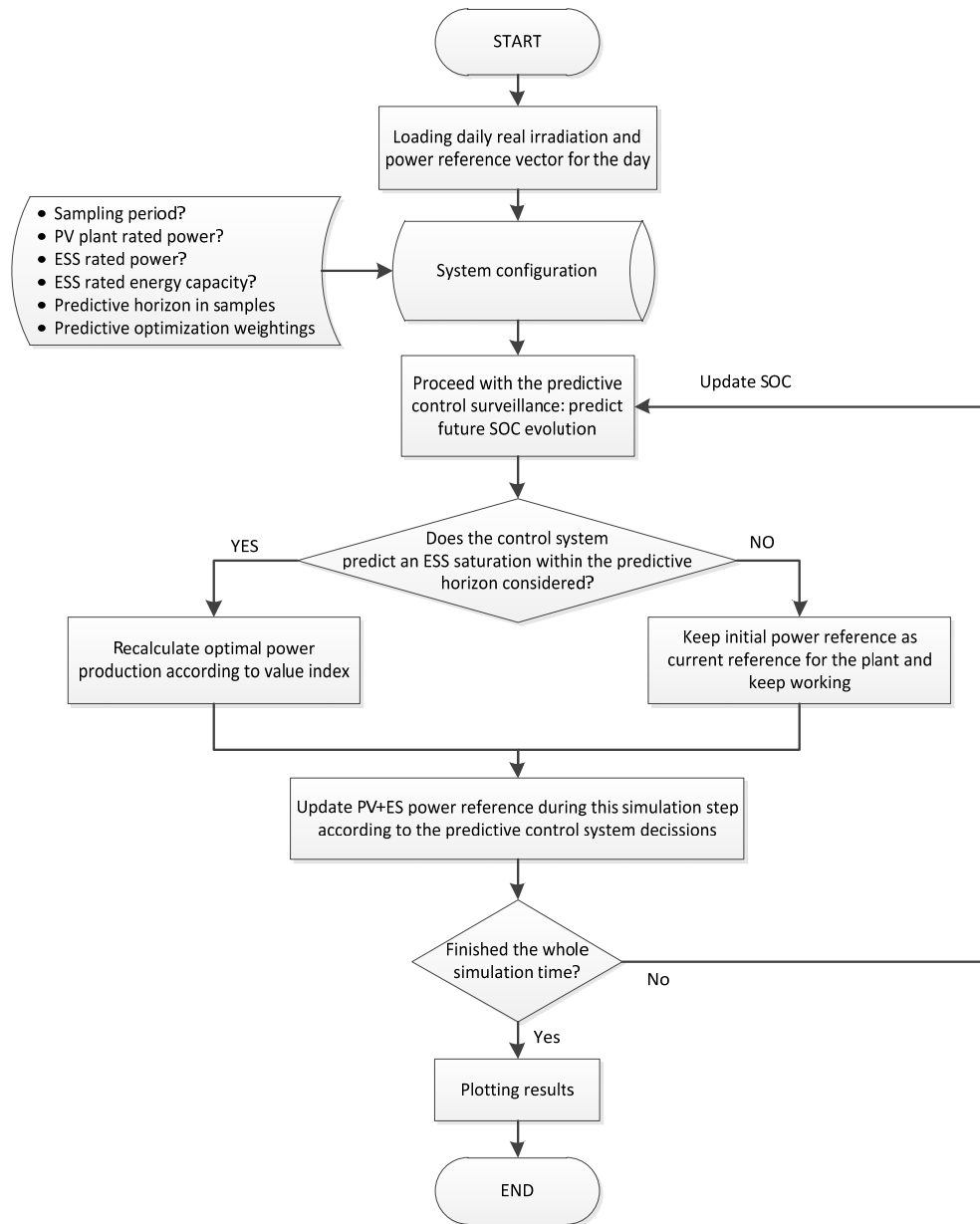
Figure 5.7 Scheme of the predictive control program.

The ES nominal power, the ES energy capacity and the ESS reference state-of-charge recovery time (τ_{SOC}) are assumed to be variable. In fact, these are the parameters which are going to be modeled and analyzed. The two first establish the ESS sizing here defined while

the latter one influence the sizing and introduces power distortions as will be analyzed in 5.2.3.

Parameter	Value
PV plant nominal power	40kW
ES nominal power	Variable
ES energy capacity	Variable
ES Charging efficiency	90%
ES Discharging efficiency	90%
Reference SOC	0.5
Location region	South of Spain
Capacity factor (C_f)	0.18p.u.
ES reference SOC recovery time	Variable

Table 5.1 PV+ES plant case study characteristics and values.

The rest of parameters are fixed. Note that the region or location where the study is associated influences the real irradiance experienced and the PV plant capacity factor (C_f). On the one hand, the irradiance data used in the analysis are those presented in Chapter II, which were obtained for a specific location and adapted to the plant rated power (40 kW). On the other hand for the C_f, the typical value for fixed PV power plants in that region has been assigned. This C_f coefficient was already defined in Chapter IV as the quotient between the estimated average power (P_{AVG}) in the period of time considered and the nominal PV power (P_N) of the plant. Therefore, it provides the annually-estimated average daily PV energy production per installed kW. A value which has been identified as 4.3 kWh / kW$_{peak}$ for this region and which is used as base for the per unit energy calculations and representations established on this Thesis. Thus, it is to note that all the analyses have been done in per unit system, and the base values used are the 40 kW for power and 172 kWh (40 kW$_{peak}$ x 4.3 kWh / kW$_{peak}$) for energy.

Therefore, after this brief introduction on the case study characteristics, the sizing requirements for the ESS working in a PV+ES power plant which can be operated under the two different EMS are presented and discussed in the following.

5.2.1. Constant power steps control strategy.

Regarding the improvement towards the desired deterministic production pattern of the PV technology, it was stated in the initial simulation results presented in Chapter IV that a relatively large fraction of the average power in a given time frame can be made available with a certain probability if ES is introduced, i.e. when using the constant power step control strategy, a certain amount of the PV nominal power can be guaranteed every day, in a

constant way, during a certain controlled duration. This effect or application is also known as PV power availability and predictability improvement, and is one of the ESS applications presented in Chapter I. Parameters such as power, energy capacity, τ_{SOC} and efficiency of the ES will determine how long this fraction of nominal power will be available along the year.

The ESS sizing analysis whose results are here introduced has been done using the program presented in Section 5.1.1. Different annual simulations have been carried out with the various possible configurations of the constant power step EMS. The constant power single step reference configuration has been mainly used in this analysis, being the step durations considered: 2, 4, 5, 6, 7, 8, 9, 10, 11, 12, 13, 14, 16 and 18 hours per day. For each of these step durations, the PV+ES power plant operation has been simulated but performing a systematic scanning of the different ESS power and energy capacities that could be implemented. For each of these possible ESS configurations, the simulation program provided the resulting annual evolutions for variable parameters such as the ESS state-of-charge level or the final PV+ES power exchanged by the plant with the EPS. From these two curves, the following interesting information has been extracted:

- On the one hand, the periods of time when the ES unit, or its corresponding connection power converter, saturate (i.e. the power required by the power plant operation exceeds the equipment rated values) while trying to track the reference. This can be extracted from the final PV+ES power exchanged curve for each of the possible ESS power ratings. In this sense, one can obtain what time along the year the PV+ES power plant is going to operate properly while tracking the defined configuration reference without activating the system power limit restrictions, for each of the possible ESS power ratings.

- On the other hand, the periods of time when the ESS energy is saturated (completely charged or discharged) can be also extracted from the SOC evolution curve for the various energy capacity ratings considered. As for the previous case, one can then obtain what time along the year the PV+ES power plant is going to operate properly while tracking the defined configuration reference without saturating (complete charge or discharge) for each of the possible ESS energy capacity ratings.

Therefore, for each of the multiple ESS configurations whose performance has been annually simulated working within a PV power plant, it would make no sense to represent their corresponding SOC and final PV+ES exchanged power annual evolution. These are

supposed to be approximately known, according to the control configuration, and could be reproduced at any moment, except for those periods when the ESS saturates (either because of power or energy limitations). Instead, a set of graphs summarizing the importance of these saturation periods (or, better yet, the non-saturation periods) have been developed and some of them here represented. These compile the extracted results for each of the multiple ESS configurations, representing on the Y axis the percentage of time with proper operation and on the X axis the ESS property which is progressively modified. Thereupon, as can be understood from the description just introduced, the goal for such figures is to easily define the annual availability of the PV controlled production (without saturation) operating the plant with a certain ES capacity under each of the EMS configuration.

In this sense, graphs such as those in Figures 5.8, 5.9 and 5.10, which are introduced in this document as examples for one type of configuration, have been obtained. While figures in the form of 5.8 or 5.9 correspond to the power saturation analysis, figures such as 5.10 correspond to the energy capacity saturation analysis.

Let's explain each of them in detail so that the reader can get a complete understanding of their content, what will help the comprehension of the conclusions:

- Figure 5.8 is the first of the three representative resulting figures. It depicts the different evolutions of the probability to operate the PV+ES plant without any power saturation as the ESS nominal power increases. Those evolutions are represented with different colors for each of the one single step possible configurations. The τ_{SOC} parameter presents a value equal to infinite for the simulated results represented here.

- Conversely, although representing the power ratings analysis too, Figure 5.9 faces the analysis from a different point of view. It depicts the nominal power (also in pu) required by the ESS in order to guarantee that the PV+ES system will not saturate along the percentage of time indicated by the line under each of the EMS configurations. This is represented, as for the previous figure for each different constant power single step reference configuration but these are introduced now on the X axis. The same τ_{SOC} parameter value is considered. Therefore, the curves represented in Figure 5.9 show the different percentages of time along the year when the rated ES power is not achieved. In this sense, when analyzing the ESS power sizing requirements obtained in that figure, one can appreciate how, although the minimum ES power to guarantee the one single constant step reference production

along the 80 % of the year is obtained for the 7 hours configuration, the minimum ES power needed to guarantee a high reference tracking (along the 99.5 % of the year) is obtained when the PV+ES plant is submitted to the 11 hours configuration.
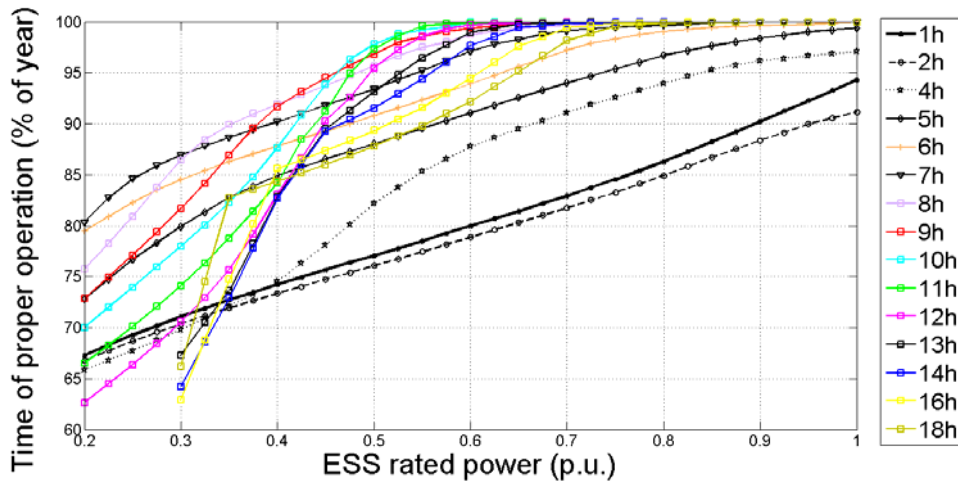
Figure 5.8 Time of proper operation (no power saturation) along the year under the one single step EMS for different ESS power values regarding the PV plant power capacity.
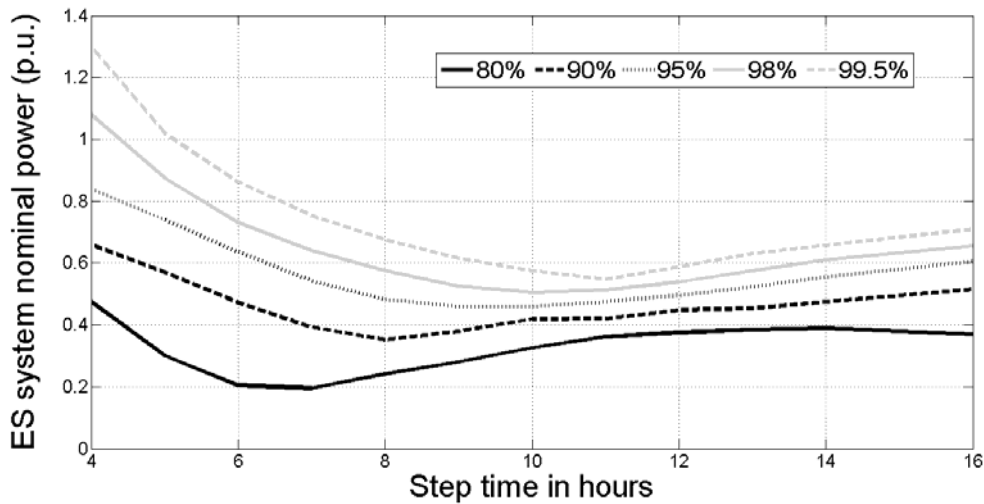
Figure 5.9 ES power to guarantee the reference tracking with different confidence levels.

Finally, Figure 5.10 represents the evolutions in the percentage of time along the year when the PV+ES power plant can track the different-duration power step references without saturation, as a function of the defined ESS energy capacity rating (τ_{SOC} = 24 hours in this

case). Therefore, this figure is the result of the energy saturation analysis extracted from the SOC evolution. By analyzing it the minimum energy capacity which guarantees the compromised production along the year with a certain percentage of probability can be established.

After describing the content of the different resulting figures some examples of lecture of their results are now described in order to further clarify them:

- For instance and regarding the power requirements, one can appreciate in Figure 5.8 how for ESS rated power values above 0.5 pu, the probability to avoid a saturation due to power limitations is above the 87 %, being below this percentage only for the one, two and four hours single constant step references. This can be understood by the fact that these tree references need to inject all the daily expected PV energy within less than four hours, what represents high values of power which cannot be assumed by the ES unit or its connection converter.

- Furthermore, it can be concluded from Figure 5.9 that if the goal is to establish a 10 hours single constant power reference to the PV power plant, the ESS power ratings required to guarantee that the PV+ES plant will properly track that reference during the 80 % of the time along the year is 0.325 pu. Similarly, the ES power capacity to guarantee that production with a 99.5 % confidence is 0.575.

- Regarding energy requirements and according to the information depicted by means of Figure 5.10, if the plant is operated with an eight hours single constant step reference, an ES energy capacity of 0.51 pu is needed to guarantee the reference accomplishment along the 90% of the year, and a capacity of 2 pu. to assure it during the 99.3 % of the time, that is 87.72 kWh and 344 kWh respectively for a 40 kW PV plant. Similarly, if the five hours single constant step reference is desired, the PV plant would need 0.2 pu to guarantee a correct operation around the 82 % of the year, and it could grant the reference tracking during the 97.5 % with an energy capacity equal to 1 pu.

Finally, it must be noted that all the evolutions represented in Figures 5.8, 5.9 and 5.10 depend on the value of the τ_{SOC} parameter if this one is used. The different values of this parameter modify the response of the system varying the saturated-time percentages. This phenomenon is further analyzed in Section 5.2.3.
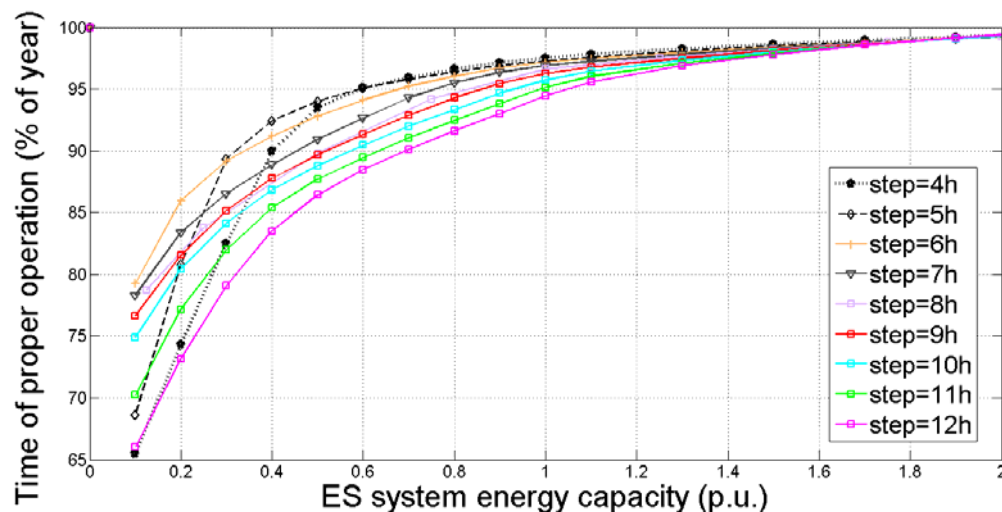
Figure 5.10 Time of proper operation (no energy saturation) along the year under the one single step EMS for different ESS energy capacity values (τ_{SOC} = 24).

5.2.2. Fluctuations reduction control strategy.

As regard to the fluctuations reduction EMS, the effect introduced by this strategy when applied to PV plants with ES comprehends a general smoothening of the PV output power, i.e. reducing the variability of the power production referred to an average value over a period (its standard deviation). This variability reduction was already stated on the frequency spectrum modification, which together with the standard deviation evolution table, were described in the initial results introduced in Chapter IV. Once that smoothening performance is confirmed, the amount of power and energy capacity required by the ESS to allow the different operation modes (filtering or smoothening degrees) for this EMS needs to be analyzed. These ESS requirements are introduced in this section.

To perform this analysis, the program presented in Section 5.1.1 has been used, as it was done for the previous sizing analysis introduced in Section 5.2.1. Again, different annual simulations have been carried out for the various configurations of the fluctuations reduction EMS. In this sense, the filtering values mainly evaluated in this analysis among all the possible range, are: 0.8, 0.85, 0.9, 0.95, 0.97, 0.99 and 0.995. For each of these filtering levels, the PV+ES power plant operation has been annually simulated, performing a systematic scanning of the different ESS power and energy capacity ratings that could be implemented. Therefore, the analysis mechanism is the same than that used for the previous

analysis. The resulting annual evolutions for the ESS state-of-charge level and for the final PV+ES power exchanged by the plant with the EPS are obtained also in this case from the different simulations and for each of these possible ESS configurations. Equally, from these two curves, the evolutions of the proper operation percentage of time along the year, as a function of the power or the energy limitations, have been processed. These evolutions are represented in Figure 5.11, for the case of the power saturation analysis, and in figures such as 5.12 and 5.13 for the case of the energy capacity saturation analysis.
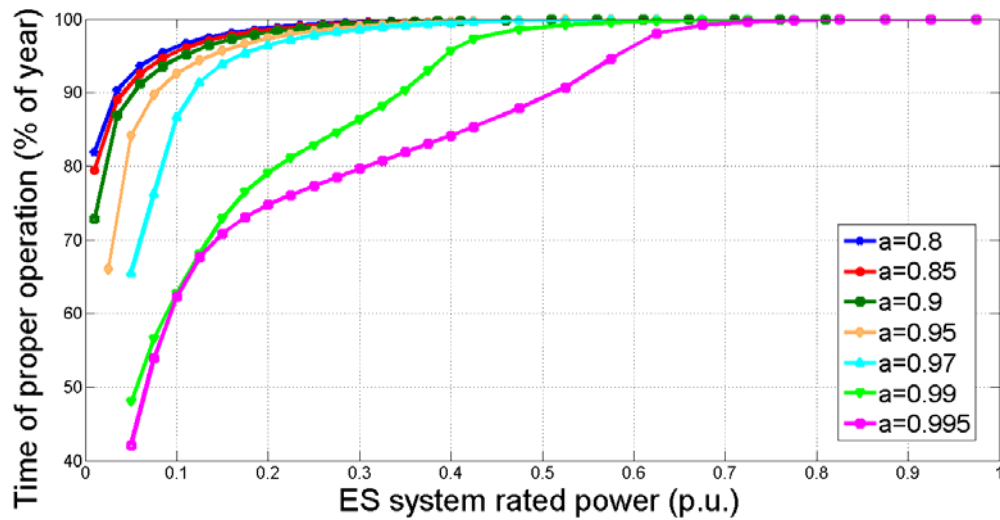
Figure 5.11 Time of proper operation (no power saturation) along the year under the fluctuations reduction EMS for different ESS power values (τ_{SOC} = 24 hours).

Thus, Figure 5.11 depicts the probability to operate the PV+ES plant along one whole year without any power saturation as a function of the ESS rated power. Those evolutions are represented with different colors for each of the different filtering levels, defined in the figure's legend, which have been considered in the analysis as possible configurations of the system. The τ_{SOC} parameter presents a value equal to 24 hours for the simulated results represented in this figure.

It can be appreciated in that figure how the power requirements to track this EMS' generated references are below those defined in Figure 5.8 for the constant power steps EMS. In fact, with an ESS nominal power of about 0.2 pu the percentage of time when the PV+ES system is going to avoid power saturations is over the 95 %, except for extreme filtering levels (a = 0.99 and a = 0.995) whose resulting reference diverges much from the

input PV production, as can be appreciated in Figure 4.14. Then, as an example according to Figure 5.11, it can be derived that if a 40 kW PV plant is operated with an ES whose power ratings are over 12 kW (0.3 pu), a proper operation regarding power saturations will be achieved along the 98 % of the time for filtering levels below $a = 0.97$.

On the other hand, Figures 5.12 and 5.13 represent the evolution in the percentage of time along the year when the PV+ES power plant tracks the different filtering level references without saturations, in this case, due to energy limitations; that is, it analyzes the proper functioning evolution as a function of the ESS energy capacity rating. The evolutions for corresponding considered filtering values' are represented by the colored lines with different types of markers. The value of τ_{SOC} has been assumed to be, respectively, equal to 24 hours and infinite time (complementary control action not active), for the simulations represented in these figures.

It can be concluded from them how, for the case of the fluctuations reduction EMS, the battery capacity must be progressively increased, as it was expected, when the PV production is desired to be more and more smoothed (a higher value of "a"), approaching it to the PV daily-averaged production. Putting this issue in numbers, a couple of examples can be introduced to help clarifying the results represented on the figures.

It can be extracted from Figure 5.12 that with an energy capacity equal to 0.02 pu, the smoothening level corresponding to $a = 0.9$ can be guaranteed along the 97 % of the year. Similarly, with an energy capacity of 0.15 pu, the smoothening level corresponding to $a = 0.97$ can be guaranteed during 98.7 % of the time along the year.

On the contrary, when the τ_{SOC} complementary control action is not active, Figure 5.13, the ESS energy capacity requirements increase. An energy capacity equal to 0.02 pu enables the PV+ES power plant to track the smoothening reference corresponding to a filtering level of $a = 0.9$ for only the 87 % of the year time. That represents a 10 % drop with regard to the previous case. Furthermore, times of proper operation above the 98 % of the year are not obtained for any filtering level, regardless of the ESS energy capacity taken, and even lower percentages, of around the 95 %, are only obtained for low filtering levels from 0.85 downwards.
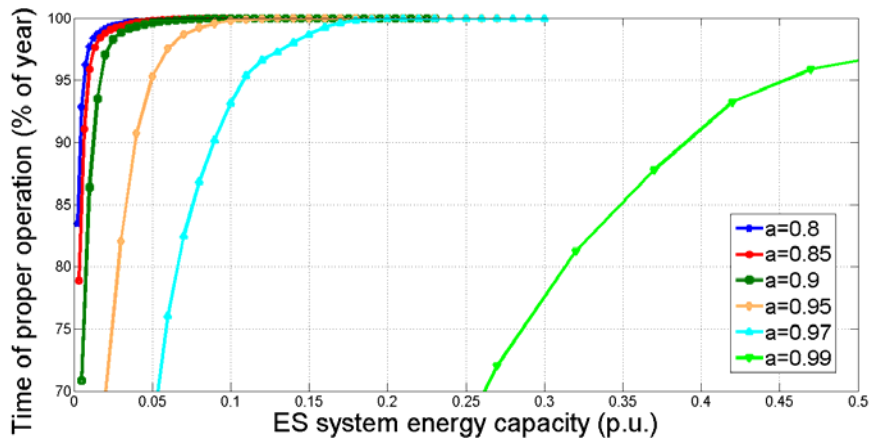
Figure 5.12 Time of proper operation (no energy saturation) along the year under the fluctuations reduction EMS for different ESS energy capacity values ($\tau_{SOC} = 24$).
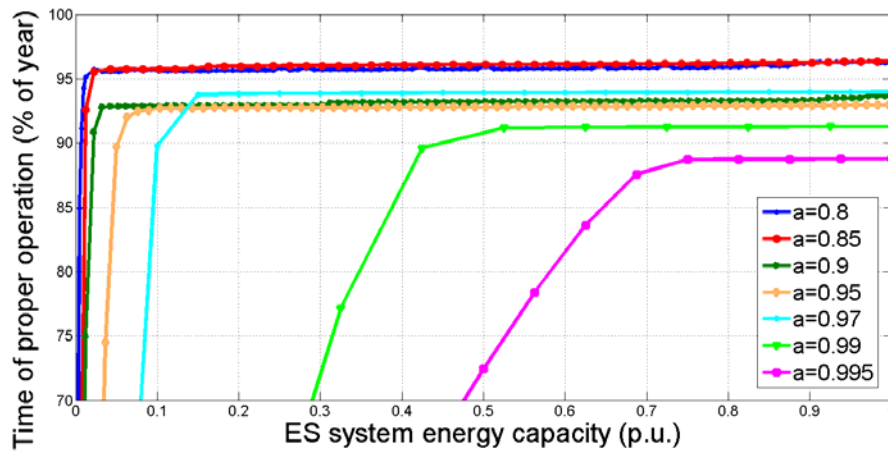
Figure 5.13 Time of proper operation (no energy saturation) along the year under the fluctuations reduction EMS for different ESS energy capacity values (τ_{SOC} = infinite).

Hence, the resulting graphs represented in this section depend on τ_{SOC} parameter value, as was also stated for the constant power steps EMS case. This influence is presented in detail in Section 5.2.3 although it can be clearly appreciated here when comparing the results in Figures 5.12 and 5.13. Therefore, sizing results presented here for the different filtering values are only valid when taken into account in combination with the τ_{SOC} value indicated on each figure's caption. Moreover, it can be concluded that the preferred state-of-charge complementary control action will have to be normally used in parallel to the fluctuations reduction EMS in order to avoid frequent saturations due to energy capacity limitations.

259

Finally, one can conclude from the results introduced in figures such as 5.10 (constant power steps EMS) or 5.12 and 5.13 (fluctuations reduction EMS) how increasing the difference (instantaneous distance) between the PV real production and power plant reference provided by any of the EMS, require a higher ESS energy capacity to obtain the same level of confidence. In fact, and not surprisingly, as it can be observed by comparing results in 5.10 and 5.12 (both obtained for the same τ_{SOC} value), the storage requirements for a significant reduction in the power variations (*a = 0.99* and upwards) approach those energy capacity requirements for a large increase in availability (a long duration constant step with a power level similar to the average PV power).

5.2.3. Tau SOC effect and approximated tradeoff.

After obtaining some reference results on the ESS capacity ratings required to operate the PV plant with ES under the two main EMS considered, this section introduces a complementary analysis to those just introduced in the Sections 5.2.1 and 5.2.2.

As previously cited, this analysis is focused on the study of the variation in the ESS energy requirements previously presented due to the introduction in the control system of the ESS reference state-of-charge (SOC) recovery time, τ_{SOC}. This complementary control action, which was already presented in Section 4.3.1, is characterized by its main goal which is to be able to reduce or limit the ESS energy power requirements by forcing the system to automatically recover a defined SOC in a given time. Therefore, when activating this option the SOC evolution is not a float parameter anymore and the control system avoids it to oscillate freely. The ES unit energy capacity requirements are in this way effectively reduced, as can be extracted from the comparison of Figures 5.12 and 5.13 described in the previous section.

However, when introducing this action, its performance implies the ESS to suffer a modification on its functioning (a power distortion) since not all the power required by the reference will be exchanged but only the power theoretically demanded minus the power that the control system estimates the ESS needs to recover its SOC_{ref} within that defined τ_{SOC}. The effect of this distortion was already presented in the previous chapter, with Figure 4.16 as an example depicting the outlook of the PV+ES power production with different values of τ_{SOC} implemented for each of the EMS mainly considered in this Thesis.

Thereupon, a tradeoff between the generated power distortion undesirable effect and the reduction obtained in the profitable ESS size due to the τ_{SOC} introduction must be achieved.

A detailed study of the effect produced by different possible values of the τ_{SOC} on the ESS energy requirements to define the tradeoff solution is introduced in the following.

For that purpose, those simulations performed for the two previous analyses and their compiled results were profited, complementing them with another set of annual simulations, to analyze the τ_{SOC} influence. These extra simulations were carried out under the same conditions (the same real irradiance solar data sampled every 120 seconds) and also adapted to the 40 kW PV power plant with its realistically simulated power curve production along the year. All the analysis has been also done in per unit though; using as base the same reference. Therefore, the ESS capacity ratings, required to be able to track the power reference without saturation during a certain percentage of time along the year, has been estimated for various EMS configurations while varying the defined τ_{SOC} value. Figures 5.14 to 5.20 agglutinate some of the resulting proper operation evolutions, as a function of the τ_{SOC} value, which help extracting some interesting conclusions on the τ_{SOC} influence. Results are described in detail in the following.

a) Results for the constant power steps EMS

For the case of the constant power steps EMS, just one single step references have been analyzed too. In this case, the durations under analysis range from 4 to 12 hours per day. For each of them, eight different τ_{SOC} values have been analyzed. These values are: 0.5 hours, 6 hours, 24 hours, 72 hours, 120 hours, 168 hours, 336 hours and infinite time.

The possible combinations are quite a lot. Thus, among all the different simulations performed, just a few combinations are reported. In this sense, Figure 5.14 is devoted to the variations in the ESS power requirements for a 1 kW PV power plant as τ_{SOC} varies ("case "a" τ_{SOC} = 6 hours, "case "b" τ_{SOC} = 24 hours and "case c" τ_{SOC} = 168 hours) which can be compared with those in Figure 5.9, obtained for the case when τ_{SOC} is equal to infinite.

Therefore, although not significant changes on the ESS power ratings, required to operating the plant under the different duration one single step constant power references with the same liability, are identified, it is true that a certain variation can be appreciated indeed among these graphs as a function of the value defined for the τ_{SOC} parameter.

On the other hand, variations in the energy capacity requirements must be analyzed too. To do that, figures as those represented in Figure 5.15, Figure 5.16 and Figure 5.17 can be used.
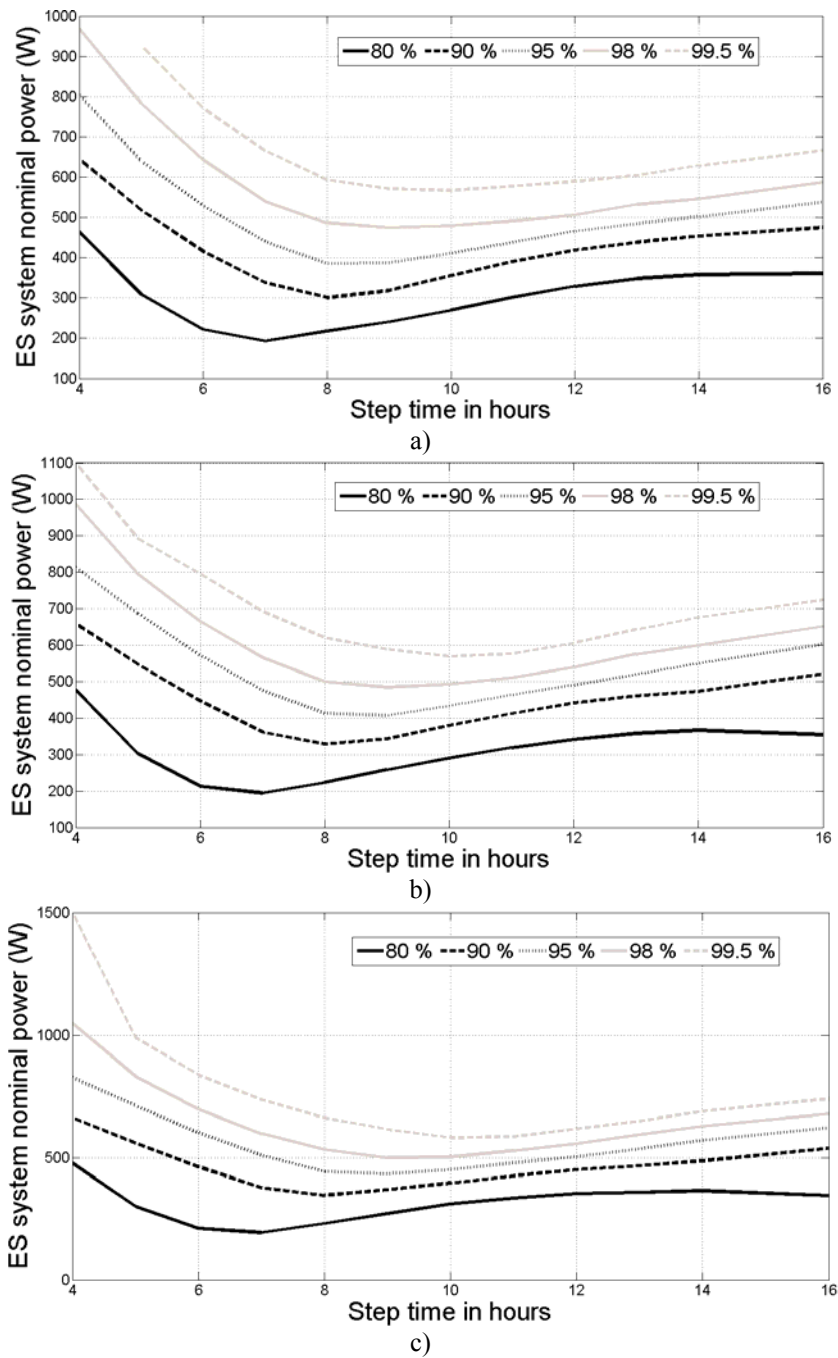
Figure 5.14 ESS power requirements evolution for different power step lengths as a function of the τ_{SOC} value: a) for 6 hours, b) for 24 hours, c) for 168 hours.

a)

b)

c)
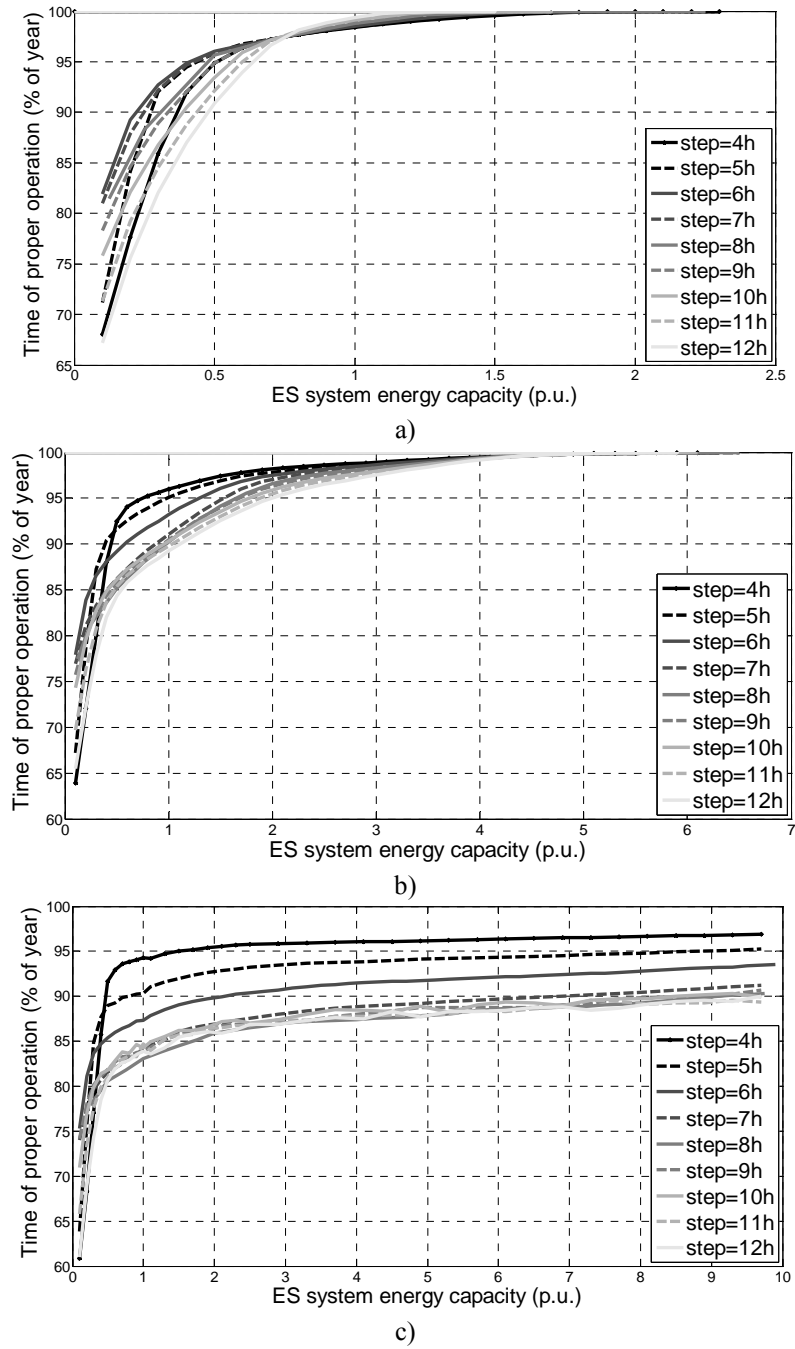
Figure 5.15 ESS energy requirements evolution for different power step lengths as a function of the τ_{SOC} value: a) for 8 hours, b) for 72 hours, c) for an infinite value.

For example, Figure 5.15 establishes the resulting evolution curves for the different step durations, as that in Figure 5.10, but calculated for different values of τ_{SOC}. More precisely, the three graphs in Figure 5.15 represent the resulting evolutions for the three values of: τ_{SOC} equal to 8 hours, τ_{SOC} equal to 72 hours, and τ_{SOC} with a value equal to infinite, respectively.

It can be observed in these figures how, as τ_{SOC} increases its value (passing from "a)" to "b)" or from "b)" to "c)") the ESS energy capacity requirements do also increase. Just note also how the abscissa axis contains values till 2.5, 7 and 10 pu, respectively.

But the influence of the τ_{SOC} parameter over the energy capacity requirements can be also observed from another point of view which, maybe, offers further information. In this sense, Figure 5.16 represents the percentage of time that the PV power plant with ES can track the six hours daily single step constant power reference without SOC saturation as a function of the nominal ES energy capacity for the different implemented values of the τ_{SOC} parameter. Similarly, Figure 5.17 contains the PV+ES power plant proper functioning evolutions achieved for the case of tracking a ten hours daily single step constant power reference and also for the different implemented values of the τ_{SOC} parameter.

Therefore, these two figures compare the operation of the power plant while trying to track a same reference with different implemented values of τ_{SOC}. It stands out in both of them how the lower the value of τ_{SOC} the smaller the required energy capacity for the ESS, hence minimizing its cost but also increasing the power distortion.
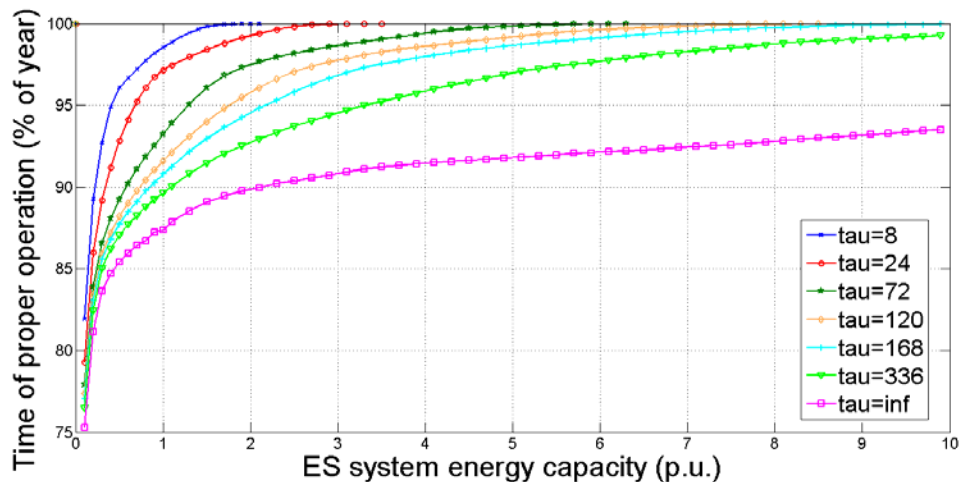
Figure 5.16 ESS energy requirements for a six hour power step as a function of τ_{SOC}.
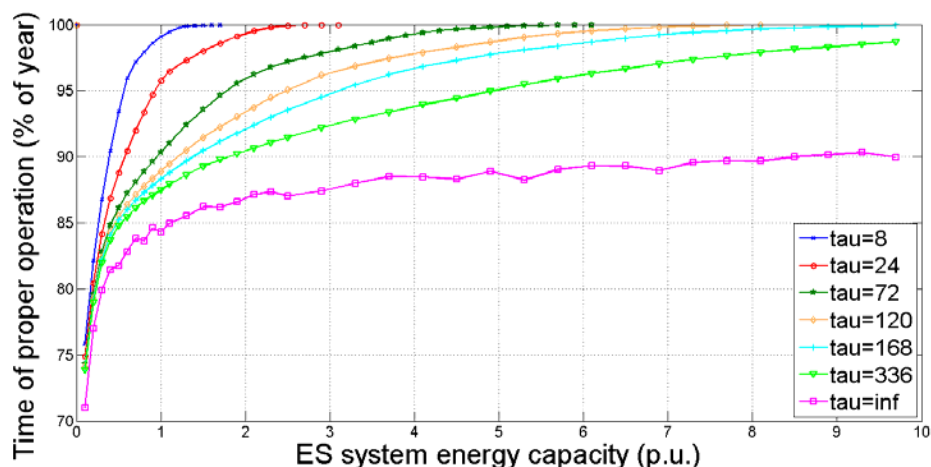
Figure 5.17 ESS energy requirements for a ten hour power step as a function of τ_{SOC}.

The following conclusions can be extracted from the multiple simulations performed whose results are mostly summarized in those figures:

- For fix step duration, as τ_{SOC} gets larger, a higher ESS energy capacity is required to be able to track the reference properly the same percentage of time. Or what is the same, as τ_{SOC} presents a lower value (higher effect and higher deformation of the reference), the ESS capacity needed to properly track that reference is reduced. This confirms that higher deformations in the production lead to lower ES capacity needs.

- If τ_{SOC} = infinite, no automatic control of the SOC_{ref} level is done. Then, percentages of time without saturation higher than 95 % cannot be achieved.

- For a same τ_{SOC} value, if it is over 72 hours, reference steps under 6 hours per day require smaller ESS energy capacities than longer step references. However, if $8h < \tau_{SOC} < 24h$, steps between 5 and 8 hours present similar evolutions.

- No important effect is detected when varying the τ_{SOC} value on the ESS power rating requirements.

Therefore, one should generally operate the power plant with τ_{SOC} values being a tradeoff between the important deformations introduced by values under 24 hours and ESS higher energy capacity requirements for values over 24 hours. For instance, using a τ_{SOC} equal to 24 hours instead of 8 hours represents increasing ESS capacity needs in around the 50 %. Furthermore, for the same change in τ_{SOC}, to achieve times of no saturation of up to 95 %

265

represents an increase in the ESS capacity of around two regardless of the constant power step duration. However, to get percentages of time over > 95 % of the year with proper operation (no saturation), ESS capacity variations among the different step durations are relatively small. Very high energy capacity values, between 0.75 pu and 2 pu, have to be considered though.

a)

b)
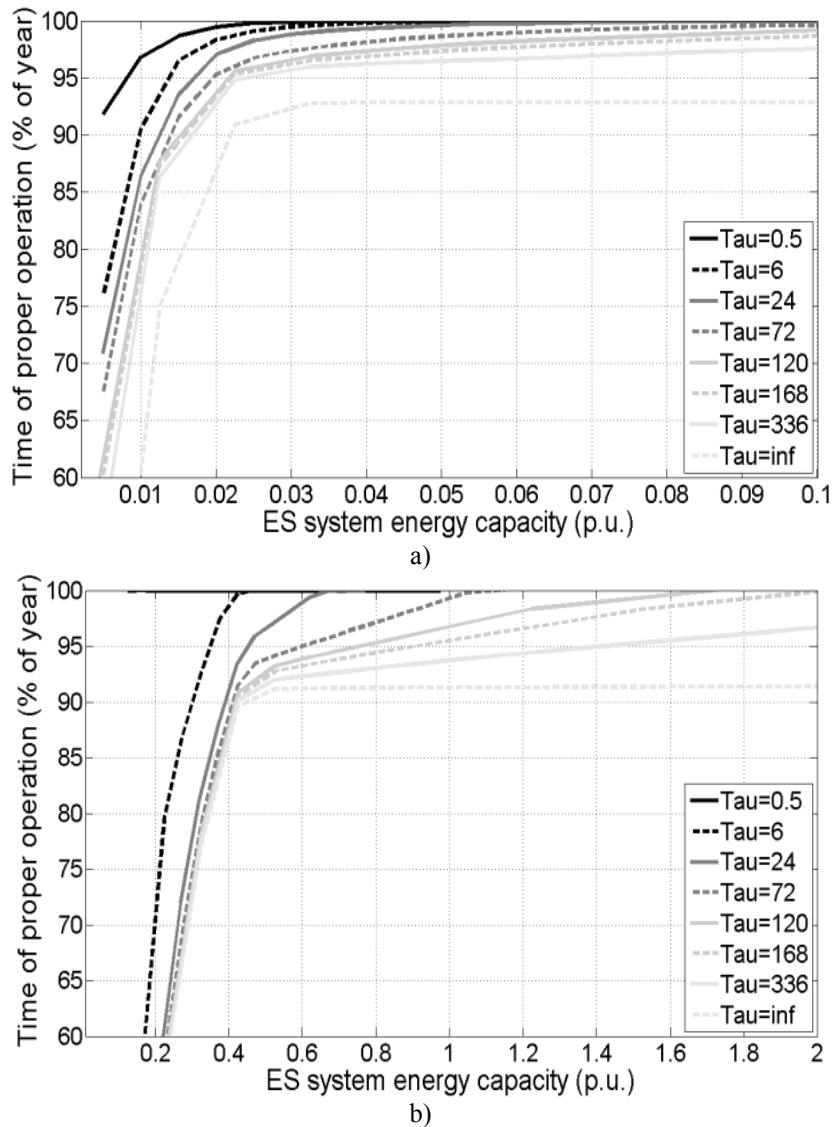
Figure 5.18 ESS energy requirements as a function of τ_{SOC} for: a) filtering level "$a = 0.9$", b) filtering level "$a = 0.99$".

a) Results for the fluctuations reduction EMS

For the case of the fluctuations reduction control strategy, some simplifications have been considered too, since many degrees of filtering can be considered. Only seven filtering levels have been analyzed (a = [0.8, 0.85, 0.9, 0.95, 0.97, 0.99, 0.995]). These have been combined with eight different τ_{SOC} values (0.5h, 6h, 24h, 72h, 120h, 168h, 336h and the infinite value).

Results for some of those combinations are presented in Figure 5.18 as well as in the Tables 5.2 and 5.3 with their associated graphical representations (Figure 5.19 and Figure 5.20, respectively).

In this sense, Figure 5.18 represents different evolutions of the energy requirements to achieve a certain degree of confidence to avoid functioning saturations along the year. The different evolutions correspond to varying τ_{SOC} values associated to this EMS with filtering levels of a = 0.9 and a = 0.99, respectively.

	τ_{SOC} = 0.5	τ_{SOC} = 6	τ_{SOC} = 24	τ_{SOC} = 72	τ_{SOC} = 120	τ_{SOC} = 168	τ_{SOC} = 336	τ_{SOC} = inf
a = 0.80	0	0	0.0029	0.00334	0.00346	0.00366	0.00373	0.0051
a = 0.85	0	0.0038	0.0050	0.0055	0.0083	0.0085	0.0088	0.0113
a = 0.90	0	0.0064	0.0079	0.0088	0.0102	0.0105	0.0109	0.0188
a = 0.95	0	0.0224	0.0284	0.0319	0.0337	0.0345	0.0356	0.0415
a = 0.97	0.0152	0.0515	0.066	0.074	0.0872	0.0881	0.0892	0.0901
a = 0.99	0	0.2287	0.313	0.332	0.338	0.341	0.345	0.348
a = 0.995	0	0.448	0.5835	0.6155	0.624	0.629	0.6375	0.647

Table 5.2 Minimum energy capacity required (in pu) to obtain 85% of time without saturation.
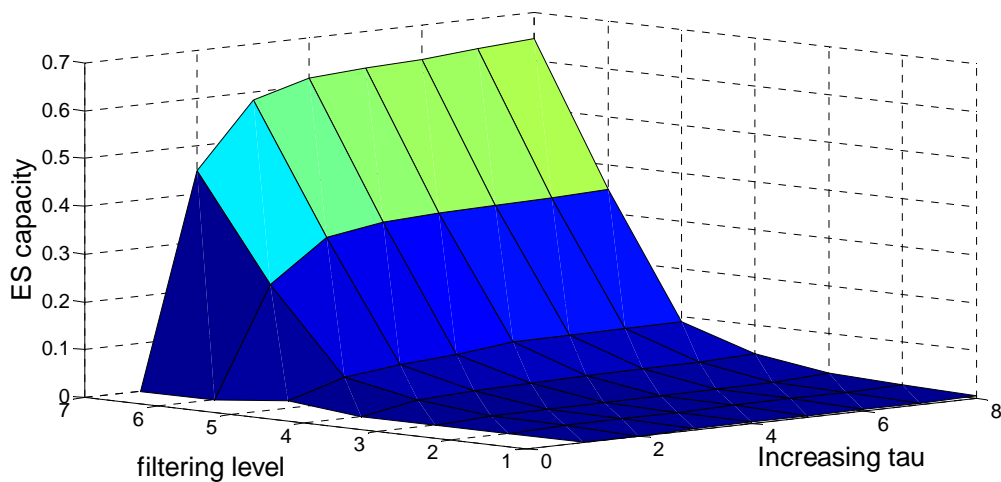
Figure 5.19 Graphical representation of the values in Table 5.2.

To get a more detailed idea of the τ_{SOC} influence while trying to summarize the big number of simulations which would be hard to represent in figures as the one in Figure 5.18, Tables 5.2 and 5.3 have been developed. These synthetize the amount of energy capacity that is required by the ESS in order to enable the PV+ES power to track the fluctuations reduction power reference without saturation, as a function of the different values of $\tau_{SOC.}$.

	$\tau_{SOC} = 0.5$	$\tau_{SOC} = 6$	$\tau_{SOC} = 24$	$\tau_{SOC} = 72$	$\tau_{SOC} = 120$	$\tau_{SOC} = 168$	$\tau_{SOC} = 336$	$\tau_{SOC} = \text{inf}$
$a = 0.80$	0.00448	0.00551	0.00658	0.00714	0.00737	0.00757	0.00802	0.012
$a = 0.85$	0.00575	0.00795	0.0094	0.00998	0.0121	0.0122	0.0123	0.02071
$a = 0.90$	0.0082	0.0137	0.0172	0.0195	0.0217	0.0222	0.0242	inf
$a = 0.95$	0.0159	0.0392	0.0494	0.0577	0.063	0.0705	0.098	inf
$a = 0.97$	0.0259	0.0885	0.1084	0.1219	0.147	0.1585	0.2295	inf
$a = 0.99$	0	0.349	0.453	0.602	0.757	0.907	1.421	inf
$a = 0.995$	0	0.5551	0.7435	1.059	1.354	1.643	2.633	inf

Table 5.3 Minimum energy capacity required (in pu) to obtain 95% of time without saturation.
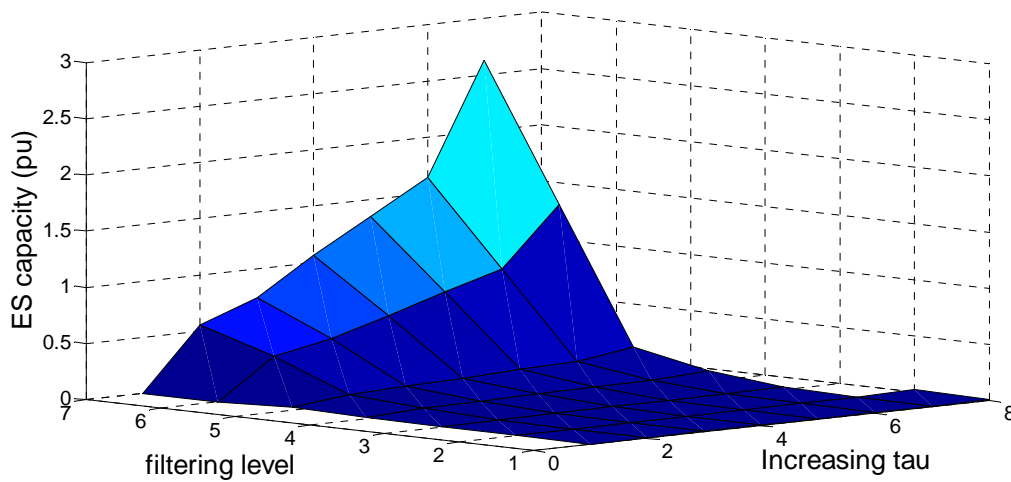
Figure 5.20 Graphical representation of the values in Table 5.3.

As for the previous strategy whose effects have been analyzed, some conclusions can be extracted here from the different figures and tables represented above. These are:

- For a fix filtering level, if τ_{SOC} increases, higher ESS energy capacity is required to track the reference the same percentage of time without saturation.

- For a fix τ_{SOC}, if the filtering level is increased, the ESS energy capacity required to track the reference a percentage of time without saturation increases too.

- To achieve times of proper operation of up to 90 % of the annual period, regardless of the filtering level, by varying τ_{SOC} from 6 to 336 hours represents that the needed ES energy capacity is increased in a range from 40 % to 80 %. However, in all these situations, ES energy requirements are kept under 1 pu, hence, no large ESS are required in absolute values.

- On the other hand, for times of proper operation over the 90% of the year, the τ_{SOC} influence is much more important for filtering levels over "$a = 0.9$".

- Till that filtering level, "$a = 0.9$", evolutions are similar to that of the previous points, but from that value upwards, ES energy requirements are more than doubled when varying τ_{SOC} from 6 to 336 hours.

- For filtering levels over "$a = 0.95$", if the time of proper operation is desired to be over the 90%, the use of τ_{SOC} values under 24 hours seems compulsory so as not to require huge amounts of ESS energy capacity. However, the generated power is distorted to a great extent within this range of τ_{SOC} values, as previously introduced. That is due to the fact that the filter time constant for these filtering levels approaches the value of the τ_{SOC} (40 minutes for 0.95, 3h20min for 0.99 and 6h40min for 0.995). Therefore, for high filtering levels, it is reasonable to achieve once again a tradeoff between the acceptable deformation in the power injected into the EPS (referred to the reference) and the value of τ_{SOC} which allows keeping the ESS energy requirements as low as possible. Nevertheless, one can conclude that, mainly for economic reasons, PV plant operators will tend to work with τ_{SOC} values as small as possible, reducing the ESS energy requirements.

b) Conclusions for the τ_{SOC} influence

The aim of this study has been to analyze one of the main issues in the integration of ESS into PV power plants, which corresponds to the variations experienced in the energy requirements of ESSs (mainly in the energy capacity needs) due to the different possible values of the ESS complementary control action called preferred state-of charge with its associated "reference SOC recovery time". These variations together with the deformation experienced by the total injected power under the two different EMS as a function of the varying τ_{SOC} have been analyzed in this section.

From the different graphical representation introduced in this document, one important conclusion that can be extracted is that for any of the two EMS analyzed, it stands out that

the τ_{SOC} influence it is much more important for the energy capacity analysis than for the power requirements analysis. While for the latter, no important modifications in the proper functioning time evolutions is detected, for the energy case the τ_{SOC} variations modify the sizing requirements in a great extent.

In this sense, it can be seen that, as τ_{SOC} gets larger in any of the strategies (complementary control less demanding), a higher ESS energy capacity is required in order to guarantee the same percentage of time along the year with proper operation (no saturation of the ESS). This is of course not economically beneficial for the power plant promoter due to the increase in the installation costs. However, also as τ_{SOC} gets larger, the total final production of the plant gets more similar to the theoretical reference imposed by the EMS, what it is really interesting from the plant operator point of view. This simplifies the operation because produces a more certain and predictable production. A tradeoff between these two divergent trends should be achieved after pondering one factor and the other, mainly in economic terms.

A possible solution that could be considered in order to avoid the big deformations introduced in the reference by low values of τ_{SOC} could be to take profit of the off-peak hours to discharge or recharge the storage in order to start the next day operation at the SOC_{ref}, rebooting the system every day and cancelling energy deviations produced in previous days. That is, the SOC_{ref} recovery control could be activated only during night hours or during those periods of time when the PV plant has no power compromise with the system operator. However, this faces the issue of the different tariffs which are applied to the electricity consumption (which could be used to recharge the ESS at night) and to the PV electricity produced. This is an issue which should be solved to allow this operation.

5.2.4. Conclusion for the ES basic sizing.

The relation between the ES power and energy ratings and the extended benefits obtained in a particular PV power plant with ES for each of the EMS have been analyzed and quantified. While the constant power control strategy allows a clear reorganization of the production, making it more constant, i.e. less stochastic and hence more predictable or deterministic, the power fluctuations reduction strategy reduces mostly the high frequency variations. Accordingly, power and energy requirements for both strategies differ significantly being in general much more significant for the constant power steps EMS.

To put some numbers to this issue regarding the ratings analysis, the ESS energy and power requirement, for a significant improvement in the availability along the year (power constant steps EMS), is found to be among 50 % to 200 % of the yearly average energy produced in one day and from 50 to 60 % of the rated power of the PV plant. Thus, for the case of a 40 kW PV plant, an ES unit rated 20 kW and 85 kWh would guarantee tracking the reference during 90% of the time along the whole year for an eight hours daily constant power step, with a τ_{SOC} below 72 hours. With much less storage requirements, ranging from 5% to 30% in terms of energy capacity and around 50% in terms of power, a significant power variability reduction (fluctuations reduction EMS) can be achieved. Therefore, once a plant is designed to operate under any EMS, it could adopt a different mode of operation to improve its incomes at a given moment (subject to economic interests). This is an option to be considered by the plan operator depending on the electricity market prices. As an example, if the plant is designed to be operated according to constant power control EMS and its high energy capacity requirements, it will present capacity enough so as to adopt the fluctuations reduction EMS profiting the extra available energy capacity to provide some ancillary services as those introduced in Chapter I (although probably not the other way round).

In this sense, different ES technologies could also be applied for each case, and even a combination of technologies could be considered for flexibility of the plant. From the possible ESS candidates reviewed in Chapter III, Lithium ion batteries are those considered to fit the best with the calculated rating needs for medium size PV power plants operating under the constant power steps EMS. However, this type of battery technology could be combined with ultracapacitors in small PV power plants for being used under the fluctuations reduction EMS.

In a general way one can conclude that, an ESS can hence be designed not to guarantee a desired reference perfect tracking at all times but to provide an improved degree of probability to get a certain production according to that reference within a given timeframe. This improved probability depends on the ES energy capacity, on the ES rated power, on the efficiency of the ESS and other considered control parameters.

It is to point out though, the big handicap introduced by the stochastic nature of the solar resources which involves large PV power production variations as a function of two main factors: its geographical dependency and the irregular irradiance evolution along the year. The first of them implies that the results presented in this Thesis have an important local

component and cannot be directly extrapolated to any different location. And the second one could suggest that an extended study should be performed analyzing the percentages of time with proper operation on the different months of the year (month by month).

Despite this handicap, the results introduced in this document, and particularly those in this section, offer a valuable and interesting tool for PV plant designers to obtain good approximations of the ESS ratings required in their plants to operate them under a specific regime of production. In other words, by using the figures presented in this document (and some complementary ones), the PV plant designer can calculate the ES characteristics that would be statistically required in order to operate the plant under any of the EMS evaluated with a certain degree of confidence. This can be useful for PV plant designers as a roughly way to estimate the costs of the PV+ES potential power plants and the hypothetical economic incomes they could receive in a properly adapted electric market.

Therefore, one can finally conclude that the proposed EMS with the ESS required ratings analysis, and its corresponding results, presented here show that a PV power plant can achieve advanced performances being capable to reduce the PV production variability and improve its predictability. In this way, the goal of reducing the stochastic nature of the solar resource and turn PV plants into deterministic systems can be certainly obtained.

5.3. UC sizing to be used in a PV+ES power plant under the constant power steps EMS.

In order to avoid the problems related to the power distortion introduced by the τ_{SOC} activation, an advanced analysis has been executed for the constant power strategy. This analysis, which combines simulation and experimental results obtained with a test bench containing ultracapacitors (UC), is based in the daily-energy adapted constant power step strategy which was introduced in the previous chapter and represented on Figure 4.8. Note that some proposal combining UC with PV power plants have already been published in the literature, most of them combining UC with other technologies as ESS solution [17, 18], or applying UC alone in isolated PV sources for feeding pulsing loads [19].

The goal of the analysis here presented is to try to determine the optimal UC' ratings (minimizing the energy capacity requirements) to be installed in a PV power plant which is desired to operate under the one single constant power step EMS. This minimization can be approximately achieved with the complementary control actions presented in Chapter IV; i.e. an accurate weather forecast combined with an on-line surveillance of the real PV power

generated along the day and the corresponding analysis of the expected production trend as well as the introduction of a predictive controller which ultimately adjusts the reference. These complementary control actions will help defining a daily constant power step reference adapted to the estimated daily PV energy yield and, in case of need, adjusting this reference by accounting the internal system losses and the possible deviations in the real daily PV evolution (referred to the estimated one) so as to finish providing the same amount of energy that the PV panels do generate each day along the year. In this sense, a more or less constant reference in duration will be obtained although these will be variable on its daily power value, Figure 4.8.

By doing this, the ESS should finish the daily operation at the same SOC it started each day (energetic balance), avoiding in this way the activation of the τ_{SOC} control and its corresponding distortion while obtaining a similar effect on the annual SOC evolution. Moreover, lower ESS energy capacities than those estimated for the analyses previously introduced in this chapter are required in this case to track a same type reference. This can be understood from the fact that the real daily PV production rarely coincides with its corresponding month's average production (which has been only statistically estimated), assumption which has been accepted for those analyses presented in Sections 5.2.1 and 5.2.2.

Therefore, a sizing analysis of a real ESS (considering in this case UC as the ES technology) installed in PV power plants to be operated according to that EMS just introduced is presented in the following.

Figure 5.21 Global appearance of the test bench used for the analysis. Courtesy of Ikerlan.

5.3.1. Test bench introduction and characteristics.

Once again, a PV+ES power plant with the configuration already described is considered although introducing in this case real components which have been tested in the lab in order to identify their real performance and underwrite in this way the simulated final sizing which results from this analysis procedure.

Experiments have been performed in the installations of the Ikerlan[2] research center. These have been done using a test bench which includes the different components that can be found in the PV+ES proposed power plant and which has been there developed at Ikerlan. The appearance of this assembly is shown in Figure 5.21.

Thus, this test bench allows reproducing the real behavior that would present a 2.5 kW PV power plant with ES. These components are enumerated and described as follows:

- The PV plant emulator: a configurable and programmable dc/ac power converter is used as a PV plant emulator. This converter has been developed at the Ikerlan center itself and operates as a programmable source which can reproduce any power shape introduced as reference in the form of a variable dc input voltage. It presents a nominal power of 2.5 kW which has to be injected as active power (always in phase with the voltage) into a 230 V one phase grid. Thus, it does not present the possibility to work on three phase system. However, although initially designed to operate with fuel cells, this converter has been very useful to reproduce the different PV daily curves being capable to emulate perfectly both clear and cloudy profiles with the sole limitations of its rated power. This can be observed in the different figures with results from the experiments introduced in Section 5.3.2. The PV power emulated by this converter has been represented with a green continuous line in all of them. This converter can be observed in the global test bench picture represented in Figure 5.21.

---

[2] The IKERLAN Technology research Centre is a private non-profit making entity with a public service vocation settled in Arrasate (Basque Country) and created in 1974 at the initiative of a group of companies and entities which today form part of the MONDRAGON Corporation. It is a reference center for the innovation and comprehensive development of mechatronic and energetic products. It also actively innovates in design and production processes. IKERLAN has over 35 years of experience in combining and applying mechanics, electronics, computing, microtechnology and fuel cell technologies.

Among the different components, it is located on the table on the top left of the figure. The two conductors which feed its dc bus, proceeding from the dc current source located on the floor can be clearly appreciated. This dc current source substitutes the potential PV panels providing the dc energy that is transformed by the converter to emulate the PV power plant. A close-up image of the converter where some components can be observed in detail is introduced in Figure 5.22.
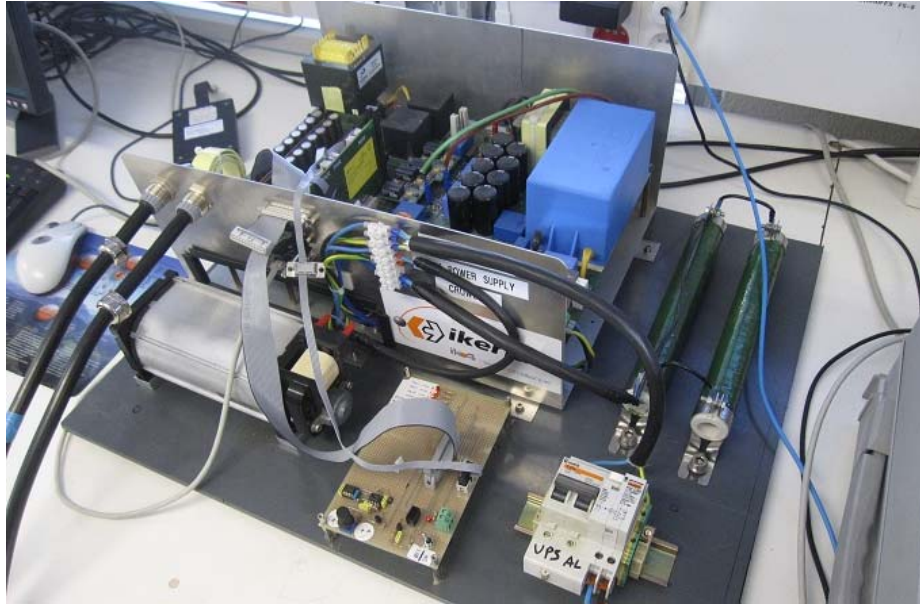
Figure 5.22 The dc/ac power converter used to emulate the PV power plant. Courtesy of Ikerlan.

- The ES unit: UC were selected and used as ES technology for the experimental tests introduced in this section due to their immediate compatibility to electric power systems, the lab conditions and the pretended experimental application. In this sense, among the Maxwell Technologies' manufacturer heavy transportation series of UC modules, the model BMOD0063 P125 B03 has been integrated within the test bench due to its power and energy capacity ratings as well as its voltage operation level. Its principal characteristics are summarized in Table 5.4. This UC package is a high performance ESS which incorporates balancing, monitoring and thermal management capabilities to ensure proper charge/discharge performance, high reliability and long operational life.

Parameter	Value
Rated capacitance	63 F
Rated voltage	125 V
Specific power	1.8 kW/kg
Stored energy	102 Wh
Specific energy	2.4 Wh/kg
Lifetime	1500 hours at max T°
Lifetime in cycles	$1 \cdot 10^6$ cycles

Table 5.4 Ultracapacitors package electrical specifications.

The appearance of this Maxwell technologies UC package is clearly appreciated in Figure 5.23, where a voltmeter showing the UC voltage has been included. The instantaneously registered voltage value that can be appreciated on the pictures (106.06 V) means that the UC unit contained at that moment a SOC equal to 63 % of its capacity.
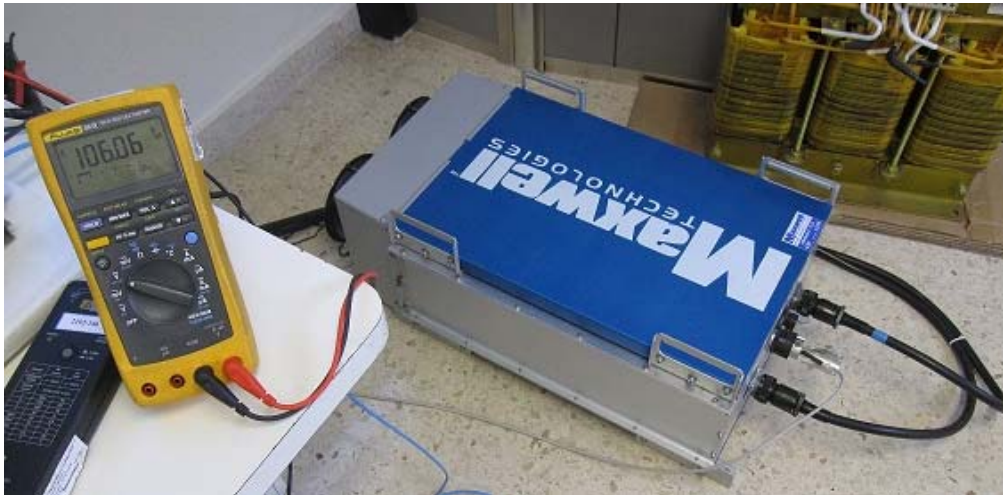
Figure 5.23 UC package from Maxwell technologies used for the analysis. Courtesy of Ikerlan.

- The ES connection converter: this is another configurable and programmable dc/ac power converter, with some different characteristics to the one used as PV plant emulator, which has been used to connect the UC package to the one phase 230 V ac grid implemented in this test bench. This converter has been also developed at the Ikerlan center itself and operates as a programmable source capable to exchange up to 3.6 kVA in the form of both active and reactive power. Thus, it provides some extended functionalities over the previous converter since it has been designed to

operate within microgrids. In this sense, it could also operate isolated from the grid, taking in this case the responsibility to fix the voltage and the frequency in the local grid as well as locally balancing energy flows (coupling generation and demand). Anyway, it has been used in these experiments in the connection mode allowing the exchange of power between the UC and the PCC of the plant so as to guarantee the overall PV+ES production to be in accordance with the power plant defined reference. Although not very clearly, this converter can be also observed in the global test bench picture represented in Figure 5.21. It is located on the table too but on the top right side, next to the voltmeter previously cited. A close-up image of this converter can be also observed with further detail in Figure 5.24.

- Measurement equipment: apart from the power converters, the dc current source feeding the PV plant emulator and the UC unit, different instruments have been introduced in the test bench in order to perform the measurements needed by the control system to drive the power plant. Moreover, different voltmeters, an oscilloscope and a network analyzer are also installed in order to allow the user to supervise the experiment and register the results as those represented in the next point. The latter two components can be observed in the Figure 5.21, being located between the two power converters.
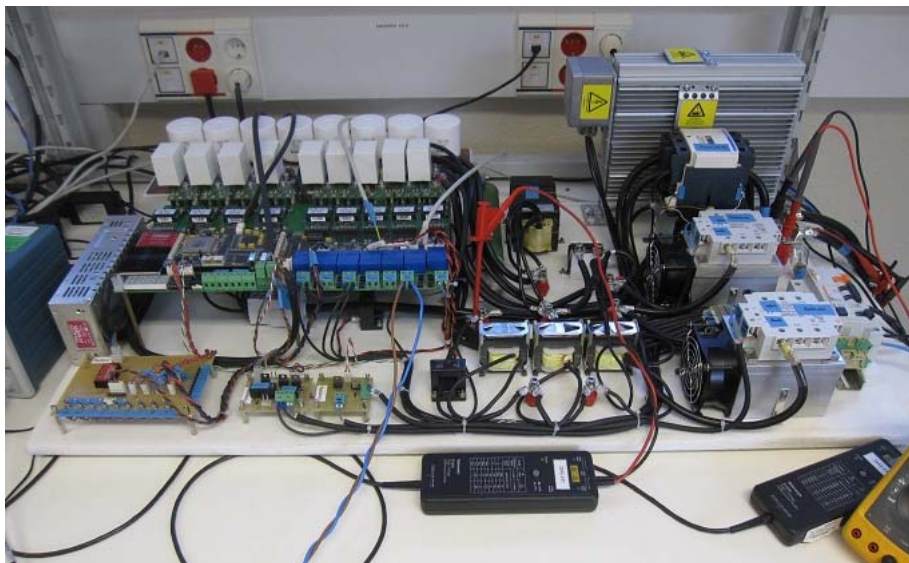
Figure 5.24 The dc/ac power converter which connects the UC to the grid. Courtesy of Ikerlan.

5.3.2. Experimental results and sizing analysis.

After introducing the different components which form the test bench, some experimental results obtained with it are presented here.

a) Experimental results

The constant power steps EMS has been the sole strategy tested on this platform in order to check the capability of the system to track a reference type as the one proposed along the introduction of this Section 1.1. In this sense, experiments redistributing the PV daily energy production by one single step or four different level constant power steps have been executed.

Figures 5.25 to 5.28 represent the resulting daily evolutions of the powers exchanged in the power plant for a 6, 8, 10 and 14 hours single step constant power reference, respectively.

Note that all the different resulting figures represent the powers along the daytime as a function, not of the time itself but, of the number of sample registered by the network analyzer. It is to point out that the network analyzer sampling frequency has been configured to be equal to 0.63 seconds for all the experiments executed in order to avoid memory saturations during the whole daytime analysis. However, one can observe how the different figures are represented for a different number of samples during the various daytime simulations. This fact can be explained by the following two reasons:
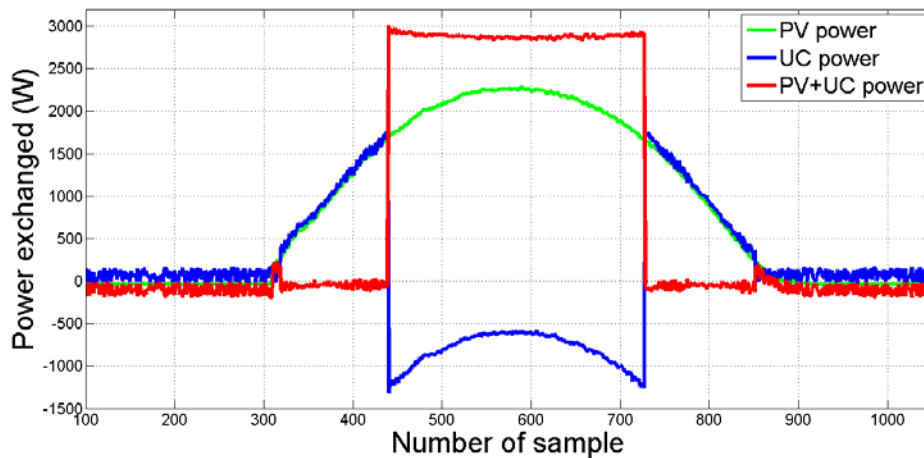
Figure 5.25 Results for a six hours constant power step energy redistribution in a clear day.
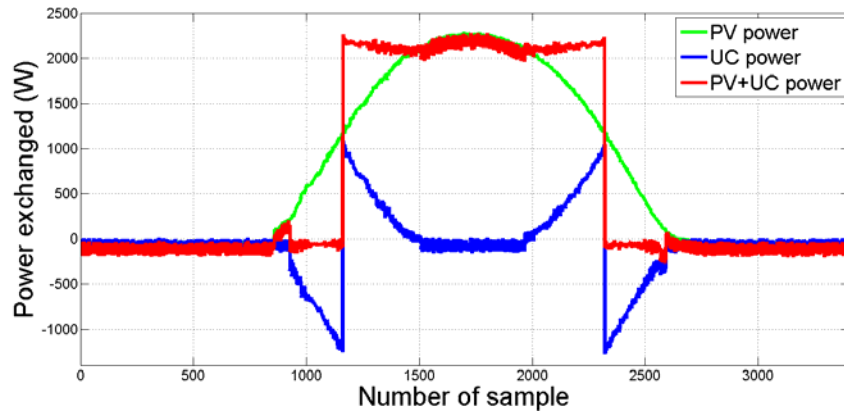
Figure 5.26 Results for an eight hours constant power step energy redistribution in a clear day.
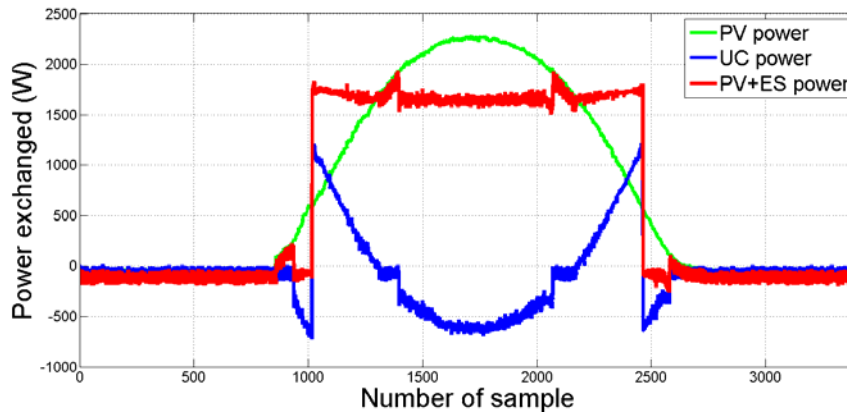
Figure 5.27 Results for a ten hours constant power step energy redistribution in a clear day.
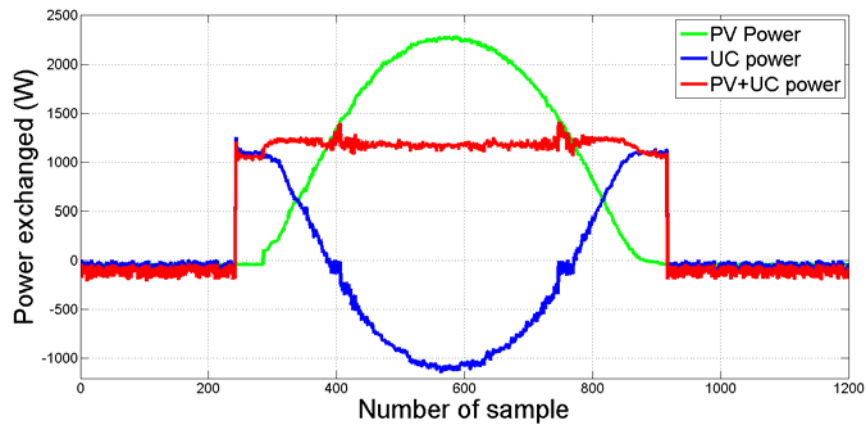
Figure 5.28 Results for a fourteen hours constant power step energy redistribution in a clear day.

- On the one hand, for a reason of time availability. If a whole daytime performance has to be tested, experiments would require 24 hours to be completed. Considering the number of different tests which would be desired to be executed, this represents a very long experiments campaign which cannot be afforded.

- On the other hand, since the UC unit included in the test bench does not contain a very large energy capacity (only 100 Wh), though being already important considering the typical UC ratings, this storage capacity would not allow a 2.5 kW PV power to track a constant power reference along the whole daytime if this was not time-scaled. Thus, by scaling the time of the experiment, the corresponding energy capacity of the UC is proportionately increased. In this sense, if each of the input power values is refreshed to the different components once a second instead of once every 120 seconds (which is the initially defined sampling frequency for the signals), the UC energy capacity is proportionately increased 120 times to acquire an equivalent capacity value of 12 kWh during that experiment.

With these considerations, it can be appreciated on Figures 5.25 to 5.28 how the one single step constant power EMS can be effectively applied during clear days when the shape of the PV production is regular. This is represented in all these figures by means of the green continuous line, makes it easy to forecast the final energy yield. The other two power evolutions represent in the figures are the power exchanged by the UC unit (the blue continuous line) and the total power exchanged by the PV+ES power plant with the grid (the red continuous line). Therefore, the power plant reference is tracked with a high degree of accuracy during the clear days as can be observed in these figures. Only in those points where the UC power exchange is close to zero some slight tracking error can be identified. This phenomenon is due to the internal functioning system of the ES connection converter which requires to permanently commutating its power switches while operating in order to avoid UC discharge and feed its dc bus which must be kept at a certain voltage level for an immediate response. Moreover, to complement this functioning mode, this converter presents a security band on its input power reference which avoids reversing its operation from charge to discharge and vice versa when the reference differs from zero in a positive (discharge) or negative (charge) way for values below that security band. This protection has been implemented to avoid continuous changes in the sense of the power exchanged by the converter due to small power reference oscillations around zero.

Apart from that strategy, also the four steps constant power EMS has been experienced in the test bench. In this sense, Figure 5.29 represents the resulting daily power evolutions for this EMS configuration.
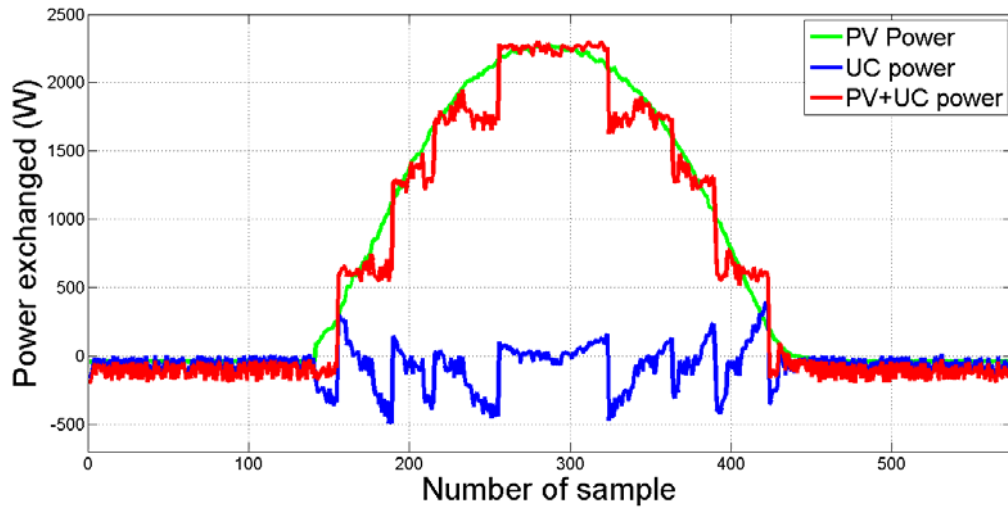
Figure 5.29 Results for a four steps constant power energy redistribution in a clear day.

strategy during a clear day. The same tracking problem can be identified every time the UC converter has to keep a power exchange close to zero. In this case, since the comparison of the plant power reference with the PV power do cross each other several times, the resulting overall power of the plant gets more distorted.

Finally, the same EMS strategies, with one and four constant power steps, have been tested while operating during cloudy days. The resulting power evolutions are represented in Figure 5.30 and Figure 5.31, respectively. Unfortunately, results obtained are not as spectacular as those achieved for the tests with clear days since the permanent crossing of the reference and the PV power curves, due to the PV permanent variability introduced by the passing clouds, forces the UC connection converter to operate more times around the zero power reference. This, as can be clearly appreciated in both figures, induces tracking errors in the system because the UC power curve does not instantly compensate the PV power changes.
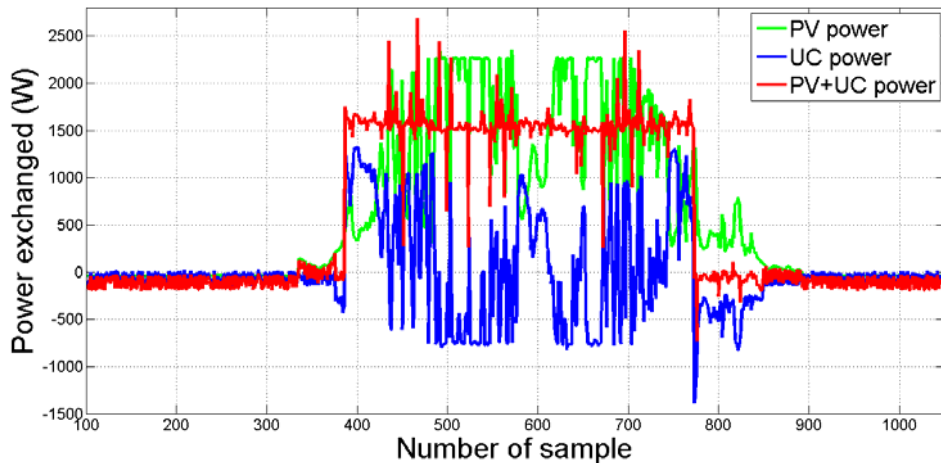
Figure 5.30 Results for an eight hours constant power step energy redistribution in a cloudy day.
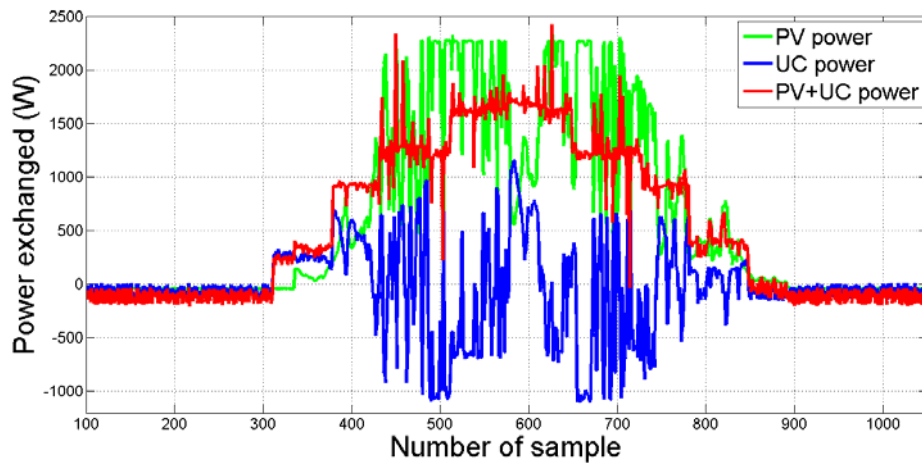
Figure 5.31 Results for a four steps constant power energy redistribution in a cloudy day.

The different experiments performed with this test bench permit to determine some functioning characteristics of the equipment which are summarized here:

- PV plant emulator converter efficiency: from the different experiments a value of 88 % can be deduced as the weighted efficiency of this converter during the tests. Losses in the converter are due to internal electric consumption of its components (fan and others) as well as to switching losses.

- UC connection converter efficiency: similarly, an efficiency value of around the 90 % can be determined for this converter according to the different tests' results. This

efficiency can be calculated from the energy balance in the plant after the experiment, by comparing the energy produced by the PV plant emulator, the energy received by the grid and the change in the SOC of the UC. There are several sources which can produce that 10% of losses such as, again, the internal components consumption and the permanent switching.

- UC self-discharge rate: this value has been identified as very low when compared with the converter losses. Furthermore, it can be accepted to be included within the UC connection converter efficiency calculations. Thus, it is considered as negligible.

These functioning characteristics of a real system are used for the simulated ESS sizing analysis which has been performed according to the EMS presented in the introduction of this section. The results for this analysis, which comprehends once again an annual evaluation of the ES requirements including this time the real system limitations just introduced, are presented in the following point.

b) Sizing analysis

The program presented in Section 5.1.1 has been also used on this occasion, although some parameters and functions have been adapted for this specific analysis. Given that the ESS efficiency has been determined to be of around the 90 %, losses in the power plant performance are assumed although these cannot be calculated in advance because they depend on the amount of energy getting in and out of the ESS. This amount mainly depends on the real irradiation variability which forces the ESS to stochastically operate in order to guarantee the power plant reference. Therefore, although the reference defined in this analysis has been designed to provide an energy injection into the EPS equal to the real energy provided by the PV panels each day, losses in the ESS will tend to unbalance this equilibrium of the system. That leads to a change in the daily final SOC (energy drop) which is equal to the amount of losses in the system (around the 10 % of the power exchanged by the battery). Thus, some recharge complementary control must be introduced again. In order to avoid the undesirable distortion in the PV+ES combined production already described when introducing the SOC recovery time constant (τ_{SOC}), this complementary control action is only activated in this study during the night hours, when no power is compromised from the PV+ES power plant and expected by the system operator. In this sense, the ESS will behave during these hours as another system load which can even help to flatten the aggregated load curve of the EPS.

The resulting appearance of the system behavior according to these considerations can be observed in Figure 5.32, where a ten hours single constant power step reference has been used and represented against the real PV production. A negative value of power can be appreciated in the reference during night hours. This negative power is the action introduced in the reference in order to recharge the ESS and start next day at a SOC level as close as possible to the reference one.

This can be done during the limited range of eight hours (from 10 pm to 6 am) which has been established so as to avoid overlaps with the power plant operation. Shorter SOC recovery periods could be defined although they would require higher negative power values to recover the same amount of energy. Therefore, these are not contemplated to avoid overcharging the UC converter. In the same way, longer periods are avoided to skip overlapping with long duration single constant step references' active hours.

After analyzing the recharge level obtained along those eight hours with different values of τ_{SOC}, a value of six hours has been defined as the optimal for this parameter and used for completing the sizing analysis. The reasons to select that value are mainly two:

- Regarding power evolutions, when introducing a six hours SOC recovery time constant, no large recharge power peaks (which could also lead to exceeding the UC recharge power limits) are achieved at the beginning of the active SOC recovery hours. This is something which is appreciated when taking lower τ_{SOC} values (below three hours).

- Regarding energy evolution, the six hours value of the τ_{SOC} parameter allows achieving a good performance of the plant, completing every night a SOC recovery beyond the 80 % regarding the daily deviation. In this sense, similar τ_{SOC} values (up to 16 hours) will produce similar recovery effects which finally lead to a very similar annual saturation percentage of time.

In this sense, it can be appreciated in Figure 5.33, which represents the UC's energy reserve evolution for those days whose powers are represented in Figure 5.32, how the SOC hardly recovers every night the reference SOC value (0.5 of battery capacity). Note that the simulated battery capacity is equal in this case to 2150 Wh (0.5 pu).
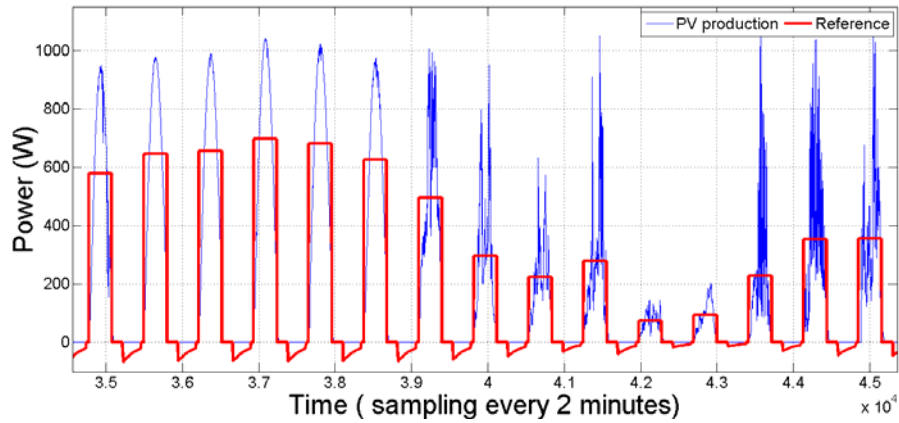
Figure 5.32 Powers evolution for the analysis.
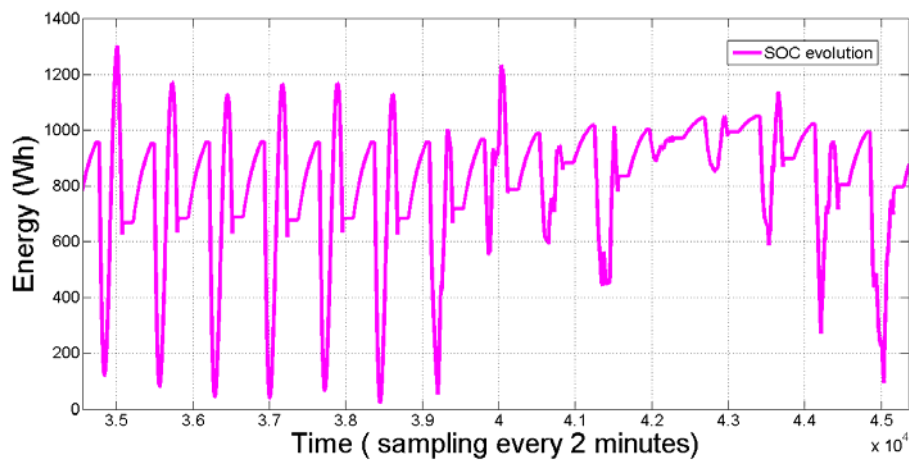
Figure 5.33 SOC evolution for the time of simulation represented in Figure 5.32.

Therefore, Figure 5.33 shows how the power plant is operated oscillating everyday around the UC's reference SOC, avoiding tripping due to energy deviations in consecutive days.

According with this control strategy and the SOC recovery adjustment just introduced, a systematic analysis of the UC energy requirements has been performed. Results for the different EMS configurations (eight different one single step durations and one four-level steps case), and for each of the different ESS energy capacities analyzed (from 0.2 pu to 0.5 pu), are represented in Table 5.5. As it was done for the analysis introduced in 5.2.1 and 5.2.2, the energy capacity considered are measured in the per unit system, taking for the

calculation the same energy base values. Therefore, each of the values in the table correspond to the percentage of time along the whole year that an UC unit with the capacity indicated for each column would not be able to guarantee the PV+ES power reference tracking (due to being completely charged or discharged), according to the EMS configuration defined for each table line.

EMS configuration	Capacity 0.2 pu	Capacity 0.25 pu	Capacity 0.3 pu	Capacity 0.35 pu	Capacity 0.4 pu	Capacity 0.45 pu	Capacity 0.5 pu
A 4 hours single constant power step	24.16	20.32	16.89	13.34	9.77	7.55	6.28
A 6 hours single constant power step	13.94	9.09	6.38	4.45	3.09	2.08	1.37
A 7 hours single constant power step	7.21	4.13	2.46	1.55	0.96	0.59	0.33
An 8 hours single constant power step	3.59	2.04	1.24	0.72	0.35	0.19	0.12
A 9 hours single constant power step	4.58	2.56	1.60	0.90	0.47	0.27	0.16
A 10 hours single constant power step	9.32	5.40	2.94	1.79	1.08	0.61	0.29
A 12 hours single constant power step	18.90	14.91	11.25	7.66	4.50	3.02	1.91
A 14 hours single constant power step	26.43	22.25	18.27	14.76	11.78	8.65	5.35
A 4-level constant power steps	2.68	1.48	0.88	0.50	0.29	0.18	0.11

Table 5.5 Percentage of time along the year when the PV power plant cannot track the different EMS references as a function of the UC energy capacity.

Different conclusions can be extracted from the results presented on the table, by comparing the different EMS configurations among them, and by comparing the results here presented with those from 5.2.1 (obtained for the same EMS). These are summarized below.

5.3.3. Discussion and conclusions.

This point is devoted to discuss over the experimental results and the sizing analysis introduced in this section.

Regarding the experimental results, the following considerations can be concluded:

- The efficiency of the power converters is more than acceptable, given that these have been operating much of the test time at power levels well below their rated value.

- On the contrary, the sensibility of these power converters should be improved in order to allow a proper operation during cloudy days. An advanced programming with a

more frequent reference update is required so as to enable a reduction in the programed security operation bands which are responsible for the injected power distortion.

- The time response of the UC technology is fast enough to respond to the PV variations due to clouds; hence, this ES technology does no present limitations in this sense.

- The UC's self-discharge ratio has been measured to be low since not very long tests were carried on. An extended analysis of this parameter should be introduced in order to account for the annual losses.

Moreover, some other conclusions can be extracted regarding the sizing analysis:

- For example, there is clear evidence that the minimal energy capacity requirements are obtained for the eight hours single constant power step reference configuration. As the step durations differs more from this optimal one, the ES capacity requirements do increase. Note how with a same ESS energy capacity, e.g. 0.3 pu, the PV+ES power plant will manage to properly track an eight-hour step reference during the 98.76 % of the year, while it would only do so during the 88.75 % of the year with a 12-hour step reference.

- Furthermore, results in Table 5.5 show the great reduction in the ESS energy capacity requirements obtained, with respect to those estimated in 5.2.1, thanks to the daily real energy adjustment which allows optimizing the power production. Note from Figure 5.10 how none of the EMS configurations achieve proper performances, beyond 85 % of the time, with an ESS energy capacity equal to 0.5 pu, while all of them are above 94 % of the time in Table 5.5 for that capacity.

- Moreover, results for the simple 4-level constant power steps configuration (which has not been optimized with any algorithm) are the best among those in Table 5.5. This confirms the capacity requirements reduction which can be achieved by evolving, within the constant steps EMS, from using a one single step to a multiple constant steps configuration. Thus, the extreme case which uses one different power step value every hour has been also analyzed in this Thesis, and its results introduced in Section 1.1.

Finally, one can conclude from the results and information here presented that, given the current UC state-of-the-art and the market prices of this technology, these do not seem the most appropriate ES solution to be used in grid connected PV power plants which pretend to be operated according to any of the possible constant power EMS configurations. According to the power and energy requirements obtained from the analyses presented in this document till here, batteries, and more precisely Lithium ion batteries, can be confirmed as the candidate ES technology to be integrated in this type of plants, as already introduced in Chapter III. That is the reason why this technology has been studied too in this Thesis. The study performed comprehends an annual ageing analysis of one commercial Lithium ion battery model which could be used in a PV+ES power plant operated under the different EMS already known. This study is presented in the following section.

5.4. Ageing analysis of Lithium ion batteries used in a PV+ES power plant.

Lithium-ion batteries technology points out to be a firm candidate to be installed in PV power plants according to the ES technologies overview presented in Chapter III, and corroborated by the power and energy requirements obtained for ES units in Sections 5.2 and 1.1. Thus, this technology has been also analyzed in this Thesis. Although there has been no possibility to get experimental results with them, a set of simulations has been carried out in order to estimate the possible ageing evolution that these will experience when used in PV+ES power plants which are operated in any of the two main EMS whose sizing results have been introduced in 5.2. For doing so, the following case study was established and analyzed.

5.4.1. Case study description.

A specific PV+ES power plant was considered for this study. It is defined as an aggregated 40kW rated power PV plant which integrates a group of Li-ion batteries whose ratings (in both power and energy capacities) are gradually modified. This ratings' change is done with the goal to determine, as for the analysis presented in 5.2, the plant operation improvement obtained with the different ES capacities introduction. But, it is also done here to determine the corresponding ageing of the batteries which present those diverse ratings.

Similarly to the studies presented in 5.2 and 1.1, this analysis was also conceived for the same Spanish southern location whose real irradiance data along the year 2009 with a sampling period equal to 2 minutes are available. Again, the expected standard irradiance

profiles are those provided by the PVGIS database. Therefore, power references for the PV power plant are defined according with the mechanisms presented in Chapter IV. By comparing these sets of data (PV real production with PV+ES power reference), the instantaneous Li-ion battery power and energy requirements along the period of time considered working are determined. Of course, as already concluded in 5.2, depending on the plant different operation modes (EMS) the power requirements do largely vary. Therefore, a different number of full cycles, with the corresponding variation in the *DoD* distribution, is extracted by the RFC algorithm (presented in 5.1.2) along one whole year of operation simulated for each EMS. Consequently, different degrees of ageing are experienced by the Li-ion batteries as a function of the power plant EMS.

5.4.2. Case study results.

In order to analyze the different ageing evolutions under the two EMS, these were simulated while modifying different control parameters. The different configurations analyzed can be appreciated in Table 5.6. This table also summarizes the resulting number of equivalent charging and discharging cycles experienced by the Li-ion batteries along the year together with its life expectancy under the corresponding plant operation conditions.

Energy Management Strategy	Strategy configuration	Battery ratings	Number of cycles	Lifetime expectancy
Constant output power	A 4 hours single constant step	20kW, 80kWh	375.9	4.6 years
Constant output power	A 6 hours single constant step	20kW, 65kWh	317.4	5.64 years
Constant output power	An 8 hours single constant step	20kW, 30kWh	363.5	5.95 years
Constant output power	A 10 hours single constant step	20kW, 35kWh	388.3	5.21 years
Constant output power	A 12 hours single constant step	20kW, 55kWh	355.1	4.87 years
Constant output power	A 14 hours single constant step	20kW, 75kWh	347.2	4.95 years
Constant output power	A 16 hours single constant step	20kW, 110kWh	330.4	5.33 years
Constant output power	4 step levels of 165minutes each	20kW, 12kWh	444.5	6.75 years
Fluctuations reduction	$a = 0.8$, $\tau = 9$ minutes	20kW, 1.5kWh	1314	2.07 years
Fluctuations reduction	$a = 0.9$, $\tau = 19$ minutes	20kW, 3kWh	964.8	2.66 years
Fluctuations reduction	$a = 0.95$, $\tau = 39$ minutes	20kW, 10kWh	500.4	5.04 years
Fluctuations reduction	$a = 0.97$, $\tau = 66$ minutes	20kW, 20kWh	392.5	5.41 years
Fluctuations reduction	$a = 0.99$, $\tau = 199$ minutes	20kW, 80kWh	283.3	6.49 years
Fluctuations reduction	$a = 0.995$, $\tau = 399$ minutes	20kW, 200kWh	220.9	9.24 years

Table 5.6 Resulting Li-Ion Battery ageing under different operating conditions.

For all the cases simulated, the values of SOC_{ref} and τ_{SOC} were fixed to 0.5 and 12 hours respectively. Moreover, among the multiple cases of Li-ion battery ratings simulated for each power plant configuration, only some of them are represented here for comparison. These correspond to those ESS rating values which assure, according with that explained in 5.2, a proper operation of the PV+ES plant (no ESS saturation) when tracking the power reference during at least the 95% of the simulated time.

From the resulting number of cycles introduced in Table 5.6, and using equations (5.4) and (5.5), the Li-ion battery capacity fading and the cycling resistance evolution can be calculated. These are represented along the year as a function of the operation mode in Figure 5.34 and Figure 5.35 which respectively depict the evolution of these two parameters when considering a rated 20kW power 20kWh energy capacity battery. An eight hours constant power step reference which generates 490.25 battery equivalent cycles in one year has been considered on the one hand, and an "$a = 0.97$" filtering value which generates 392.5 equivalent cycles on the same year on the other hand.

The life consumption difference experienced by the same battery along one year, when operating in a PV+ES power plant which is controlled with the two different EMS, stands out. Finally, note how the evolution along the year is not regular since the temporal variability of the solar radiation along the year, and even along each day, makes the battery to be differently demanded as time goes by. This forces the battery to stochastically exchange more or less power in order to guarantee the power plant reference tracking and, hence, experiencing different ageing as a function of the season and even the day.

5.4.1. Discussion and conclusions.

Different conclusions can be extracted from this study, which summarizes the ageing experienced by the Li-ion batteries under different operation EMS, and its corresponding results presented in Table 5.6 and in Figures 5.34 and 5.35.

On the first hand and according with the results shown in that table, a similar number of experienced cycles can be forecasted for the battery regardless of the EMS taken if the battery energy capacity is properly adapted to its expected type of operation.

On the other hand, for the same battery energy capacity, the constant power strategy is more demanding than the fluctuations reduction strategy in terms of battery life. This can be observed in the figures.
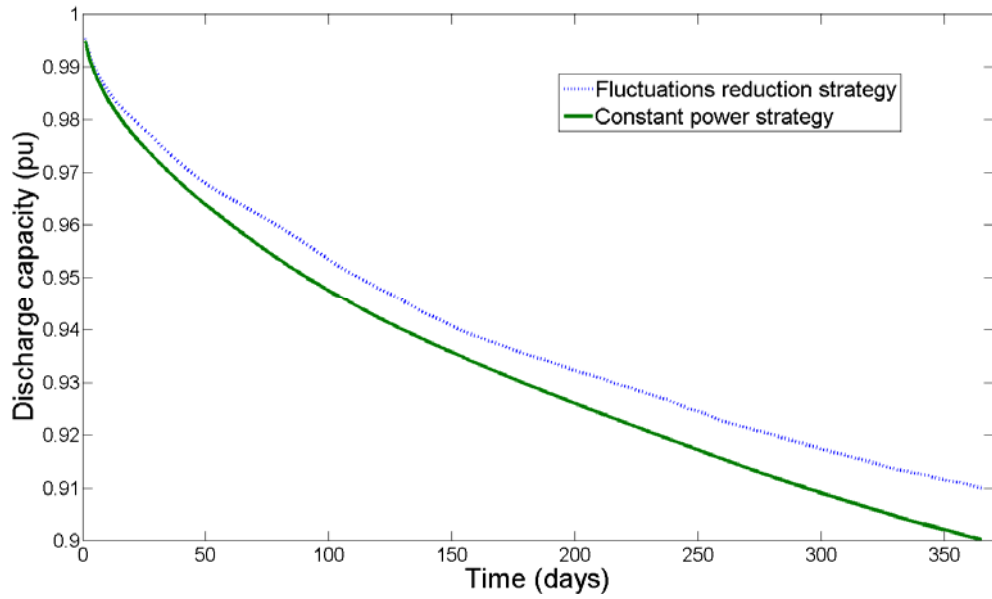
Figure 5.34 An 80kWh Li-ion battery capacity evolution under the different EMS.
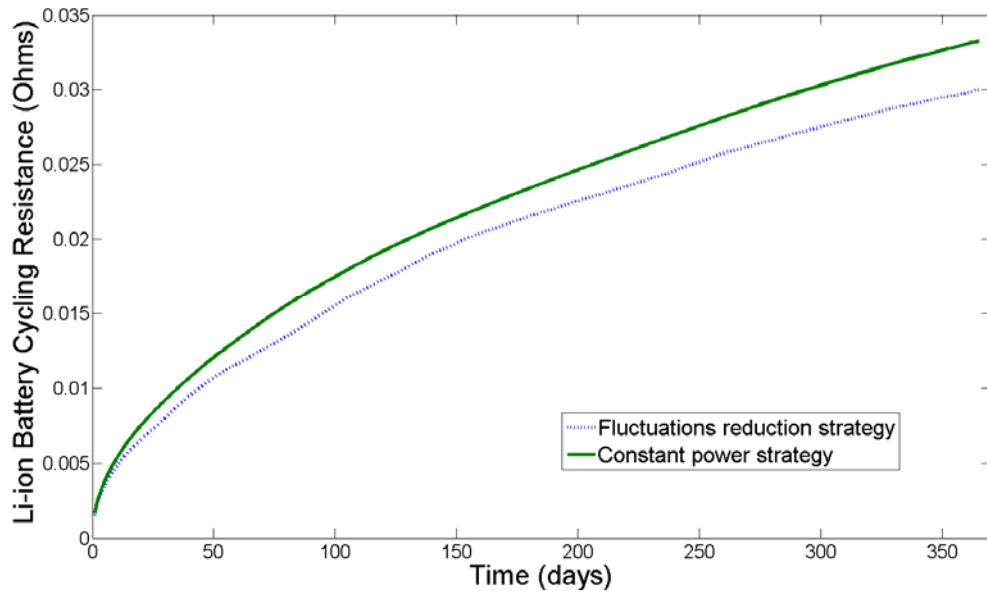
Figure 5.35 Cycling resistance evolution as a function of the different EMS.

Moreover, the ageing suffered by the battery not only depends on the number of cycles, which has been counted with two different methods whose results differ in less than 1%, but also on the *DoD* of the partial cycles. This can be concluded from the life expectancy

difference between the six and the eight hours constant power step results presented in the table. In this sense, increasing the size of the battery supposes reducing its ageing (smaller *DoD* cycles under the same operation conditions) although increasing its price.

Furthermore, note that although the study is envisaged here for a whole year time, different periods along the year will have to be compulsory analyzed separately since PV production varies largely from winter to summer due to both irradiance change and to the different quantity of cloudy hours per month. These variations will limit or require some monthly adjustments to the introduced in the EMS for a more precise analysis. Therefore, an advanced analysis of the constant energy management strategy under cloudy conditions should be further performed.

Finally, it seems clear that, according with the life expectancy results here presented, Lithium ion batteries are a very promising technology to be used in PV power plants. Some commercial models, which are already being applied in the automotive industry already present acceptable power and energy ratings, could allow a controlled operation of 10 to 20 kW PV plants. And their investment costs could briefly approach a profiting economic panorama. Therefore, a further effort on development, which should go hand in hand with the one already being experienced within the electric vehicle industry, should be by renewables industry in order to accelerate an advance technical and economic viability of this type of PV+ES power plants.

5.5. Sizing results for advanced constant power EMS.

Finally, apart from the two basic EMS analyzed in Section 5.2 and the improved daily energy-adapted constant power steps EMS configuration studied in 1.1, a third systematic sizing analysis has been developed. This has been carried out for the advanced constant power steps EMS proposal which establishes an hourly-adapted constant power steps reference. This strategy, which aims to reduce the ESS capacity requirements, seeks to establish a reference as close as possible to the real PV production (hourly-averaged) using its associated complementary controls. Both, this EMS configuration and the possible complementary control actions which can be used to apply it effectively were already introduced in Chapter IV. These were presented in those sections dedicated to: the meteorologically-based adjustment (4.3.3), the progressive power step optimization (4.3.4) and the intra-hourly predictive control (4.3.5).

A combination of the programs described in 5.1.1 and 5.1.3 has been used for this analysis. While the first one has been executed once again in order to calculate the percentage of time when the system saturates or not, the latter program has been the one used to establish the PV+ES power plant annual references, as a function of the different advanced constant power steps EMS configurations. That is, the second program generates a reference adapted to the real PV instantaneous production, more or less accurate, leaning on the different periodically-implemented adjustments, which can be optionally included for each case.

Therefore, the results here presented provide a quite precise idea on the ESS sizing requirements that should be covered to operate a PV+ES power plant along one whole year as a conventional dispatchable PV power plant, with an hourly-scheduled production, which can turn to electricity markets.

5.5.1. Advanced EMS possible configurations.

A PV+ES generic power plant is considered once again for the simulations carried out in this section. A bunch of different hourly-based constant power steps EMS configurations have been considered and their corresponding ESS energy capacity requirements analyzed. These configurations correspond to the introduction of the different complementary control actions described in Chapter IV, combining them in some cases in order to try to achieve more accurate power references for the power plant. The different configurations which have been analyzed are classified as shown in Figure 5.36.

According to this scheme, the advanced EMS can be divided into two main groups of configurations: those which take as reference the real sky (RS) PVGIS models and those which take into account the clear sky (CS) PVGIS models. Although the meteorologically-based adjustment (presented in 4.3.3) was only referred to the clear sky conditions, a similar adjustment can be defined and calculated for the real sky model dataset. This adjustment has been considered too in this analysis, with the goal of exploring more possibilities and it allows finding what the best control option would be when trying to optimize the ESS energy requirements.
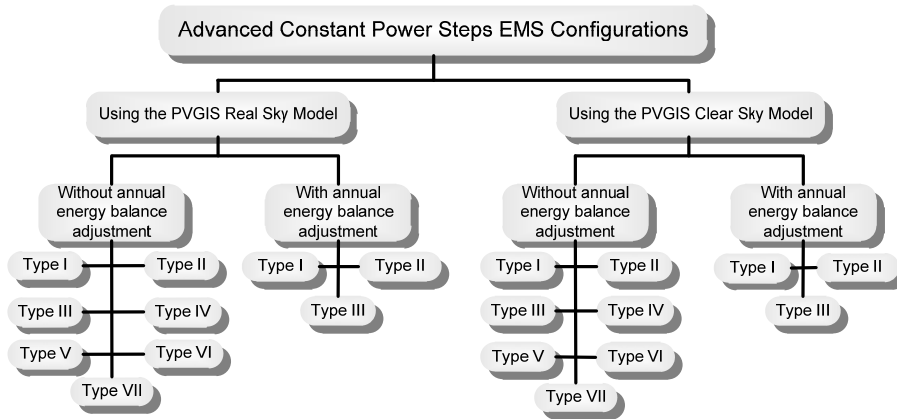
Figure 5.36 Advanced constant power steps EMS possible configurations.

Within each of these two groups, other two different subgroups can be identified. These are: those configurations which keep the RS or CS model as it is provided by PVGIS, and those which modify both models in order to adapt their overall annually-produced energy to the climatic conditions expected for that year (i.e. consider if the year is expected to be dry or wet compared with statistically-averaged climatic data?). For instance, and as it was already introduced along the input solar data description in Chapter II, the real PV energy production for the location under study during the year 2009 was just 90 % of that predicted by the RS PVGIS model. That represents the 72.9 % of the CS PVGIS model. Therefore, this global annual adjustment has been also considered, as it was done in the analyses introduced in 5.2, providing results with and without its implementation.

Finally, different specific configurations are included in each subgroup. These take into account: the meteorologically-based adjustments and the progressive power step optimizations (according with the different intraday electricity market periods). These specific configurations are labeled with different "Type" numbers, and can be described and identified as follows:

- Type I – generates a power reference with hourly-adapted steps, which is exclusively calculated at the beginning of the day according to the PVGIS RS or CS models without any further adjustment.

- Type II – generates a power reference with hourly-adapted steps, which does not take into account any meteorologically-based adjustment but which is updated at every

intraday market period to adjust it to the current SOC (takes into account deviations in the current daily energy production between PVGIS model and real PV production).

- Type III – generates a power reference with hourly-adapted steps, which is calculated at the beginning of the day according to any PVGIS RS or CS models, and which is updated in the intraday market periods using as feedback information not only the current SOC but also the *Cloudiness Coefficient* (introduced in 4.3.3) for the 6th and the 1st intraday.

- Type IV – generates a power reference with hourly-adapted steps, which includes the *Meteo Coefficient* (according to the expected weather and extracted from Table 4.3). This coefficient is already used when defining the reference at the beginning of the day, and it is kept active during all the intraday periods.

- Type V – Similar to the previous one. This configuration generates a power reference with hourly-adapted steps but including an ideal *Meteo Coefficient.* This ideal coefficient, which could be calculated only a posteriori (it is the optimal weather forecast), would modify the PVGIS model in which the reference is initially based so as to adapt this model to the day weather conditions. It represents an ideal PV daily energy estimation, as that considered in the analysis in Section 1.1. Therefore, it supposes a refinement of that *Meteo* value used in the previous "Type IV". Again, this coefficient is used when defining the hourly-adapted power reference at the beginning of the day, and kept active during all the intraday periods.

- Type VI – generates a power reference with hourly-adapted steps, which combines the use of the two coefficients included in the meteorologically-based adjustment: the *Meteo* and the *Cloudiness Coefficient*. While the first one is used when defining the reference at the beginning of the day and for the 5th programmed intraday market, the latter is used for the 6th intraday and the 1st intraday of the next day.

- Type VII – Similar to the previous one, this type also comprehends a power reference with hourly-updated steps which combines the use of the two coefficients included in the meteorologically-based adjustment being used each of them in the same situation. The sole difference is that the *Meteo* value used is the ideal one also calculated for the "Type V" configuration.

As can be observed in Figure 5.36, not all the seven types of configurations are included within each subgroup. That's because it makes no sense to distinguish among those cases

295

considering the annual energy balance adjustment and those who do not for types "IV" to "VII" given that these EMS configurations do already involve an energy adjustment which overlaps the annual one.

5.5.2.   Different EMS configurations results.

As previously introduced, the references generation program presented in 5.1.3, which provides signals as that represented in Figure 5.37, has been initially used in the analysis.
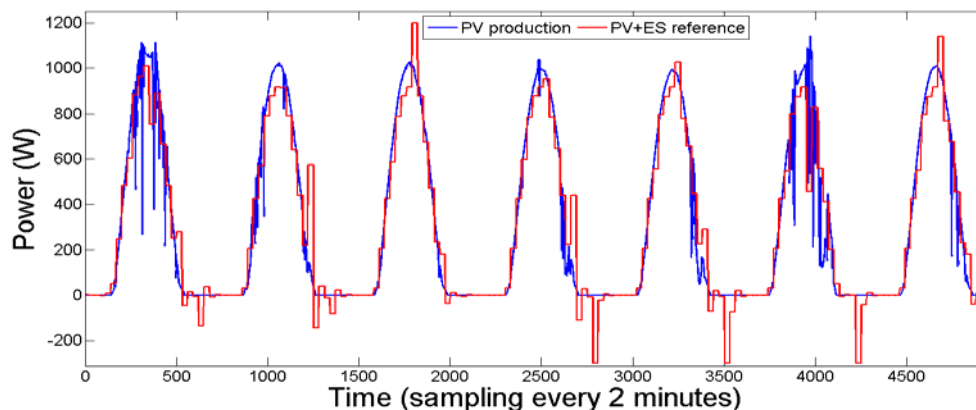
Figure 5.37 Example of hourly-defined reference for a week operation under "Type VI" EMS.

Signals in Figure 5.37 correspond to the PV panels real production overlapped with the hourly-stepped reference, generated by that program for a generic week, corresponding to a PV+ES plant operation according to the EMS configuration "Type VI" within the CS subgroup.

Apart from annually defining the power reference for the plant, according to each of the different EMS configurations, this program does also already calculate the annual SOC evolution of the ESS integrated within the PV plant. From this SOC evolution, the program can derive the maximum and minimum ESS energy capacity values required each day along the year which have been required to provide the PV+ES power plant with capacity enough so as to track the defined reference reliably, without ES saturations. These daily limit-values can be represented for each EMS configuration in figures like the one which can be observed in Figure 5.38. This represents the maximum and minimum daily energy deviations of the ESS' SOC (in pu and taking the same energy base-value as in 5.2) with regard to the reference SOC value (normally 50% of the ES capacity) when analyzing the performance of

the PV+ES power plant operated under the same EMS configuration of Figure 5.37, "Type VI" within the CS subgroup.
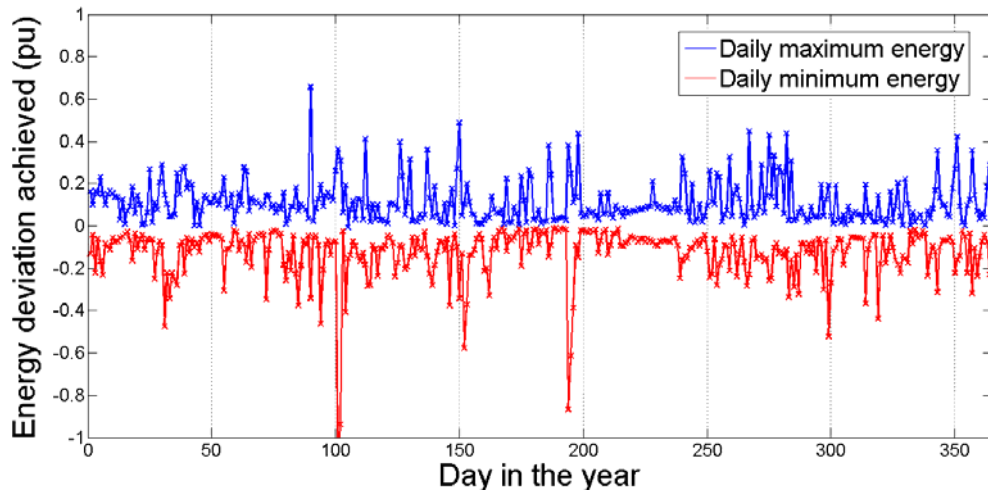
Figure 5.38 Daily maximum and minimum energy values along the annual SOC evolution.

Information as that represented in Figure 5.38 is valuable because it provides an initial idea of the ESS energy capacity required to operate the PV+ES power plants under any of the advanced EMS configurations. Figures as this one have been helpful to define the range of energy capacity values to be systematically simulated, with the program 5.1.1, in order to establish the different percentages of time along the year when the system operates properly. Note that most of the days in Figure 5.38 present an energy variation within the ±0.5 pu range. However, these limits are exceeded some days as it can be appreciated in the figure. These have been analyzed in detail to determine their peculiar behavior and their corresponding detailed power evolutions appearance represented in Figure 5.39 and Figure 5.40.

In this sense, days numbered 101, 152 and 194 (two of them represented in Figure 5.39) present a very deep discharge level because their morning PV productions are similar to those expected for their clear equivalent day, what makes the control system to correct the reference for the afternoon hours to be in accordance with that PV production defined trend. However, the current PV production drops suddenly to zero, what forces the ESS to deeply discharge in order to allow PV+ES coping with the updated reference tracking while PV production lacks. It can be noted that, according to the PV production evolutions' strange

appearance in Figure 5.39, the simulation is probably dealing with a real PV production measurement problem for these days.
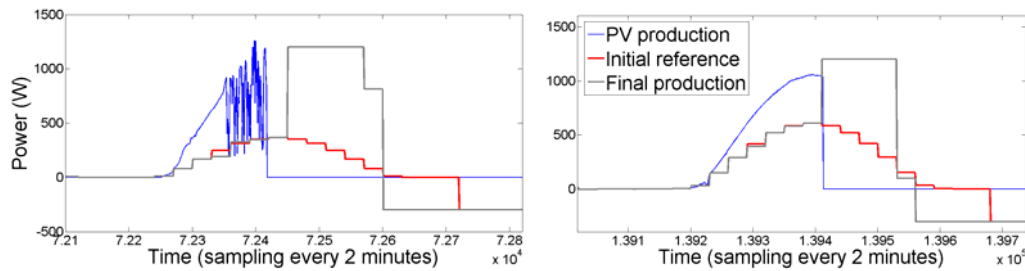
Figure 5.39 Evolution of PV production Vs. initial and final PV+ES references for the days 101 and 194 in the year 2009, respectively.

Conversely, the situation for days number 90 and 150 (Figure 5.40) is the opposite one. Very low PV production is registered in the morning, what makes the control system to reduce the updated PV+ES power plant reference for the afternoon. Then, it suddenly gets clear and the PV production does increase a lot, what forces the ESS to charge all the energy produced by the PV panels which exceed the defined updated reference. Finally, the ESS releases some energy after the sunset so as to recover the reference SOC level before starting next day's operation.
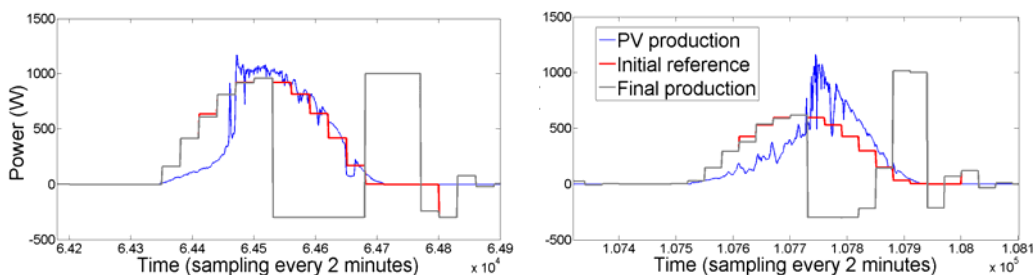
Figure 5.40 Evolution of PV production Vs. initial and final PV+ES references for the days 90 and 150 in the year 2009, respectively.

For the rest of the days in the year, since PV production is more homogeneous along the whole period, the corrections in the updated reference elaborated at each intraday negotiation period are not so important. Thus, the final production of the plant is much more similar to the initial production reference calculated at the beginning of the day. This can be observed in the two examples represented in Figure 5.41, one for an overcast day (day 116 of the year) and another one for a clear day (day 156 of the year).

Therefore, the ESS capacity requirements for days with an approximately constant PV energy production trend are smaller because the tendency can be anticipated and the reference corrected. With that reference correction, the power compromised at the PCC in the coming hours will defined more similar to the expected PV production and, hence, the ESS will have to compensate lower levels of energy.
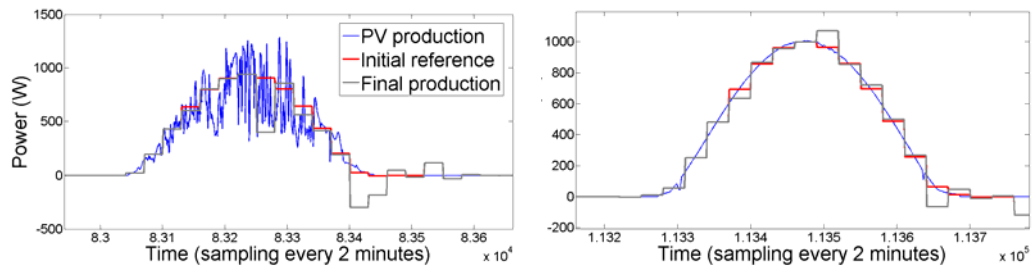
Figure 5.41 Evolution of PV production Vs. initial and final PV+ES references for the days 116 and 156 in the year 2009, respectively.

All these graphical results have been obtained when analyzing the performance of the PV+ES power plant operated, as previously introduced, always under the same EMS configuration: "Type VI" within the CS subgroup. However, similar results would be obtained for the other advanced EMS configurations here analyzed. Figure 5.42 a) and b) are introduced so as to provide a comparative idea of the various EMS configurations' performances for a generic clear day and a generic cloudy day, respectively. The different strategies to manage the PV energy production associated to each of the control configurations can be clearly understood and extracted from the various reference evolutions represented in Figure 5.42. The variability in the accuracy and the efficiency of the different EMS configurations when trying to convert the stochastic solar production into an hourly-constant production can be there appreciated. This cited variability has its implications in the ESS requirements for each of the strategies, what is described in the following.

As it has been done to obtain the results presented in Sections 5.2 and 1.1, the program described in 5.1.1 has been also used in this analysis. Equivalent results for this case have been compiled in Table 5.7. These represent the percentage of time along the whole year 2009 (percentage of sampling periods) that the ES unit with the energy capacity indicated for each column would not be able to guarantee the PV+ES power reference tracking (due to saturations of the ESS related to a complete charged or discharged state). And this has been calculated for each of the possible EMS configurations previously defined and which are classified in Table 5.7 on each line.

a)

b)
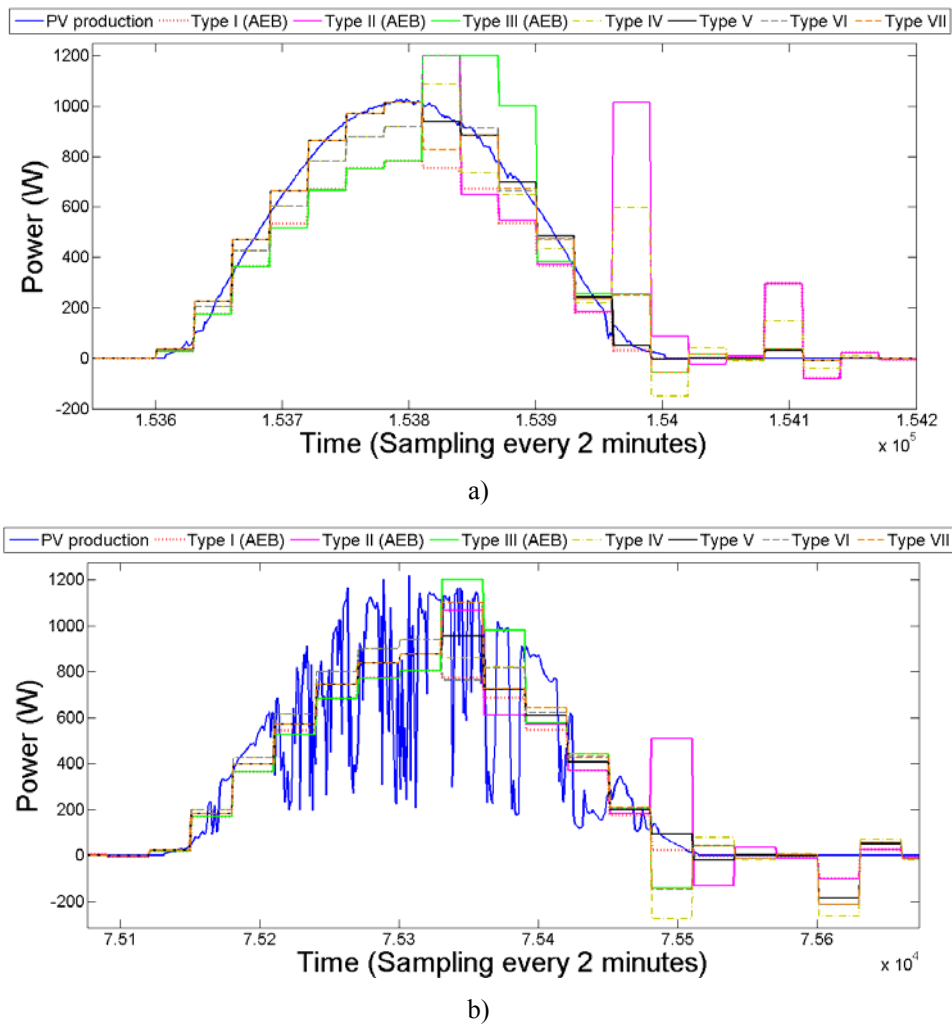
Figure 5.42 Graphical comparison of the PV+ES power references generated by different hourly-defined EMS configurations during a: a) clear day and b) overcast day.

Altogether, although twenty different advanced EMS configurations were contemplated in Figure 5.38, only fourteen of them have been taken into account for the analysis. This is because configurations "Type I", "Type II" and "Type III" are not optimized at all if these do not include any kind of external energy adjustment. For those cases, the energy difference between the PVGIS model (RS or CS) and the real PV radiation could differ so much that the ESS would require an enormous energy capacity to be able to provide a reliable proper operation to the plant. This is a second important conclusion of this analysis which is here highlighted and anticipated. Therefore, these configurations have not been studied in those

subgroups where the annual energy balance adjustment is not active. The rest of them, fourteen, have been organized in Table 5.7 (from top to bottom) according to their order of appearance in Figure 5.38 (from left to right). Moreover, note that those included in a subgroup with annual energy balance adjustment are denoted with the "(AEB)" indicator.

For each of these configurations considered, the performance of the plant (considering an efficiency of the ESS equal to 90 %) with seven different ESS energy capacity values (from 0.25 pu to 2 pu) have been annually studied. Note that the ESS energy capacity values introduced in Table 5.7 are defined in the per unit system once again. The energy value which it has been taken as energy base value for the pu calculation is also the daily energy that would produce a 1 kW PV power plant installed in a determined location. This value is equal to 4.3 kWh/kW$_{peak}$ for the location where the sizing analysis has been carried out. Thus, a 0.5 pu represents that an energy capacity of 2.15 kWh in ES units should be installed for each rated kilowatt of PV panels installed.

EMS configuration	Capacity 0.25 pu	Capacity 0.5 pu	Capacity 0.75 pu	Capacity 1 pu	Capacity 1.25 pu	Capacity 1.5 pu	Capacity 2 pu
RS (AEB) – Type I	17.68	9.60	5.36	3.26	2.1	1.26	0.30
RS (AEB) – Type II	16.21	5.22	1.71	0.81	0.33	0.11	0.02
RS (AEB) – Type III	14.95	4.92	1.47	0.54	0.20	0.08	0.01
RS – Type IV	4.67	0.51	0.07	0	0	0	0
RS – Type V	1.50	0.12	0.01	0	0	0	0
RS – Type VI	6.64	1.62	0.46	0.14	0.07	0.03	0.01
RS – Type VII	5.55	1.65	0.52	0.15	0.08	0.05	0.01
CS (AEB) – Type I	20.20	11.70	6.05	3.52	2.56	1.70	0.52
CS (AEB) – Type II	18.72	6.22	2.00	1.02	0.46	0.16	0.01
CS (AEB) – Type III	16.23	5.54	1.93	0.76	0.34	0.12	0.02
CS – Type IV	2.78	0.28	0.01	0	0	0	0
CS – Type V	1.49	0.13	0.01	0	0	0	0
CS – Type VI	6.16	1.62	0.46	0.15	0.074	0.047	0.01
CS – Type VII	5.53	1.57	0.53	0.17	0.09	0.06	0.01

Table 5.7 Percentage of time along the year when the PV power plant cannot track the different advanced EMS configurations' references as a function of the ESS energy capacity.

5.5.3. Discussion and conclusions.

Interesting conclusions can be extracted from the results introduced in the previous point. For instance, it has already been anticipated how the ESS capacity requirements for days with an approximately constant, or homogeneous, PV energy production trend are smaller since their tendency can be anticipated and the reference corrected. With that reference correction, the power compromised by the PV plant at the PCC in the coming hours will be defined more similar to the expected PV production and, hence, the ESS will have to compensate lower levels of energy.

Apart from that, it has also been highlighted along the previous point that EMS configurations of "Type I", "Type II" and "Type III" are not optimized since they do not incorporate any kind of energy adjustment, and this applies regardless of the PVGIS dataset used as model, RS or CS. For those three configurations, the energy difference between any of the PVGIS models and the real radiation is so large that the ESS would require an enormous energy capacity to be able to annually guarantee the reference tracking without saturations. Therefore, a second conclusion of this analysis is that an energy adjustment of the reference results compulsory, regardless of the EMS configuration, if the ESS is wanted to present a logical and economically viable size.

This second conclusion links straightly with the results presented in Table 5.7. From them, some considerations can be extracted when comparing the annual performance of the PV+ES plant operating under the different configurations. These are:

- Firstly, and related with the second conclusion just introduced, a clear improvement in the sizing results can be observed as more precise energy adjustments are introduced in the control system. In this sense, if "Type I" and "Type II" were excluded of the final analysis due to the high ESS requirements diagnosed already in the initial analysis, their corresponding versions with AEB adjustment do already provide reasonable results which could be considered. However, even like this, these are not the optimal control strategies since refined configurations of "Type III" to "Type VII" with daily meteorological adjustment do present much better results.

- Secondly, when comparing "Type I" and "Type II" results, it can be concluded that, as could be logically anticipated, if the PV plant can access to the intraday markets correcting its future power commitment, being this correction only based on the current SOC of the ESS, the ES capacity requirements are reduced.

- Moreover, if the *Cloudiness Coefficient* is also introduced for the 6th and the 1st intraday corrections, "Type III" configuration, results do improve the ES capacity requirements which have been calculated for the "Type II" configuration.

- Elsewhere, although the real sky PVGIS model dataset provides better annual operation results for "Type I" to "Type III" configurations, both clear and real sky models provide similar results for the advanced configurations with daily energy adjustment. This can be understood by the simple fact that the *Meteo Coefficient* introduced in "Type IV" to "Type VII" adapts the PVGIS model, used to predict the theoretical daily PV production, to the weather forecast anticipated for each day (regardless if the PVGIS irradiation dataset is that of RS or that of CS).

- Regarding the comparison of "Type III" with the rest of configurations which include the meteorological adjustment, "Type IV" to "Type VII", the first one is the sole which does not incorporate the *Meteo Coefficient*. Therefore, according to their results which are quite better for all the cases introducing the *Meteo*, this coefficient turns to be a key parameter for the optimal design of the ESS reducing its cost.

- Furthermore, the two configurations "Type V" and "Type VII" collect results for ideal cases in the definition of the *Meteo Coefficient* since, as was presented in the configurations' description, the value assigned to this coefficient is the exact quotient between the model predicted energy production and the real energy finally produced that day. This value could only be calculated when finishing the day, once the reference has already been generated and tracked. Therefore, only results obtained for configurations "Type IV" and "Type VI", which consider an approximated *Meteo* value estimated for the type of day as the weather forecast predicts the current day will be, can be accepted as realistic and achievable. "Type V" and "Type VII" configurations only provide information on the optimal case that could be achieved.

- Considering the configurations "Type IV" and "Type VI" resulting performances, the latter turns to be more demanding in terms of ESS. However, this comparison is based on a good *Meteo Coefficient* definition and a proper selection of this coefficient every day along the year. This last selection has to be done by the PV plant operator based on the available weather forecast and although should not be a very difficult decision to take if good weather information is available, some human estimation error can be introduced. In this sense, the "Type IV" configuration would be more sensitive to this

error factor than the "Type VI" configuration, which bases two of its daily reference corrections on the *Cloudiness Coefficient*. Therefore, both configurations have to be considered when it is to decide the optimal operation mode of the plant.

- Finally, since "Type IV" and "Type VI" configurations are concluded as the optimal strategies to be considered, some conclusions over the capacity values can be highlighted from the results presented on the Table 5.7. In this sense, if ES capacity values of 0.25 to 0.5 pu were installed in the PV plant, the hourly constant production could be assured annually for more than the 98% of the time. A percentage which could be even increased if the predictive control system, introduced in Chapter IV, was implemented. This overlapped reference control would avoid ES saturations within each hour. This would be done by profiting that the energy commitment that the DG plants agree with the market is not compulsory constant in power during that hour-period. Only the final energy delivered in the whole period must agree with that compromised, what leaves some leeway to modify the power reference throughout each hour.

5.6. Results summary and economic considerations.

This chapter has been devoted to the presentation of the various ESS' sizing results obtained for each of the different analyses carried out corresponding to the various EMS introduced in Chapter IV. Prior to the results, the Matlab programs which have been developed and used to perform the analyses have been introduced. And then, each of the analyses is described pointing out its goals and its characteristics as well as introducing the main results obtained for it. Finally, some partial conclusions related to each of the analyses have also been highlighted on the corresponding sections.

In summary, it can be concluded from the different results that, since each of the EMS pursues a different goal, in terms of improved operability of the PV power plant, and there are different adjustments which can be activated or not in the control, quite different levels of ES capacity are required in the various analyses. In this sense, while the constant power steps EMS pretends to render the PV technology production pattern deterministic and predictable, the fluctuations reduction EMS only comprehends a general smoothening of the PV output power, i.e. reducing the variability of the power production referred to an average value over a period (its standard deviation). Therefore, it was logical to advance that the ES energy requirements would be much smaller for the latter, as it has been confirmed when comparing

the results summarized in 5.2.1 and 5.2.2. However, results in 1.1 and 1.1 demonstrate how advanced control options complemented with precise adjustments based on real measurements and accurate weather information can facilitate the reduction of the ES capacity requirements to operate the PV+ES plant under an hourly-constant production EMS. This improved operation mode would provide PV power plants with a predictable and reliable production which would foster their participation in the electricity markets.

This wide range of ES energy capacity requirements will pave the way to the economic viability of some control strategies, closing the door to the others. Taking into account that recent cost estimations of Lithium Ion batteries used in the electric vehicle industry are around 500 €/kWh, some of the proposed EMS configurations with better results (facilitating proper plant performance with a liability over the 98 % along a regular year) could be evaluated to present an extra cost to the PV plant of around 750-1000 €/kW. Assuming that current PV plants are being installed with an estimated cost of 4000 €/kW nowadays, this would represent an extra investment of around the 20 to 25 %.

This extra investment should be economically compensated with a power commitment complementary revenue which could be assigned to the currently intermittent and stochastic RES if these were forced to provide an hourly constant power. Something similar to the way CHP units and other DGs are already operating nowadays within the Spanish electricity markets. Moreover, a power production shift could be controlled in order to program more power to be injected to the grid during peak hours, when electricity price is higher, reducing production during lower demand hours which usually coincide in Spain during the daytime with the maximum solar radiation period (remind Figure 1.15). These power production shifts are feasible given that, as can be observed in Figures 5.37 and 5.43, the same advanced EMS configurations do already introduce some energy shifts along the day, injecting and absorbing energy regardless of the current real production in such a way that the ESS capacity needs are minimized. These energy operation periods should be also shifted during the night time so as to adapt the periods when the ESS is energy-updated to recover the reference SOC before the next day's operation starts to those hours of the night when the electricity prices are more convenient (in both sense, to charge or discharge the ES).

As for the case of the "Type VI" EMS configuration whose defined reference has been represented for one whole week in Figure 5.37, the "Type IV" EMS configuration resulting reference is here represented in Figure 5.43 for a four days period. The automatic energy shift introduced with this control strategy can be clearly appreciated, and it stands out how

305

the resulting power plant production presents a peak positive production some of the days during the peak energy consumption hour, placed around 9 pm in the Iberian electric system. The two latter days the plant would consume during that period instead of supporting the grid. This grid's critical-period extra consumption could and should be shifted to the following hours during the night when electricity prices are reduced.
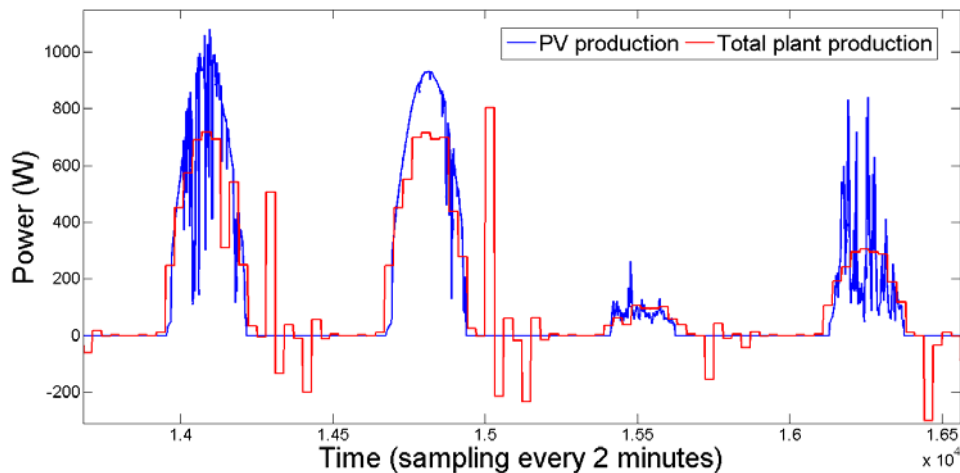
Figure 5.43 Hourly-defined reference for a four days operation under "Type IV" EMS.

All these shifting mechanisms could be easily incorporated to the EMS reference definition system just by introducing some weighting coefficients to assign different values or importance to the different one-hour periods along the day.

5.7. References

[1] SAFT Corporation. Http://www.saftbatteries.com/Technologies_Lithium_Liion_301/Language/en-US/Default.aspx. 2010.

[2] D. U. Sauer and H. Wenzl, "Comparison of different approaches for lifetime prediction of electrochemical systems—Using lead-acid batteries as example," J. Power Sources, vol. 176, pp. 534-546, 2/1, 2008.

[3] S. D. Downing and D. F. Socie, "Simple rainflow counting algorithms," Int. J. Fatigue, vol. 4, pp. 31-40, 1, 1982.

[4] M. Frendahl and I. Rychlik, "Rainflow analysis: Markov method," Int. J. Fatigue, vol. 15, pp. 265-272, 7, 1993.

[5] C. Amzallag, J. P. Gerey, J. L. Robert and J. Bahuaud, "Standardization of the rainflow counting method for fatigue analysis," Int. J. Fatigue, vol. 16, pp. 287-293, 6, 1994.

[6] R. J. Anthes, "Modified rainflow counting keeping the load sequence," Int. J. Fatigue, vol. 19, pp. 529-535, 10, 1997.

[7] G. Glinka and J. C. P. Kam, "Rainflow counting algorithm for very long stress histories," Int. J. Fatigue, vol. 9, pp. 223-228, 10, 1987.

[8] I. Rychlik, "A new definition of the rainflow cycle counting method," Int. J. Fatigue, vol. 9, pp. 119-121, 4, 1987.

[9] L. Schluter, Programmer's Guide for LIFE 2's Rainflow Counting Algorithm. Sandia National Laboritories, 1991.

[10] E. Schaltz, A. Khaligh and P. O. Rasmussen, "Influence of Battery/Ultracapacitor Energy-Storage Sizing on Battery Lifetime in a Fuel Cell Hybrid Electric Vehicle," IEEE Transactions on Vehicular Technology, vol. 58, pp. 3882-3891, 2009.

[11] E. Schaltz, A. Khaligh and P. O. Rasmussen, "Investigation of battery/ultracapacitor energy storage rating for a fuel cell hybrid electric vehicle," in Vehicle Power and Propulsion Conference, 2008. VPPC '08. IEEE, 2008, pp. 1-6.

[12] E. Meissner and G. Richter, "The challenge to the automotive battery industry: the battery has to become an increasingly integrated component within the vehicle electric power system," J. Power Sources, vol. 144, pp. 438-460, 6/15, 2005.

[13] R. Dufo-López and J. L. Bernal-Agustín, "Multi-objective design of PV–wind–diesel–hydrogen–battery systems," Renewable Energy, vol. 33, pp. 2559-2572, 12, 2008.

[14] O. Erdinc, B. Vural and M. Uzunoglu, "A dynamic lithium-ion battery model considering the effects of temperature and capacity fading," in Clean Electrical Power, 2009 International Conference on, 2009, pp. 383-386.

[15] R. Spotnitz, "Simulation of capacity fade in lithium-ion batteries," J. Power Sources, vol. 113, pp. 72-80, 1/1, 2003.

[16] P. Ramadass, B. Haran, R. White and B. N. Popov, "Mathematical modeling of the capacity fade of Li-ion cells," J. Power Sources, vol. 123, pp. 230-240, 9/20, 2003.

[17] J. D. Maclay, J. Brouwer and G. S. Samuelsen, "Dynamic modeling of hybrid energy storage systems coupled to photovoltaic generation in residential applications," J. Power Sources, vol. 163, pp. 916-925, 1/1, 2007.

[18] M. Uzunoglu, O. C. Onar and M. S. Alam, "Modeling, control and simulation of a PV/FC/UC based hybrid power generation system for stand-alone applications," Renewable Energy, vol. 34, pp. 509-520, 3, 2009.

[19] A. Andreotti, F. Mottola, M. Pagano and G. Velotto, "Design of ultracapacitor based filter for isolated PV source feeding pulsing load," Electr. Power Syst. Res., vol. 78, pp. 1038-1046, 2008.

Conclusions, contributions and future works

This Thesis has addressed some fundamental issues on the future further integration of PV technology into the electric power system, with particular emphasis on the possibility to convert the stochastic weather dependent PV production into a constant and tradable production. In this sense, topics such as the PV technology evolution, the electricity market configuration, the solar resource characteristics or the ES technologies have been reviewed in order to determine their influence on the future PV penetration degree that the electric power system will be able to manage.

The different reviews, proposals and theories performed along the different chapters of this Thesis, as well as the results from the proposals analysis achieved, yielded to a number of individual findings which have been successively introduced along this dissertation. This chapter presents now a series of general conclusions, based on the knowledge gained from the work carried out, that summarize these findings as well as providing an overall idea of the work completed in this Thesis.

In the same way, new contributions have been described, simulated and tested along the different chapters. These contributions are also stated in this chapter where a list of the various scientific papers, which have been submitted to different international conferences and journals, is also provided.

Finally, a set of new ideas and concerns which raised along the research but which have not been explored in depth for different reasons are briefly described at the end of this chapter. These ideas represent the future lines of research to be undertaken as the logical continuation to the work completed in this Thesis.

6.1. Conclusions.

As already introduced, the presented research work has addressed several key issues related to the design and control of PV power plants integrating ESS in order to facilitate their further integration into the EPS, stressing the goal of providing access to the electricity markets to this type of currently stochastic power plants. This has been done paying also special attention to the analysis of the ESS energy capacity needs which are required to operate the PV+ES power plants under different EMS. It is noteworthy that the different chapters of this Thesis dissertation divide and summarize the work performed, providing different individual conclusions which are compiled in the following.

In Chapter I, a general introduction to the current EPS structure (with a high level of DGs penetration, many of them presenting the big handicap of an intermittent production) is presented together with the future RES installation trends, especially for the case of the PV technology. The analysis of these topics, combined with the description of the associated problems which can arise from this EPS tendency, allow concluding that the ES is going to be a key technology in order to allow a further penetration for PV power plants. Moreover, the ES introduction into the stochastic PV power plants will enable this type of plants to provide a number of different applications and functionalities, such as ancillary services, improved supply quality services, flexible energy management… The implementation of one or the other, or even two of them overlapped, will depend on the ESS ratings. These various applications are also described in Chapter I, highlighting the renewables energy management functionality which provides PV+ES power plants with the capability to modify their power production spectrum, decoupling it from the current irradiation, and offering PV power plants a flexible and controlled production.

Prior to the analysis of the ESS requirements needed to operate the PV power plant according to any controlled energy management strategy, which allows modifying the PV panels' instantaneous production, a good knowledge of the solar resource is essential. In this sense, Chapter II presents an extensive review of the current solar radiation modeling

techniques complemented by an overview of the solar resource data information sources. Many different techniques and data information sources with different degrees of accuracy and liability are found. Each of them is more accurate for a certain location or presents an accuracy which depends on the input information available. Among them, the PVGIS database is concluded as the optimal to provide PV monthly-averaged production models which can be used for an ESS sizing analysis as the one performed in this PhD Thesis work. The PV models from PVGIS, both for clear and real sky conditions, are compared with current data measured throughout one whole year in situ in a Spanish southern location, resulting in good agreement. Therefore, the PVGIS database can be concluded to be a reliable source of PV production data, and the current data, available every two minutes, a representative sample of the real PV annual production.

Apart from that, note that many different ES technologies can be already found nowadays. However, not all of them are commercially available or some may still present limitations related to cost, energy and power ratings, ageing and lifetime or geographical dependence. An updated and complete compilation of their current state-of-the-art has been presented in Chapter III. When comparing the different ES technologies to determine their suitability to be used in PV power plants many factors are analyzed. Thanks to the tremendous stimulus that this technology is receiving from the electric vehicles industry, the Li-ion batteries are concluded as the optimal candidate for the use under study.

In Chapter IV, different energy management strategies to control PV power plants integrating an ESS have been described. These can be grouped into two main categories: those which aim to reduce the PV production variability (the fluctuations reduction EMS) and those which aim to turn the PV production as constant as possible (the constant power steps EMS). In this sense, while the fluctuations reduction EMS only achieves to smooth out the PV production, the constant power steps EMS turns the PV production constant in periods, adapting the power on each period to the standard monthly-averaged PV power profiles defined for a certain location by PVGIS. This provides a more regular cumulative probability distribution of the PV production which converts this EMS in the most advantageous to enter the electricity markets. In this sense, different configurations of the constant power steps EMS are defined, with a varying number of steps, so that their performance and energy requirements can be compared.

On this basis, Chapter V provides results on the amount of ES energy capacity that would be required to allow PV+ES power plants to track the power references defined by each of the different EMS configurations. Simulated results have been mainly obtained and experimental results have also been introduced in some section to support the validity of the simulated results. In this sense, the good agreement obtained between the simulation sizing analysis of the ultracapacitors and the experimental results obtained in the lab test bench, which are presented in Section 5.3, allows verifying a high degree of accuracy of the digital programs and the models considered.

Regarding the comparison of results obtained for the different EMS sizing analyses, the great advantage of the fluctuations reduction EMS is that it requires much less ES energy capacity, for most of the filtering levels contemplated, than the constant power steps EMS does. Nonetheless, for increased filtering levels which produce very constant power references, energy requirements get increasingly large, so large that these configurations should not be considered given that, with the same amount of energy capacity, the PV+ES power plant could provide constant power references and participate in electricity markets. This is not possible with the fluctuations reduction EMS which, although smoothening out the PV production, keeps being unstable and irradiation-dependent. Apart from that, among the constant power steps configurations examined, it is clear that the higher the number of steps introduced throughout the day, the lower the energy capacity requirements. Therefore, optimal strategies are those introducing 24 different one-hour-length steps when operating in the Spanish electricity market. And within these hourly-based configurations, it can be concluded that significant differences can be achieved with the various meteorologically-based energy adjustments described in Chapter IV. In this sense, results in Chapter V demonstrate how the ES energy capacity requirements can be reduced by a factor of ten when using the so-called *Meteo* and *Cloudiness* coefficients. These are therefore key parameters which should not be forgotten in a future optimal calculation of the PV+ES capacity requirements. The "Type VI" configuration is proposed, in rivalry with "Type IV" configuration, as the optimal EMS to be implemented within PV+ES power plants. The choice for one or the other will depend on the accuracy and credibility of the weather forecast service used to refine the power plant EMS. The less reliable it is, the most the "Type VI" configuration takes advantage over the "Type IV" given that the latter only relies on the weather forecast while the earlier also takes into account the past PV production.

To set down in figures what the introduction of an ESS into a PV power plant would represent, one must note that in an ideal situation where the weather forecast could be perfectly anticipated, providing a perfect prevision of the daily PV production, storage capacities of around 900 kWh / MW_{peak} would be required to track an hourly-based constant programed reference with a confidence level higher than 98 % ideally. Knowing that PV installation costs are close to 4000 €/ kW nowadays and that some ESS are around 500 €/ kWh, as it is the case of the Li-Ion batteries implemented in new prototypes of electric vehicles, the introduction of this type of batteries into large scale PV plants would represent an extra investment of approximately 12 %. To get a similar proper performance confidence level under not an ideal but a realistic constant power steps EMS configuration, the optimal "Type VI" should be implemented. With this EMS configuration, the extra costs due to the ES introduction would double those of the ideal situation but still would be in a range rounding the 25 % of the PV power plant cost. An extra cost which should be compensated in order to be economically viable by a good trading in the electricity markets and new feed-in tariffs offered by the electric system to renewables for granting a constant power production; that is a new regulatory frame. Something that, in opinion of the author, is not unreasonable. This new regulatory frame should address different problems which would stand out according to the current regulatory frame. One of them, the need for energy recharging that most of the EMS configurations require during night hours. This poses an issue due to the current feed-in tariffs associated to renewables. If the goal is to achieve a new regulatory frame in which PV power plants with constant production are encouraged, by means of improved feed-in tariffs for granting constant power as well as a determined power reserve, it results hard to assume that the system operator is going to allow these PV+ES power plants to recharge during night hours as a normal consumer (low electricity price) for a later discharge of this energy reserve complementing the PV instantaneous production (at an increased price).

However, it is noteworthy to remark as a final conclusion that, according to the ESS sizing results the hourly-stepped EMS configuration supported by a proper meteorologically-based energy adjustment, can be asserted as a technically viable option to operate PV power plants with ES in the near future. This EMS configuration will effectively provide access to the electricity markets to the PV+ES technology although a new regulatory frame, more favorable than the current one to the incoming renewable hybrid technologies, should be developed to achieve the economic viability.

6.2. **Contributions.**

As can be extracted from this Thesis dissertation, and summarized with the previous conclusions, this research work introduces a series of contributions which, in the opinion of the author, can be mainly enumerated as:

- The validation of the PVGIS solar database by comparing its PV production models with real production measured data for a location in the south of Spain. Both real measured and statistically-based PVGIS models are used in the Thesis analysis work.

- A proposal for introducing ESS into grid-tied PV power plants in order to achieve a more constant and predictable production which could be reliably traded on electricity markets.

- A review of the multiple ES technologies which can be currently integrated with renewables comparing them in terms of different characteristic parameters.

- The proposal of two main energy management strategies with completely different control philosophies (fluctuations reduction and constant power steps) for PV power plants which integrate ESS.

- The definition of different energy balance adjustments, some of them based on the meteorological conditions (in both past conditions which are measurable and future weather forecast), which are used to regulate the power reference demanded to the PV+ES plant, mainly when operating under the constant power steps configuration.

- The introduction of a recharge time constant in the ESS control equation which allows reducing the ESS size although distorting the final power production shape. A compromise solution between distortion and ESS requirements reduction is studied.

- The proposal of various advanced EMS configurations which establish constant power steps references adapted hour by hour. These EMS configurations use an optimization method which pretends to reduce the deviation of the current SOC of the ESS with regard to a predefined reference SOC.

- The definition of a meteorologically-based energy adjustment, formed by two different coefficients (the *Meteo* and the *Cloudiness* coefficient), turns to be crucial for the optimal sizing of the ESS, reducing the ESS requirements by a factor of ten when applied to these advanced hourly-based EMS configurations.

- An analysis of the frequency spectrum variation and of the cumulative probability distribution reorganization experienced by the PV power production when the PV power plant with ES is operated under each of the two basic EMS.

- The development of a cycle-counting tool which has been programed to determine the number of battery charge-discharge equivalent full cycles for a given period when operating the ESS under any control strategy. It is only function of the SOC evolution along that period. This information will help studying the potential ageing suffered by different types of batteries integrated within PV power plants.

- The experimental validation showing that UC can be used in parallel to PV generators in order to provide a more controlled production. However, this is concluded not to be the best option nowadays for these applications given their current state of development and their corresponding power and energy commercial rated levels. Li-ion batteries are contemplated as the strongest candidate ES technology to be installed in PV power plants for this kind of applications.

- A precise definition of the ESS energy capacity, defined in the per unit system (taking as base values the PV plant rated power and its daily energy production), that is needed to provide the PV+ES power plant with capability enough so as to track any of the introduced power references with a defined level of confidence.

- The sizing procedure itself which, developed to analyze the ESS requirements as a function of the PV plant rated power, could be adapted to any other location and any other EMS for which the ESS capacity requirements were desired to be established.

- The definition of one, among the various advanced EMS configurations described and analyzed in this Thesis, as the optimal strategy to be implemented in PV power plants integrating an ESS which are conceived to trade their production in electricity markets.

- A brief economic analysis of the costs increase that would represent introducing an ESS to operate the PV+ES plant under this optimal EMS.

- The proposal of introducing predictive control algorithms to continuously supervise the power injected by the PV+ES power plant, according to the reference defined by any EMS, in order to avoid saturations of the ESS due to estimation errors on the

available energy to be yielded. This can happen whenever weather forecast is not accurate. The introduction of this supervisory control in a different programming layer could help reducing even more the ESS energy requirements to track a defined reference.

Finally, note that most of these contributions are reflected in a series of papers which have been submitted to different international conferences and journals:

- H. Beltran, M. Swierczynski, A. Luna, G. Vazquez and E. Belenguer, "Photovoltaic plants generation improvement using li-ion batteries as energy buffer", in *Proc. of the IEEE International Symposium on Industrial Electronics,* ISIE, GDansk, Polland, 2011.
- H. Beltran, I. Candela, J. Rocabert, E. Belenguer and P. Rodriguez, "Influence of the Reference SOC Recovery Time on Energy Storage Ratings for PV Power Plants", in *Proc. of IEEE Industrial Electronics Society Annual International Conference*, IECON, Melbourne, Australia, 2011.
- E. Perez, H. Beltran, N. Aparicio, and P. Rodriguez, "Predictive Power Control for PV plants with Energy Storage", under review in *IEEE Transaction on Sustainable Energy Special Issue on "Applications of Solar Energy to Power Systems"*.
- H. Beltran, E. Perez, N. Aparicio, and P. Rodriguez, "Daily Solar Energy Estimation for Minimizing ES Requirements in PV Power Plants", under review in *IEEE Transaction on Sustainable Energy Special Issue on "Applications of Solar Energy to Power Systems"*.
- H. Beltran, E. Belenguer, I. Etxeberria and P. Rodriguez, "Energy Storage System Ratings and Management Strategies for increased PV Plant Operability", under review in *IEEE Transaction on Industrial Electronics Special Section on "Distributed Generation and Microgrids"*.
- H. Beltran, E. Bilbao, E. Belenguer, I. Etxeberria and P. Rodriguez, "Energy Requirements for Ultracapacitors used to render PV Power Plants Production Predictable", under review in *IEEE Transaction on Industrial Electronics Special Section on "Smart Devices for Renewable Energy Systems"*.

6.3. Future works.

Research efforts always pretend to provide solutions for every day upcoming problems and most of the times these hopefully achieve their goal. Nonetheless, solutions are never unique and can always be improved what, combined with the multiple collateral and complementary issues which arise during each research process, pave the way to new unexplored lines which could be further investigated in the future. Therefore, according to the conclusions and contributions summarized for this Thesis, the following research lines are proposed for future works:

- To analyze the functioning of a hybrid system using two types of ESS technologies (e.g. Li-ion batteries and UC) in order to compensate the distortion introduced in the power injected according to the basic constant power steps EMS when defining the preferred state-of-charge complementary control action.

- To check what the energy requirements would be for the PV+ES power plant operated under the basic constant power steps EMS (with the various step durations) if this preferred state-of-charge complementary control action is only activated at night time.

- To modify the filter equation governing the fluctuations reduction EMS, or establish another type of equation, which allows controlling the level of reduction of fluctuations in a clearer and more precise way. For instance, an equation or a series of control rules which limit the power variations to a certain percentage of the power averaged every 30 minutes and determine in this way the ESS capacity requirements.

- To reproduce the ES requirements analysis with a refined clear sky irradiation model. This could be done by taking into account the day by day irradiance variation for a determined location and program it as a function of geometrical considerations or by interpolating the monthly average PVGIS model to provide a different exact model for each day along the year.

- To try to define some rules which allow generalizing the results obtained here for a single location in the south of Spain. Similar analysis for certain characteristic sites could be performed in order to determine some relations among the resulting ESS requirements.

- To analyze the ageing experienced by Li-ion batteries when introduced in a PV power plant which is managed according to the optimal advanced EMS proposed in this Thesis.

- To establish an economic evaluation of the ESS introduction into PV power plants determining what its introduction payback period would be, taking into account the installation cost increment and contemplating different future EPS regulatory scenarios (feed-in tariffs and pool prices for daily and intraday markets as well as system imbalance costs which configure imbalances prices).

- To estimate the optimal ESS size that would be obtained if, instead of the intraday markets configuration used in the analysis presented in this Thesis (that of the Spanish electricity market nowadays), a different configuration with more frequent intraday periods and a shorter gap between the bids closure period and the operational settlement period was considered (as are the cases for instance of the Australian and Irish electricity markets with hourly markets). In fact, note that a new configuration with eight intraday markets is already being proposed to the Spanish Ministry by the Iberian electricity market operator (OMEL-OMIE).

- To calculate the ESS size reduction that could be achieved if the daily initial SOC was optimized according to meteorological information.

- To introduce the predictive control methodology, whose configuration has been described in this dissertation, to acquire the capability to modify the PV+ES production within each hour so as to provide the energy compromised while avoiding potential ES saturations. This should allow an ES size reduction for the same EMS.

- To analyze the possibility of using the ESS, introduced to achieve a controllable PV production, to provide energy shifting capability to the PV+ES power plant and determine what would be the payback period if this functionality was introduced.

- To experimentally analyze the performance of a PV+ES system introduced in a microgrid which, apart from injecting energy to the PCC in a controlled way as it is proposed in this Thesis, should also keep some energy reserve so as to cooperate with the primary frequency control of the microgrid.

320

322